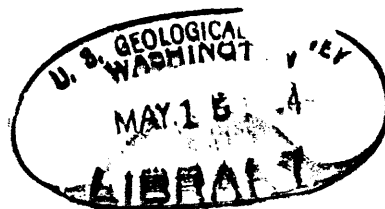


THE GEOLOGY, MINERALOGY, AND PARAGENESIS OF THE  
CASTROVIRREYNA LEAD-ZINC-SILVER DEPOSITS, PERU

۳۳

By Richard Wheatley Lewis, Jr.



U. S. Geological Survey  
OPEN FILE REPORT

This report is preliminary and has not been edited or reviewed for conformity with Geological Survey standards or nomenclature.

### ABSTRACT

The Castrovirreyña mining district lies in the Andean Cordillera of South Central Peru, and has been worked sporadically since its discovery in 1591. Supergene silver ores were first mined. Currently the district produces about 20,000 tons of lead-zinc ore and 5000 tons of silver ore annually.

The district is underlain by Tertiary andesitic rocks interbedded with basalts and intruded by small bodies of quartz latite porphyry. The terrane reflects recent glaciation and is largely covered by glacial debris.

The ore deposits are steeply dipping veins that strike N. 60° E. to S. 50° E., and average 60 centimeters wide and 300 meters long. The principal veins are grouped around three centers, lying 5 kilometers apart along a line striking N. 55° E. They are, from east to west: San Genaro, Caudalosa, and La Virreyña. A less important set of veins, similarly aligned, lies 2 kilometers to the north. Most of the veins were worked to depths of about 30 meters, the limit of supergene enrichment; but in the larger veins hypogene ores have been worked to depths over 150 meters.

Galena, sphalerite, chalcopyrite, and tetrahedrite are common to all veins, but are most abundant in the westernmost veins at La Virreyña. In the center of the district, around Caudalosa, lead sulfantimonides are the commonest ore minerals, and at the eastern end, around San Genaro and Astohuaraca, silver sulfosalts predominate.

Supergene enrichment of silver is found at shallow depths in all deposits. Silver at San Genaro, however, was concentrated towards the surface by migration along hypogene physico-chemical gradients in time and space, as vein material was reworked by mineralizing fluids.

The pattern of wallrock alteration throughout the district grades from silicification and sericitization adjacent to the veins, through argillization and propylitization, to widespread chloritization farther away.

Mineralization can be divided into three stages:

- 1) Preparatory stage, characterized by silicification and pyritization;
- 2) Depositional stage, characterized by the deposition of base-metal sulfides; and
- 3) Reworking stage, characterized by the formation of lead sulfantimonides from galena at Caudalosa, and the deposition of silver sulfide and sulfosalts at San Genaro.

Maximum temperatures, indicated by the wurtzite-sphalerite, famatinite-enargite and chalcopyrite-sphalerite assemblages, did not exceed 350° C. The low iron content of sphalerite suggests that most of the base-metal sulfides were deposited below 250° C. The colloidal habits of pyrite and quartz in the preparatory and reworking stages imply relatively low temperatures of deposition, probably between 50° and 100° C.

Mineralization was shallow and pressures ranged from 17 atmospheres in the silver deposits to over 45 atmospheres in the lead sulfantimonide deposits.

Mineralization at Castrovirreyne represents an open chemical system in which mineralizing fluids constantly modified the depositional environment while they themselves underwent modification. The deposits formed under nonequilibrium conditions from fluids containing complex ions and colloids. Reworking and migration along persistent physico-chemical gradients in time and space, from a deep source to the west concentrated base-metal sulfides in the western half, lead-antimony minerals in the center, and silver-antimony minerals in the eastern part of the district. Silver, antimony, and bismuth were kept in solution as complex ions until low temperature and pressure prevailed. They document in situ reworking by reacting with existing minerals.

Physico-chemical gradients controlled the type of minerals deposited, whereas vein structure controlled the quantity deposited.

Vein fissures formed by the equivalent of from east-west compression during Andean orogenesis and mineralization probably came from the underlying Andean Batholith.



# TABLE OF CONTENTS

	Page
Abstract .....	iv
Introduction .....	1
Purpose and scope .....	1
Previous work .....	2
Acknowledgments .....	2
I Geography .....	3
A. Location .....	3
B. Access .....	5
C. Relief and topography .....	6
D. Climate and vegetation .....	7
II Regional geology .....	8
A. Extrusive rocks .....	9
1. Andesite .....	9
2. Andesitic vitrophyres and glass .....	11
3. Andesite flow breccias .....	11
4. Andesite vent breccias .....	13
5. Basalt .....	14
B. Pyroclastic rocks .....	16
1. Andesitic pyroclastic rocks .....	16
2. Rhyodacitic pyroclastic rocks .....	17
C. Intrusive rocks .....	19
1. Quartz latite porphyry .....	19
2. Adamellite .....	20
D. Glaciation .....	21
E. Regional structure .....	22
1. Folding and tilting .....	22
2. Faulting .....	22
III Mineral deposits of the region .....	24
A. History .....	24
B. General features .....	27
C. Mineralogy .....	30
1. General .....	30

# TABLE OF CONTENTS

	page
III Mineral deposits of the region (continued)	
C. Mineralogy (continued)	
2. Description of individual mineral species --	33
a. Native elements -----	33
b. Sulfides -----	33
c. Sulfosalts -----	37
d. Oxides -----	41
e. Halides -----	42
f. Carbonates -----	42
g. Sulfates -----	43
h. Silicates -----	45
i. Mineraloids -----	47
D. Wallrock alteration -----	48
1. Chloritization -----	48
2. Propylitization -----	48
3. Argillization -----	49
4. Sericitization -----	49
5. Silicification -----	49
6. Alteration processes -----	49
E. Oxidation and leaching -----	51
F. Supergene enrichment -----	53
1. Base-metal veins -----	53
2. Silver veins -----	55
G. Hypogene enrichment of silver -----	59
1. Base-metal veins -----	59
2. Silver veins -----	59
a. Surficial zone -----	60
b. Intermediate zone -----	60
c. Protore zone -----	64
d. General considerations -----	64
H. Nature of veins -----	67
I. Structural features of the ore deposits -----	72
1. Pre-mineral faulting -----	72
2. Faulting contemporaneous with mineralization -----	74
3. Post-mineral faulting -----	74
4. Origin of vein fracture system -----	75
J. Mineralization -----	78
1. Paragenesis -----	78
a. Preparatory phase -----	79

# TABLE OF CONTENTS

	page
III Mineral deposits of the region (continued)	
J. Mineralization (continued)	
1. Paragenesis (continued)	
b. Depositional phase -----	79
c. Reworking phase -----	105
i. Lead-antimony veins -----	106
ii. Silver-antimony veins -----	116
K. Physico-chemical conditions of mineralization ----	129
1. Temperature -----	129
2. Depth of formation -----	132
3. Pressure -----	134
4. Physical states -----	134
5. Chemical conditions -----	135
L. Localization of oreshoots and zoning -----	144
1. Structural controls -----	144
2. Zoning -----	145
Conclusions -----	148
Economic -----	148
General -----	149
Appendix I. Mine descriptions -----	152
A. Astohuaraca mine -----	153
B. La Griega area -----	154
C. Rápida area -----	155
D. San Genaro mine -----	157
E. The Madona area -----	169
F. Caudalosa mine -----	171
G. Candalaria area -----	175
H. Bonanza-Seguridad-Yahuarcocha area -----	176
I. Cerro Reliquias area -----	178
J. La Virreyena area -----	181
K. Miscellaneous mines -----	185
Appendix II. Mine production -----	187
Appendix III. Mineralogical investigations -----	192
A. Techniques -----	193
1. X-ray methods -----	193
2. Spectrographic methods -----	194
B. Supporting investigations -----	194

## TABLE OF CONTENTS

	page
Appendix IV. X-ray powder diffraction data with commentary -----	196
Appendix V. Spectrographic analyses -----	245
Bibliography -----	257

# LIST OF TABLES

	page
Table I Distribution of vein-forming minerals of the Castrovirreyna mining district -----	31
Table II Veins of the Cerro Reliquias area -----	182
Table III Miscellaneous mines in the Castrovirreyna district -----	186
Table IV Mine production and grade of ore, Carmen mine, 1941-1958 -----	188
Table V Metal production, Caudalosa mine, 1927-1957 -----	189
Table VI Mine production and grade of ore, Lira mine, 1941-1958 -----	190
Table VII Metal production, San Genaro mine, 1928-1955 -----	191
Table VIII X-ray powder diffraction pattern of acanthite ---	197
Table IX X-ray powder diffraction pattern of aramayoite --	201
Table X X-ray powder diffraction pattern of bournonite -----	203
Table XI X-ray powder diffraction pattern of chalcostibite -----	207
Table XII X-ray powder diffraction pattern of enargite ----	210
Table XIII X-ray powder diffraction pattern of famatinite --	213
Table XIV X-ray powder diffraction pattern of ferrous sulfates -----	216
Table XV X-ray powder diffraction pattern of geocronite --	219
Table XVI X-ray powder diffraction pattern of miargyrite --	223
Table XVII X-ray powder diffraction pattern of pearceite ---	226
Table XVIII X-ray powder diffraction pattern of polybasite --	229
Table XIX X-ray powder diffraction pattern of pyrargyrite -	233
Table XX X-ray powder diffraction pattern of semseyite ---	237
Table XXI X-ray powder diffraction pattern of zinkenite ---	241

# LIST OF TABLES

		page
Table XXII	Spectrographic analysis of aramayoite -----	246
Table XXIII	Spectrographic analyses of bournonite -----	246
Table XXIV	Spectrographic analysis of chalcostibite -----	247
Table XXV	Analyses of enargite -----	247
Table XXVI	Analyses of famatinite -----	248
Table XXVII	Spectrographic analysis of ferrous sulfate (pozenite) -----	248
Table XXVIII	Spectrographic analysis of galena -----	249
Table XXIX	Spectrographic analyses of geocronite -----	250
Table XXX	Spectrographic analysis of miargyrite -----	250
Table XXXI	Analyses of polybasite -----	251
Table XXXII	Spectrographic analyses of pyrargyrite from the San Genaro mine -----	252
Table XXXIII	Spectrographic analysis of semseyite -----	252
Table XXXIV	Spectrographic analyses of sphalerite -----	253
Table XXXV	Spectrographic analysis of stibnite -----	254
Table XXXVI	Spectrographic analyses of tetrahedrite -----	255
Table XXXVII	Spectrographic analysis of zinkenite -----	256

# LIST OF FIGURES

	page
Figure 1. Index map showing location and generalized geology of the Castrovirreyra mining district -----	4
Figure 2. View of Cerro Quespijahuar, a volcanic neck -----	12
Figure 3. View of Santa Inés from the south, with Cerro Quespijahuar in the background -----	12
Figure 4. Graph showing relation of lead and copper to silver in typical base-metal ores -----	54
Figure 5. A typical supergene replacement of galena -----	56
Figure 6. Supergene sphalerite on stibnite -----	57
Figure 7. Typical quartz-carbonate silver ore from intermediate depths -----	62
Figure 8. Open boxwork of quartz resulting from hypogene leaching -----	63
Figure 9. Base-metal sulfides cut by quartz-silver veinlet --	65
Figure 10. Colloform, band ore showing a typical depositional sequence -----	68
Figure 11. Sketch of typical cross-section of lead-antimonide vein -----	70
Figure 12. Sulfide depositional sequence showing brecciation between last two stages of deposition -----	71
Figure 13. Vein orientation frequencies, Castrovirreyra mining district, Peru -----	73
Figure 14. Sketches of typical ore shoots, showing structural features controlling ore deposition -----	76
Figure 15. Colloform pyrite deposited around a silicified fragment of wallrock -----	80
Figure 16. Stalactitic knot of sulfides from vug showing typical sequence of minerals deposited with declining temperatures -----	82

# LIST OF FIGURES

	page
Figure 17. Two distinct periods of pyrite deposition -----	83
Figure 18. Pyrite showing three well marked growth rings, on a partially dissolved original grain -----	84
Figure 19. Porous "ball" of pyrite with base-metal sulfides -	85
Figure 20. Typical age relations between early pyrite and base-metal sulfides -----	86
Figure 21. Quartz deposited after galena and before sphalerite -----	87
Figure 22. Early base-metal sulfides replaced by early sulfantimonides -----	89
Figure 23. Typical depositional sequence during rising temperatures -----	90
Figure 24. Typical base-metal sequence deposited during rising temperatures -----	91
Figure 25. Typical galena-tetrahedrite relations -----	92
Figure 26. Sketch of typical base-metal ore showing paragenetic relations during the depositional and reworking phases -----	93
Figure 27. Ambiguous relationships between sphalerite and galena -----	94
Figure 28. Indefinite relationship between sphalerite and galena -----	95
Figure 29. Late galena replacing sphalerite -----	96
Figure 30. Galena replaced by late sphalerite -----	97
Figure 31. Layered textures typical of base-metal deposition with declining temperatures -----	98
Figure 32. Pseudo-eutectic, arborescent intergrowth of base-metal minerals -----	99
Figure 33. Typical association of chalcopyrite with tetrahedrite and sphalerite -----	101



# LIST OF FIGURES

	page
Figure 34. Chalcopyrite replaced by sulfides deposited in the reworking stage -----	102
Figure 35. Assemblage of copper sulfosalts -----	103
Figure 36. Typical reaction interface between galena and tetrahedrite -----	104
Figure 37. Typical specimen of lead sulfantimonide ore -----	107
Figure 38. Galena altered to lead sulfantimonides -----	108
Figure 39. Detail of replacement of galena by lead sulfantimonides -----	109
Figure 40. An equilibrium assemblage of sinkenite, quartz, and pyrite -----	111
Figure 41. Typical habit of only copper mineral, bournonite, deposited with lead sulfantimonides -----	112
Figure 42. Typical mineral sequence of the reworking phase --	113
Figure 43. An equilibrium assemblage of sphalerite, sinkenite, and quartz -----	114
Figure 44. Late quartz-pyrite mineralization -----	115
Figure 45. Remnant grain of early base-metal minerals in banded silver ore -----	117
Figure 46. Sketch of typical banded, colloform ore -----	119
Figure 47. Corrosion of galena by early mineralizing fluids of the reworking phase -----	120
Figure 48. Galena replaced by silver minerals -----	121
Figure 49. Antimonian alteration of scanthite -----	122
Figure 50. Typical silver sulfantimonide sequence -----	124
Figure 51. Typical knot from banded, colloform ore -----	125
Figure 52. Detail of knot of late hypogene minerals, showing depositional sequence -----	126

# LIST OF FIGURES

	page
Figure 53. Typical example of late hypogene -----	128
Figure 54. Graph showing relation of FeS content in sphalerite to temperature -----	130
Figure 55. Assemblage diagram of silver and lead sulfantimonides -----	137
Figure 56. Sketch map showing principal veins of the San Genaro area -----	159

## LIST OF PLATES

- Plate 1. Geologic map of Peru
- Plate 2. Geologic map of the Castrovirreyna District, Peru
- Plate 3. Map showing principal mines, prospects, and veins of the Castrovirreyna mining district
- Plate 4. Diagram showing sequence of deposition of vein-forming mineral and qualitative estimates of the changes in the chemistry of the mineralizing fluids with time
- Plate 5. Underground workings of the San Genaro mine
- Plate 6. Composite vein map of the San Julián section, San Genaro mine
- Plate 7. Vein map of the 623 level of the Madona mine
- Plate 8. Plan and longitudinal sections of the Caudalosa mine workings
- Plate 9. Composite vein map of the Caudalosa vein, Caudalosa mine
- Plate 10. Composite vein map of the San Pedro vein, Caudalosa mine
- Plate 11. Sketch map of mine workings and vein outcrops in the Cerro Reliquias area
- Plate 12. Composite vein map of the Santa Teresita mine
- Plate 13. Map of workings and vein outcrops, La Virreyna area
- Plate 14. Composite vein map of the principal levels, Lira mine
- Plate 15. Composite vein map of the Carmen mine

## INTRODUCTION

### Purpose and Scope

The study of the Castrovirreyna mining district was part of the systematic appraisal of the base-metal resources of Peru carried out from 1947 to 1957 by the United States Geological Survey in collaboration with the Instituto Nacional de Investigación y Fomento Mineros of the Ministerio de Fomento y Obras Publicas of the Peruvian government, under the auspices of the program of technical cooperation (Point IV) of the United States Department of State. Emphasis was placed on ore genesis, as these deposits are typical of the shallow, low temperature, lead-zinc-silver mineralization of the Andean Cordillera.

Field work was done intermittently from July to November, 1954, and for short periods from 1955 to 1957; field work totaled 20 weeks. Surface geology was mapped on aerial photographs with approximate scales of either 1:30,000 or 1:10,000, and compiled on a 1:25,000 topographic base by Masias (1929). Mine geology was mapped at a scale of 1:500 on maps provided by local mining companies or made with compass and tape by the author. About 27 kilometers of mine workings were mapped; the most important were compiled and are included herein.

More than 400 samples of ore and rock were collected, and 50 polished sections and 40 thin sections prepared. About 200 X-ray powder diffraction photographs were taken and 80 semiquantitative spectrographic analyses made.

### Previous Work

Previous reports on this area are generalized economic studies and contain little geologic data. The earliest geologic report (Raimondi, 1878) described the general geology, mineralogy, and mining activity of the district. The first geologic map of the area was published by Masias (1929). More recently, the author published a preliminary report on this area (Lewis, 1956).

### Acknowledgments

Credit is due my Peruvian associates of the Instituto Nacional de Investigación y Fomento Mineros: to Ingeniero Dante Brambilla, for mapping the geology of the San Julián section of the San Genaro mine, to Ingeniero Eleodoro Bellido for mapping the 4610 level of the Caudalosa mine, and to Ingeniero Sigfredo Narvaéz for able assistance in the field.

Cordial thanks go to the Castrovirreyra Metal Mines Company, the Corporación Minera Castrovirreyra, and Mr. Francisco Pozo for opening their mines and hospitality to us. I wish to thank in particular Messrs. Clyde Russel and Ernesto Baertl M., mine superintendents of the aforementioned companies, for their personal help and kind hospitality.

Dr. Frank S. Simons, former chief of the United States Geological Survey Mission to Peru supervised this investigation.

Special gratitude is due to Prof. C. F. Park, Jr., Dean of the School of Mineral Sciences of Stanford University, ~~under whose guidance this dissertation was prepared,~~ for his personal help, advice, and counsel; to Prof. C. O. Hutton, Professor of Mineralogy at Stanford University, whose constant advice and encouragement made the mineralogical studies possible; and to Dr. Wolfgang Mahrholz for assistance in editing and reviewing this manuscript.

## I. GEOGRAPHY

### A. Location

The mining district of Castrovirreyna is in south central Peru in the Provincia de Castrovirrayna, Departamento de Huancavelica, at approximately latitude  $13^{\circ}15'S$ . and longitude  $75^{\circ}00'W$ . Although only 100 kilometers airline from the Pacific Coast (see Figure 1), the district lies on the continental divide.

The mineralized area forms a belt 16 kilometers long and 8 kilometers wide that runs along the north shores of the lakes, Laguna Orcococha and Laguna San Francisco. It is bounded on the west by Laguna Pacococha and on the east by Laguna Choclococha. The town of Castrovirreyna (population: 2000) is 10 kilometers south of Laguna Pacococha, and 60 kilometers southwest of Huancavelica, a railhead served from central Peru.

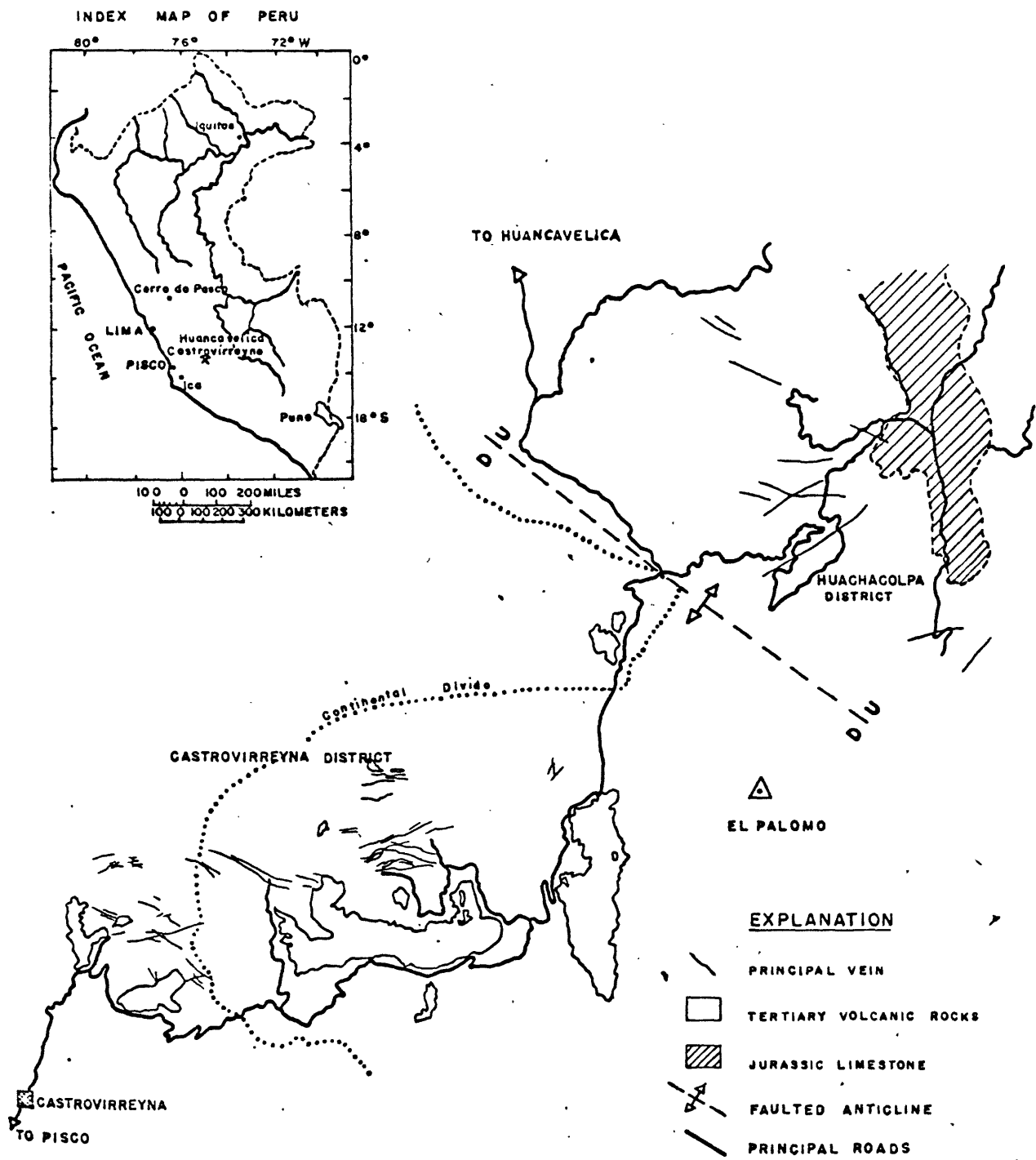


FIGURE 1 — INDEX MAP OF THE CASTROVIRREYNA MINING DISTRICT, PERU

B. Access

The district is accessible from Pisco, a port on the Pacific Coast, over 175 kilometers of good all-weather dirt road, and from Huancavelica, over 80 kilometers of good all-weather dirt road. The principal mines in the Castrovirreyna district are accessible by road from the Pisco-Huancavelica road, which passes along the southern edge of the district.



### C. Relief and Topography

The altitudes of the region range from 4300 to 5250 meters. The areas of greatest relief are along the continental divide, on the western and northern sides of the district, where differences in elevation range from 100 to 300 meters and slopes are 20 to 60 degrees or more. Elsewhere topography is more subdued; relief ranges from 1 to 5 meters on upland plains, and 50 to 150 meters in hilly areas.

The topography of the area shows the effects of alpine glaciation of flat-lying volcanic rocks. Slopes are steep and may have steplike profiles, in most places terminating in rugged peaks or sheer cliffs. Valleys are deep and characteristically U-shaped. Upland plains, or pampas, are numerous but usually small in extent, and are dotted with small, shallow seasonal lakes.

Laguna Orcococha and Laguna Choclococha, two large perennial glacial lakes 8.5 to 9 kilometers long, dominate the area (see Figure 1 and Plate 2). Laguna Orcococha drains into Laguna Choclococha, which lies 2.5 kilometers east and 125 meters lower. The overflow of these lakes belongs to the Atlantic watershed but has been diverted for irrigation of the Ica valley, 75 kilometers southwest. The area contains several smaller lakes, 750 to 2000 meters in diameter. The most important of these are Laguna La Virreyna and Laguna Pacococha, which supply water for irrigation of the Pisco valley.

#### D. Climate and Vegetation

Because of the high altitude, the climate of the region is cool and temperate in spite of its proximity to the equator. Temperatures range from about -4°C to 20°C. The year is divided into two seasons: a dry, cold winter from May to October and a cool, snowy summer from November to April. During winter, the days are pleasant and very clear, but temperatures drop to below freezing at night. During summer, hail or snow usually falls every afternoon, but seldom accumulates to any extent because of rapid melting and sublimation during the sunny mornings. Permanent ice and snow are encountered only above 5100 meters altitude.

The cool climate and high altitude restrict vegetation to a sparse covering of bunch grass on flat areas and less precipitous slopes, occasional recumbent bushes in the shelter of rocks and gullies, and thick muskeg-type mosses in poorly drained depressions and valley bottoms. There are no trees, and agricultural activity is limited to herding sheep, and the hardy alpaca and llama. The area is only sparsely inhabited.

## II. REGIONAL GEOLOGY

Andesite flows and flow breccias of the Castrovirreyna district are part of the extensive fields of Late Tertiary volcanic rocks that cover most of the mountainous region of southern Peru (see Plate 1). These rocks underlie about 60 percent of the district (see Plate 2). They are interbedded with irregular beds and lenses of rhyodacitic to andesitic pyroclastic rocks. The thickness of these volcanic rocks around Castrovirreyna is at least 1200 meters, by extrapolation from the highest peaks down to the altitude of the exposed contact with the underlying Andean batholith.

These rocks are generally tilted slightly to the south, but commonly show small local variations in attitude. A prominent faulted and tightly folded northwestward trending anticline lies 10 kilometers northeast of the district (see Figure 1).

Several bodies of andesitic glass or vitrophyre, some of which probably mark former volcanic vents, were recognized. Small intrusions of quartz latite porphyry crop out sparsely throughout the northern half of the district.

Unconsolidated glacial fill and glacial outwash deposits cover about 20 percent of the area.

## A. Extrusive Rocks

### 1. Andesite

About 45 percent of the rocks of the region consist of andesite lavas. Individual flows are 5 to 50 meters thick and are fairly uniform in appearance and texture. Megascopically, they are fine-grained and porphyritic, and are greenish black to dark reddish brown, when fresh. In mineralized areas these andesites are greenish gray to white, according to the intensity of alteration.

In thin section, the andesites consist of: (1) one or two generations of labradorite phenocrysts, (2) occasional phenocrysts of ferromagnesian minerals, and (3) a matrix of plagioclase microlites with interstitial glass, specks of iron ore, rare pyroxene grains, some ilmenite, and small apatite crystals. The overall texture is porphyritic with phenocrysts tending to group together glomeroporphyritically.

Textures of the groundmass range from vitrophyric, in which swarms of tiny semiparallel crystallites and microlites are scattered through a matrix of glass, to pilotaxitic, in which small feldspar microlites are packed so tightly that no glass remains. The most common texture is hyalopilitic, in which a felt of small feldspar microlites is suspended in a glass matrix. Intersertal textures, in which larger laths of feldspar lie at random in a mesostasis of glass and augite grains, were also observed.

The amount of glass ranges from 5 to 35 percent of the rock and averages about 25 percent. Phenocrysts comprise 10 to 50 percent of the rock and average about 30 percent. They fall into two size groups, one of labradorite laths 0.25 to 1.0 millimeters long, and the other of labradorite and ferromagnesian crystals 2 to 5 millimeters long.

The average composition of the larger labradorite phenocrysts is  $An_{65}$ . Zoning is pronounced and is normal or normal-oscillatory; cores may be as calcic as  $An_{85}$ , whereas rims average  $An_{55}$  in composition. The smaller phenocrysts are also zoned and are similar in composition to the larger ones or slightly more sodic ( $An_{60}$ ). The plagioclase microlites range from  $An_{40}$  to  $An_{55}$  in composition and average  $An_{45}$ . In unaltered rocks, plagioclase is occasionally flecked with clay, sericite, and calcite, and slightly albitized in small patches. Many phenocrysts have spongy centers or rims, filled with the glass of the matrix, indicating either very rapid growth or partial remelting.

Augite is the most common ferromagnesian mineral, comprising 5 to 10 percent of these rocks. From 2 to 5 percent biotite, and up to 3 percent hornblende were also noted. Where preserved, augite and hornblende crystals are surrounded by halos of iron-rich carbonate, and iron oxides and hydroxides. Biotite is slightly bleached. Ferromagnesian minerals are seldom preserved, however, even in the freshest rocks, and are usually represented by heterogeneous, fine-grained masses of calcite, bowlingite, chlorite, epidote, finely divided anatase, iron-rich carbonate, and iron oxides and hydroxides.

Matrix glass is devitrified or hydrated to a material resembling palagonite. Devitrification is irregular in both intensity and character, and its products include quartz, albite, and chalcedony. These minerals form micro- or cryptocrystalline aggregates showing mottled extinction under crossed nicols, or monomineralic mosaics and aggregates of fine radiating fibers.

The calcic nature of the plagioclase classify these rocks as calcic or labradorite andesites. The abundance of glass in the matrix, the

textures, the scarcity of ferromagnesian minerals, the low amount of iron ore in the groundmass, and the complete absence of olivine preclude the classification of these rocks as basalts.

## 2. Andesitic Vitrophyres and Glass

Four occurrences of andesitic vitrophyre and glass were noted in the district (see Plate 2). The largest, a spine of vitrophyre, forms the core of a volcanic neck called Cerro Quespijahuar on the west shore of Laguna Choclococha (see Figures 2 and 3). This neck is about 600 meters in diameter and is surrounded by an irregular belt of andesite vent breccia 375 to 1500 meters wide and scattered lenses of andesitic pyroclastic rock.

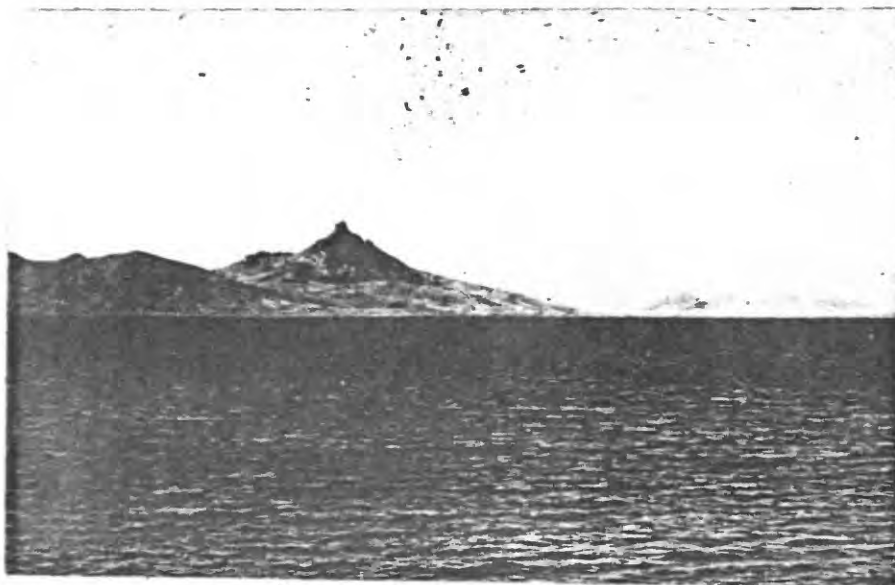
A small lens of andesitic glass was observed with rhyodacitic tuffs south of Laguna Orcococha; the two other lenses were seen incalated with andesitic pyroclastic rocks north of Laguna Choclococha.

The andesitic vitrophyre is dark brown to black, whereas the andesitic glasses are dark green, and commonly show spherulitic texture.

In thin section, the vitrophyre consists of 10 to 40 percent of plagioclase microlites, set in glass flecked with tiny skeletal crystals and grains of opaque minerals. The andesitic glass, on the other hand, contains no microlites, few opaque grains, and less than one percent crystallites.

## 3. Andesite Flow Breccias

Andesite flow breccias comprise about 5 to 10 percent of the rocks of the region. They are unequally distributed throughout the volcanic sequence and are found in beds and lenses 2 to 5 meters thick, intercalated irregularly with unbrecciated lava. They commonly contain lenses and large masses of unbrecciated andesite, and contacts between the breccia



**Figure 2.** View of Cerro Quespijahuar, a volcanic neck, from east shore of Laguna Choclococha. Note the rocky spine of andesite vitrophyre, which rises above the surrounding terrain.



**Figure 3.** View of Santa Inés from the south, with Cerro Quespijahuar in the background. The end moraine which dams the east end of Laguna Orcococha, the ruins of an old mine, and the present hydroelectric plant penstock, lie behind the camp.

and the ordinary lavas are uneven and at places gradational. These breccias are best developed west of the Caudalosa mine and in the cliffs above the La Virreyña area. They were not mapped as a separate unit but are included with andesite lavas (see Plate 2).

The flow breccias are composed of fragments of andesite 1 to 100 centimeters in diameter in a matrix of andesite lava, which, in some localities, contains small amounts of pyroclastic material. They show no bedding or lineation. Some sorting is evident, however, as the fragments at any one locale tend to be roughly the same size. The matrix, which comprises from 30 to 70 percent of these rocks, is lava, similar in texture and composition to the fragments, but different in color, often strikingly so. These breccias are generally more intensely altered than the andesite lavas, because of possible volatile activity during brecciation and cooling, or more intense weathering due to higher permeability, or both.

The origin of these breccias is problematical. The lack of stratification, the absence or low percentage of identifiable pyroclastic material, the absence of glass, the angularity of the fragments, and an igneous matrix similar to the fragments indicate an igneous rather than pyroclastic origin. Fragmentation could have been caused by autobrecciation either during extrusive flow or while in the volcanic conduit prior to extrusion. Their irregularity, thinness, and intercalation with massive lava suggest, however, that they were formed by fracturing of hardened flow surfaces and subsequent incorporation of fragments by the still fluid cores of flows during movement.

#### 4. Andesite Vent Breccias

Thick, irregular lenses of andesite breccia flank the known volcanic



vents, associated with lavas and pyroclastic rocks. The most conspicuous occurrence is a belt 200 to 300 meters wide on the western and southern flanks of the volcanic vent, Cerro Quespijahuar (see Plate 2). W. A. Lyons (oral communication, 1961) reported similar breccias within the San Genaro mine that crosscut flat-lying volcanics with apparent intrusive relationship on the north and west flanks of a suspected volcanic vent at Cerro Quaspiasisa.

These breccias are similar in appearance, composition, and texture to the flow breccias, but are classified as vent breccias because of their association with volcanic vents and crosscutting relations to bedded volcanic rocks.

### 5. Basalt

Olivine-free basalts (tholeiites) are interbedded with andesite flows and breccias and intrude them in dikes and sill-like bodies. These rocks, which probably comprise about 5 percent of the total, were not mapped as a separate unit, but are included with the andesite flow rocks (see Plate 2), because in the field they were generally indistinguishable from andesite.

In contrast to the andesites, the plagioclase of these basalts is more calcic and more abundant; the groundmass contains more iron ore, has little or no glass but more pyroxene and larger feldspar laths; textures are intergranular to pilotaxitic with a strong tendency for phenocrysts to cluster.

Phenocrysts in the basalts range in length from 1 to 5 millimeters and make up 10 to 30 percent of the rock. Most of the phenocrysts are bytownite, averaging An<sub>76</sub> in composition. Phenocrysts of ferromagnesian minerals were common, but have been altered to aggregates of chlorite,

calcite, bowlingite, epidote, halloysite (?), finely divided anatase, and iron oxides and hydroxides. Remnants of augite are also present. The groundmass consists of labradorite (An<sub>55</sub>) laths, 0.2 to 0.3 millimeter long, set in a mesostasis of tiny augite grains, iron oxides, and small amounts of glass. Most plagioclase in phenocrysts and groundmass is fresh, although it may be flecked with clay; partly albitized; or locally replaced by sericite, epidote, and chlorite.

The glass of the groundmass is commonly concentrated in small globules and clouded with tiny opaque particles, probably of an iron mineral. It is always altered either to palagonite which, in turn, may be enveloped by fibrous celadonite, or it is altered to fine-grained aggregates of chlorite, albite, iron-rich carbonate, iron oxides and hydroxides, and clay minerals of the kaolin group.

## B. Pyroclastic Rocks

### 1. Andesitic Pyroclastic Rocks

Pyroclastic rocks are found throughout the district but are most abundant in the northeast and along the southern edge (see Plate 2). They grade from fine tuff, in which most particles are smaller than 0.25 millimeter, to tuff breccia with particles averaging 50 to 100 millimeters. Vitric tuffs or lapilli tuffs comprise more than 70 percent of these rocks, and are composed of ash and cinders which range in size from 0.5 to 10 millimeters. Interbedded with the pyroclastic rocks are a few water-laid tuffs that grade into tuffs of nonaqueous origin.

The coarse-grained fractions, which include lapilli, fragments of andesite lava or pyroclastic rock, and crystal fragments, are set in a matrix of compacted glass shards. Crystal fragments include plagioclase, biotite and altered ferromagnesian minerals, magnetite, and quartz. The composition of the plagioclase ranges from  $An_{20}$  to  $An_{60}$ , and averages  $An_{50}$ . All ferromagnesian minerals, except occasional biotite flakes, have been altered to aggregates of chlorite, iron oxides and hydroxides, and finely divided anatase. The form of some of the pseudomorphs is suggestive of hornblende. Quartz is rare and is associated with the more sodic plagioclases. Glass is seldom preserved, and devitrification or alteration products are cryptocrystalline, granular, spherulitic, or even fibrous. Ghosts of former shards are visible where the devitrification or alteration has not been too intense. Refractive indices of the glass shards in the freshest material available, collected just north of Laguna Choclococha, range from 1.490 to 1.575. Partial devitrification or hydration, rather than wide differences in original composition,

probably caused this variation (George, 1924).

Pyroclastic rocks are white, gray, brownish gray, pink, and red and commonly porphyritic. Lapilli tuffs show good lineation due to flattening of lapilli and shards, and all of the pyroclastic rocks have been at least partly welded. The more highly indurated tuffs may be ignimbrites.

In the northeastern part of the district (see Plate 2), these rocks attain an aggregate thickness of at least 200 meters, and individual beds, 1 to 40 meters thick, extend over several tens of square kilometers. The two most extensive units of pyroclastic rocks crop out between the Caudalosa and San Genaro mines (see Plate 2). Each unit is 10 to 140 meters thick and they are separated by 200 meters of lavas. They consist of interbedded tuffs and tuff-breccias and the lower part of each unit includes 10 to 30 meters of medium-grained water-laid tuff.

Tuff breccias occur only locally in beds 10 to 30 meters thick intercalated with both tuffs and andesite flows.

Fine tuffs are found sporadically throughout the district in small lenses, 1 to 3 meters thick and 20 to 50 meters in diameter, and in thin beds of limited areal extent. The small uniform grain size suggests that these tuffs were deposited by wind in small depressions or as dunes.

The water-laid tuffs form beds 10 to 30 meters thick; they are usually red and exhibit graded bedding. They are composed of altered ash and cinders, small amounts of plagioclase and altered ferromagnesian minerals, and rarely quartz. Clastic grains are subangular, have a sphericity of 0.6 to 0.8, and are cemented by iron oxides and hydroxides, iron-rich carbonate, and a kaolinitic clay.

## 2. Rhyolitic Pyroclastic Rocks

In the north and south-central parts of the Castrovirreyna district

are two extensive outcrops of rhyodacitic pyroclastics (see Plate 2). These rocks cover only a small part of the area studied, but are common in adjacent areas, especially to the south.

These rocks are light colored, usually gray, white, or yellow, similar in texture to the andesitic tuffs, but contain from 5 to 10 percent quartz and from 1 to 2 percent orthoclase fragments.

The southernmost and largest outcrop lies just south of Laguna Orcococha, covering andesitic pyroclastics and lava. It consists of irregular lenses and beds of fine-grained vitric rhyodacitic tuff.

The northern outcrop of rhyodacitic tuff lies just north of the San Genaro mine and is a relatively massive body of lithic tuff.

## C. Intrusive Rocks

### 1. Quartz Latite Porphyry

Numerous, small bodies of light-green quartz latite porphyry intrude the andesite flows in the northern part of the district (see Plate 2). The largest of these, an irregular body about 850 meters long by 250 meters wide, lies just south of La Griega mine. A discontinuous arcuate line of quartz latite dikes on the south side of the valley, Quebrada Callejón Grande, near the Bonanza mine, appears to be outcrops of a single dike 2.5 kilometers long that strikes about N. 60° E. Numerous intrusions of quartz latite, 10 to 50 meters in diameter, crop out near the San Julián portal of the San Genaro mine.

This rock consists of phenocrysts of labradorite and sparse augite in a granular groundmass of labradorite, orthoclase, quartz, and finely divided opaque minerals. Phenocrysts comprise about 30 percent of the rock and range in size from 1 to 5 millimeters. The average composition is 52 percent labradorite, 25 percent orthoclase, 10 percent quartz, and 10 percent ferromagnesian minerals. Accessory minerals include clear apatite and rarely zircon. The labradorite is flecked with clay and replaced by calcite, epidote, opaline silica, and albite along cracks and the edges of grains. Orthoclase is heavily coated with clay minerals. The groundmass is generally impregnated with chlorite and epidote. Ferromagnesian minerals include augite and biotite. Most augite is altered to chlorite, calcite, epidote, rarely iron oxides and hydroxides, and finely divided anatase. Biotite is slightly bleached or chloritized and in places rimmed with fine-grained aggregates of siderite, and iron oxides and hydroxides.

## 2. Adamellite

A single occurrence of calcic adamellite (quartz monzonite), 50 meters in diameter, was found in the center of the quartz latite outcrop at La Criega. It was too small to be distinguished from quartz latite on the geologic map (see Plate 2). The adamellite is dark, mottled gray and is medium-grained with a hypidiomorphic equigranular texture. It is composed of approximately 35 percent labradorite, 30 percent quartz, 15 percent microcline, 12 percent biotite, and 8 percent common hornblende, plus minor amounts of magnetite, clear apatite, zircon, dravite, and schorlite. Slight deuteric alteration has formed specks of kaolinite and montmorillonite on microcline, and partly converted biotite to chlorite. Small aggregates of epidote develop along the edges of ferromagnesian minerals.

The adamellite is interpreted as a coarse-grained equivalent of the quartz latite, even though differences in composition are apparent.

#### D. Glaciation

Glaciation during Pleistocene and Recent times has formed arêtes and serrate ridges, faceted spurs, cirques, deep U-shaped valleys, hanging tributary valleys, step-like long valley profiles, quarried surfaces, and striated outcrops. The larger lakes of the region were formed by morainal damming, and many of the smaller ones occupy cirques. Some of the small seasonal ponds in level areas occupy rock basins scoured by glaciers.

Glacial till deposits are abundant (see Plate 2) and form ground, lateral, and end moraines. Ground moraines are most extensive in the lower parts of wide valleys, where they are characterized by hummocky, poorly drained terrain. Lateral moraines are generally poorly preserved and are found only along the sides of the larger valleys. End moraines are developed near valley mouths, and the accumulated glacial material is more than 50 meters thick in some instances. The larger valleys have three to four end moraines.

The lower limit of glaciation in the region is at 3900 meters elevation, and is marked, just above the town of Castrovirreyna, by a large terminal moraine, an abrupt change in valley profile from U- to V-shaped, and a sharp steepening in the long-valley profile. A few small ice and permanent snow caps still exist northeast of the area, near the continental divide, above 5100 meters elevation.

Glacial debris, consisting of rounded and subrounded boulders, cobbles, and pebbles of andesitic volcanic rock in a matrix of sand and rock flour, is poorly sorted, unconsolidated, and shows little or no sign of weathering.



## E. Regional Structure

Deformation of the rocks of the district during the uplift and compression of the Andean Cordillera in late Tertiary time is minimal and resulting structures are rather simple. This deformation is recorded in two ways: 1) by folding and accompanying tilting, and 2) by faulting.

### 1. Folding and Tilting

The dominant structure of the region is a simple tightly folded anticline, about 10 kilometers northeast of the district (see Figure 1). This anticline trends N.  $45^{\circ}$  W. and can be traced for more than 60 kilometers.

Within the Castrovirreyna district the rocks have gentle dips,  $5^{\circ}$  to  $20^{\circ}$ . Locally they tend to conform to surface features of the original volcanic terrain, and dip away from topographic highs which represent original volcanic vents. In general, all rocks are slightly tilted to the south.

### 2. Faulting

The only major fault noted in the region is a high angle fault trending N.  $45^{\circ}$  W. along the axial plane of the anticline (see Figure 1). Apparent vertical displacement along this fault is about 400 meters with the northeast block lifted up.

All minor faults in the district can theoretically be related to the same stresses that caused the folding and faulting of the anticline, although no direct evidence of this was found. Faults generally dip at high angles and have small displacements. Three periods of faulting were recognized; pre-mineral, contemporaneous with mineralization, and post-mineral. Pre-mineral faulting formed the vein fissures. Faulting during

mineralization reopened certain veins by shear or tension, permitting the deposition of new vein material and its accumulation at offset flexures. Post-mineral faults are rare, and cut veins at high angles with small displacement.

For further details on faulting, see the section on Structural Features of the Ore Deposits.

### III. MINERAL DEPOSITS OF THE REGION

#### A. History

Many colorful legends about the Castrovirreyna silver mines exist. Unfortunately, few substantiated facts and no production records, except for recent years, are available. Old reports, abandoned camps and roads, and more than 200 mine workings indicate an intense, yet sporadic, exploitation of silver bonanzas in the past. Eight mines were operating in 1957, but only San Genaro was producing silver as its major metal, the others were producing lead and zinc. For location and identification of mines and veins, see Plate 3.

The Castrovirreyna deposits were discovered at the end of the 16th century (Montesinos, 1591). During the first half of the 17th century, the mines produced about 92,000 kilograms of silver per year, and were considered among the richest silver deposits in South America, ranking with Potosí and Oruro, in Bolivia, and Pasco (Cerro de Pasco) and Nuevo Potosí (Morococha), in Peru (Masias, 1929). Most of this mining activity was centered around the Cerro Reliquias area, in the western part of the Castrovirreyna district. Silver production declined rapidly upon exhaustion of easily accessible ore, and from about 1670 to 1770 mining activity was negligible.

The advent of the Cornish pump and new smelting techniques at the end of the eighteenth century permitted the exploitation of deeper silver deposits. Between 1769 and 1852 interest in the district was revived and several economic studies were made (Monroy, 1769; Vives de Echevarría, 1812; Manetti, 1845). In the early nineteenth century, law suits, epidemics, lack of easily accessible ore, and water problems nullified attempts to revitalize the district (Crosnier, 1852). In the eastern part of the

district, however, at the Astohuaraca, Quespisisa, and San Julián mines, where silver sulfide ore continued in depth, successful operations recommenced about 1840.

Following the installation of pumps, the Astohuaraca mine was worked sporadically throughout most of the nineteenth century, but lack of fuel, improper machinery, water at depth, and lack of ore caused complete cessation of operations around 1900.

The San Julián and Quespisisa veins were reopened about 1860 by Don Carlos Reynaldo Pflücker. Several sizeable ore shoots in both veins were discovered. The most famous of these, La Boya de la Cruz in the Quespisisa vein, yielded 3,000,000 ounces of silver (Masias, 1929). The San Julián and Quespisisa mines, now called the San Genaro mine, were sold in 1920 to Don Tomás Marsano who formed the Compañía Minera de Santa Inés y Morococha, installing a hydroelectric plant at Santa Inés and replacing the two concentrating plants at Santa Inés and San Julián by a new plant near the main entrance of the Quespisisa mine. In 1945, the mine was leased to Leon Rosenshine and Associates who formed the present Castrovirreyna Metal Mines Company.

Pflücker's success at the San Genaro reawakened interest elsewhere in the district, and around 1870 mining was resumed at the Caudalosa, La Virreyna, and Cerro Reliquias areas, largely by the Picasso family, who also installed a mill and a crude smelter below the town of Castrovirreyna. Small-scale mining operations were carried out at Caudalosa by the Picasso family until about 1927, when the mine was leased to Don Agustín Arias Carrecedo, who had been operating mines in the nearby Bonanza area. Arias held this lease for about 5 years, during which time he built a small concentrating plant and drove more than 5 kilometers of workings.

Upon termination of the lease, the Picasso family again assumed administration of the mine and formed the present Corporación Minera Castrovirreyna. The Caudalosa mine has become the major lead and zinc producer of the region.

Although the La Virreyna and Cerro Reliquias areas had been the major producers of the district in early colonial times, interest in these areas was only sporadic throughout the latter part of the nineteenth century and the early part of the twentieth century. Several small yet determined efforts to open up old mines in the 1920's and 1930's lead the Banco Minero del Perú to install a 60-ton-per-day custom concentrating mill at Pacococha in 1945. Although the production of the area is still modest, its potential is being explored. Active mines in the La Virreyna area include Carmen, owned and operated by the Francisco Pozo family, and Lira owned by Dante Castagnola. In the Cerro Reliquias area the Corporación Minera Castrovirreyna is operating the Santa Teresita and Matilde mines.

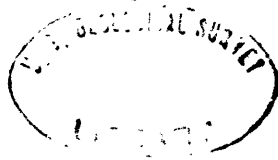
For the production records of the four principal mines of the district (Carmen, Caudalosa, Lira, and San Genaro) see Appendix II.

### B. General Features

The ore deposits of the region are veins that dip steeply, usually to the south, and range in strike from N. 60° E. to S. 50° E. The veins are 25 to 2000 meters long, averaging about 300 meters, and 10 to 300 centimeters wide, averaging about 60 centimeters. Most deposits have been worked to depths of only 25 to 30 meters, the limit of supergene enrichment; but many of the larger veins have been developed to depths of 150 meters or more.

The majority of these veins, including the most productive, are grouped around three centers, spaced about 5 kilometers apart and having an alignment that strikes N. 55° E. (see Plates 2 and 3). These mineralized centers are, from east to west, Rapida and San Genaro, Madona and Caudalosa, and Cerro Reliquias and La Virreyas. Another group of less important deposits similarly aligned lies 2 kilometers to the north. These include, from east to west, Astohuaraca, La Griega, Sorococha, Ruperto, Bonanza, Seguridad, and Yahuarcocha. The western half of the area contains a few scattered, weakly mineralized veins, which do not fit into these alignments.

Mineralization is typical of the upper mesothermal to epithermal mineral deposits. Galena, sphalerite, tetrahedrite, and chalcopyrite are common throughout the district. Around the Caudalosa mine, antimonian minerals are abundant, and the veins are characterized by lead antimonides, stibnite, and copper sulfosalts. In the eastern section of the district, around the San Genaro mine, mineralization is typical of the bonanza-type silver-antimony deposits, and veins are characterized by abundant silver antimonides, especially near the surface. The deposits of the Castro-virreyas district probably formed at relatively shallow depths, 50 to



350 meters; low pressures, 15 to 45 atmospheres; and low temperatures, 100° to 350°C.

The mineralization originated from a single source, probably related to the Andean batholith, and took place during one prolonged period, which can be divided into three stages. In the first or preparatory stage, initial mineralizing fluids conditioned fault and breccia zones for subsequent mineral deposition, by alteration of wallrock and removal of finely triturated material. The deposition of quartz and small amounts of pyrite characterize this stage. In the second or depositional stage, the bulk of the vein-forming minerals was deposited. During the final or reworking stage, many minerals were redistributed or reacted with antimony-rich mineralizing fluids forming abundant lead and silver antimonides and producing silver enrichment towards the surface.

Most of the veins of this district were mineralized by replacement and removal of triturated material in faults and fault zones. The veins at San Genaro, however, were formed in open fissures. The fracture system that provided mineral deposition sites was probably formed by the same tectonic forces that folded and faulted the rocks northeast of the district (see Figure 1).

The chemistry of mineralization controlled the character and, to some degree, the concentration of ore minerals. The near-surface concentration of silver was caused by supergene and hypogene processes; the extremely rich, surficial silver ores common to the district were deposited by descending supergene solutions, whereas the increase in silver and antimony upon approaching the surface at the San Genaro mine was caused by ascending hypogene solutions. Supergene enriched ores

extend to 30 meters depth. The hypogene enriched ores are found from 25 to 150 meters below the surface.

Ore shoots reflect the physical environment of deposition and are generally at flexures, where brecciation of the wallrock was most intense or where open fissures were widest after offset. Ore shoots range from 1 to 3 meters wide, 15 to 300 meters long, and 20 to 100 meters high.

Alteration of the wallrock follows the same pattern throughout the district, and reflects the intensity rather than the stage or type of mineralization. Within or immediately adjacent to vein structures, silicification and sericitization are predominant. Proceeding outward from the veins a narrow zone of argillization is first crossed, then a wide zone of propylitization, and finally a zone of wide-spread chloritization.



## C. Mineralogy

### 1. General

The mineralogy of the veins of the Castrovirreyña district is complex, but can be divided into several groups on the basis of genesis and distribution. Table I is a tabular resumé of the vein-forming minerals identified in the Castrovirreyña district, arranged both by genesis and geographic distribution. Individual mineral descriptions following this table are arranged according to Dana's system. For location of mines referred to in these descriptions, see Plate 3.

Identification of all of the sulfosalts and many of the oxides and sulfates was made by X-ray powder diffraction methods. For X-ray and spectrographic data on many of these minerals, see Appendices IV and V.

For photographs illustrating many of the mineral habits and relationships mentioned, see the sections on the Nature of the veins and Paragenesis.

**Table I: Distribution of vein-forming minerals of the Castrovirreyna mining district**

<u>PRINCIPAL DEPOSITS</u>		
<u>Base-metal deposits</u>	<u>Lead-antimony deposits</u>	<u>Silver-antimony deposits</u>
Lira mine Carmen mine Santa Teresita mine Matilde mine Bonanza mine Rápida mine La Griega mine	Caudalosa mine Candelaria mine Ruperto mine	San Genaro mine Astohuaraca mine

SECONDARY MINERALS

Oxidation and Leaching products

Azurite Calcite Cerussite Malachite Chalcanthite Gypsum Melanterite Quartz Limonite	Antimony oxides Azurite Calcite Cerussite Malachite Chalcanthite Gypsum Jarosite Melanterite Pozenite Quartz Limonite Wad	Azurite Calcite Cerussite Malachite Chalcanthite Gypsum Quartz Limonite Wad
---	---	---

Supergene Minerals

Copper Silver * Acanthite * Chalcocite Covellite Galena Marcasite Sphalerite Miargyrite Pyrargyrite	Silver * Acanthite * Chalcocite Covellite Galena Marcasite Sphalerite Miargyrite Pyrargyrite	Silver Acanthite Chalcocite Covellite Galena Miargyrite Polybasite Pyrargyrite Cerargyrite
--	--	--

Table I -- continued

<u>PRIMARY MINERALS</u>		
Base-metal deposits	Lead-antimony deposits	Silver-antimony deposits
Gold	Gold	Gold
Chalcopyrite	Chalcopyrite	Acanthite
Galena	Galena	Chalcopyrite
Pyrite	Orpiment	Galena
Sphalerite	Pyrite	Pyrite
Tetrahedrite	Realgar	Sphalerite
Hematite	Sphalerite	Stibnite
Calcite	Stibnite	Wurtzite *
Rhodochrosite	Wurtzite	Aromayosite
Barite	Bournonite	Bournonite
Kaolinite	Chalcostibite	Miargyrite
Montmorillonite	Enargite	Pearceite
Quartz	Famatinite	Polybasite
Sericite	Geocronite	Pyrargyrite
	Semseyite	Hematite
	Zinkenite	Rhodochrosite
	Hematite	Siderite
	Rhodochrosite	Barite
	Barite	Allophane
	Gypsum	Dickite *
	Kaolinite	Hyalophane
	Montmorillonite	Kaolinite
	Quartz	Montmorillonite
	Sericite	Quartz
		Sericite

\* Reported occurrence, not confirmed.

## 2. Description of Individual Mineral Species

### a. Native Elements

Copper - Small amounts of native copper, associated with chalcocite, were seen in the Lira mine, forming friable crusts and granular masses filling cracks in the vein wall, some 40 meters below the surface.

Gold - All of the ores assay small amounts of gold, but notable amounts have been reported only from the San Genaro mine. Minute grains of gold are associated with antimonial minerals, especially those of silver.

At least two prospects have been worked for gold, Siglo Nuevo, east of the Rápida mine (Enock, private report, 1910) and the Tres Paisanos prospect, on the north shore of Laguna San Francisco, but neither was successful because of low tenor.

Silver - Native silver was one of the principal ore minerals in the zone of supergene enrichment overlying both base metal veins and silver veins (Crosnier, 1852). During this study it was seen only in the Juan de Dios adit, San Genaro, about 20 meters below the surface, as isolated wires, and thin sheets in massive and platy barite.

### b. Sulfides

Acanthite - Acanthite was identified in silver ores of the San Genaro mine, and plata negra (acanthite) was abundant in the surficial ores of the Cerro Reliquias area according to Crosnier (1852). At San Genaro acanthite has two habits: 1) lacy mats, interstitial laminæ, and sooty coatings on hypogene and supergene vein minerals near the surface; and 2) isolated anhedral grains in quartz and in the centers of polybasite crystals in the deeper, unaltered vein material.

Acanthite is the low temperature dimorph of argentite and is the stable modification below 175°C, the temperature of transformation (Kracek, 1942; and Ramsdell, 1943).

Chalcocite - Small amounts of sooty chalcocite are present in most of the supergene ores, but less so over the silver ores than elsewhere. It coats and replaces hypogene sulfide minerals as sooty films and aggregates.

Chalcopyrite - Chalcopyrite, common to the district in small amounts, is a major mineral only in the westernmost mines and in certain sections of the San Genaro mine. It forms anhedral grains with quartz, sphalerite and tetrahedrite, and tiny veinlets or blebs in sphalerite. In the Lira and Carmen mines, chalcopyrite lines vugs along with quartz, sphalerite, and tetrahedrite, and lies in the centers of large tetrahedrite crystals.

Covellite - Small amounts of covellite are widely distributed in the near-surface vein material, as thin films on sphalerite, pyrite, chalcopyrite, and tetrahedrite, and in association with native silver, acanthite, and supergene galena. Moreover, covellite forms iridescent films on sphalerite far below the zone of enrichment.

Galena - Galena, an important and abundant ore mineral throughout the district, forms massive bands, knots, and coarse-grained aggregates, in association with quartz, sphalerite, tetrahedrite, pyrite, and chalcopyrite. In the San Genaro mine, galena is associated with both base-metal sulfides and silver antimonides, and is also in small sub-hedral octahedral to cubo-octahedral crystals in drusy aggregates of barite and sphalerite. In the Caudalosa mine, galena is generally accompanied by zones of the lead antimonides, geocronite, semseyite, and sinkenite. Streaky bands of fine-grained "steel" galena, showing curved

cleavage in polished section, and galena crystals 5 centimeters across are characteristic of the Carmen and Lira mines.

Marcasite - Small amounts of marcasite were identified in polished sections of near-surface ores from localities, principally in the Caudalosa mine. It replaces pyrite along small quartz-filled cracks or occurs as isolated grains in quartz.

Pyrite - Pyrite was abundant in every deposit examined, disseminated in quartz or sulfides, in wallrock, and in bands of polycrystalline aggregates with quartz, sphalerite, or tetrahedrite. At the Caudalosa mine, pyrite is also in colloform, semimassive vuggy stringers, 1 to 20 centimeters thick and thick, porous shells rimming isolated breccia fragments. Pyrite crystals are subhedral pyritohedrons, or cubes, when disseminated in massive quartz or wallrock. They commonly have two to six growth rings. Spongy balls of pyrite, with centers of sphalerite, tetrahedrite, or galena, were noted in massive and banded quartz.

Realgar and Orpiment - Realgar was observed only in the Caudalosa vein of the Caudalosa mine as tiny stringers in siliceous vein material, as short prismatic crystals coating massive banded pyrite, or as tiny inclusions in late barite crystals.

Orpiment is an alteration product of realgar, usually coats it.

Sphalerite - Sphalerite, the commonest ore mineral of the district, forms monomineralic stringers 5 to 50 millimeters wide, knots mixed with quartz and sulfides, crystals lining vugs, or irregular buttons and colloform crusts. Its habit is massive, or finely to coarsely crystalline. Crystals are 1 to 4 millimeters in diameter, but in the Lira mine are up to 5 centimeters across. Colors range from dark reddish or greenish brown to bright orange and golden yellow.

The darker sphalerites commonly contain tiny blebs of chalcopyrite, and are associated with galena, chalcopyrite, pyrite, quartz, bournonite, tetrahedrite, and wurtzite. The lighter sphalerites never contain chalcopyrite and are characteristically associated with lead and silver sulfosalts. The buttons and colloform crusts of reddish sphalerite, associated with barite and galena, line vugs and cracks throughout the district. Bright yellow, fragile acicular aggregates of sphalerite were detected in the Caudalosa vein pseudomorphing stibnite.

The iron content of sphalerite is low, ranging from about 0.01 percent in the lighter colored varieties to a maximum of about 0.9 percent in the darker ones (see Table 37). In thin section, many sphalerite crystals show oscillatory zoning, with colored bands separated by zones of clear sphalerite.

Stibnite - Stibnite was observed in the Caudalosa and Pitonisa mines, with rhodochrosite and quartz, in gouge-filled fault zones that cut or parallel veins, cementing brecciated siliceous vein material, or lining vugs, cavities, and small fractures in veins. W. A. Lyons (personal communication, 1961) reported stibnite and rhodochrosite on the A level of the San Genaro mine in veinlets paralleling the Bella and San Julián veins. Stibnite forms columnar masses or radiating or confused aggregates of elongate prismatic or acicular crystals, commonly covered with a second generation of hair-like crystals.

Wurtzite - Wurtzite was identified in ore from the 4570 level of the Caudalosa vein in aggregates of short prismatic crystals 5 to 8 millimeters across and rosettes of tiny hexagonal plates, associated with sphalerite and lead sulfosalts, especially bournonite. Wurtzite also was

reported from the Quespisisa vein, San Genaro (Palache and others, 1944) as tabular crystals up to 8 millimeters across.

c. Sulfosalts

Aramayoite - Aramyoite was found in the rich near-surface silver ores of the San Julián section of the San Genaro mine, as isolated anhedral blebs or subhedral plates in quartz, or intergrown with massive miargyrite, pyrargyrite, and polybasite.

Bournonite - Bournonite is a common mineral in the Caudalosa, Candelaria, and Ruperto mines, but elsewhere is rare. It forms massive stringers 0.5 to 10.0 millimeters wide associated with other lead sulfosalts, generally senesite and zinkenite; as thin bands separating masses of tetrahedrite and galena; or as irregular stringers, patches, or blebs in tetrahedrite. It also lines vugs as stubby or elongate prisms, comparable to those from Harz, Germany (Palache and others, 1944), or rosettes of subparallel wheel-like plates, both less than 1 millimeter across. Small amounts of bournonite are associated with galena and tetrahedrite at San Genaro.

Chalcostibite - Small quantities of chalcostibite coat famatinite and tetrahedrite or replace enargite as thin mats of fine crystals in the Caudalosa vein. Crystals are usually tabular and comparable to crystals from Cejar, Spain (Palache and others, 1944).

Enargite - Enargite was observed only in the Caudalosa vein, associated with colloform, banded pyrite. Stevanovic (1903) reported tabular or prismatic pseudohexagonal enargite crystals from a vug in this mine associated with "antimonian-luzonite" (famatinite) and stylotypite, which was identified as tetrahedrite by Rardohr (1943). Enargite is massive and commonly intergrown with famatinite. Enargite and famatinite have



been largely replaced by younger tetrahedrite and tetrahedrite-bourmonite-pyrite mixtures.

Famatinite - Famatinite is found only in the Caudalosa vein, Caudalosa mine. It is massive and associated with enargite and colloform pyrite, tetrahedrite, bourmonite, and chalcocite.

Geocronite - Geocronite is an abundant lead sulfosalt in the Caudalosa, Candalaria, and Ruperto areas. It rims galena or replaces it in tiny stringers and blebs. It also replaces sphalerite or forms isolated knots in semseyite and bourmonite. Geocronite is usually massive or very fine-grained granular, but stubby prismatic crystals or mats of irregular elongate plates and acicular crystals line cavities. Small (less than 0.5 millimeter) equidimensional subhedral grains interstitial to quartz and other lead sulfosalts were also seen. Geocronite is usually enveloped by semseyite, and was never observed in direct contact with any sulfides other than galena, sphalerite, semseyite and rarely bourmonite and pyrite.

Miargyrite - Miargyrite is abundant at the San Genaro mine and is not common elsewhere. It is a principal constituent of the semicrystalline aggregates of silver sulfantimonides filling quartz-lined cavities, or cementing quartz fragments. Miargyrite is also found in the colloform banded ores of San Genaro and, at depth, as crystals in quartz-lined vugs or as anhedral grains in quartz. Miargyrite, together with pyrite, tetrahedrite, galena, and sphalerite, fills or coats fractures in vein material throughout the San Genaro mine and the shallow parts of the veins around Cerro Reliquias. Crystals are usually thick, tabular prisms, often triangular in cross section, and seldom more than 2 millimeters in length. Crystal faces commonly show two sets of well-developed striae.

Pearceite - Pearceite, identified only in silver ores from the 35 level of the Quespisisa vein, San Genaro mine, occurs in flat subhedral tabular crystals in a veinlet of clear quartz cutting banded quartz containing tetrahedrite, galena, and chalcopyrite.

Polybasite - Polybasite is common in the San Genaro and Astohuaraca mines, but was not identified elsewhere. It forms massive or semicrystalline aggregates intimately associated with pyrargyrite, or isolated crystals and anhedral grains in quartz, associated with acanthite. Crystals are short, tabular plates, 0.5 to 2.0 millimeters in diameter, commonly showing well-developed triangular striae.

Pyrargyrite - Pyrargyrite is the principal ore mineral in the San Genaro and Astohuaraca mines. Minor quantities were seen in the near-surface ores of the Cerro Reliquias area and it is probably the rosicler referred to by Crosnier (1852) and others. At San Genaro pyrargyrite has many habits. In supergene ores it forms thin laminae and films coating barite or quartz and replacing tetrahedrite, associated with sooty chalcocite and acanthite, and wire silver. Pyrargyrite is a major constituent of the massive and semicrystalline aggregates of sulfides filling cavities in vein quartz and cementing quartz fragments. It is also in banded, colloform quartz, associated with hematite, manganiferous siderite and miargyrite. Anhedral grains of pyrargyrite appear in seams of clear crystalline quartz in vein centers or cross-cutting older vein material, along with miargyrite, polybasite, and acanthite. Finally, Pyrargyrite fills cracks in vein material, coating sulfides and gangue minerals alike throughout the San Genaro mine and the near-surface ores of the Cerro Reliquias area.

Semseyite - Semseyite is an abundant constituent of the lead antimonide ores of the Caudalosa, Candelaria, and Ruperto mines, but was not seen elsewhere in the district. It is fibrous and generally forms 1-to 10-millimeters bands or fibrous mats coating or replacing geocronite. Fibrous aggregates of semseyite in barite fill small cavities. Crystals are generally elongate prisms 0.1 to 1.0 millimeter long, but one occurrence of eight-sided tabular plates of semseyite, 0.5 to 3.0 millimeters across, was noted coating tetrahedrite.

Tetrahedrite - Tetrahedrite is found with all types of mineralization in the district, as small stringers, crystals in vugs, in the interior of multilayer knots of sulfides, and mixed with medium- to coarse-grained aggregates of sulfides. In the base-metal veins, it forms massive knots and bands 3 to 100 millimeters wide and commonly contains small amounts of disseminated quartz and pyrite. In the silver veins at San Genaro, it is intergrown with pyrargyrite, coats voids as tiny sublimate-like branching clumps, and fills cracks as granular aggregates or subhedral prismatic crystals along with pyrargyrite, niargyrite, or galena and sphalerite. Crystals are generally tetrahedral and at the Lira mine measure up to 5 centimeters across. At San Genaro small dodecahedral crystals were observed.

Zinkenite - Zinkenite is common in the Caudalosa, Candelaria, and Ruperto mines and traces were noted in veins at the Madona area. It is associated with other lead sulfantimonides and stibnite, as well as very late or even supergene minerals. Zinkenite typically forms cross-cutting veinlets together with quartz and pyrite or fibrous bands coating semseyite. Small patches of zinkenite form in semseyite, sphalerite and

bourbonite. Although associated with galena and geocronite, zinkenite is never found in contact with them. Late zinkenite coats stibnite, or fills small cavities in quartz, sphalerite, semseyite, or bourbonite in mats and aggregates of loosely packed, minute crystals, and is associated with covellite, gypsum, anglesite, and micaceous hematite. Crystals are acicular and seldom more than 0.5 millimeter long. The largest crystals observed, about 2.0 millimeters in length, were grouped like sheaves of wheat. The usual color is steel gray and crystal aggregates have a soot-like appearance. Some zinkenite, however, is golden tan, rust red, or iridescent purple, probably resulting from thin films of covellite or hematite.

#### d. Oxides

Antimony Oxides - White to yellow, granular or fine-grained antimony oxides coat the lead-antimony ores at the Caudalosa mine and elsewhere. They are found in dump material and in old workings, associated with gypsum, jarosite, hydrous iron oxides and sulfates, and rarely chalcantite. Most of this oxide is probably the hydrated oxide stibiconite, but identification was not verified.

Hematite - Fine-grained disseminations of hematite in quartz were observed in all of the deposits of the district. It is especially abundant at San Genaro where it occurs sporadically throughout the colloform ores in quartz bands that have a low silver content, as disseminated needles, characteristically grouped around corroded base-metal sulfide grains. It is most abundant in the breccia bands in the Trabajo vein and may have been derived from the breakdown of pyrite.

Loose films or mats of fine micaceous hematite also fill vugs in sulfides deep within the San Genaro and Caudalosa mines. Furthermore,

hematite was seen as inclusions in late barite and quartz. It is not, however, a common mineral in the zone of oxidation, and is noticeably absent in the supergene ores.

e. Halides

Cerargyrite - Cerargyrite is a rare mineral in the district and no mention was made of it in old reports. Tiny, yellow-brown, waxy buttons and thin crusts of cerargyrite coating quartz were seen in oxidized silver ores of the east or Grau section of the Trabajo vein at San Genaro, associated with limonite.

f. Carbonates

Calcite - Calcite is a notable vein-forming mineral in the Madona area, where it forms massive bands and fills vugs in the banded base-metal and rhodochrosite ores, and at the La Griega mine, where it forms fibrous bands and drusy coatings on quartz. Small amounts of calcite are associated with oxidation products in the near-surface portions of veins as tiny crystals and fibrous laminae coating vein minerals and filling cracks throughout the district. Calcite is also a common, but not a plentiful, product of wallrock alteration.

Cerussite - Small amounts of cerussite were observed throughout the district in the oxidized vein material, as grainy films, usually on galena, and associated with limonite, wad, quartz, calcite, and copper carbonates.

Malachite and Azurite - Small amounts of malachite and traces of azurite in efflorescent clumps form on the oxidized ores throughout the district, generally in well-aerated places, such as old surficial workings, old fill, and mine dumps. They are more abundant in the western part of the area, where the copper content of the veins is higher and abandoned mine dumps are more numerous.

Rhodochrosite - Rhodochrosite is common to the district but is most abundant in the Caudalosa vein, where, with stibnite, it fills fault zones, late fractures and vugs, or cements siliceous breccia. It is massive, with highly contorted banding, or forms semimassive to crust-like aggregates of small, flattened rhombohedral crystals. At the Madona mine, crystalline and massive rhodochrosite is interbanded with base-metal sulfides (especially galena) and calcite, and with quartz near the vein centers. It was also reported (W. A. Lyons, personal communication, 1961) in the upper levels of the Bella vein, at the San Genaro mine, interbanded with quartz. Elsewhere in the district, rhodochrosite is found as isolated crystals in cavities, or filling small fractures cutting all other vein-forming minerals.

$M_F'$  for Castrovirreyuna rhodochrosite ranges from 1.705 to 1.718, indicating relatively pure manganese carbonate (Winchell, 1951).

Siderite - Small amounts of mangiferous siderite were noted in the intricately banded, colloform quartz at the San Genaro mine, either as anhedral grains associated with sericite and silver antimonides or intimately mixed with fine-grained quartz and associated with abundant disseminated hematite.

$M_F'$  ranges from 1.735 to 1.750, indicating mangiferous iron carbonate (Winchell, 1951).

#### g. Sulfates

Barite - Barite is common at the San Genaro mine, in the upper part of the San Pedro vein at Caudalosa, and in the Mata Caballo vein at Cerro Reliquias. Elsewhere it is not common. Barite is massive or forms aggregates of thin tabular plates filling or lining vugs and fractures, or occurs as scattered single crystals in massive quartz or

rhodochrosite. Individual crystals are 1 to 2 centimeters square by 1 to 2 millimeters thick and are often coated with a second generation of smaller barite crystals containing inclusions of realgar (San Pedro vein) or finely divided hematite (San Genaro mine). Throughout the district, but especially at Caudalosa and San Genaro, barite forms drusy aggregates with galena and sphalerite. At San Genaro it is commonly associated with the rich silver ores.

Chalcanthite - Chalcanthite, the most common oxidation product of copper minerals in the district, forms fragile, matted encrustations of thin tabular crystals on the walls and vein surfaces in old mine workings. It also forms tiny buttons and plates coating copper sulfides. Hydrous iron and antimony oxides are its commonest associates. When dry, chalcanthite is commonly coated with a greenish-white, translucent powder, probably  $\text{CuSO}_4 \cdot \text{H}_2\text{O}$  (Palache and others, 1951). Chalcanthite accumulates wherever water, percolating down through old fill or brecciated vein material, evaporates; and is frequently found in mine workings far below the zone of oxidation. The most notable occurrence of chalcanthite is at the Candelaria mine where it coats the walls of the lower adit with extensive, fragile sheets 2 to 20 millimeters thick.

Gypsum - Gypsum forms throughout the district in or near the zones of leaching and enrichment or below fill or fractured vein material as scales, crusts, and fibrous aggregates, in association with hydrous iron and antimony oxides and hydrous ferrous and cupric sulfates. Gypsum is also in hypogene ores as acicular crystals, up to 3 centimeters long, coating vugs and cavities in unaltered vein material in association with stibnite, barite, and quartz.

Jarosite - Small amounts of jarosite were identified as very fine-grained, powdery aggregates in cavities in oxidized vein material, associated with hydrous iron and antimony oxides.

Melanterite and Pozenite - In the Caudalosa mine, melanterite was identified glazing partially oxidized vein material, associated with antimony oxides and limonite. It is quite common in the upper parts of the mine in old fill or stopes.

Pozenite forms as a dessication product of melanterite, which it coats as a translucent white powder.

#### h. Silicates

Clay minerals - No formal study of the clay minerals was undertaken, but perfunctory studies indicate that minerals of the kaolinite group predominate in both altered wallrock and vein material.

Kaolinite is a major constituent of the argillized wallrock surrounding the veins throughout the district. In vein quartz, kaolinite is found as disseminations and in wallrock fragments. At San Genaro, it was also identified together with sericite, quartz, and barite in the white powder that coats vein material, fills vein cavities, and forms irregular patches in quartz or carbonate bands.

Halloysite and allophane were identified optically in the thin glaze coating small intergrown sphalerite, galena, and quartz crystals from vugs and cavities in the banded quartz at San Genaro. This glaze is thicker on the under side of the crystals, giving it the appearance of having been sprayed on.

Illite was reported in the argillized rocks of San Genaro (W. A. Lyons, personal communication, 1961). The presence of dickite in these rocks is suspected, but not confirmed.



Montmorillonite group clays were identified optically in the argillized rocks in and adjacent to veins, closely associated with kaolinite.

Quartz - Quartz, the most common vein-forming mineral in the district, forms narrow stringers, thick bands, semicrystalline porous aggregates, anhedral grains mixed with sulfides, crystals lining cavities, and microcrystalline impregnations in wallrock fragments within the veins. The typical habit is massive, however, prismatic crystals, 1 to 10 millimeters long, are also common.

Massive quartz is coarsely crystalline, somewhat milky in appearance, and flecked with inclusions of altered wallrock and disseminations of pyrite and clay minerals. Banded quartz, which is best developed at San Genaro, shows intricate, contorted, and commonly variegated or colloform banding. Individual bands are cloudy, clear, or colored, and either microcrystalline or coarsely crystalline. They are solid and dense or porous and vuggy with comb structures. Individual bands may be pure quartz or contain sulfides, chlorite, crystals of barite or siderite, disseminations of hematite, or pockets of sericite and kaolinite. Some bands show bracciation healed by younger quartz or silver antimonides. Some of the massive milky quartz shows dessication cracks, and bands of impurities extending through several contiguous crystals implying that it precipitated as a hydrous, colloidal gel, which later dehydrated and crystallized.

Amethystine quartz is common at San Genaro, sparingly present at Caudalosa, and rare elsewhere in the district. Small amounts of jasper are found in all deposits. Chalcedony is common in the volcanic rocks of the region, especially the pyroclastic rocks, where it forms banded

or mottled red and white veinlets and pods.

Sericite - Sericite is characteristic of the intensely altered or sericitized zone of wallrock adjacent to vein structures. Within the veins, sericite is found as disseminations and pods in massive or banded quartz. Sericite is also found with pyrargyrite, miargyrite, tetrahedrite and other late minerals lining narrow, cross-cutting seams.

#### 1. Mineraloids

Limonite (hydrous iron oxides) - Considerable amounts of limonite are found in the oxidized zone of the veins of the district as earthy, loose or porous masses, and varnish-like coatings on vein material. It is associated with manganese oxides, hydrous antimony oxides, and other oxidation products. Some limonitic gossan contains appreciable amounts of auriferous quartz (Enock, private report, 1910), but most of it is without value.

MnO<sub>2</sub> (manganese oxides) - Small amounts of indeterminable black manganese oxides were observed mixed with hydrous iron oxides in gossans and oxidized ores or coating weathered rhodochrosite. This mineraloid is most abundant in the oxidized parts of the Caudalosa vein, but was also noted elsewhere in small amounts. It appears to have formed solely from the decomposition of rhodochrosite.

#### D. Wallrock Alteration

In the Castrovirreyna district hydrothermal alteration of the wallrock is zoned around the veins. The alteration scheme is the same throughout the district and can be separated into five gradational zones, which are, in order of increasing intensity, the zones of chloritization, propylitization, argillization, sericitization, and silicification. The width of these zones depends on the permeability of wallrock and the size of the enclosed vein. The intensity and type of alteration is a function of temperature and the circulation of hydrothermal fluids, and is apparently independent of the type, character, and stage of associated mineralization. Chloritization, the lowest degree of alteration, is the oldest and the most distant from the veins.

##### 1. Chloritization

The most extensive, but least intensive alteration is chloritization. Nearly all the rocks of the district have been somewhat chloritized; glass is devitrified and pyroxenes and amphiboles are partially or completely converted to chlorite and magnetite; biotite is partially bleached; and sericite has formed on plagioclase.

##### 2. Propylitization

From 10 to 100 meters from the veins the rocks are propylitized. Ferromagnesian minerals are completely converted to chlorite and finely divided anatase; groundmass is altered to kaolinite, chlorite, iron oxides and albite; and calcic feldspars are largely converted to sericite, albite, calcite, kaolinite, and opaline silica. The original textures of these rocks are still easily recognizable.

### 3. Argillization

The rocks are completely altered to clay, quartz, and some calcite, albite, and iron oxides within 1 to 10 meters of the veins. Original macrotextures can still be discerned, but groundmass textures are completely destroyed. Kaolinite is the dominant clay mineral and montmorillonite, illite, and dickite are suspected to be present.

### 4. Sericitization

Adjacent to the veins, wallrock is sericitized in a zone 5 to 100 centimeters wide. The rock is completely bleached and converted to an aggregate of sericite, hydronica, and clay, into which varying amounts of calcite, quartz, barite, and disseminated pyrite have been introduced. All traces of original textures have been destroyed.

### 5. Silicification

Within or immediately adjacent to the vein structures, quartz completely replaces wallrock. Minor amounts of sericite, kaolinite, and montmorillonite are present as well as disseminations of pyrite that commonly outline former breccia fragments.

### 6. Alteration Processes

Rock alteration involved three different yet concomitant processes: decomposition, leaching, and addition. The dominant process in the zones of chloritization and propylitization, was decomposition of rock-forming minerals, without essential changes in the bulk chemical composition. Mafic minerals decomposed first, followed by the groundmass and finally the feldspars.

As the circulation of hydrothermal fluids and temperature increased decomposition was complete and leaching became important. Ferrous iron and magnesium were first removed, then potassium, calcium, sodium, and

finally ferric iron and titanium. The end products of this hydrothermal leaching were argillized rocks, consisting mainly of simple aluminum silicates and quartz. Complete removal of calcium, sodium, potassium and ferric iron was seldom observed, and even the most intensely argillized rocks contain small amounts of calcite, albite, hydromica, and hematite.

Where alteration was most intense, addition played an important role. In the immediate vicinity of the veins potassium was introduced into the previously argillized rock, forming sericite and hydromica. At the same time small amounts of quartz, calcite, and pyrite were deposited. Within and adjacent to the veins, silica accompanied by minor quantities of barite and pyrite almost completely replaced altered wallrock.

### 8. Oxidation and Leaching

Although the upper parts of most veins are inaccessible and outcrops excavated or covered with debris, enough information on leaching and oxidation was obtained to draw general conclusions.

Vein outcrops are massive to semiporous quartz and seldom are more than a meter high. Above the ground surface they are generally leached of all metallic constituents except for minor amounts of iron and manganese oxides. Massive vein quartz from outcrops or float in the San Genaro area, however, may assay 100 grams or more of silver per ton, due to tiny grains of primary silver minerals locked interstitially between quartz grains and protected from weathering.

In the first 10 to 50 centimeters below the surface minerals residual from extreme weathering appear, such as, hematite and manganese oxides. Below 50 centimeters depth chalcantite, azurite, malachite, calcite, cerussite, gypsum, anglesite, jarosite, ferrous sulfate, limonite, wad, and hydrous antimony oxides form. Cerussite and calcite are the only secondary carbonates found at more than a meter's depth, but sulfates do form wherever percolating waters evaporate.

Complete oxidation of the metallic constituents of the veins seldom extends more than a meter or two in depth, but partial oxidation, especially of copper and antimony minerals, extends to depths of 20 meters or more. The shallow depth of oxidation is probably caused by a high water table. Wherever the water table has been lowered recently, either naturally or by mine workings, partial oxidation extends to depths of 50 meters or more.

Although the oxidized vein material does not generally have economic value, limonitic quartz at Siglo Nuevo prospect in the Rápida area was reported to have up to an ounce of gold per ton (Enock, private report, 1905).

## F. Supergene Enrichment

Information on supergene ores of the district is incomplete because near-surface workings are inaccessible and old reports lack reliable data. According to Montesinos (1591), Monroy (1769), Crosnier (1852), and others, early mining activities exploited near-surface ores rich in plata blanca (native silver), plata negra (sacanthite), and plata roja or rosicler (silver sulfantimonides) to depths of 10 to 25 meters on both the base-metal veins and the silver veins.

### 1. Base-metal veins

The zone of supergene enrichment in the base-metal veins of the Caudalosa, Cerro Reliquias, and La Virreyena areas (see Plate 2) extends from about 2 to 25 meters below the surface. Supergene minerals, however, may form 10 to 25 meters deeper.

Silver is the principal metal enriched, but small amounts of copper and smaller amounts of lead and zinc are also concentrated. The tenor of these supergene ores is not accurately known because no modern data are available. Monroy (1769) stated that surficial ores of the Cerro Reliquias area contained from 200 to 1700 grams of silver per ton, and Crosnier (1852) said that veins at Cerro San Francisco (Cerro Reliquias area) ran 50 to 60 kilograms of silver per ton, and that grab samples from the Caudalosa mine averaged 5 kilograms of silver and 20 percent copper per ton.

Modern analyses of the protores from these veins show silver content averaging between 250 and 350 grams per ton. Overall silver content in these protores shows better correlation to copper values than to lead (see Figure 4) and semiquantitative spectrographic



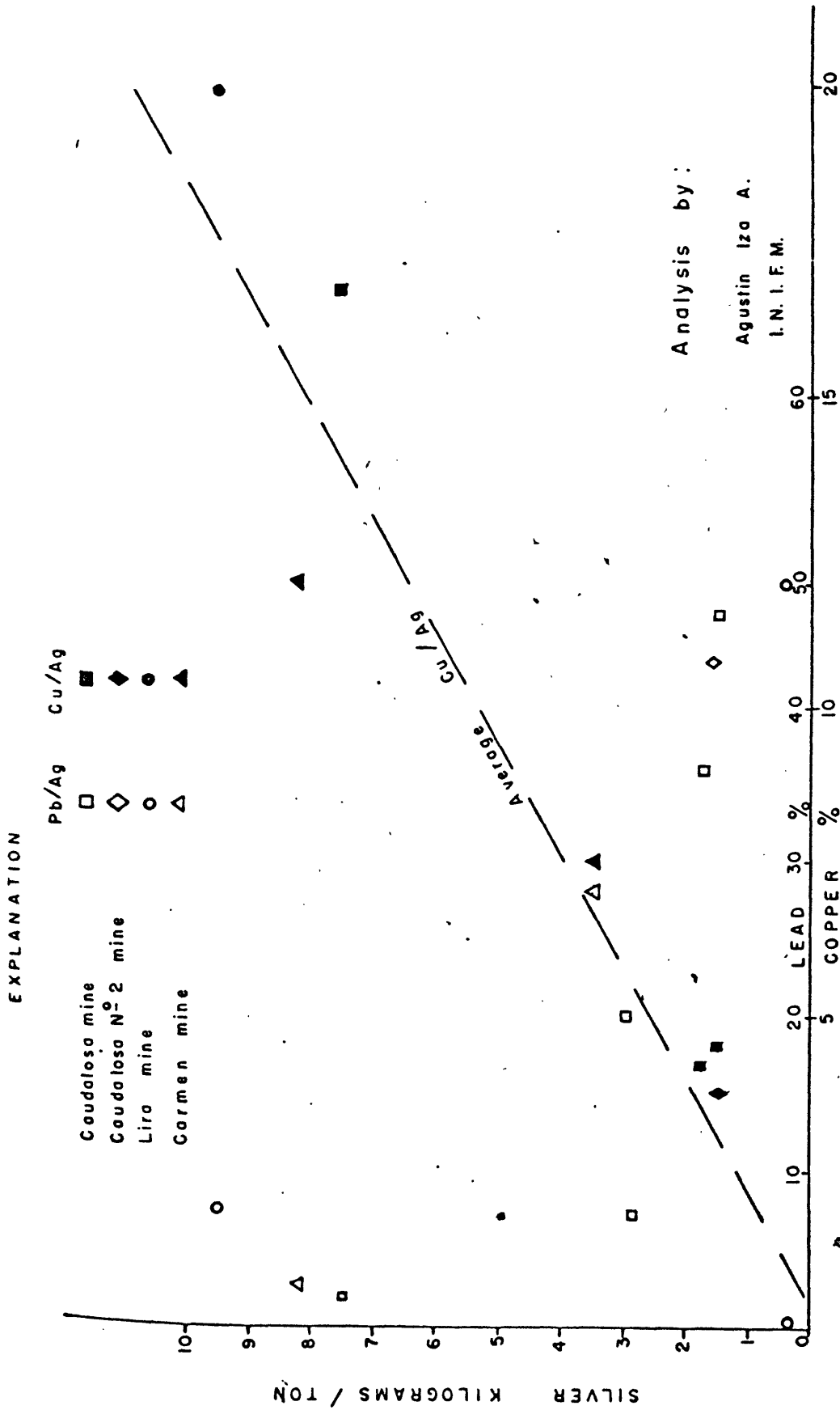


FIGURE 4—Graph showing relation of lead and copper to silver in typical base-metal ores, Castrovirreyna, Peru.

analyses show more silver in tetrahedrite than in other base-metal sulfides (see Appendix V) indicating that most silver was carried in tetrahedrite rather than in galena.

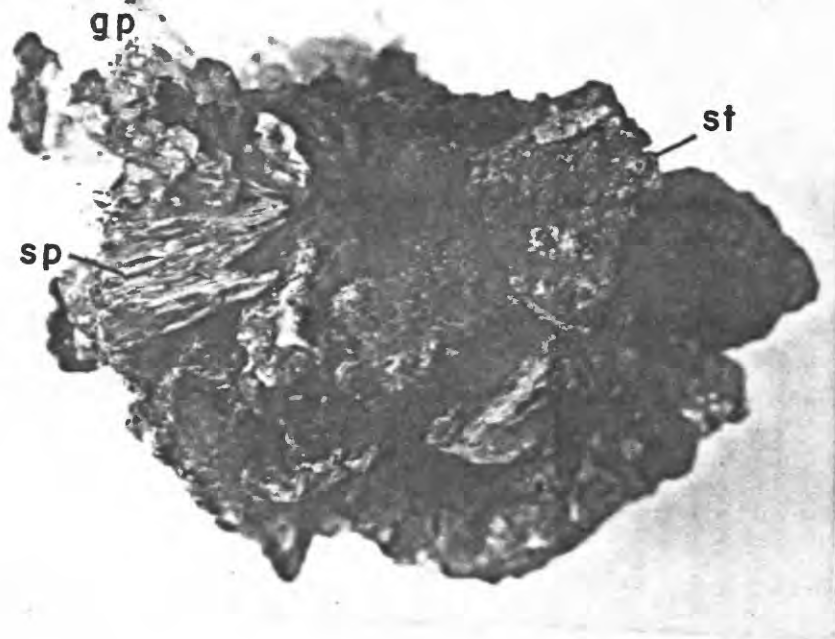
Supergene minerals found over the base-metal veins include sooty acanthite, pyrargyrite, miargyrite, covellite, sooty chalcocite, galena, sphalerite, and native copper, in order of decreasing abundance. These minerals are found typically in thin films and fine-grained granular, lacy, or plumose aggregates, commonly in association with limonite and sulfates. Figures 5 and 6 show typical supergene textures. Nonsulfide hypogene gangue minerals are coated but not replaced by supergene minerals; whereas, hypogene sulfides are selectively replaced near fractures (see Figure 5). Tetrahedrite and chalcopyrite are replaced first, followed by galena, sphalerite, stibnite, lead antimonides, and finally pyrite.

## 2. Silver veins

It is difficult to evaluate the full extent and importance of supergene enrichment in the silver veins because late hypogene solutions contributed to the enrichment of silver near the surface, depositing similar minerals. In the upper 20 to 25 meters of the silver veins the dominant enrichment process was supergene, as indicated by the abundance of sooty acanthite, native wire silver, and other minerals generally considered typical of supergene mineralization. Below 25 meters depth, however, the general textures and mineral associations of the silver ore suggest hypogene rather than supergene mineralization, even though sooty acanthite, chalcocite, covellite, and supergene sphalerite were found in small quantities as deep as 35 to 45 meters. See the following section on Hypogene



**Figure 5.** A typical supergene replacement of galena. Veinlets of covellite (cv) and a nonopaque mineral (ac), perhaps anglesite or cerussite, replace galena (ga). Quartz (qz). Caudalosa vein, uppermost working, Caudalosa mine (x 150).



**Figure 6.** Supergene sphalerite on stibnite. A semifibrous aggregate of stibnite (st) is replaced by thin fibers of bright yellow sphalerite (sp), which pseudomorph the stibnite. Gypsum (gp) crystals are associated with the sphalerite. Caudalosa vein, 4610 level, Caudalosa mine (X 1).

Enrichment for details.

The supergene ores at the San Genaro and Astohuaraca silver mines were very rich; Manetti (1845) reported tenors of 100 to 250 kilograms of silver per ton, and Crosnier (1852) said that waste from the San Genaro mine ran 1600 grams of silver per ton. Near-surface ore mined at San Genaro at the time of this study contained 5 to 15 kilograms of silver per ton.

The supergene ores in the silver veins are characterized by abundant sooty acanthite, pyrargyrite, and miargyrite, some native silver and small amounts of sooty chalcocite, covellite, galena, and cerargyrite. Sooty acanthite and chalcocite form lacy mats and plumose aggregates on other sulfides. Pyrargyrite, miargyrite, and covellite coat hypogene minerals in thin films and fill cracks and other cavities. Native wire silver forms thin sheets and wires on gangue minerals, especially barite. Supergene galena is in minute, isolated, colloform knots in lacy acanthite and tiny clumps of cerargyrite coat quartz in partially oxidized ores. These minerals are commonly associated with small amounts of limonite, gypsum, and chalcantite. Supergene mineralization is generally best shown in the more porous or fractured parts of the veins.

## G. Hypogene Enrichment of Silver

The enrichment of silver near the surface in the base-metal veins of the Castrovirreyña district can be accounted for by supergene processes, when evaluated in terms of depth of enrichment, textures, and species of minerals involved, amount of post-ore erosion, and tenors of the enriched ore and the protore. On the other hand, a similar evaluation of the silver veins of the district indicates that supergene processes alone cannot account for the enrichment of silver towards the surface, even though the silver sulfide and sulfantimonides composing these enriched silver ores are considered typical of supergene enrichment (Cooke, 1913; Raviaz, 1915; Emons, 1915; Bastin, 1924).

### 1. Base-metal veins

In the base-metal veins of the Caudalosa, Cerro Reliquias, and La Virreyña areas (see Plate 2), hypogene vein material below 30 meters depth is cut by small cracks containing pyrargyrite, miargyrite, sericite, and barite. These minerals merely fill the cracks without replacing enclosing sulfides. The lack of selective replacement, the presence of sericite, and the absence of other indicative criteria suggest that this mineralization is due to deposition by late hypogene fluids.

### 2. Silver veins

In the silver veins at San Cenaro the richer ore shoots are near the surface, and the silver content decrease with depth so that below the 70 level, which is 100 to 150 meters below the outcrop, mining is not economical. The silver minerals forming these ore shoots appear

to be younger than the bulk of the base-metal minerals and are commonly concentrated in voids in the vein material or in quartzose veinlets that cross-cut older vein material. On the basis of the tenor of silver, the mineral assemblages, and the textures present the veins at San Genaro can be divided into three zones: 1) a surficial, highly enriched zone, 2) an intermediate, enriched zone, and 3) a nonenriched, protore zone at depth.

a. Surficial zone

The surficial zone, which extends from just below the surface to 25 or 30 meters depth, contained the richest silver ore and shows mineralization and textures typical of supergene silver ores. See the preceding section on Supergene Enrichment.

b. Intermediate zone

The intermediate zone extends 75 to 125 meters below the surficial zone, down to 100 to 150 meters below the vein outcrop. Silver values range from 100 to over 1500 grams per ton and average about 500 grams per ton. Silver minerals of this zone include, in order of abundance, pyrargyrite, miargyrite, polybasite, massive acanthite, aramayoite, and pearceite. They are found in two principal habits: 1) as massive aggregates filling and cementing quartz breccia, and 2) as isolated grains and small aggregates in the colloform, banded quartz.

The massive silver ores consist of aggregates of pyrargyrite, miargyrite, and minor amounts of polybasite, pearceite and aramayoite, lining vugs, filling voids, or cementing brecciated quartz. These silver minerals are found as tightly packed anhedral to euhedral crystals, and are commonly intergrown with sphalerite, galena, and tetrahedrite with which, in places, they show mutual boundary

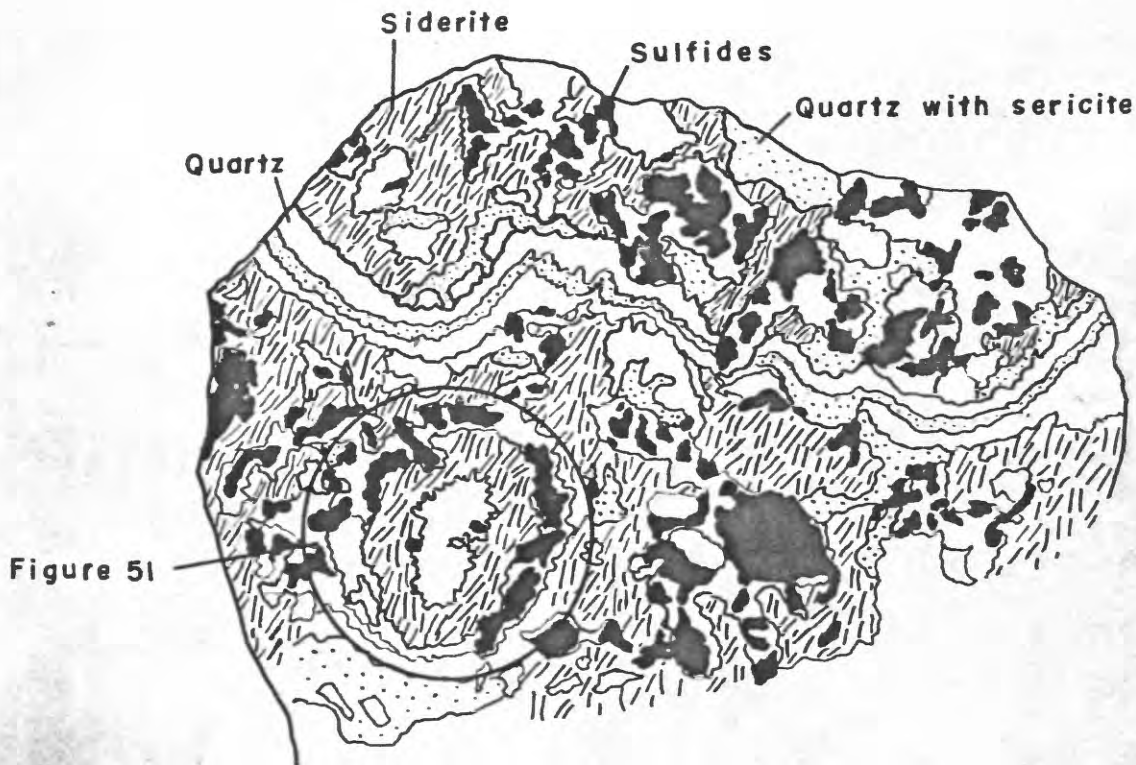
relations. They may replace galena and tetrahedrite and, in turn, may be coated with younger sphalerite, galena, and barite. Replacement by silver minerals is independent of fracturing, and boundary relations are intricate and irregular. Silver minerals are almost always deposited in order of increasing antimony content, viz. polybasite, miargyrite, and pyrargyrite. Well-developed crystals of these minerals were observed in many places, averaging 1 to 3 millimeters in diameter, and crystals of pyrargyrite 10 millimeters across were seen. The crystal form is not always constant, as both tabular and prismatic crystals of polybasite were seen, and simple prismatic and complex rhombohedral crystals of pyrargyrite observed.

The second type of silver mineralization in the intermediate zone is associated with layers rich in sericite and siderite in the colloform, banded quartz (see Figure 7). Pyrargyrite, miargyrite, and some polybasite are characteristically concentrated in the siderite-rich bands, and to a lesser extent in sericitic layers or quartzose bands. Silver minerals form anhedral grains replacing or closely associated with base-metal sulfides.

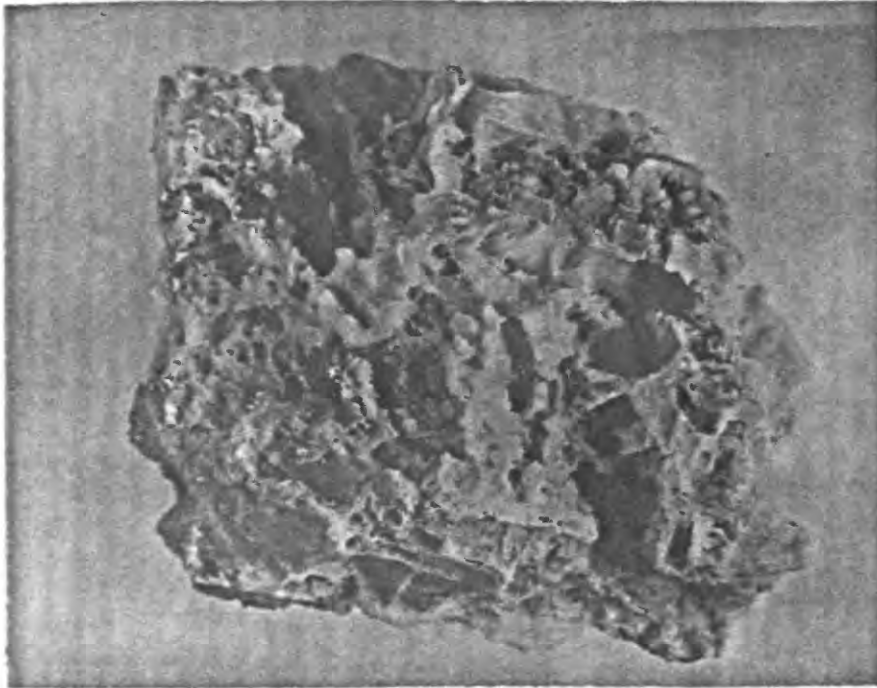
The silver sulfantimonides mentioned above are also found as isolated anhedral grains in massive vein quartz throughout the intermediate zone. Acanthite also is found throughout the intermediate zone in massive vein quartz associated with polybasite. Aramayotta occurs in massive vein quartz in the upper part of this zone, associated with pyrargyrite and miargyrite.

Open boxworks of quartz from which all barite and sulfides have been leached (see Figure 8) are commonly associated with the silver mineralization in this zone. The open spaces of these boxworks are,





**Figure 7 - Typical quartz-carbonate-silver antimonide ore from intermediate depth. Colloform quartz (white), sericite (stippled), and siderite (hatched) contain pyrrargyrite, wargyrite, and other sulfides (solid black) concentrated in the quartzose bands. The area covered by the photomicrograph in Figure 51 is marked. San Julián Sur vein, 70 level, San Genaro mine (x 6).**



**Figure 8.** Open boxwork of quartz resulting from hypogene leaching. The cavities are tabular and cubic, suggesting that barite and galena were the minerals removed. Late crystals of sericite, barite, quartz, sphalerite, and galena are commonly found on the sides of these cavities, indicating that leaching is hypogene. San Julián vein, above San Genaro level, San Genaro mine (X 1).

in places, partially filled with sericite and coated with a few tiny crystals of quartz, barite, sphalerite, and galena.

#### c. Protore zone

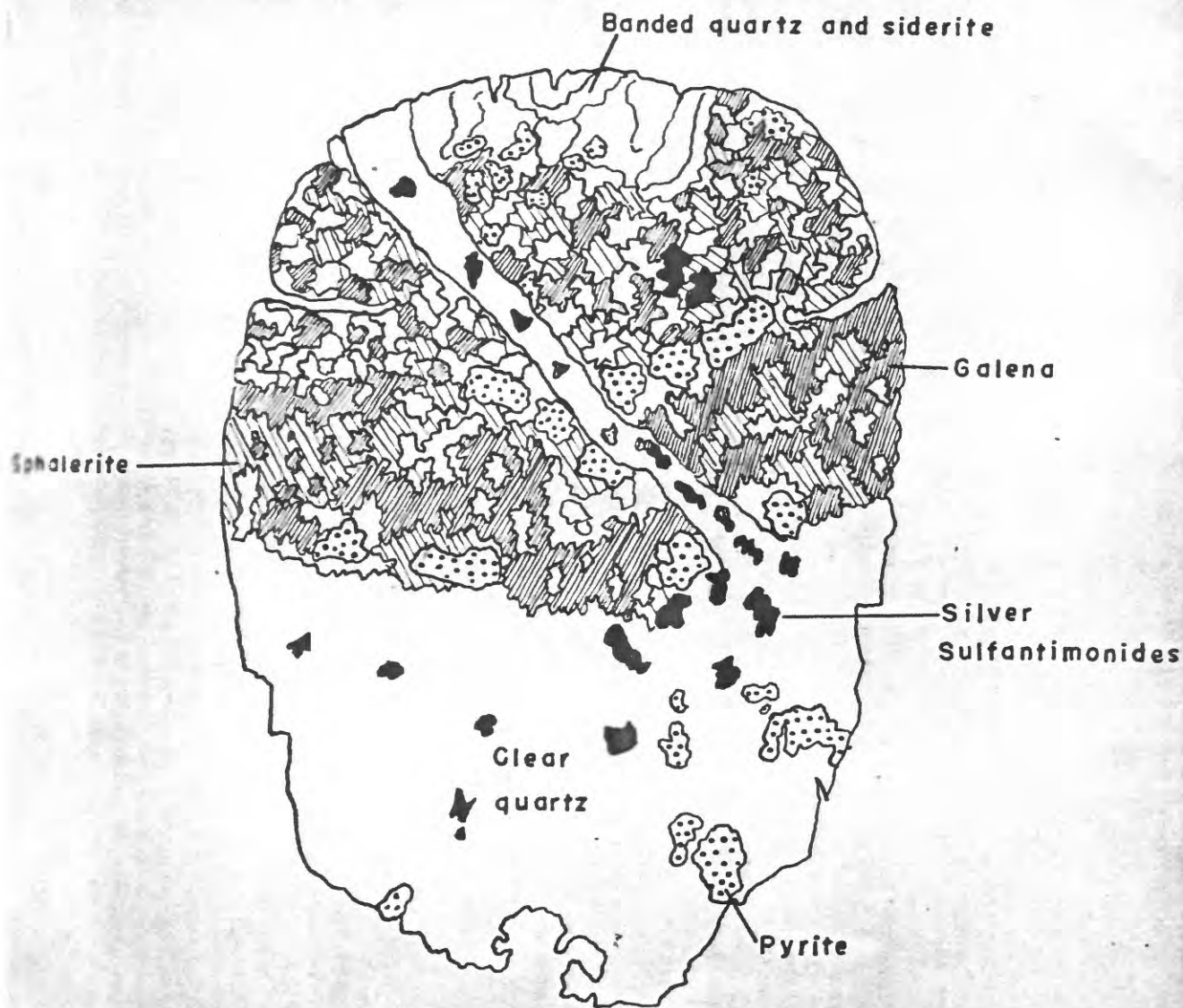
The protore zone lies below the intermediate zone, and extends from 100 or 150 meters below the outcrop to known depths of at least 200 meters. Silver values range from 50 to 350 grams per ton and average about 200 grams per ton. At least 20 to 30 percent of this silver is contained in tetrahedrite, which is associated with both base-metal and silver minerals. The silver minerals form in two distinct habits: 1) as grains in quartz veinlets, and 2) as aggregates filling small cracks. Both habits were observed in the overlying intermediate zone.

The veinlets, composed of clear quartz, cut the base-metal portions of the veins (see Figure 9) and contain anhedral grains of pyrrargyrite, miargyrite, polybasite, and acanthite, and small amounts of gold.

The silver minerals filling cracks are pyrrargyrite and miargyrite. They form massive or fine-grained aggregates coated with sericite and barite and are commonly intergrown with tetrahedrite, galena, and sphalerite. Silver minerals coat, without replacement, both sulfides and gangue minerals. Isolated crystals of the silver minerals are small, ranging in size from 0.2 to 1.0 millimeter. These fillings average 1.5 millimeters in width.

#### d. General considerations

The texture and mineral assemblage of the silver ores in the surficial zone are typical of supergene ores, and are interpreted as such.



**Figure 9 - Base-metal sulfides cut by quartz-silver antimonide veinlet. Granular mixture of galena (densely lined) and sphalerite (lightly lined) and pyrite (stippled) is replaced by veinlet of clear quartz (white) containing silver sulfantimonides (solid black). This is a typical habit of silver ore in the protore, and illustrates that silver antimonides were introduced after base-metal sulfides. San Julián Sur vein, 35 level, San Cenaro mine (X 4).**

In the intermediate zone, the interlocking textures of the massive silver minerals, their ordered deposition and tendency to form anhedral crystals, and their association with late sphalerite, galena, tetrahedrite, barite, and sericite strongly suggest hypogene deposition. The textures and mineral associations of the silver minerals in the colloform, banded quartz are also indicative of hypogene mineralization. The association with open quartz boxworks suggests that hypogene enrichment followed a period of hypogene leaching (see Lacy and Hosmer, 1956).

In the protore zone, silver mineralization in quartz veinlets is undoubtedly hypogene. The silver minerals filling cracks are interpreted as deposited by late hydrothermal solutions.



## 8. Nature of Veins

Most of the veins of the Castrovirreyana district formed by the replacement of triturated material filling faults or narrow breccia zones formed by shear. They grade from veins consisting completely of introduced material to those composed almost entirely of brecciated, altered wallrock cemented by minor amounts of introduced material. The process of vein formation apparently consisted of gradual digestion and mechanical removal of gouge and small fragments by rising mineralizing fluids. Fragments too large to be carried away were replaced after prolonged contact with mineralizing fluids or remained as inclusions in vein material. Vein-forming minerals precipitated from solution concomitantly with the removal of brecciated wallrock, and large gaping fissures seldom existed. Vein walls are commonly marked by thin seams of gouge, although in places the contact between the vein and wallrock is gradational and ill-defined.

In contrast, many veins at San Genaro and in the Astohuaraca and La Griega areas appear to have formed by deposition in fissures opened under tension. These veins are characterized by crustified banding, comb structures, numerous vugs, colloform-banded quartz, and cockade textures (see Figure 10). Most vein material formed in open fissures was deposited from solution; however, much of the quartz and some of the clay at San Genaro have habits suggesting deposition from colloidal suspension.

Many veins show indications of movement during mineral deposition. Shearing during mineralization is illustrated at Caudalosa by cementing of quartz or siliceous breccia by later minerals and by the formation of separate veins of late minerals, within or adjacent to the major



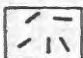



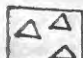



Figure 10. Colloform, banded ore showing a typical depositional sequence. The outer band of colloform quartz (cqz) is followed by a layer of brecciated base-metal sulfides (S), mostly sphalerite with minor amounts of galena, pyrite, and chalcopyrite, and cemented by quartz. The center of the vein is filled with crystalline quartz (qz). Along the inner and outer edges of the sulfide band are thin, alternating layers of quartz and quartz with hematite that give the ore its characteristic colloform, banded appearance. Silver minerals in this type of ore are restricted to the inner vuggy quartz band (qz). Milagro vein, Niño Jesús level, San Genaro mine (X 0.5).

veins (see Figure 11). In the La Virreyana area movements during mineralization are shown by the formation of "steel" galena with curved cleavage and fractured vein material covered by younger unfractured material (see Figure 12). Reopening of fissure veins by tension during mineralization is shown at San Genaro by the incorporation of brecciated vein material in the highly banded and crustified vein material, especially near flexures (see Figure 10).



# LEGEND

- 1  BASE-METAL SULFIDES
- 2  PYRITE
- 3  ENARGITE AND FAMATINITE
- 4  LEAD SULFANTIMONIDES
- 5  SILICIFIED WALLROCK
- 6  ARGILLIZED WALLROCK
- 7  BRECCIA
- 8  GOUGE

SCALE - 1:100  
0 1 2 3 4 meters

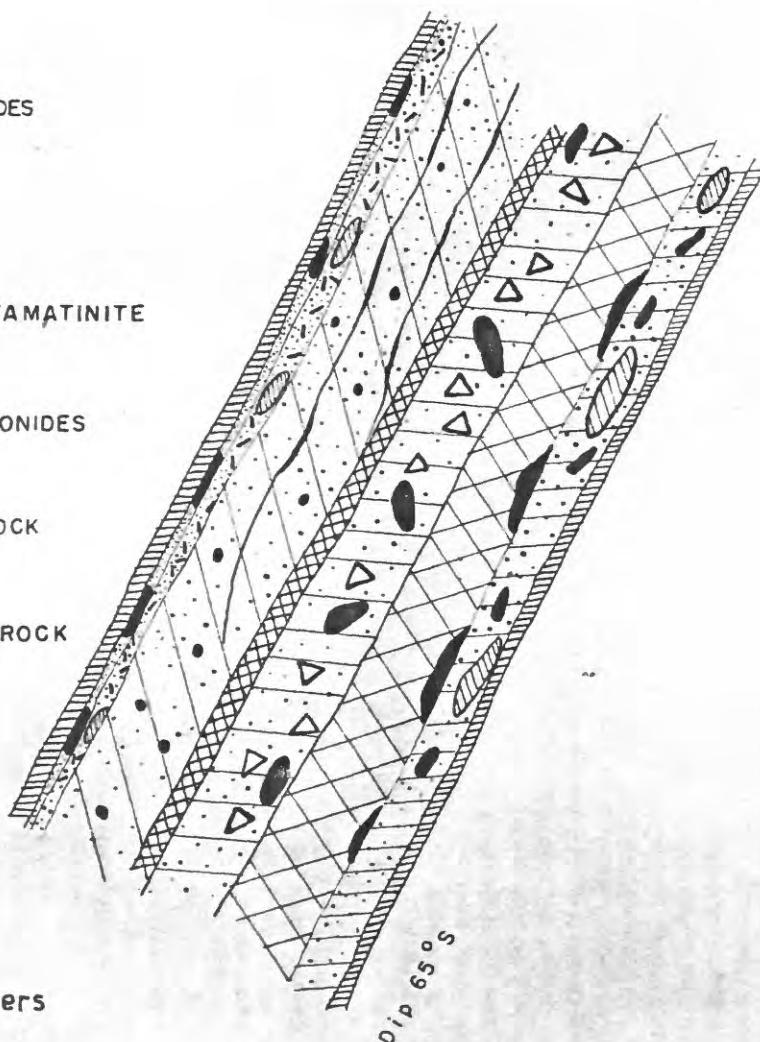
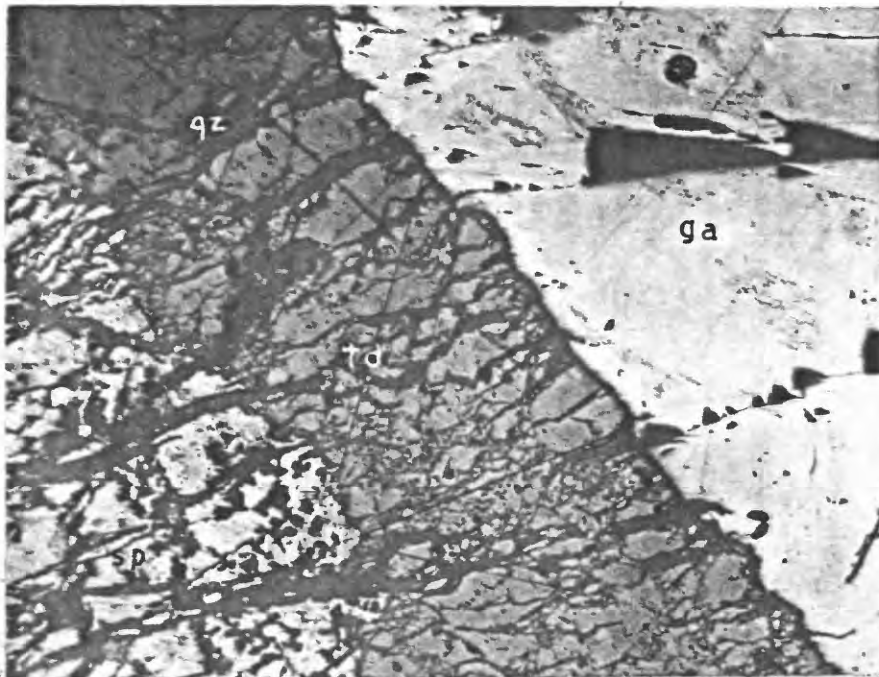


FIGURE II — SKETCH OF TYPICAL CROSS-SECTION  
OF THE CAUDALOSA VEIN, ABOVE 4610 METER LEVEL,  
CAUDALOSA MINE.



**Figure 12.** Sulfide depositional sequence showing bracciation between last two stages of deposition. Sphalerite (sp), with blebs of chalcopyrite is followed by tetrahedrite (td); and both are fractured and cut by quartz (qz). Subsequently galena (ga) was deposited on the tetrahedrite. Constante vein, above 35 level, Carmen mine (X 90).

## 1. Structural Features of the Ore Deposits

In the Castrovirreyra district only a few faults other than vein fissures were recognized. It was possible, however, to distinguish three periods of faulting: before, during, and after mineralization.

### 1. Pre-mineral faulting

Over ninety percent of the pre-mineral faults, or vein fissures, at Castrovirreyra have orientations between N. 60° E. and N. 50° W. (see Figure 13). The orientations of about 150 veins fall along a semi-arithmetic curve, with two principal peaks, at N. 75° E. and N. 80° W. On the other hand, inspection of the vein pattern (see Plate 3) and the frequency diagram of all vein orientations weighted for length of mineralization (see Figure 13, top diagram) shows three preferred orientations centered around N. 75° E., N. 80° W., and N. 35° W. Plotting vein orientations by type of mineralization (see Figure 13) shows base-metal mineralization concentrated approximately in the three orientations mentioned above, with a preferred weighted orientation of N. 50° W. Lead-antimony mineralization is preferably concentrated in veins trending N. 75° E. and N. 60° W. Most of the silver veins strike between N. 60° E. and N. 75° W., with maximum orientation frequencies at N. 80° W., N. 85° E., and N. 65° E.

The amount and direction of movement in the vein fissures prior to mineralization could not be determined with certainty. Horizontal and vertical displacements were probably only a few meters. The largest horizontal displacement was observed at the San Genaro mine in a quartz vein whose north side is displaced 34 meters to the west (left-lateral movement) by the northwestward-trending Aranzazu vein. Displacement of a bed of tuff at Caudalosa indicated reverse dip-slip

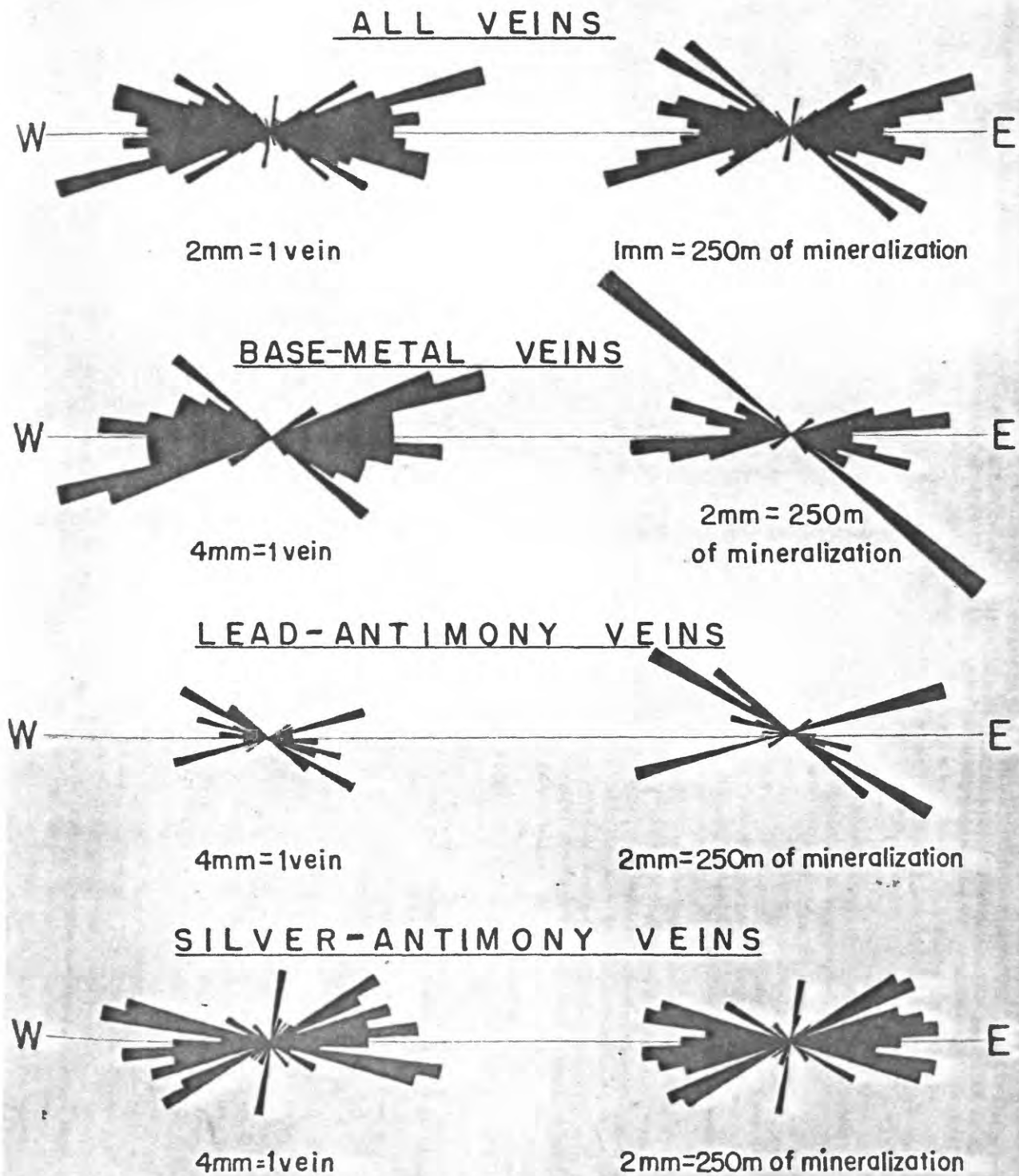


FIGURE 13-Vein orientation frequencies,  
Castrovirreyna Mining District, Peru

movement along the San Pedro vein, with a total apparent vertical displacement of 30 meters. Position of ore pockets and displacements of pyroclastic beds suggest left-lateral movements along the northwesterly group of veins, and right-lateral movements along the northeasterly veins.

## 2. Faulting contemporaneous with mineralization

Reopening of veins during mineralization under tension opened fissures with minimal displacement of vein walls and is best shown in the eastward-trending Trabajo vein, at San Genaro. Existing vein material was partially brecciated and recemented by subsequent mineralization (see Figure 10).

The formation of shear planes during mineralization is confined to veins trending northwesterly or northeasterly and is usually indicated by brecciation and seams of gouge. These shear planes are best shown in the veins at Caudalosa, where seams of gouge and breccia containing stibnite cut and parallel the veins. Judging from the size and direction of ore shoots, the amount of displacement was about 1 to 3 meters horizontally and 3 to 10 meters vertically.

The directions of movement during this period of faulting are not known, except at San Genaro where W. A. Lyons reported (personal communication, 1961) signs of nearly horizontal, left-lateral movement in slickensides in northwestward-trending veins.

## 3. Post-mineral faulting

Only a few post-mineral faults were observed in the district. They are steep, cut veins at high angles, and show left-lateral displacement of about 2 or 3 meters. Most of these faults strike N. 45°-30° E., but one strikes east and another N. 75° W.



#### 4. Origin of vein fracture system

The vein pattern in the district is most easily explained as the result of stresses equivalent to east-west compression. Such stresses would produce two sets of shears, making angles of less than 45 degrees with the axis of maximum compression, and one set of tension fractures parallel to the axis of maximum compression (McKinstry, 1955). The preferred orientations of veins at Castrovirreyna of N. 75° E. and N. 55° W. represent these conjugate shears, and the N. 80° W. veins the tension fractures. Initial movements along these shears, as indicated by early formed ore pockets, correspond to movements expected from east-west compression, left-lateral in the northwesterly set and right-lateral in the northeasterly set (see Figure 14).

Movements during mineralization were more complex. Distribution and orientation of ore pockets in northeasterly and northwesterly veins containing breccia and gouge seams are not consistent, and some displacements are contrary to those expected from the equivalent of east-west compression; to wit, right-lateral in the northwesterly veins and left-lateral in the northeasterly set (see Figure 14). This suggests that release of stress or east-west tension was followed by reverse compensatory displacements.

Post-mineral faulting is left-lateral and shows preferential orientations between N. 45°-60° E., indicating continued release of stress or tension with a slight shift clockwise.

As the major stresses involved in the Andean orogeny were east-west compressions (Oppenheim, 1948), it is logical to relate the structural formation of the Castrovirreyna veins directly to major Andean tectonics. Moreover, the types of movement shown by these

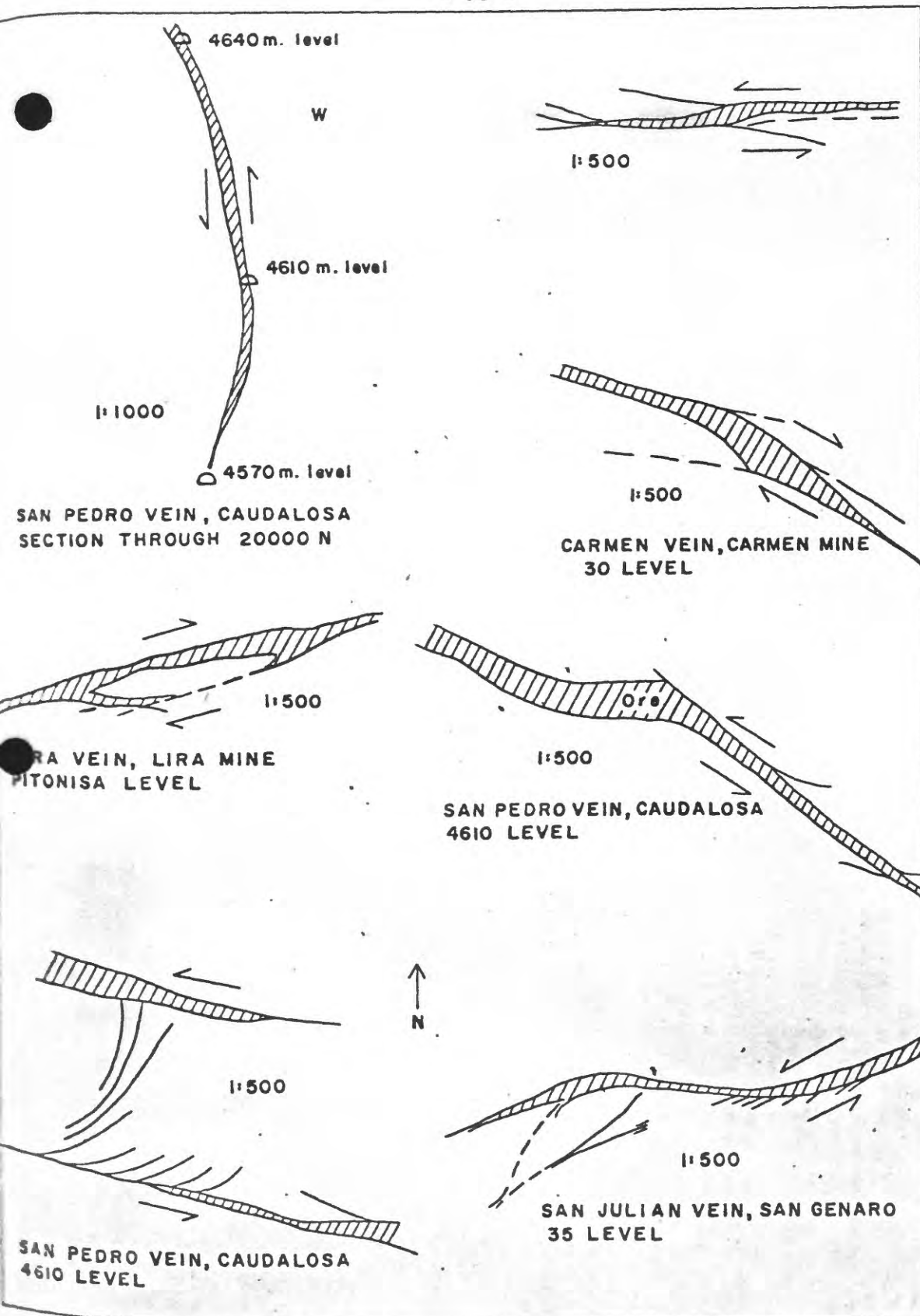


FIGURE 14 - SKETCHES OF TYPICAL ORE SHOOTS, SHOWING  
STRUCTURAL FEATURES CONTROLLING ORE DEPOSITION

veins, principally dip-slip and right- and left-lateral offsets in the same vein, are consistent with the types of movements that would result from block faulting in the Andes, through compression and relaxation of orogenic forces.



## J. Mineralization

### 1. Paragenesis

The mineralization history of the Castrovirreyña deposits is divided into three phases: 1) a preparatory phase, 2) a depositional phase, and 3) a reworking phase. These phases represent successive chemical stages, in time and space, of a single, extensive period of mineralization, and not distinct pulses of mineralization from different sources. These phases were not mutually exclusive nor wholly distinctive, but were overlapping and somewhat analogous, because each was the sum total of various types and intensities of similar and dissimilar chemical activities. Thus, although each phase is represented by characteristic mineral assemblages, many minerals are formed in more than one phase.

Conditions controlling precipitation or dissolution of the vein-forming minerals varied locally, so that a detailed paragenetic sequence applicable to a whole vein or group of veins and correlation of minerals formed along physicochemical gradients in space with those formed along similar gradients in time are conjectural. Thus, the following discussion gives only a general paragenetic sequence and avoids all overly specific correlative connotations, such as "pyrite I".

The first two phases were recognized in all the major veins of the district by characteristic mineral assemblages (see Table I and Plate 4). During the final phase, however, different mineral assemblages formed at different localities, correlation of which is admittedly tenuous.

a. Preparatory phase

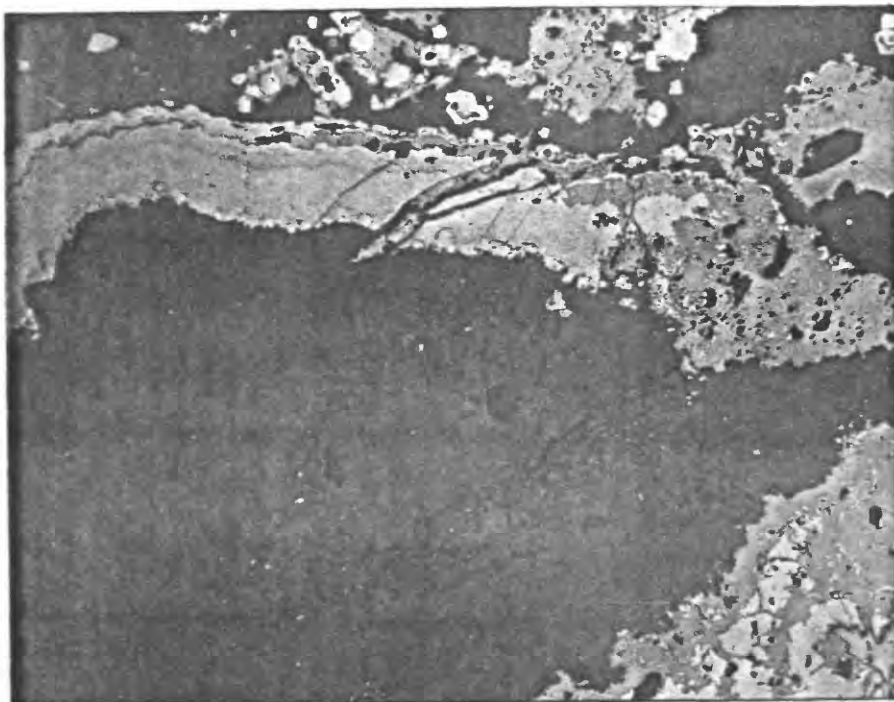
The preparatory phase of mineralization is characterized by ground preparation and conditioning of depositional environment. Prior to precipitation of ore minerals, the permeability along vein fissures was increased by removal of comminuted rock in the vein fractures, thereby facilitating circulation of mineralizing fluids; and by silicification of fracture walls, allowing the formation of porous, siliceous breccia upon continued movement of walls. The environment was conditioned chemically by raising the temperature, introducing silica, and altering the wallrock.

The only vein-forming minerals deposited during the preparatory phase were quartz and pyrite. The quartz at places shows colloform banding and is flecked with cloudy inclusions of clay and altered wallrock. Pyrite was deposited as small disseminated crystals or colloform bands suggestive of deposition from colloidal suspension (Lasky, 1930) (see Figure 15).

The presence of early quartz and pyrite, and siliceous breccia; the lateral termination of many veins as siliceous breccia; and the numerous small, sterile veins consisting only of quartz or silicified wallrock with disseminations of pyrite suggest that initial and farthest penetrating mineralizing fluids were aqueous solutions of silica, iron, and sulfur, and represent the original mineralizing fluids which had lost their metal content through discharge at points closer to the source of mineralization.

b. Depositional phase

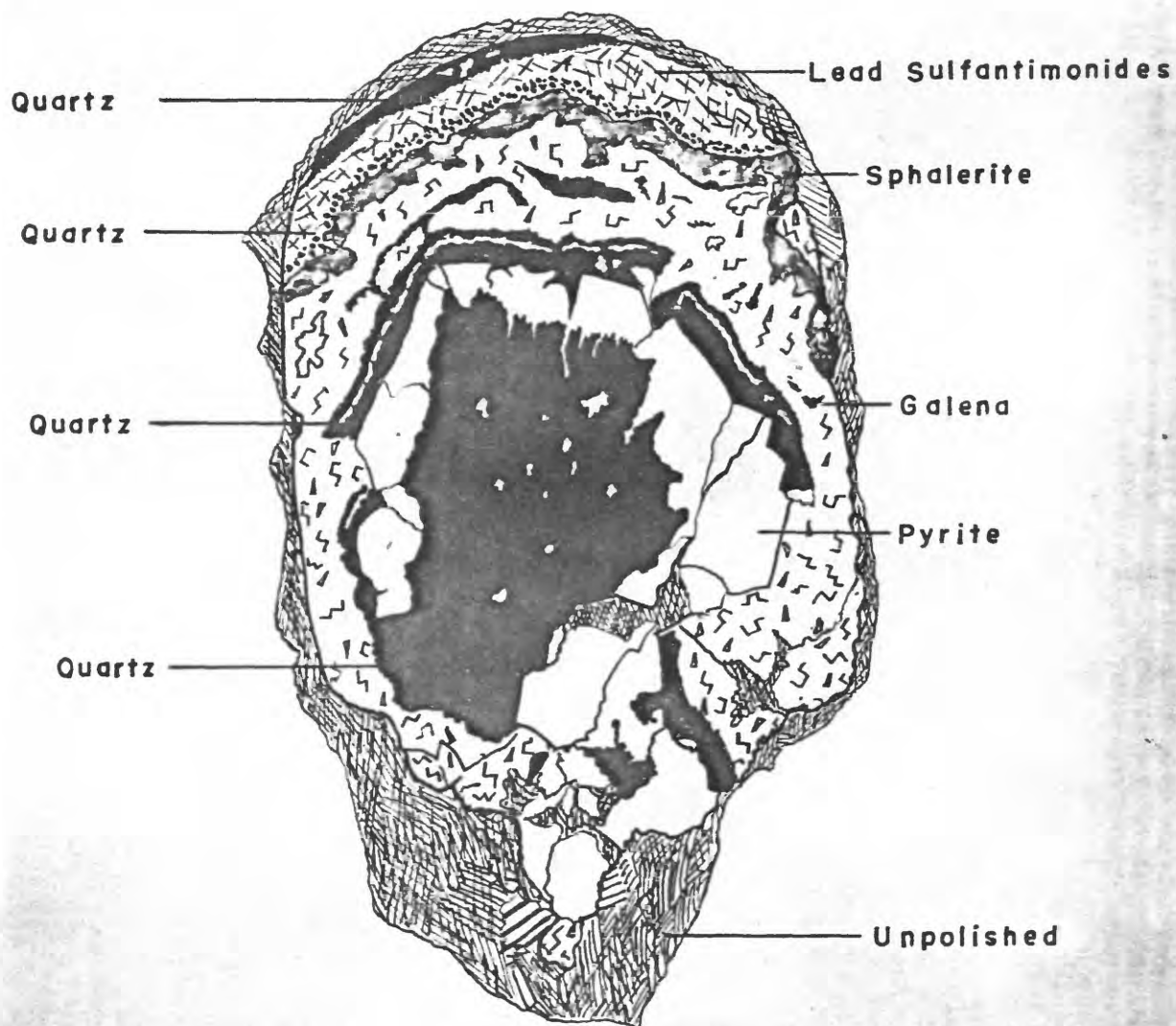
During the second phase of mineralization, the bulk of the vein and ore minerals was deposited and the maximum temperatures reached.



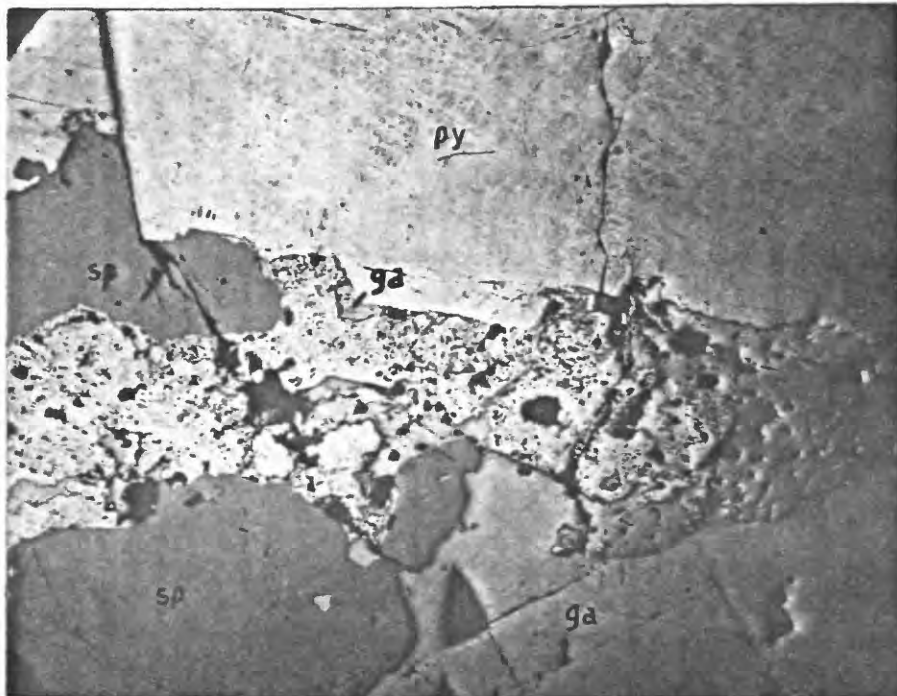
**Figure 15.** Colloform pyrite deposited around a silicified fragment of wallrock. Pyrite (white) is replaced by tetrahedrite (gray) along certain bands and is set in a matrix of quartz (black). San Pedro vein, Victoria Nueva level, Caudalosa mine (X 37).

Minerals characteristic of this phase are the simple sulfides of iron, lead, and zinc, and the complex sulfides of copper (see Plate 4). Textural relationships are complex and hard to interpret as temperatures and the effective concentrations of various elements rose to a maximum and then declined, creating two points in time (on either side of the maximum of temperature), at which the deposition of a particular mineral might be favored (see Plate 4). The general sequence of deposition is: pyrite, sphalerite, galena, chalcopyrite and tetrahedrite, enargite and famatinite, tetrahedrite and bournonite, galena, and finally sphalerite.

Quartz and pyrite were the first minerals deposited (see Figure 16), and continued to form throughout this phase as they replace, and, to a lesser extent, are replaced by most minerals (see Figures 17 to 21). It is difficult to estimate how much quartz and pyrite were deposited at any one time. Figure 17 shows two periods of pyrite deposition: an early stage of large subhedral to euhedral crystals and a later stage of spongy pyrite with base-metal sulfides. Some early crystals show growth rings due to subsequent deposition (see Figure 18). Figure 19 shows pyrite mixed with galena and sphalerite of different ages in a porous "ball." Figure 20 shows pyrite cut by stringers of base-metal sulfides and figures 16, 21, and 22 show quartz deposited during and after base-metal deposition. Euhedralism of quartz and pyrite is interpreted as chemical stability (see Figure 17) rather than an indication that they are younger than enclosing minerals. The general insolubility of quartz and pyrite suggest that they were transported as colloids rather than in solution. On the other hand, figure 15 shows that both quartz and pyrite were dissolved

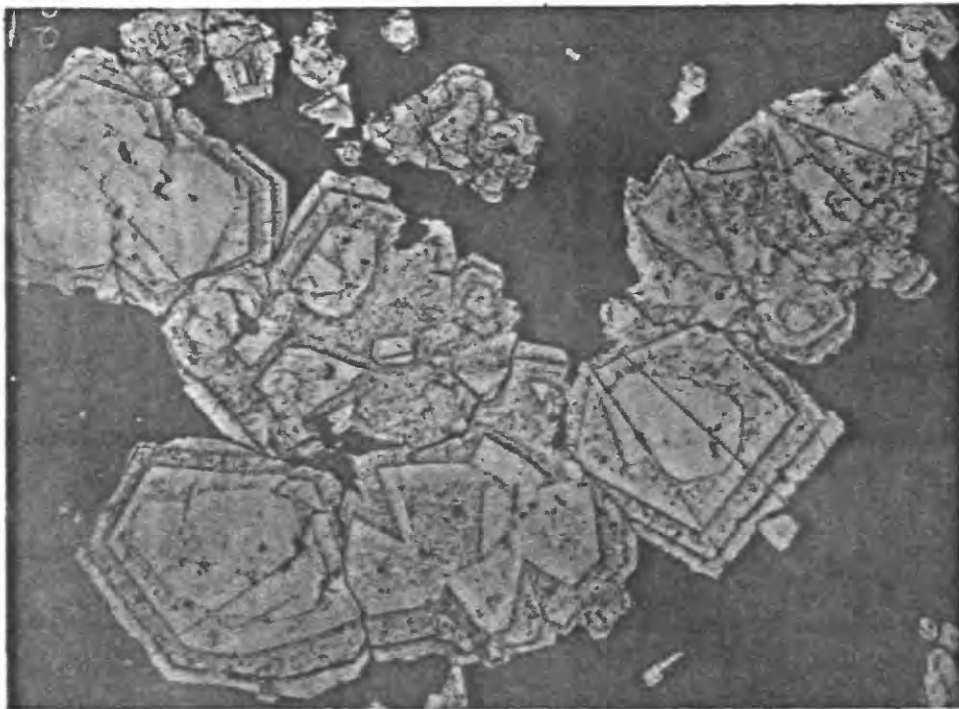


**Figure 16 - Polished cross-section of stalactitic knot of sulfides from vug, showing typical sequence of minerals deposited with declining temperatures. San Pedro vein, 4640 level, Caudalosa mine (X 2.5).**

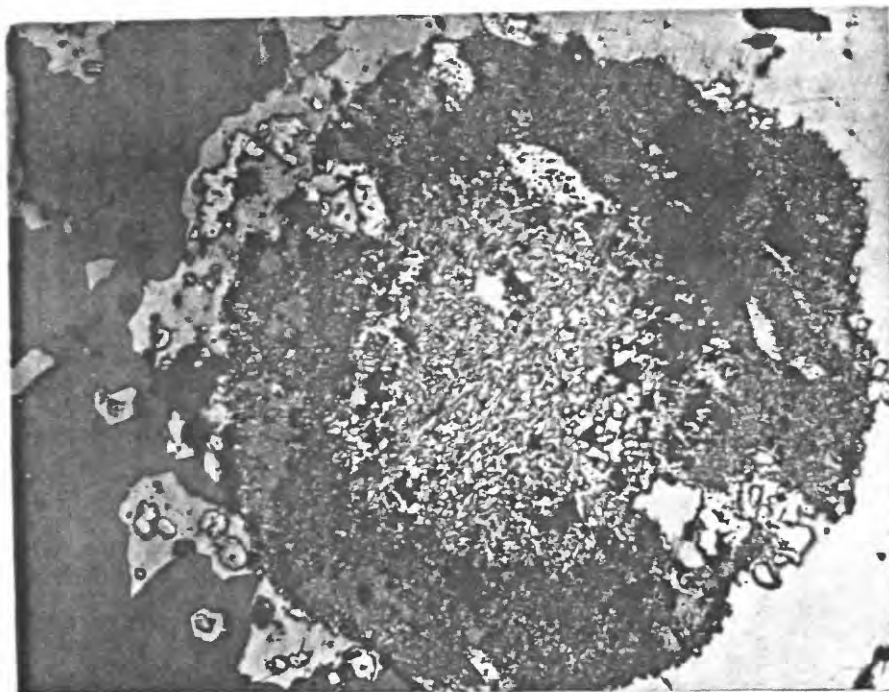


**Figure 17.** Two distinct periods of pyrite deposition. The euhedral grain of early pyrite (py) is partially replaced by sphalerite (sp), tetrahedrite (td), galena (ga), and late spongy pyrite (spy). This shows the relative resistance to corrosion of the large euhedral early pyrite crystals. San Pedro vein, 4640 level, Caudalosa mine (X 44).





**Figure 18.** Pyrite showing three well-marked growth rings, on a partially dissolved original grain. Note the rounded shape of the original grain and the "embayment" in the outermost ring. The texture is interpreted as representing fluctuating equilibrium and nonequilibrium between the grain and mineralizing fluids, causing deposition and dissolution. Matrix is quartz. Caudalosa vein, uppermost working, Caudalosa mine (X 70).



**Figure 19.** Porous "ball" of pyrite mixed with base-metal sulfides. The center is a pseudo-eutectic intergrowth of pyrite and galena (p-g) and is surrounded by sphalerite containing disseminations of pyrite (s-p). The ball is rimmed by galena (ga) and pyrite crystals (py). The ball was probably formed by successive flocculation of impure or mixed colloids. Quartz (qp). This shows the extensive time span of pyrite deposition. Caudalosa vein, Temerario level, Caudalosa mine (X 75).



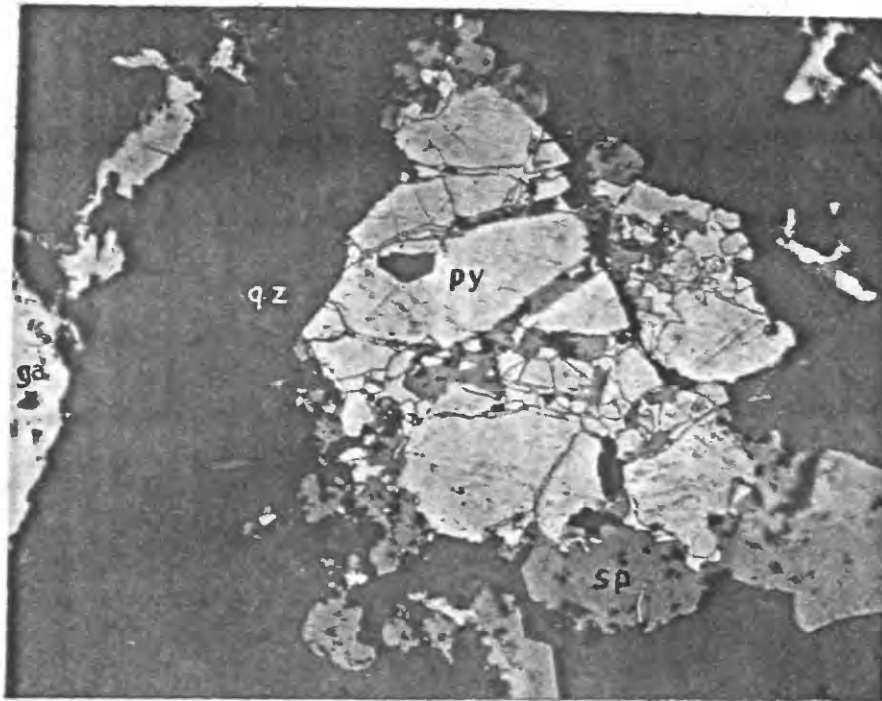
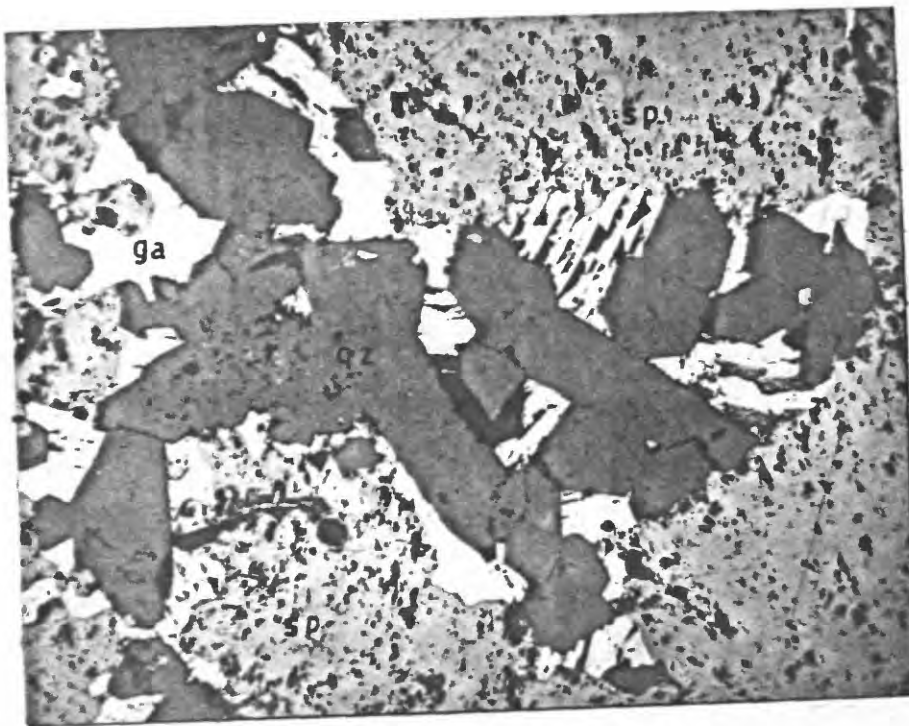


Figure 20. Typical age relations between early pyrite and base-metal sulfides. Pyrite (py) grain is fractured and partially replaced by galena (ga) and sphalerite (sp) containing chalcopyrite blebs. Quartz (qz). Milagro vein, Niño Jesús level, San Genaro mine (X 100).



**Figure 21.** Quartz deposited after galena and before sphalerite. Quartz (qz) replaces galena (ga) and both are replaced by sphalerite (sp) which preferentially attacks galena and barely corrodes the tips of quartz crystals. Contacto vein, Niño Jesús level, San Genaro mine (X 55).

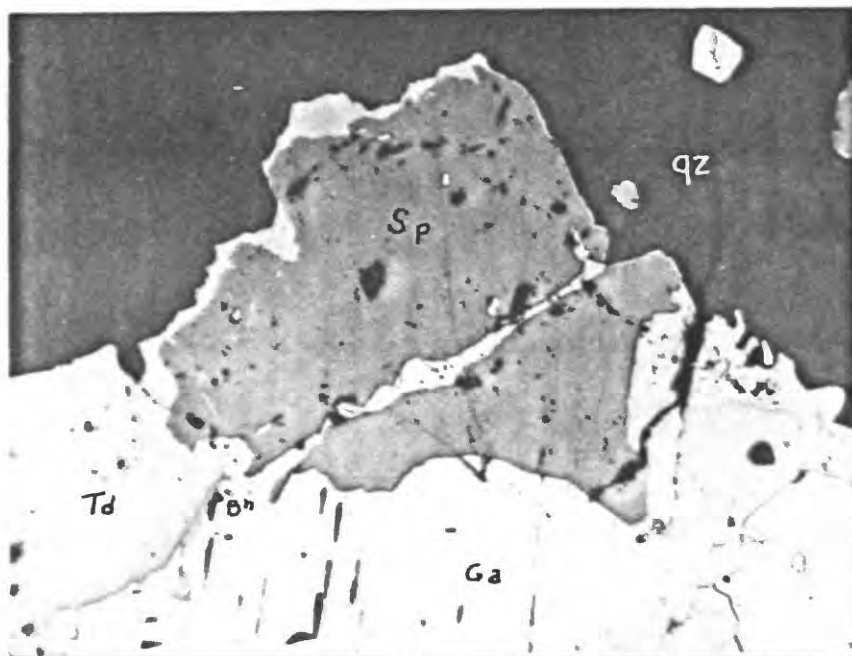
locally.

Sphalerite and galena were deposited in two main stages in this phase. Early sphalerite and galena follow pyrite, partially replacing it (see Figures 16 and 20), and precede chalcopyrite and tetrahedrite (see Figures 22 and 23) which generally replace them along thin veinlets (see Figure 24). Massive replacement of galena or sphalerite by tetrahedrite was also observed, favoring crystallographic directions (see Figure 25). Late sphalerite and galena follow late tetrahedrite (see Figure 26) with some replacement. The older galena and sphalerite, in contrast to the younger, are coarser grained. Furthermore, the older sphalerite contains blebs of chalcopyrite, and more iron, is darker colored, and is associated with wurtzite.

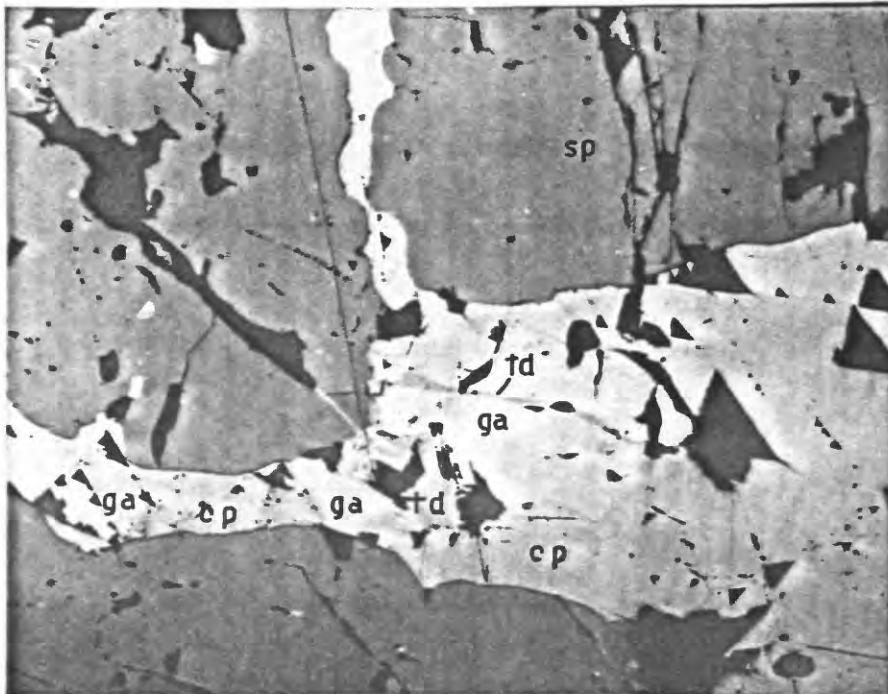
The textural relations between galena and sphalerite are commonly ambiguous (see Figure 27) or uninterpretable (see Figure 28), and mutual boundaries are not diagnostic. Some sphalerite shows obvious evidence of replacement by galena (see Figures 23 and 29). Most of the interpretable textures, however, indicate that sphalerite followed galena with appreciable replacement (see Figures 16, 30, and 31).

The close association of galena and sphalerite, their non-diagnostic borders and their dual age relationship imply that they are stable under practically the same conditions, and frequently formed contemporaneously. This contemporaneity is well shown by the pseudoeutectic, arborescent texture of a galena-sphalerite-quartz assemblage from San Genaro (see Figure 32).

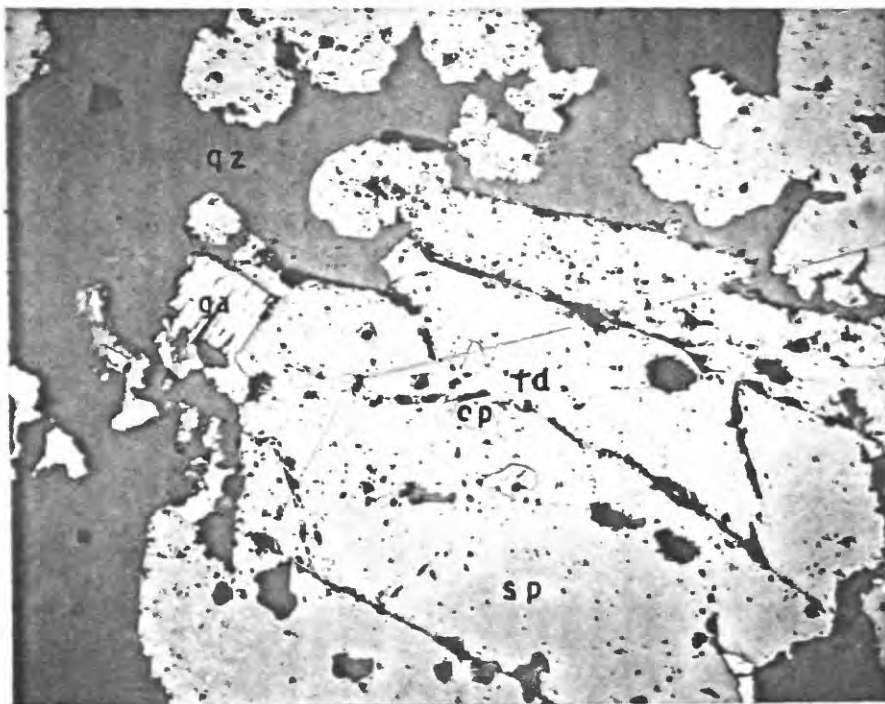
The relations of wurtzite from the Caudalosa vein to other sulfides are not clear but it appears to be contemporaneous with bournonite and younger than early sphalerite.



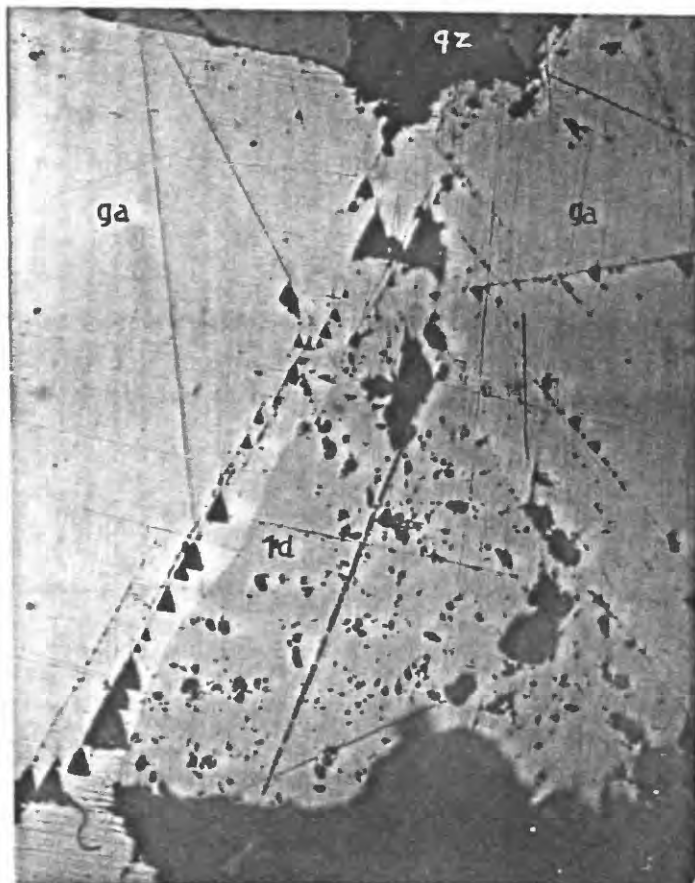
**Figure 22.** Early base-metal sulfides replaced by early sulfantimonides. Galena (ga), sphalerite (sp), and pyrite (py) are replaced by tetrahedrite (td) and bournonite (bn). Bournonite is contemporaneous with tetrahedrite and probably formed by a reaction of copper-antimony solutions with galena. Quartz (qz). San Pedro vein, 4640 level, Caudalosa mine (X 82).



**Figure 23.** Typical depositional sequence during rising temperatures. Sphalerite (sp) replaced by chalcopyrite (cp) and galena (ga), all of which is replaced by tetrahedrite (td). Shows typical depositional sequence and habits formed with ascending temperatures, Matilde vein, main level, Matilde mine (X 200).



**Figure 24.** Typical base-metal sequence deposited during rising temperature. Early sphalerite (sp), with large blebs of chalcopyrite (cp) is slightly replaced by galena (ga). A veinlet of tetrahedrite (td) cuts all of these. Quartz (qz), preferentially replaces tetrahedrite and galena, and to a lesser extent sphalerite. Milagro vein, Niño Jesús level, San Genaro mine (X 55).



**Figure 25.** Typical galena-tetrahedrite relations. Galena (ga) replaced by tetrahedrite (td) along crystallographic directions. Note similarity in shape of tetrahedrite to cleavage pits in galena. Sphalerite (sp) and quartz (qz). San Pedro vein, Intermedio level, Caudalosa mine (X 125).



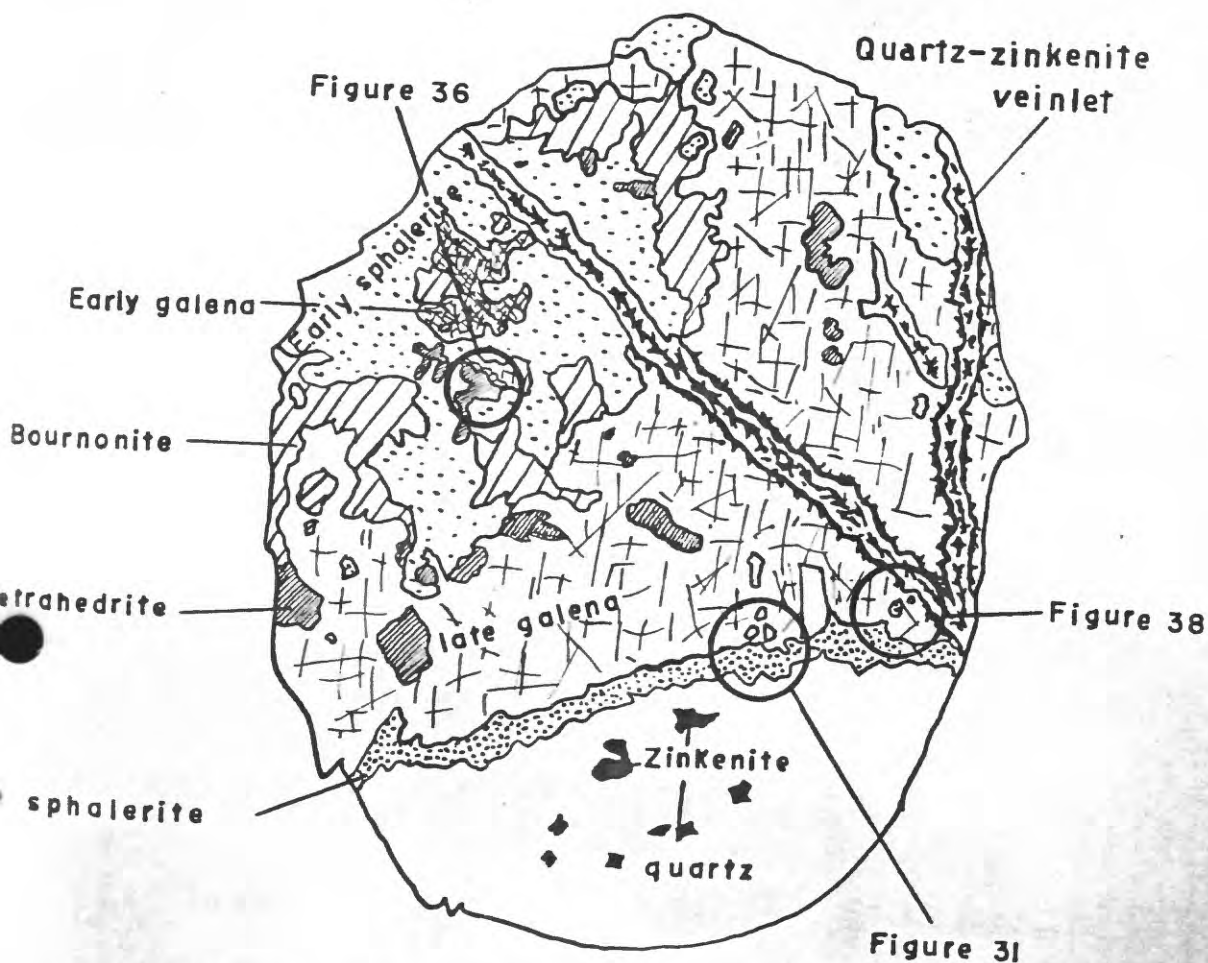
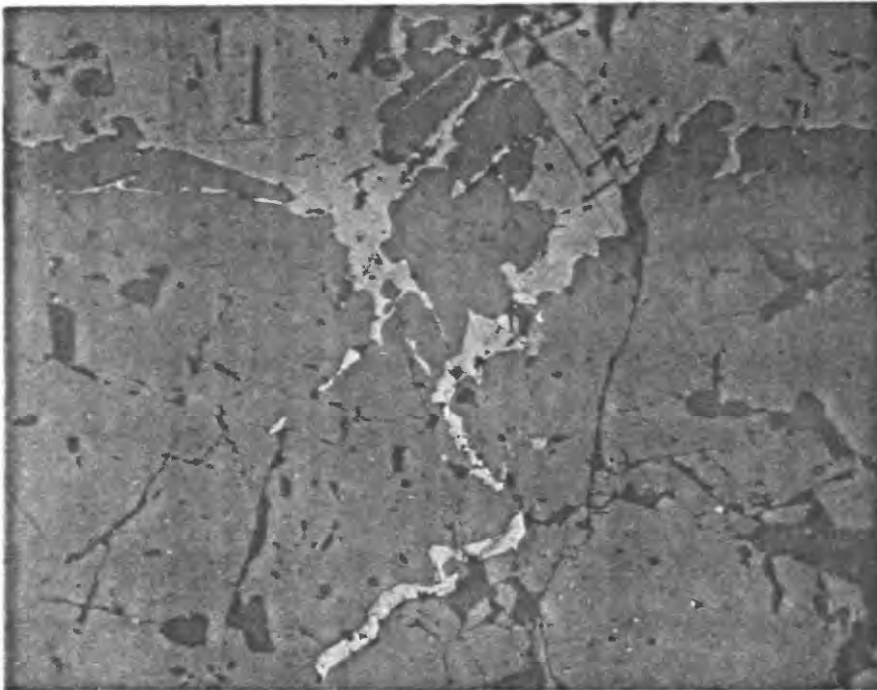
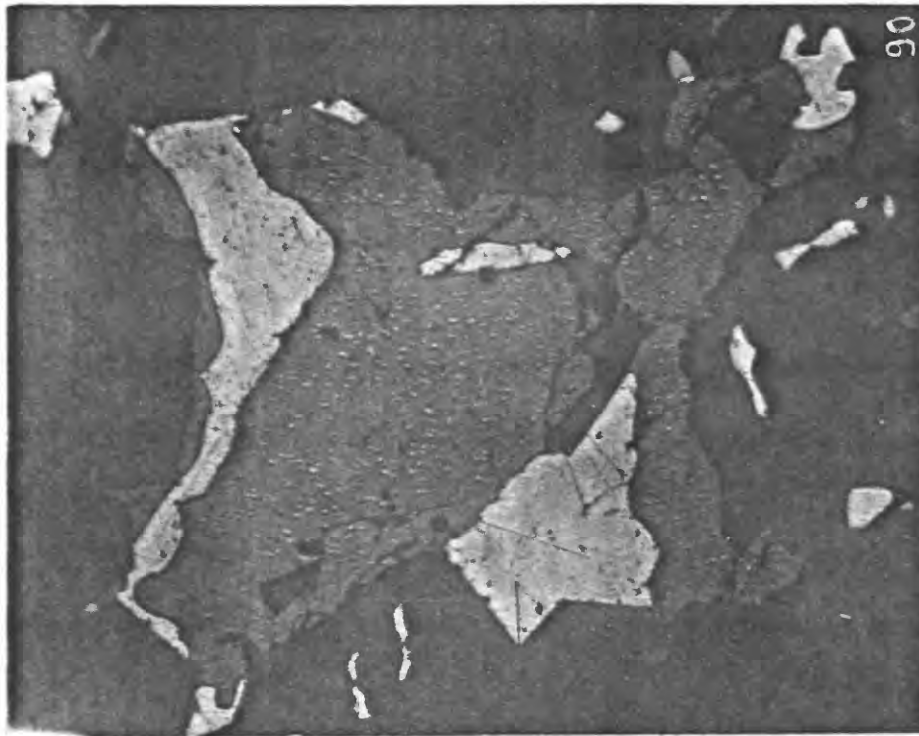


Figure 26 - Sketch of typical base-metal ore showing paragenetic relations during the depositional and reworking phases. Early galena surrounded and possibly replaced by sphalerite, which in turn is partially replaced by tetrahedrite. A second generation of galena formed around this, reacting with tetrahedrite to form bournonite. A thin seam of late sphalerite coats and slightly replaces the late galena. Veinlets of quartz with disseminated sinkenite cut all minerals. Where galena is cut by these veinlets it is altered to lead sulfantimonides (solid black). This sketch shows the two stages of galena and sphalerite, the formation of bournonite from tetrahedrite, and sulfantimonide mineralization. Areas covered by photomicrographs are marked. Caudalosa vein, San Félix level, Caudalosa mine (X 10).





**Figure 27.** Ambiguous relationships between sphalerite (gray) and galena (white). Cusping is well developed into both minerals. The seam of galena in the lower center can be interpreted as a cross-cutting veinlet or a remnant of extensive replacement. Likewise, the thin stringers of galena may be penetrations of galena along crystallographic planes in sphalerite or remnants of extensive replacement of galena along crystallographic directions. Matilde vein, main level, Matilde mine (X 75).



**Figure 28.** Indefinite relationship between sphalerite and galena. Both sphalerite (gray) and galena (white) are replaced by quartz (black). Sphalerite contains exsolution blebs of chalcopyrite. Texture is typical of early formed base-metal ores. San Antonio vein, Pique level, Lira mine (X 60).

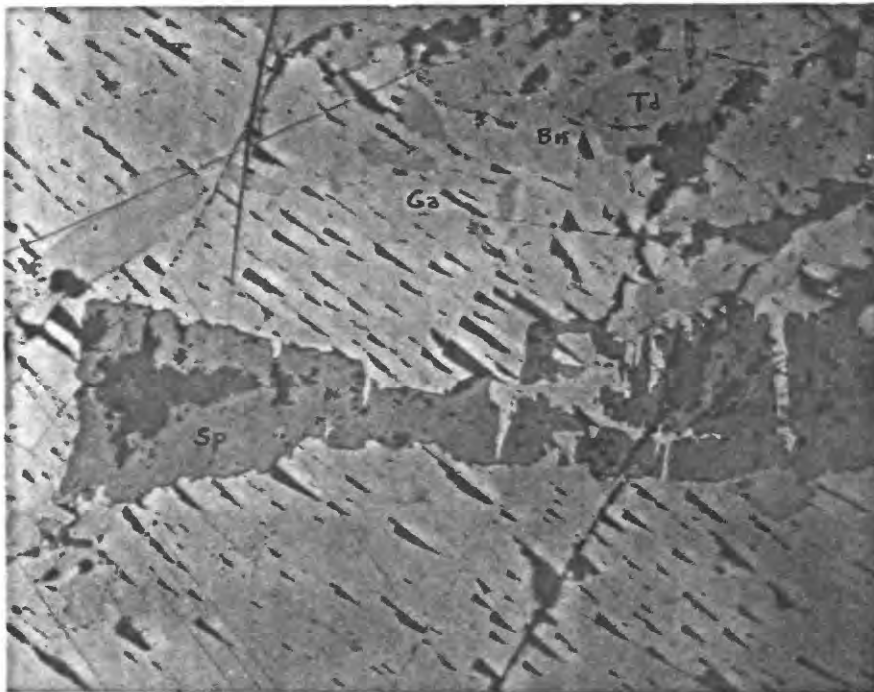


Figure 29. Late galena replacing sphalerite and tetrahedrite. Galena (ga) replaces early sphalerite (sp) along crystallographic directions. Galena also replaces tetrahedrite (td) forming bournonite (bn) at the expense of tetrahedrite. San Pedro vein, Intermedio level, Caudalosa mine (X 100).

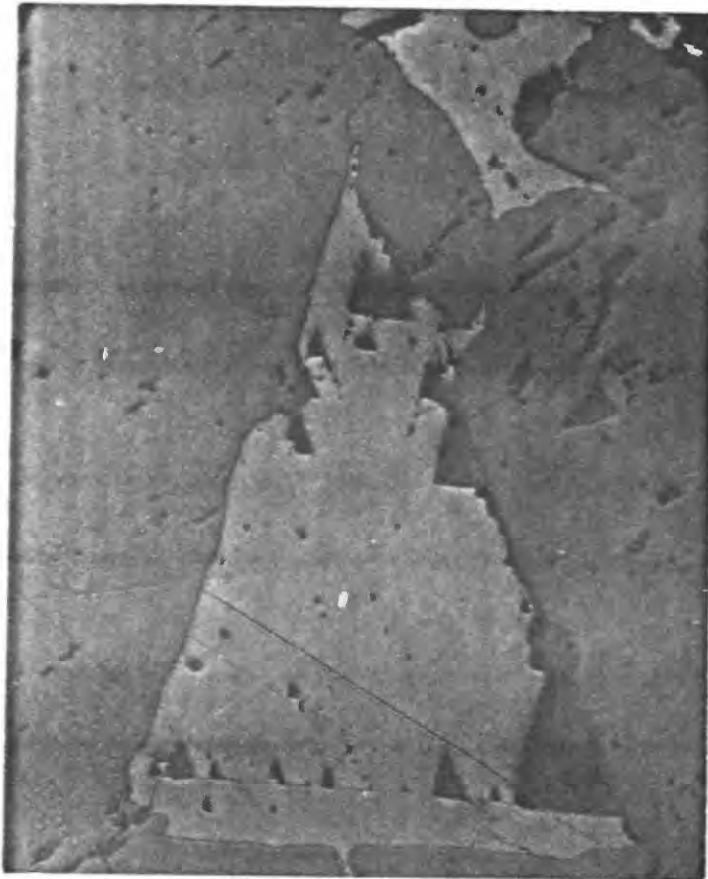
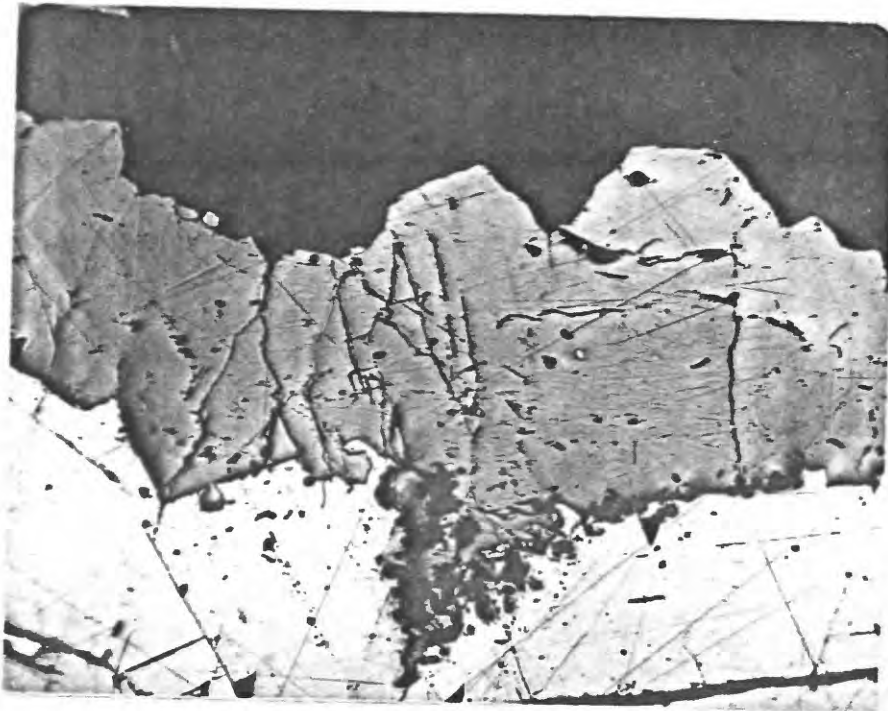


Figure 30. Galena replaced by late sphalerite containing chalcopyrite blebs. Note that the outline of the galena (white) remnant corresponds with the cleavage pits. Compare with Figure 25. Grau vein, Niño Jesús level, San Genaro mine (X 150).



**Figure 31.** Layered texture typical of base-metal deposition with declining temperatures. Sphalerite (gray) and quartz (black) are deposited on and partially replace galena (white). Massive quartz slightly corrodes the sphalerite. See Figure 26 for overall relations. Caudalosa vein, San Félix level, Caudalosa mine (X 30).

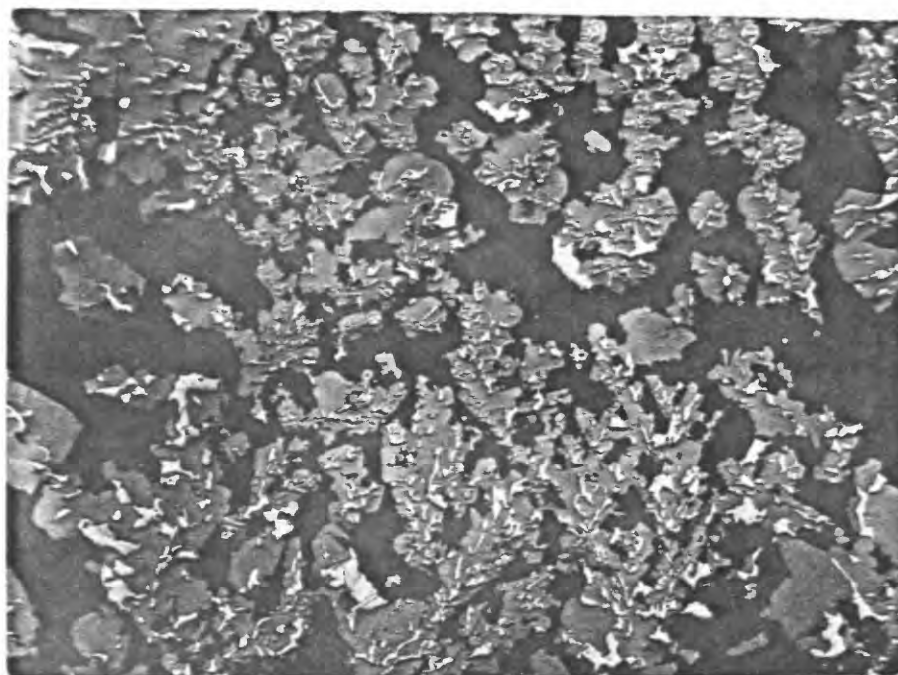
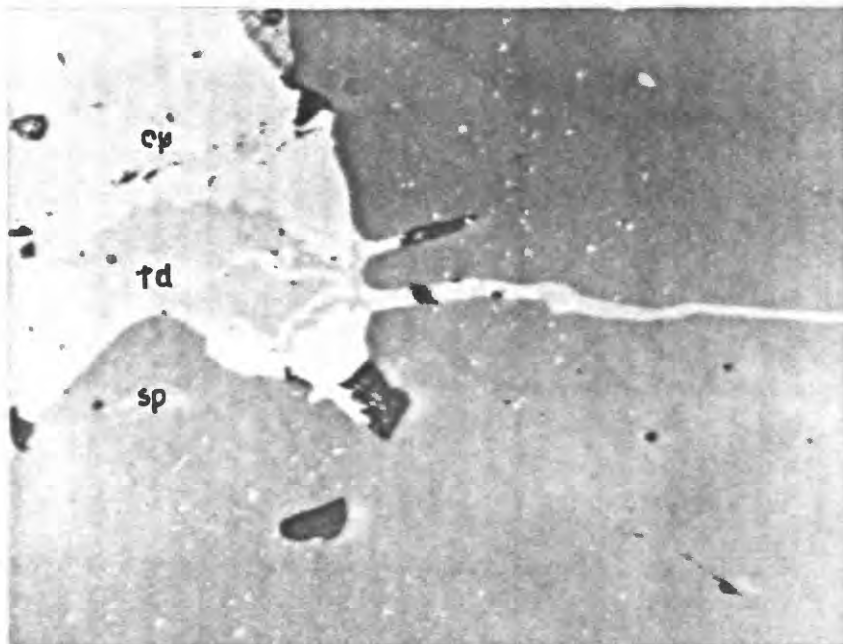


Figure 32. Pseudotectic, arborescent intergrowth of base-metal minerals. Galena (white), sphalerite (gray) with blebs of chalcopyrite, and quartz (black), have been deposited simultaneously. Milagro vein, 35 level, San Genaro mine (X 30).

Chalcopyrite is contemporaneous and slightly younger than early sphalerite. Initially chalcopyrite formed exsolution blabs in sphalerite (see Figures 28 and 32) and later, formed cross-cutting veinlets (see Figure 33) and isolated masses along the periphery of early sphalerite grains. Chalcopyrite is contemporaneous with early tetrahedrite (see Figure 33), but is not commonly associated with minerals deposited after maximum temperatures were attained (see Plate 4) and where it is, chalcopyrite is always replaced by them (see Figure 34).

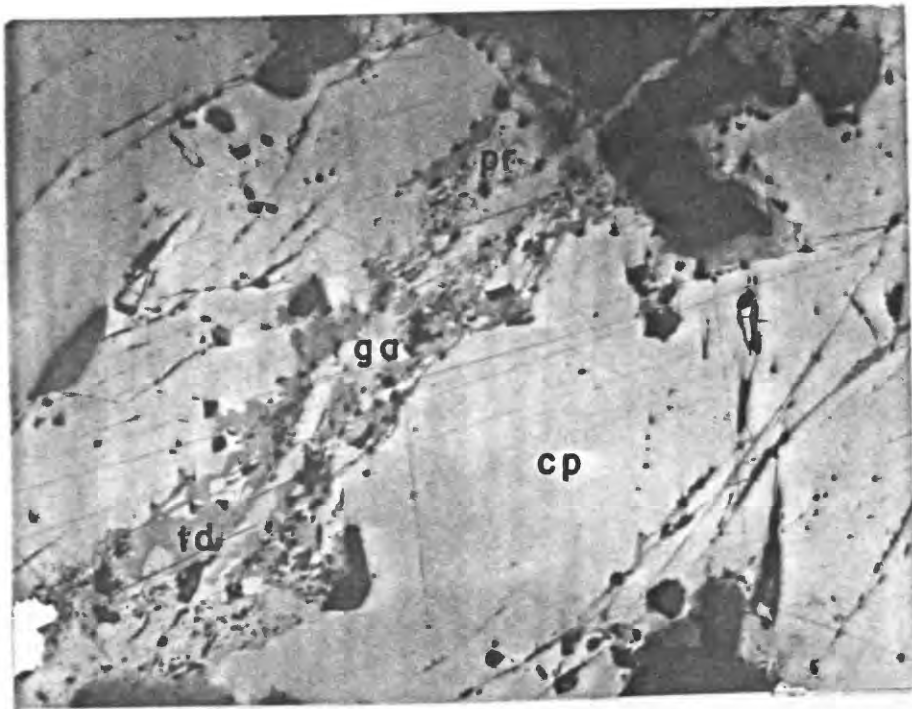
Famatinite and enargite occur only in the Caudalosa vein, associated with massive banded pyrite. They are intergrown and were deposited simultaneously. They are younger than quartz and banded pyrite, and are replaced by tetrahedrite (see Figure 35), chalcostibite, and tetrahedrite-bournonite-pyrite assemblage. Famatinite and enargite formed early in the mineralization history and are the only minerals found that are diagnostic of mesothermal deposits (Lindgren, 1933). They are vestiges of the highest temperatures developed in these deposits, i.e., 300°-350°C.

Tetrahedrite was the principal copper mineral precipitated during this phase and was deposited in two distinct periods (see Plate 4). Early tetrahedrite formed contemporaneously with chalcopyrite (see Figures 24 and 33), preferentially replacing early galena (see Figures 24 and 25) and sparingly replacing early sphalerite (see Figure 33) and pyrite (see Figures 15, 17, 19 and 22). Late tetrahedrite preferentially replaces galena, forming bournonite (see Figure 22) as well as chalcopyrite, famatinite, and enargite (see Figures 34 and 35). Late tetrahedrite is replaced by late galena, forming bournonite (see Figures 26 and 36).

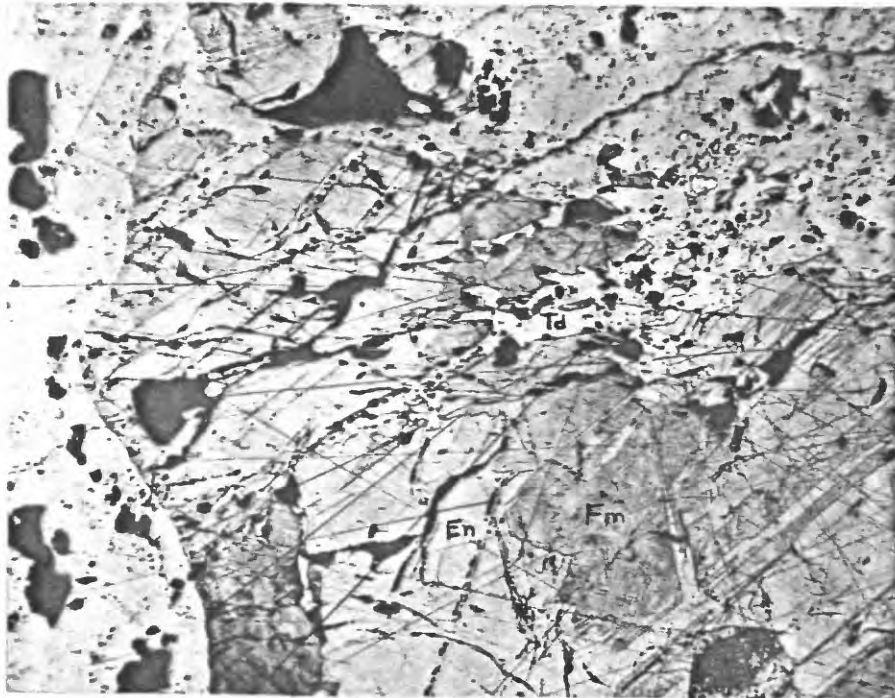


**Figure 33.** Typical association of chalcopyrite with tetrahedrite and sphalerite. Veinlet of tetrahedrite (td) and chalcopyrite (cp) cutting sphalerite (sp) which contains blebs of chalcopyrite. Oscillatory banding of tetrahedrite and chalcopyrite probably denotes equilibrium and contemporaneity. Matilde vein, main level, Matilde mine (X 550).

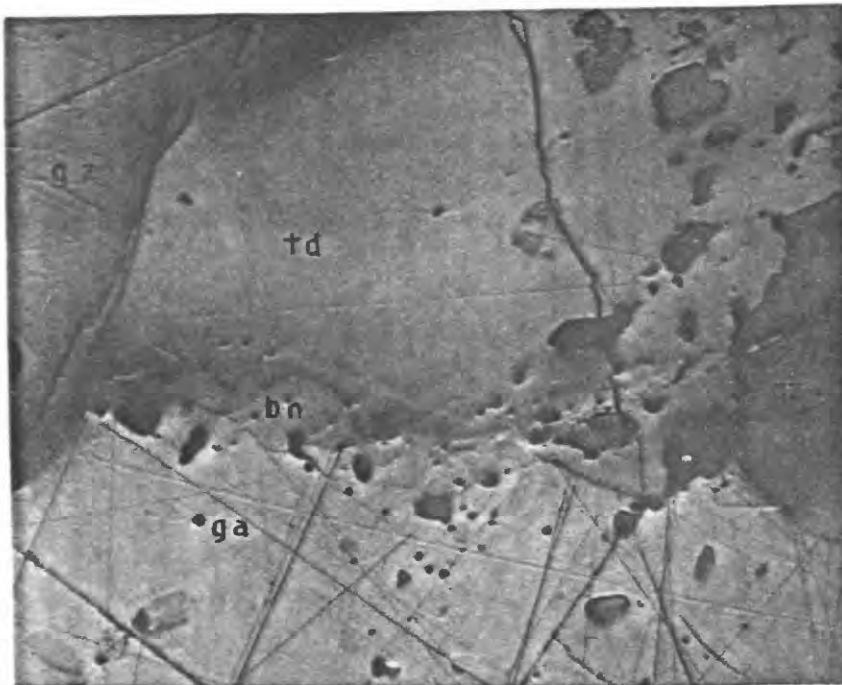




**Figure 34.** Chalcopyrite replaced by sulfides deposited in the reworking stage. Chalcopyrite (cp) rimmed and veined tetrahedrite (td). The largest veinlets of tetrahedrite contain pyrargyrite (pr) and a center of galena (ga). This shows the instability of chalcopyrite in late mineralizing solutions. San Julián Sur vein, 70 level, San Genaro mine (X 50).



**Figure 35.** Assemblage of medium-temperature copper sulfosalts. An exsolution intergrowth of enargite (en) and famatinite (fm) is partially replaced by late tetrahedrite. This assemblage probably represents the maximum temperatures developed in the district. Section stained with KCN. Caudalosa vein, 4610 level, Caudalosa mine (X 70).



**Figure 36.** Typical reaction interface between galena and tetrahedrite. Bournonite (bn) formed on tetrahedrite (td) by reaction with the solutions depositing the late galena (ga). The small blebs of bournonite in galena formed contemporaneously with galena from copper and antimony derived from the dissolving tetrahedrite. Shows an antimonial reaction typical of the lead-antimony veins of the district. See Figure 26 for overall relations. Quarts (qa). Caudalosa vein, San Félix level, Caudalosa mine (X 60).

Bournonite forms irregular stringers, patches and blebs in tetrahedrite and galena (see Figure 22) or thin bands separating galena and tetrahedrite (see Figure 36) that were formed by reaction between tetrahedrite and the mineralizing fluids depositing galena, or vice versa. The patches of bournonite in tetrahedrite or galena probably formed contemporaneously with the enclosing mineral from excess lead or copper in the mineralizing solutions. Varied textural relations of bournonite and its common absence in the tetrahedrite-galena assemblage (see Figure 24) preclude the formation of bournonite as an intermediate solid phase between galena and tetrahedrite (Ross, 1956).

c. Reworking phase

The third phase of mineralization followed movements that reopened the principal veins at San Genaro and Caudalosa which had become so clogged with vein-forming minerals that circulation of mineralizing fluids had probably all but ceased. The fresh mineralizing solutions had lower temperatures and higher effective concentrations of silica, antimony, silver, and bismuth than those of the preceding phase. New minerals were deposited and pre-existing minerals were partially replaced, redistributed, and altered along the reopened channels.

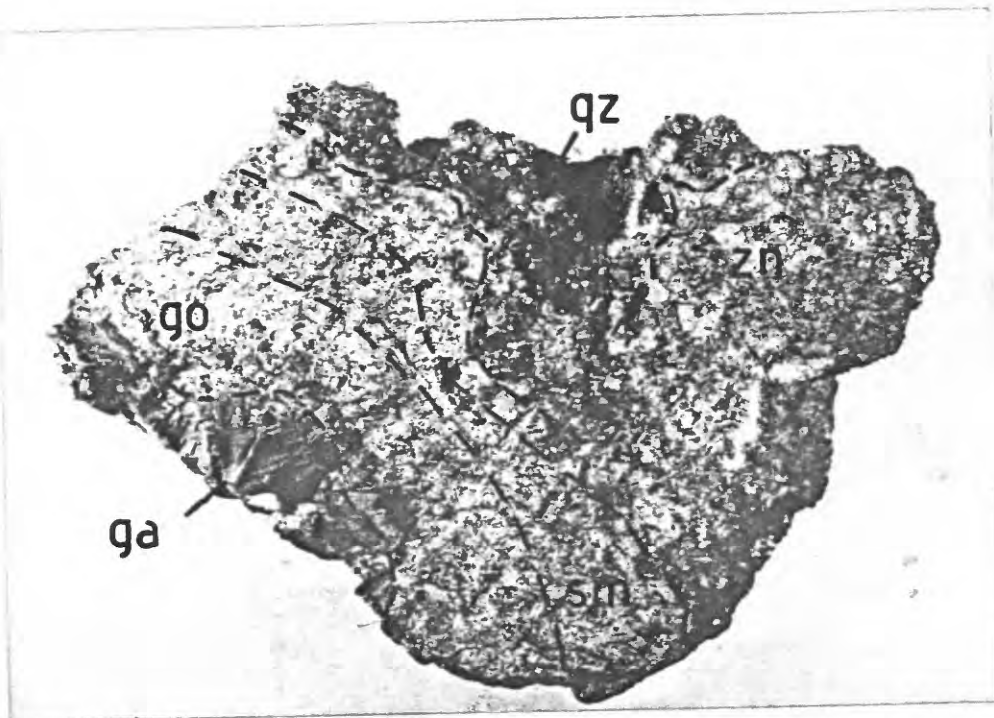
Minerals characteristic of and restricted to the third phase are the lead antimonides, geocronite, seneseyite, and zinkenite; the silver sulfosalts: pyrargyrite, pearceite, polybasite, miargyrite; the silver-bismuth sulfide: aramayoite; the simple sulfides: acanthite, stibnite, realgar, and orpiment; and the gangue minerals: barite, rhodochrosite, siderite, allophane, halloysite, and hematite. In addition galena, sphalerite, tetrahedrite, bournonite, sericite, and quartz, which are recognized in previous phases, were also deposited.

The events in the reworking phase have the following sequence in both the lead-antimony and the silver-antimony veins: 1) reopening of veins and the introduction of antimonian and argentian solutions, forming sulfantimonides of lead and copper at Caudalosa and of silver at San Genaro at the expense of existing sulfides; 2) direct precipitation of sulfantimonides, quartz, pyrite, sphalerite, stibnite, siderite, rhodochrosite, barite, hematite, realgar, and orpiment; 3) slight hydrothermal leaching of barite and galena; 4) redistribution of silver minerals towards the surface (hypogene enrichment); and 5) deposition of minor amounts of galena, sphalerite, tetrahedrite, pyrite, barite, hematite, and gypsum in cracks and voids.

#### (1.) Lead-antimony veins

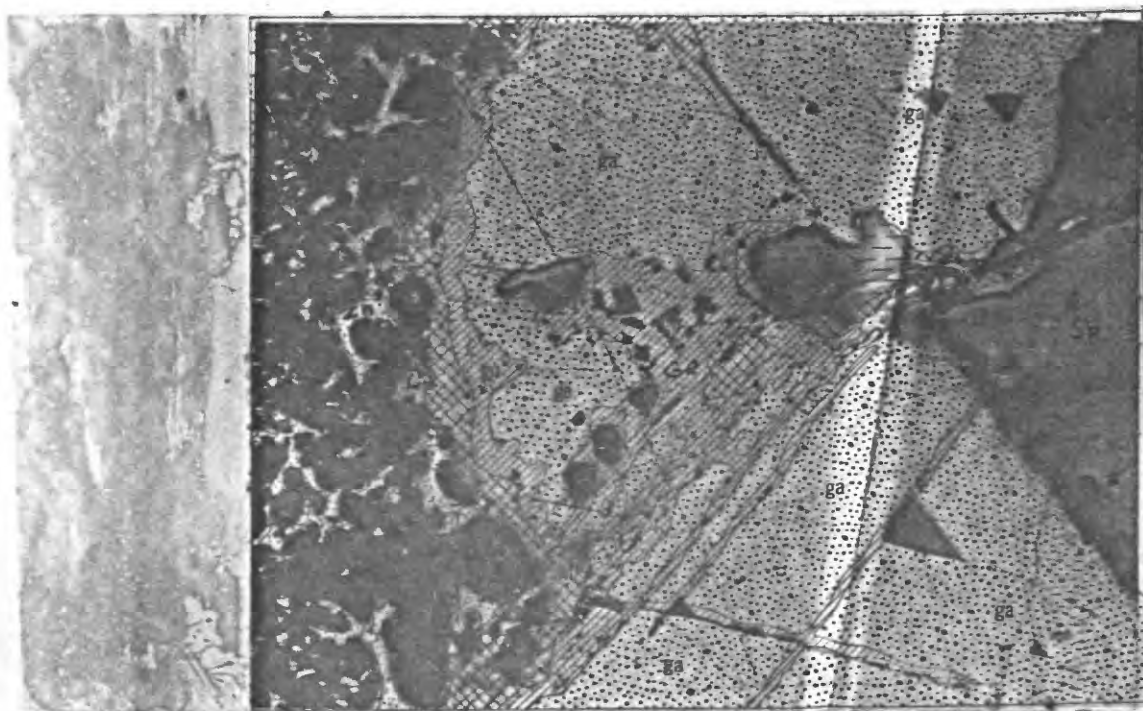
During the reworking phase the deposition of lead sulfantimonides is confined to a belt in the central part of the district, extending from the Madona mine northwestward to the Caudalosa, Candelaria, and Bonanza mines (see Plate 2). The lead sulfantimonides are bournonite, geocronite, semseyite, and zinkenite. With the exception of bournonite, these lead sulfantimonides are commonly found in zones around galena grains (see Figures 37 and 38). The least antimonian, geocronite  $[\text{Pb}_{27}(\text{Sb},\text{As})_{12}\text{S}_{45}]$ , is the only one in direct contact with galena (see Figure 39). The most antimonian, zinkenite  $(\text{Pb}_6\text{Sb}_{14}\text{S}_7)$ , is found only in contact with stibnite and semseyite. Semseyite  $(\text{Pb}_9\text{Sb}_8\text{S}_{21})$  is found in contact with both geocronite and zinkenite but not with galena or stibnite (see Figure 39).

These mineralogical associations suggest the alteration of galena by antimonian mineralizing fluids, forming first geocronite, then the subsequent partial alteration of geocronite to semseyite, and finally

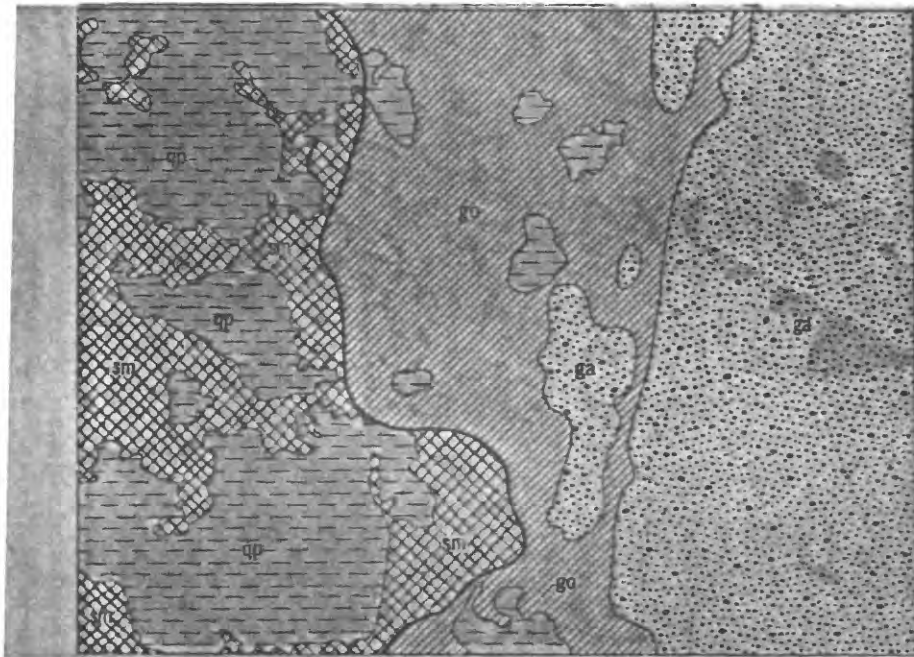


**Figure 37.** Typical specimen of lead sulfantimonide ore. Galena (ga) is surrounded by consecutive bands of lead sulfantimonides, which are, in order of increasing antimony, geocronite (go), semseyite (sm) and zinkenite (zn). Zinkenite is mixed with quartz crystals (qz). Caudalosa vein, 4570 level, Caudalosa mine (X 1).





**Figure 38.** Galena altered to lead sulfantimonides. The lead sulfantimonides are zonally arranged around galena (ga) in order of increasing antimony content, geocronite (go), semseyite (sm), and sinkenite (zn) which is mixed with quartz (qp). At right, galena is coated with younger sphalerite (sp). Typical example of local zoning caused by localized equilibrium. For overall relations see Figure 26. Caudalosa vein, San Félix level, Caudalosa mine (X 30).



**Figure 39.** Detail of replacement of galena by lead sulfantimonides. Geocronite (go) rims galena (ga) and replaces it along crystallographic directions, and in turn is rimmed with semseyite (sm) and quartz (qp). Note that semseyite is not in direct contact with galena. Caudalosa vein, San Félix level, Caudalosa mine (X 200).



the partial alteration of semseyite to zinkenite. Lead taken into solution by this process, recombined with antimony and precipitated, first as geocronite where lead concentration was very high, next as semseyite, and then as zinkenite (see Figure 40), indicating a supply of lead diminishing with time. Finally, when no more lead was available, stibnite was deposited.

Alteration of copper minerals at Caudalosa during this phase is manifested by rare occurrences of chalcostibite coating and partially replacing famatinite and enargite. Tetrahedrite was not deposited nor attacked during the early stages of the reworking phase of mineralization in the lead sulfantimonides veins, and any copper in solution early in this phase was precipitated as bournonite, which was later replaced by other lead sulfantimonides (see Figure 41).

Existing sphalerite was partially replaced by the sulfantimonides, particularly geocronite, especially near galena (see Figures 41 and 42). Towards the end of the period of maximum deposition of sulfantimonides, however, sphalerite was deposited in equilibrium with zinkenite and quartz (see Figure 43), and later was slightly corroded during quartz deposition (see Figure 44).

Throughout the entire period of sulfantimonide deposition, quartz and to a lesser extent pyrite, were deposited in small amounts (see Figures 38 and 42). Major deposition took place during and after the formation of zinkenite (see Figures 40 and 44).

Following the deposition of the bulk of lead antimonides, small amounts of fibrous semseyite, zinkenite, and small crystals of realgar, orpiment, micaceous hematite, and barite precipitated in existing voids. Subsequently, stibnite, rhodochrosite, and quartz formed in late cross-

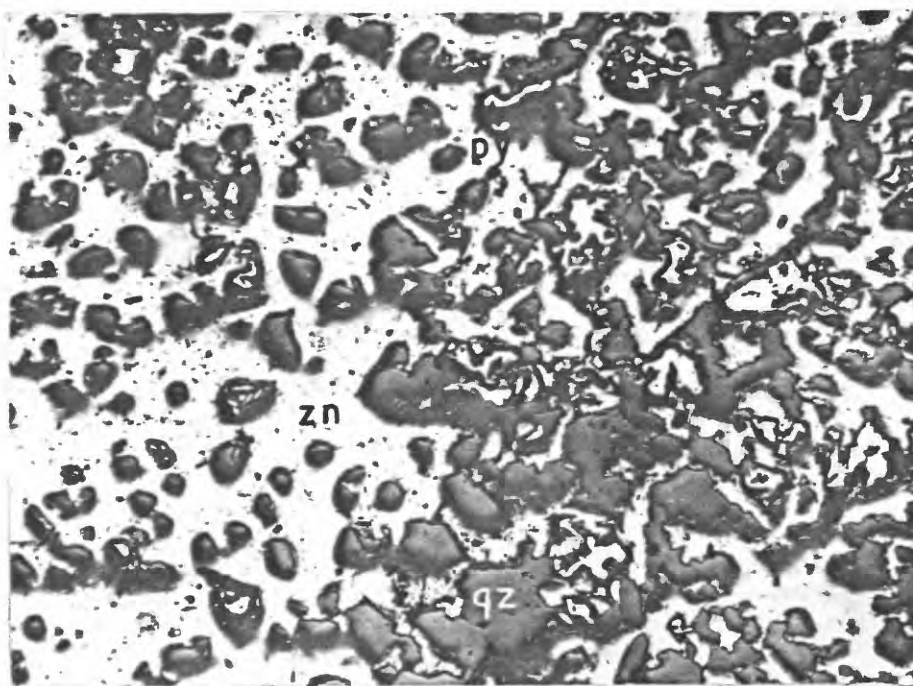
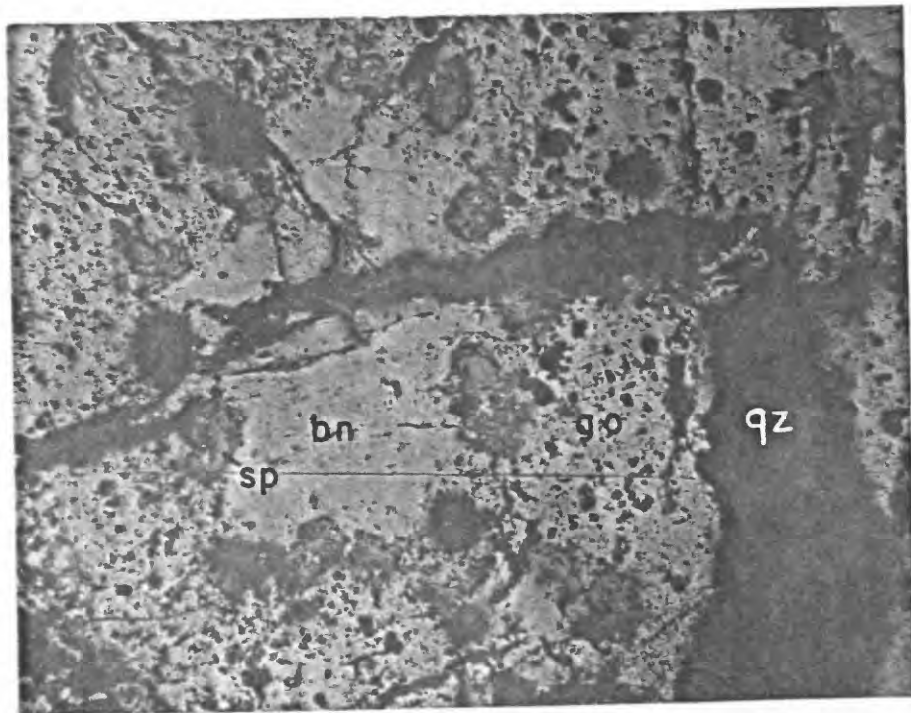
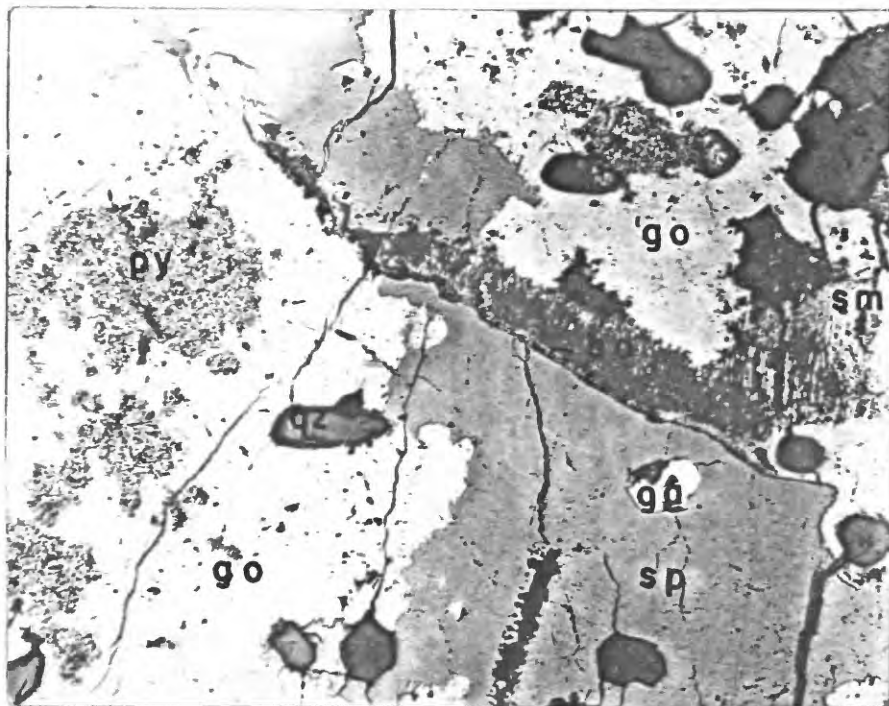


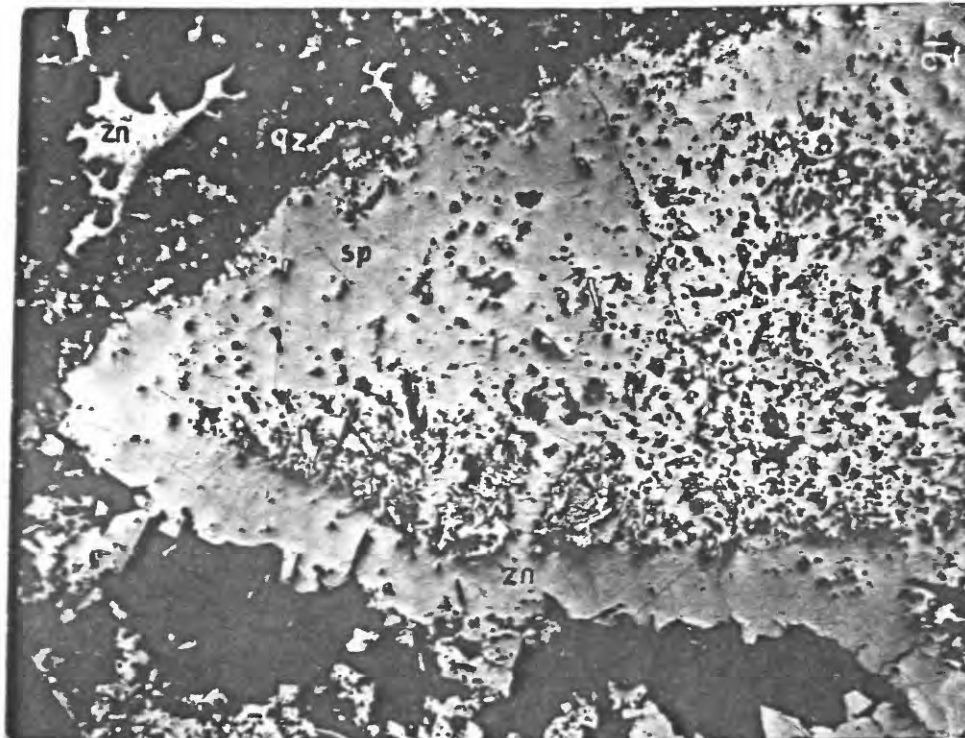
Figure 40. An equilibrium assemblage of zinkenite, quartz, and pyrite. An intergrowth of zinkenite (zn), quartz (qz), and pyrite (py), from veinlet of lead sulfantimonides, shows contemporaneous deposition of these three minerals. Caudalosa vein, Pompeyo level, Caudalosa mine (X 100).



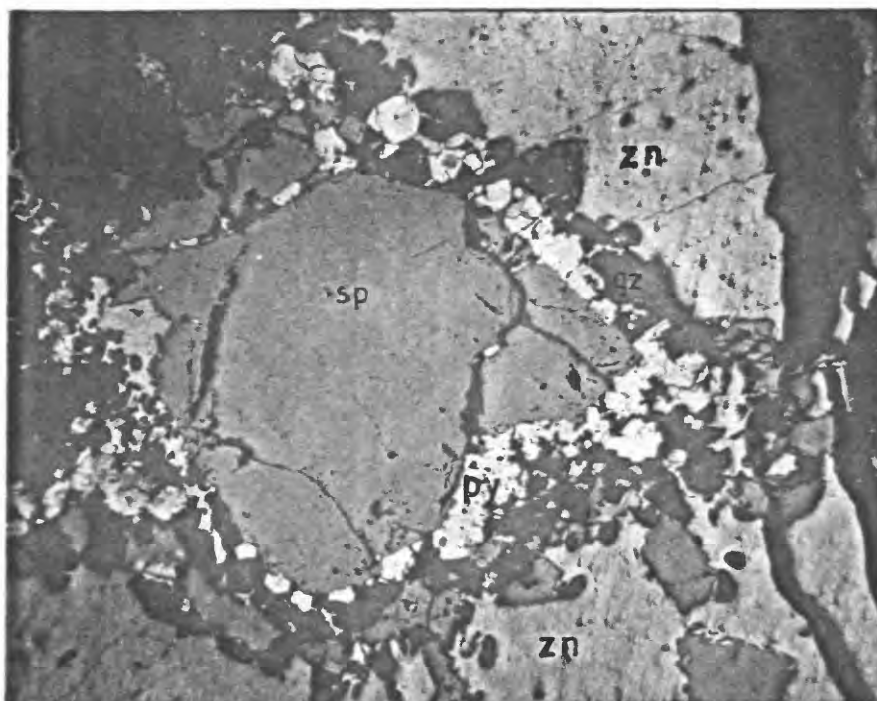
**Figure 41.** Typical habit of only copper mineral, bournonite, deposited with lead sulfantimonides. Bournonite (bn) set in matrix of geocronite (go) surrounded by ragged grains of sphalerite (sp) and cut by quartz (qz). Note association of sphalerite with bournonite. Caudalosa vein, Temerario level, Caudalosa mine (X 250).



**Figure 42.** Typical mineral sequence of the reworking phase. Geocronite (go) with spongy pyrite (py) replacing sphalerite (sp), and in turn being replaced by fibrous semseyite (sm) and barite (ba). Sphalerite has replaced galena (ga). Quartz grains (qz) are probably older than geocronite and younger than sphalerite. Ruperto mine, dump (X 100).



**Figure 43.** An equilibrium assemblage of sphalerite, sinkenite and quartz. Sphalerite (sp) was deposited simultaneously with sinkenite (zn) and quartz (qz). Later pure sphalerite was deposited and finally quartz and sinkenite formed. Shows separation of minerals due to slight fluctuations in concentrations. Caudalosa vein, San Felipe level, Caudalosa mine (X 30).



**Figure 44.** Late quartz-pyrite mineralization. Quartz (qz) preferentially replaces sphalerite (sp) which is partially replaced by zinkenite (zn). Note pyrite (py) preferentially deposited on sphalerite without apparent replacement. Caudalosa vein, Pompeyo level, Caudalosa mine (X 42).



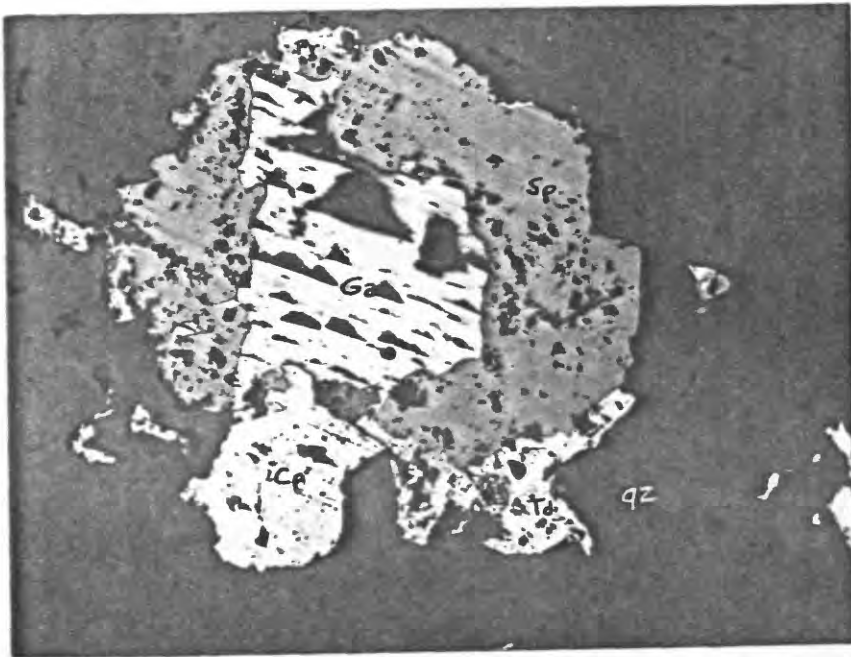
cutting fractures or in vugs, marking the close of antimonian mineralization in the lead-antimony veins. The presence of zinkenite and stibnite at Madona, without antimonian alteration of galena, and the quartz-stibnite-rhodochrosite assemblage in the upper parts of the Caudalosa vein may represent physico-chemical gradients in space rather than in time. Thus, correlation in time is not possible.

Hydrothermal leaching, which followed major deposition in this phase, was observed only at the Madona mine where galena crystals have been corroded in a step-like fashion nicely revealing their cubic nature. Hypogene enrichment of silver minerals was not seen in the lead-antimony veins; however, the final phase of hydrothermal deposition in which minor amounts of sphalerite, galena, pyrite, barite, gypsum, and hematite were deposited is well documented throughout the lead-antimony veins.

#### (11.) Silver-antimony veins

Correlation of the silver-antimony mineralization at San Genaro and Astohuaraca with the reworking or antimonian phase of mineralization in the central part of the district, is based on comparable increases in antimony in the depositional sequence following similar base-metal mineralization.

The base-metal mineralization of the silver-antimony veins at San Genaro are similar in mineralogy to base-metal mineralization elsewhere in the district: sphalerite contains exsolution blebs of chalcopyrite, galena-sphalerite-tetrahedrite-chalcopyrite assemblage is typical (see Figures 32 and 45), and iron content of sphalerite is the same (see Table XXXIV).



**Figure 45.** Remnant grain of early base-metal minerals in banded silver ore. Galena (ga) enveloped by sphalerite (sp) and chalcopyrite (cp). Silver-antimony mineralizing fluids have partially replaced chalcopyrite by tetrahedrite (td) and galena by polybasite (po) and pyrargyrite (pr). Grain enclosed in colloform quartz (qz). Milagro vein, Niño Jesús level, San Genaro mine (X 82).



Following the deposition of base-metal sulfides at San Genaro, the veins were reopened and mineralizing fluids bearing silica, silver, antimony, iron, and small amounts of gold, arsenic, and bismuth were introduced in the central parts of the veins, cross-cutting and partially replacing the base-metal minerals (see Figures 9, 46 and 47) and depositing silver sulfantimonides (see Figure 48).

The silver mineralization at San Genaro began with the deposition of silver sulfide, became progressively more antimonian in time, and terminated with the deposition of a silver-bismuth sulfantimonide, aramayoite. The silver minerals are: acanthite ( $\text{Ag}_2\text{S}$ ), polybasite ( $\text{Ag}_{16}\text{Sb}_2\text{S}_{11}$ ), pearceite ( $\text{Ag}_{16}\text{As}_2\text{S}_{11}$ ), pyrargyrite ( $\text{Ag}_3\text{SbS}_3$ ), miargyrite ( $\text{AgSbS}_2$ ), aramayoite [ $\text{Ag}(\text{Sb},\text{Bi})\text{S}_2$ ]. Polybasite, the least antimonian of the sulfantimonides, is the only one in direct contact with acanthite. Miargyrite, the most antimonian mineral of this assemblage, was observed only with pyrargyrite. Stibnite was reported near the present surface in the Bella vein (W. A. Lyons, personal communication, 1961), and, as at Caudalosa, it occurs with rhodochrosite.

The first minerals deposited in the third phase of mineralization at San Genaro were quartz and hematite (see Figure 46), followed by acanthite (see Figure 49). Most of the acanthite was subsequently altered to polybasite, but some still remains locked between quartz grains and in the centers of polybasite grains (see Figure 49). Following the precipitation of acanthite, polybasite and pearceite were deposited, then pyrargyrite and miargyrite. Age relationships between sulfosalts are not always clear as they were redistributed after initial deposition and concentrated near the surface. It is apparent, however, that miargyrite tends to replace pyrargyrite (see

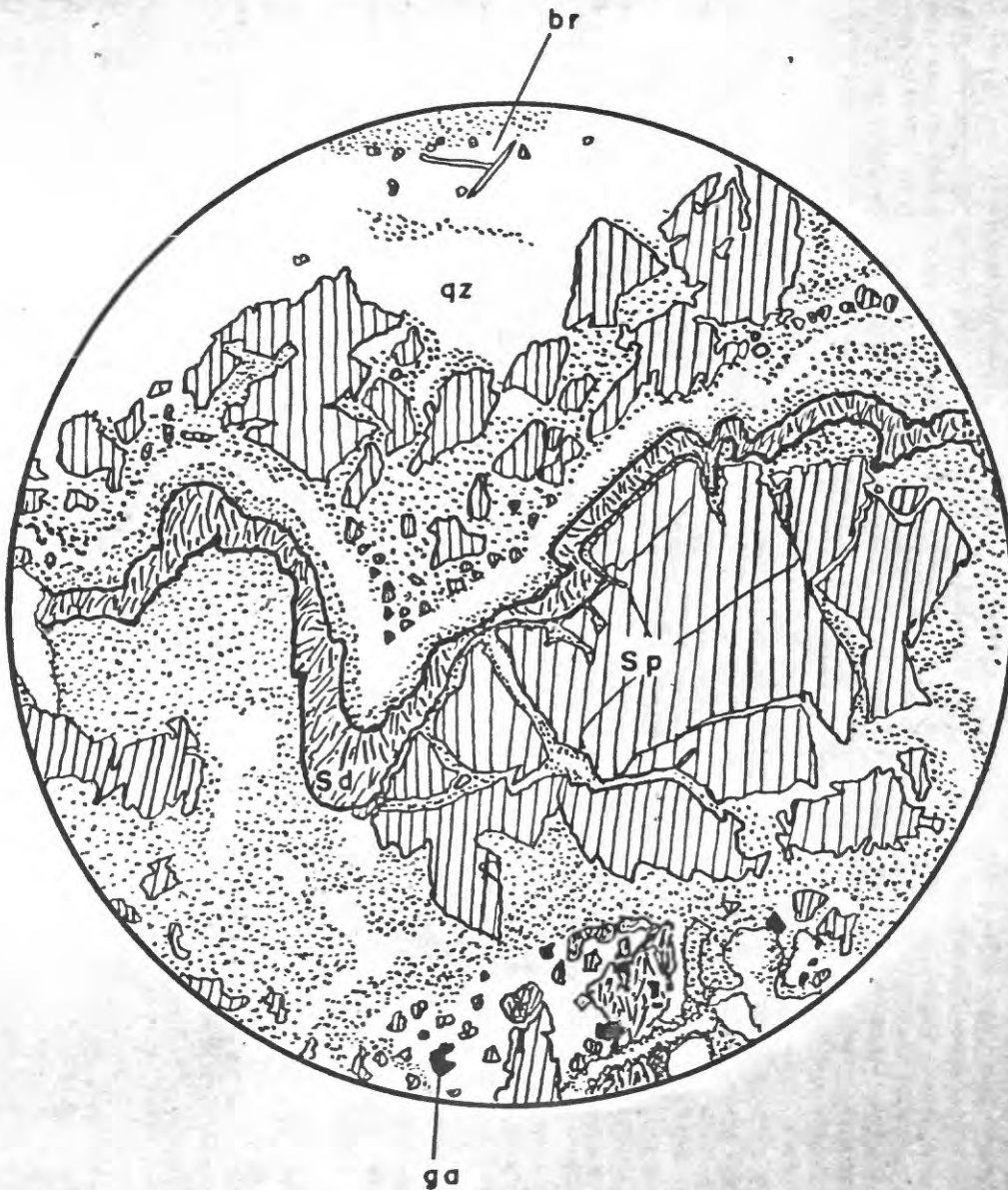
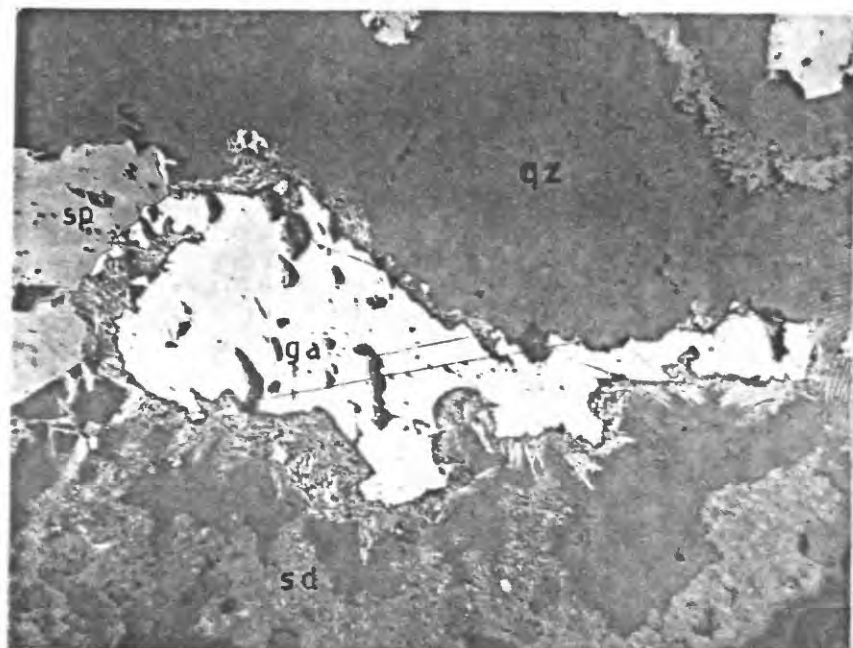
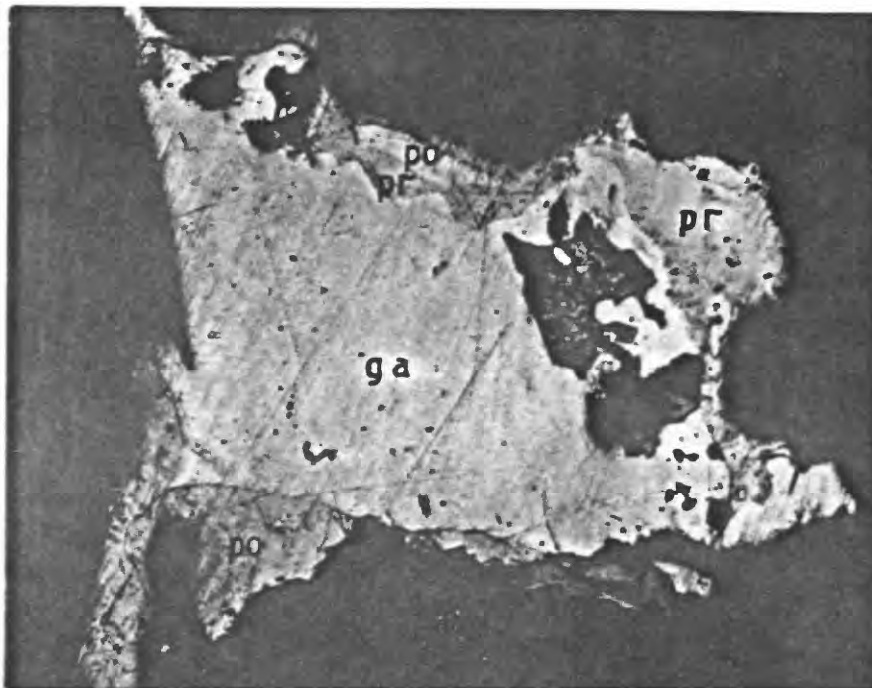


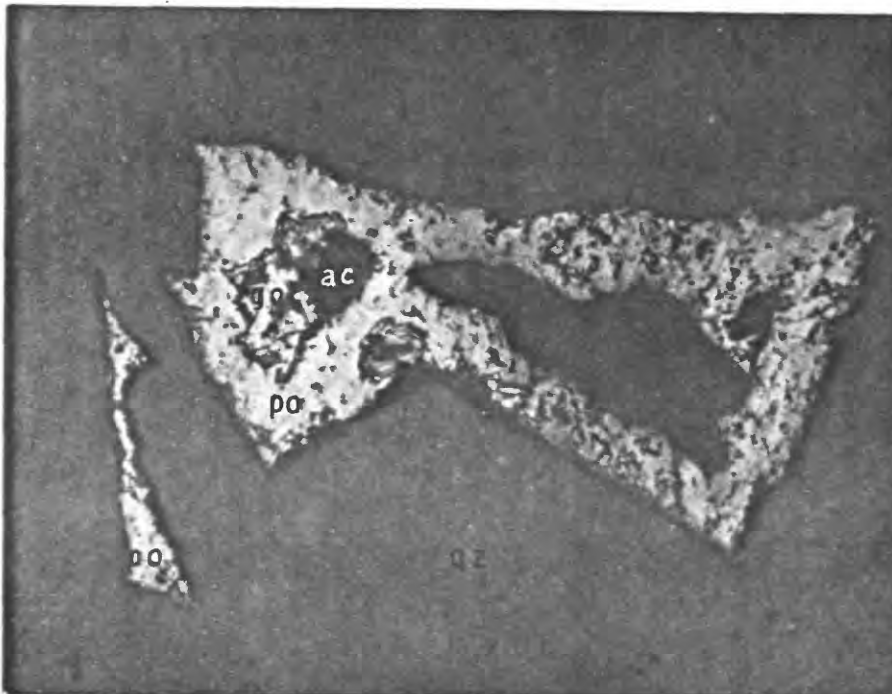
Figure 46 - Sketch of typical banded colloform quartz ore. Quartz (qz) and siderite (sd) coat and envelope fractured grains of sphalerite (sp). Banding in quartz marked by hematite needles (dots). Note that only quartz with hematite corrodes sphalerite. Barite (br) and galena (ga). Genaro vein, 35 level, San Genaro mine (X 5).



**Figure 47.** Corrosion of galena by early mineralizing fluids of the reworking phase. Galena (ga) preferentially replaced by quartz (qz) with hematite needles. Sphalerite (sp) is not attacked. Quartz is interbanded with siderite (sd) containing disseminations of hematite. Note the precipitation of hematite in quartz only around galena. Milagro vein, Niño Jesús level, San Genaro mine (X 63).



**Figure 43.** Galena replaced by silver minerals. An isolated grain of galena (ga) from quartz veinlet shown in Figure 9, which is replaced by polybasite (po) and pyrargyrite (pr). San Julián Sur vein, 35 level, San Genaro mine (X 202).



**Figure 4Q.** Antimonian alteration of acanthite. Acanthite (ac) and gold (go) surrounded by polybasite (po) and enclosed in quartz (qz). Gold and acanthite are remnants of initial mineralization in the reworking phase. Acanthite subsequently reacted with antimonian fluids forming polybasite. San Julián Sur vein, 35 level, San Genaro mine (X 350).

Figure 50).

During the early stage of silver sulfosalt deposition quartz was the principal gangue mineral. It was accompanied by minor amounts of hematite and pyrite (see Figure 46) and mineralizing fluids corroded or replaced existing base-metal sulfides (see Figure 47). As silver mineralization continued, siderite and sericite became important gangue minerals, forming intricately banded, colloform quartz-siderite-silver ores (see Figures 7 and 51). Small amounts of pyrite, galena, tetrahedrite, sphalerite, and barite were also deposited with these colloform ores. The replacement of existing chalcopyrite by tetrahedrite, galena, and pyrargyrite (see Figure 34) probably took place at this time. This early stage of antimonial mineralization culminated in the deposition of stibnite and rhodochrosite.

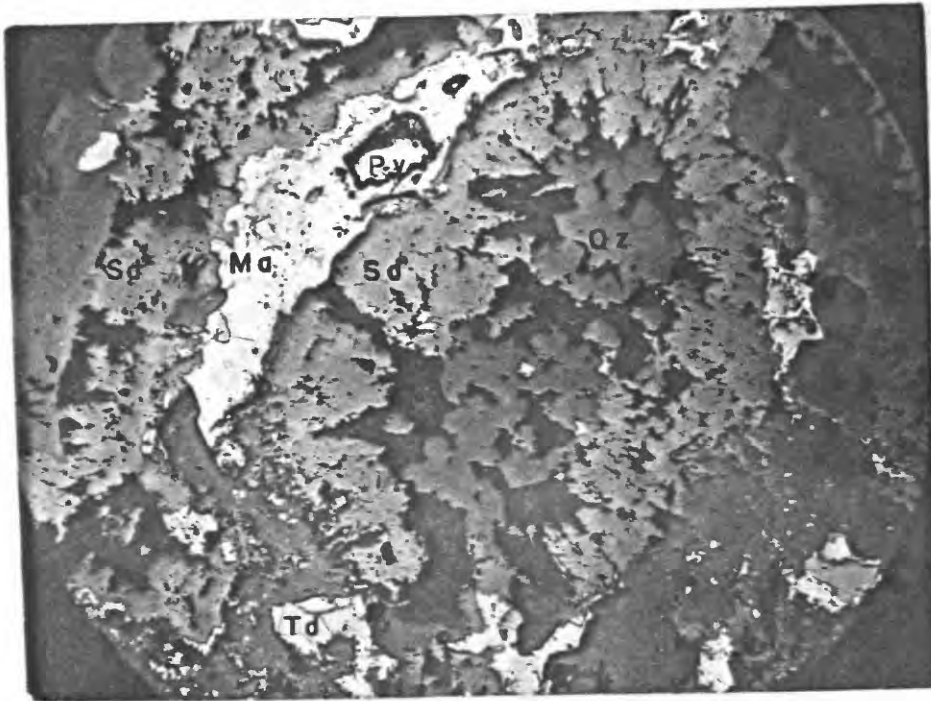
Early deposition was followed by a period of slight hydrothermal leaching, wherein barite and possibly sulfides were leached out of vein quartz leaving open boxworks (see Figure 8). Thereupon, silver sulfantimonides were remobilized and concentrated near the surface, filling voids provided by leaching and brecciation (see Figure 10). Aramayotte, a silver-bismuth sulfantimonide, is characteristically associated with these enriched ores.

Hypogene mineralization at the close of the reworking phase is marked by the deposition of minor amounts of base-metal, gangue, and silver minerals in cracks and voids in vein material. In the upper levels of the San Genaro mine, nodular growths of late materials were observed filling vugs (see Figure 52). The typical depositional sequence is pyrite, chalcopyrite, galena, sphalerite, tetrahedrite, quartz, and barite (see Figure 52). Drusy growths of galena, sphaler-



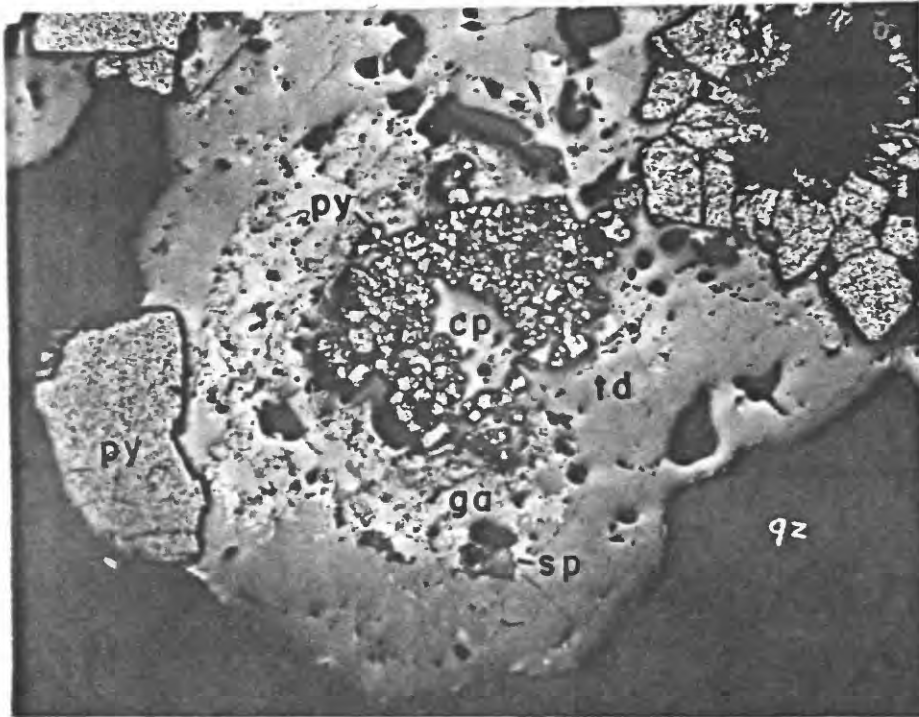


**Figure 50.** Typical silver sulfantimonide sequence. Massive pyrargyrite (pr) is replaced by miargyrite (mr), which has a higher antimony content. San Julián Sur vein, 35 level, San Genaro mine (X 50).



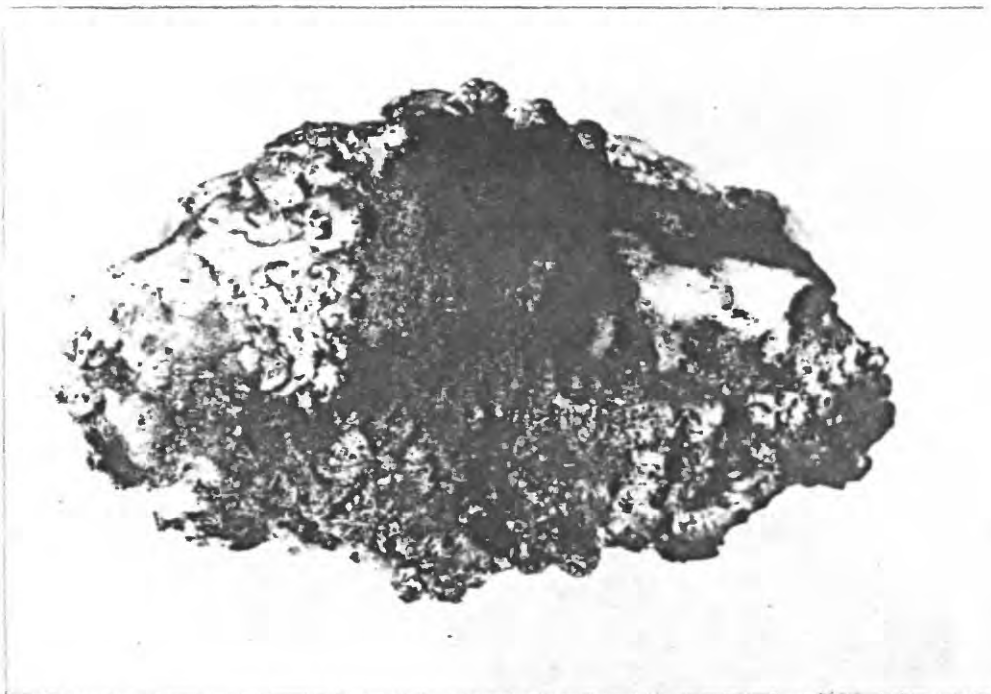
**Figure 51.** Typical knot from banded, colloform ore. Crystalline quartz (qz) surrounded by siderite (sd) followed by a layer of margaryite (mr), pyrite (py), tetrahedrite (td) and massive quartz, another band of siderite, and finally quartz. See Figure 7. San Julián Sur vein, 70 level, San Genaro mine (X 30).





**Figure 52.** Detail of knot of late hypogene minerals showing depositional sequence. Granular pyrite (py) and chalcopyrite (cp) enclosed by galena (ga) followed by minor amounts of sphalerite (sp) and massive tetrahedrite (td) which partially replaces galena and pyrite. Late pyrite grains (mottled gray) around edge. Quartz (qz). San Julián Norte vein, San Genaro level, San Genaro mine (X 30).

ite, and quartz, glazed with allophane, are characteristic of late mineralization at San Genaro. Other manifestations of late hypogene mineralization at San Genaro include: 1) thin seams of pyrargyrite, miargyrite, sericite, barite, tetrahedrite, galena, and sphalerite (also observed in the Cerro Reliquias area); 2) drusy encrustations of late barite, galena, and sphalerite (common in the district); and 3) buttons of late sphalerite encrusting all other vein minerals (see Figure 53) (also well developed at the Santa Teresita mine).



**Figure 53.** Typical example of late hypogene mineralization. Tiny buttons of sphalerite (dark) and tabs of barite (white) deposited on vein quartz. San Julián Norte vein, San Genaro level, San Genaro mine (X 1).

## K. Physico-chemical conditions of mineralization

### 1. Temperature

An indication of the temperatures developed in Castrovirreyna deposits is given by the iron content of sphalerite. This is small, regardless of color, locality, depth, and paragenesis, and ranges from 0.003 to 0.88 percent, with an average less than 0.5 percent (see Table XXXI). The uniform paucity of iron and the absence of pyrrhotite suggest that sphalerite was not in equilibrium with iron and formed in the presence of excess sulfur. The curves of Kullerud (1953) are based on a sphalerite-pyrrhotite system, hence temperatures for the Castrovirreyna area extrapolated from these curves will be lower than the true temperatures of formation and should be considered minimal (Kullerud, 1959). Although the low iron content of Castrovirreyna sphalerites place them beyond the limits of accurate extrapolation (see Figure 54), temperatures between 50° and 200°C. can be assumed.

The enargite-famatinite mixture found in the Caudalosa vein indicates temperatures above 325°C., the inversion point of enargite-luzonite, and below 600°C., the melting point of enargite (Skinner, 1960, and Barton, personal communication, 1963).

Another estimate of temperature is derived from the wurtzite-sphalerite mixtures identified by X-ray diffraction in material taken from the 4570 level of the Caudalosa vein. These minerals were deposited with declining temperatures after maximum temperatures were reached. This mixture must have formed by direct precipitation and not inversion as the wurtzite-sphalerite inversion point of 1020°C. is much higher than the melting points of associated lead antimonides (Kracek, 1942). Allen and others (1914) precipitated wurtzite and

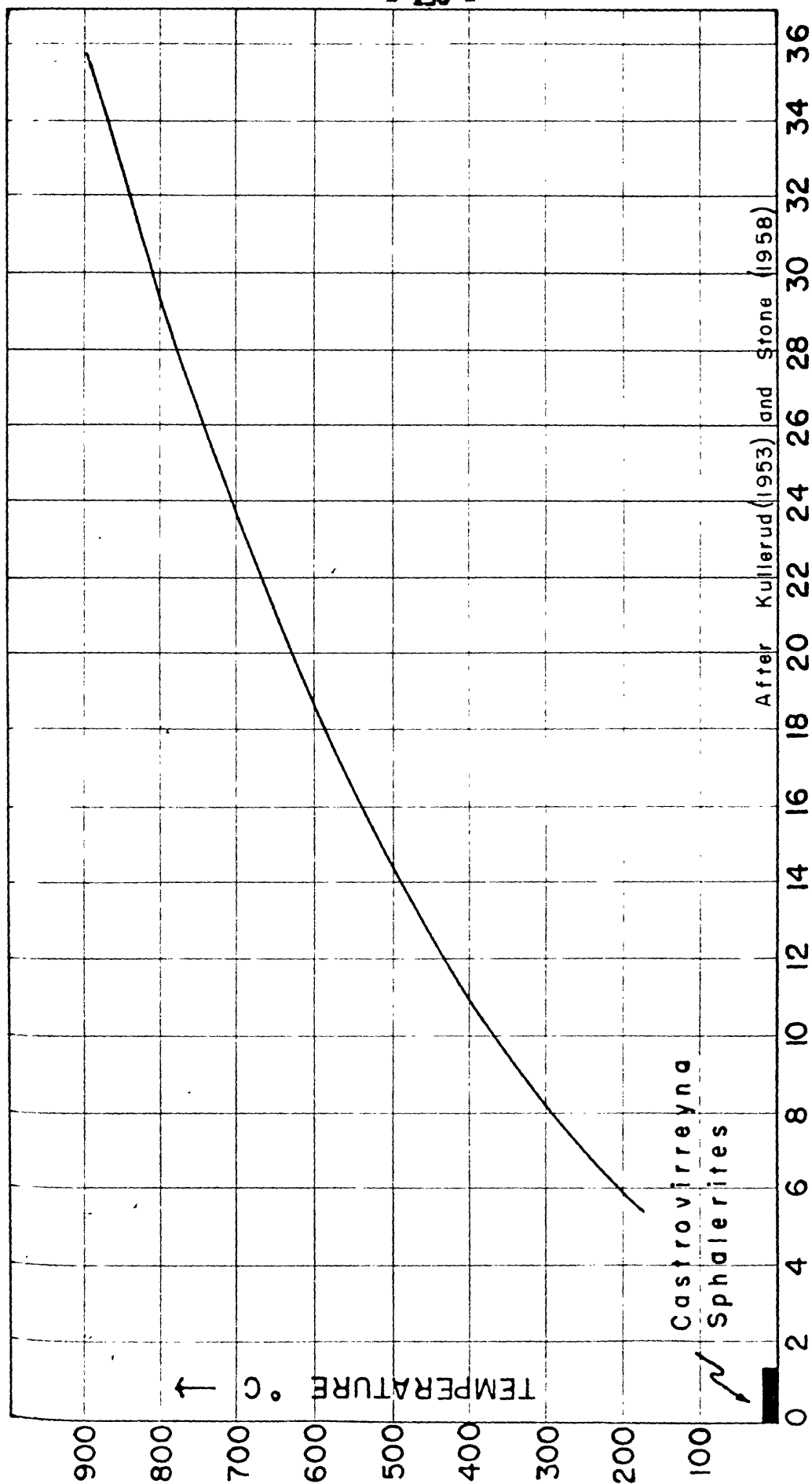


Figure 54 : Graph showing relation of FeS content in sphalerite to temperature

wurtzite-sphalerite mixtures from slightly acid solutions (pH 5 to 6) at temperatures from 250° to 350°C. and completely converted the wurtzite thus formed to pure sphalerite, in the same slightly acid solution, by raising the temperatures to above 350°C. Therefore, the temperature of formation of the wurtzite-sphalerite mixture at Castrovirreyna may not have exceeded 350°C. The extremely low iron content of this mixture (see Table XXXI, analysis 11), suggests that the formation temperature was considerable lower than 350°C.

A further clue to the temperature is provided by the sphalerite-chalcopryrite exsolution mixtures which are found in small amounts in all veins in the district (see Figure 28). Swarms of chalcopryrite blebs in sphalerite are, according to Buerger (1934) and others, a product of exsolution between 350° and 400°C. Barton (personal communication, 1961) concurs that chalcopryrite will exsolve from sphalerite at these temperatures if cooling is very rapid, but found that cooling over periods of 6 to 24 months depress the exsolution point to at least 250°C.

Kaolinite and sericite, common to all the veins at Castrovirreyna, indicate moderate temperatures. Kaolinite forms only below 310°C. (Ewell and Insley, 1935), and sericite forms from feldspar (sericitization) above 200°C. (Folk, 1947).

Criteria for the lower temperatures of hypogene mineralization at Castrovirreyna are less conclusive than those for maximum temperatures. Colloform banding in the very early and late quartz suggests deposition from a colloidal suspension which probably could not exist above 100°C. (Barton, 1959). The lower temperatures of hypogene mineralization probably ranged from less than 50° to over 100°C.

The formation temperature of these deposits thus probably ranged from 50° to 350°C. The highest temperatures were developed in the depositional phase of mineralization; but the low iron content in most sphalerite suggests that the bulk of the base-metal and associated minerals of this phase was deposited at temperatures ranging from about 150° to 250°C. The very low iron content of late sphalerite and the abundance of colloform textures suggest that the temperatures during the reworking phase ranged from about 25° to 125°C., the bulk of mineralization taking place between 50° and 100°C.

## 2. Depth of Formation

The maximum vertical range of mineralization in any one mine in the Castrovirreyna district is unknown because none of the mines has reached the lower limit of sulfide mineralization. Order-of-magnitude calculations of the average depths of formation can be based, however, on estimates of the probable amount of post-ore erosion and the known depths at which different ore suites are concentrated.

Mineralization is considered younger than all of the volcanic activity because rocks of all ages are cut by mineralized structures. Thus, an estimate of post-ore erosion is found in the relation of Cerro Quispejahuar with the surrounding terrane.

Cerro Quispejahuar is a volcanic neck that rises about 355 meters above the surrounding andesite flows (see Figure 2). The core of this neck consists of vitrophyre and forms a spine that protrudes 180 meters above the sloping base. The vitric core is surrounded by a well-indurated vent breccia, which, in turn, is surrounded by massive andesite flows. As the core of this neck could not have resisted erosion sufficient to permit the removal the more resistant breccia and

flow rocks, this spine must have protruded above the original terrane. Therefore, the 175 meters between the base of the spine and the base of the volcanic neck massif represent a maximum figure for the depth of normal erosion in the area, after the formation of the neck, discounting glacial scouring.

Based on this assumption of 175 meters of post-ore erosion, the following figures indicate the approximate depth certain ore suites tended to concentrate.

Hypogene silver sulfide and sulfantimonides are most abundant from the present surface to depths of 150 meters. Thus, hypogene concentration of silver minerals was at original depths of 175 to 325 meters.

An estimate of the depth of formation of the lead-antimony ores at the Caudalosa mine is more tenuous because the veins crop out on the side of a glacially scoured valley. Reconstructing the pre-glacial valley profile from a break in slope above the upper workings and adding 175 meters of cover removed by normal post-ore erosion, indicate that lead sulfantimonides were best developed at original depths of 235 to at least 425 meters.

Galena, sphalerite, chalcopyrite, and tetrahedrite are most abundant in the La Virreyna area, which lies in the bottom of a glaciated valley. Judging from the height of the moraines on the valley walls, the depth of scouring did not exceed 100 meters. Thus, the original depth at which this type of mineralization was best developed was about 275 meters. For lack of better evidence, the lower limit of concentration of this base-metal mineralization is considered the same as that for lead sulfantimonide mineralization, which was superimposed



on base-metal mineralization.

### 3. Pressure

The pressures at which these deposits formed were equal at least to the hydrostatic head overlying each deposit, and at most not much greater than the lithostatic head. Using depth of formation values mentioned in the preceding section and 2.18 as the average density of andesite, the following maximum and minimum pressures were calculated.

<u>Ore type</u>	<u>Depth range</u>	<u>Hydrostatic pressure</u>	<u>Lithostatic pressure</u>
Silver antimonides	175-325 meters	17-31 atmos.	47-87 atmos.
Lead antimonides	235-425 meters	22-41 atmos.	63-114 atmos.
Lead-zinc-copper sulfides	275-425 meters	26-41 atmos.	74-114 atmos.

These deposits formed at relatively shallow depths in fissures that probably terminated at the surface in hot springs or aqueous fumaroles similar to those of the Huachocholpa lead-zinc district 25 kilometers to the northeast (see Figure 1). Thus, the lower pressure values, calculated on the basis of a hydrostatic head, are probably more realistic.

### 4. Physical States

Consideration of the temperatures, pressures and textural relations suggest that the ore fluids were predominantly in the liquid phase during mineral deposition. Most of the sulfide and gangue deposition is thought to have taken place below 250°C., although temperatures probably ranged from 25° to 350°C. Thus, pressures from 15 to 45 atmospheres would place the depositional environment very near or below the boiling-point curve of water. Colloform banding of quartz and pyrite, colloform encrustations of allophane, well-developed

crystals in cavities, and comb structures are all suggestive of a liquid environment.

### 5. Chemical Conditions

Interpretation of the chemistry of mineralizing fluids is difficult because of the lack of specific physico-chemical data and the fact that the resulting mineralization is only a fragmentary record of the complete mineralizing history.

Although it was possible to make order-of-magnitude calculations for the temperatures and pressures developed in the Castrovirreyne deposits (see Physical Conditions) from available geologic and mineralogic data, estimates of the compositions of the mineralizing fluids can be made only if certain basic assumptions are fulfilled. Holland (1956), Barnes and Kullerud (1957) and Barton (1957) stated that in order to calculate the composition of ore fluids from mineralogic data one must assume the following: 1) equilibrium conditions existed during precipitation, 2) the environments of deposition of any two minerals used for calculating concentrations were the same, 3) minerals used for calculations did not undergo post-depositional changes, and 4) colloids were not important. Furthermore, they stated that the following must be evaluated: 1) the relative distribution and types of ions present, and 2) the activity coefficients of aqueous ions as functions of temperature, pressure, ionic species, and ionic strength.

Consideration of the paragenesis of the Castrovirreyne ores indicates that the above assumptions and evaluations usually could not be made. The cyclical nature of the base-metal mineralization and the marked concentration of antimony, silver, and bismuth in time and space indicate that the Castrovirreyne deposits represent an open, dynamic

chemical system in which mineralizing fluids constantly modified the solid phases while they themselves changed. As long as fluids continued to circulate through the system they continuously met new environments with which they were not in equilibrium and, thus, maintained a general state of nonequilibrium. Complete equilibrium was attained only after the system became static, i.e., when mineralization ceased. Locally, however, equilibrium tended to establish itself, even though the system as a whole was out of equilibrium (Thompson, 1959). The attainment of equilibrium locally in a general state of nonequilibrium is well documented by the antimonian alteration of galena to lead sulfantimonides at Caudalosa and to a lesser extent, by the antimonian alteration of scanthite to sulfantimonides at San Genaro. These sulfantimonides are arranged around the simple sulfide in zones in which the antimony content increases with the distance from the sulfide. As the compositions of these sulfantimonides lie on a straight line between galena or scanthite and stibnite (see Figure 55), only two minerals can be in equilibrium at a given point. Thus, these assemblages represent the attainment of local equilibrium between mineral pairs in an overall state of nonequilibrium in the assemblage as a whole. The lead sulfantimonides appear to have formed by the reaction of antimonian fluids and galena. Once the first sulfantimonide, geocronite, formed by replacement of  $PbS$  molecule by  $Sb_2S_3$ , the galena was effectively sealed off from further contact with the antimonian solutions. These solutions then reacted with the geocronite, replacing  $PbS$  molecule with  $Sb_2S_3$ , forming semseyite, and so on (see Figure 38).

The silver sulfantimonides are not so markedly distributed around scanthite in zones of increasing antimony content. However, alternating

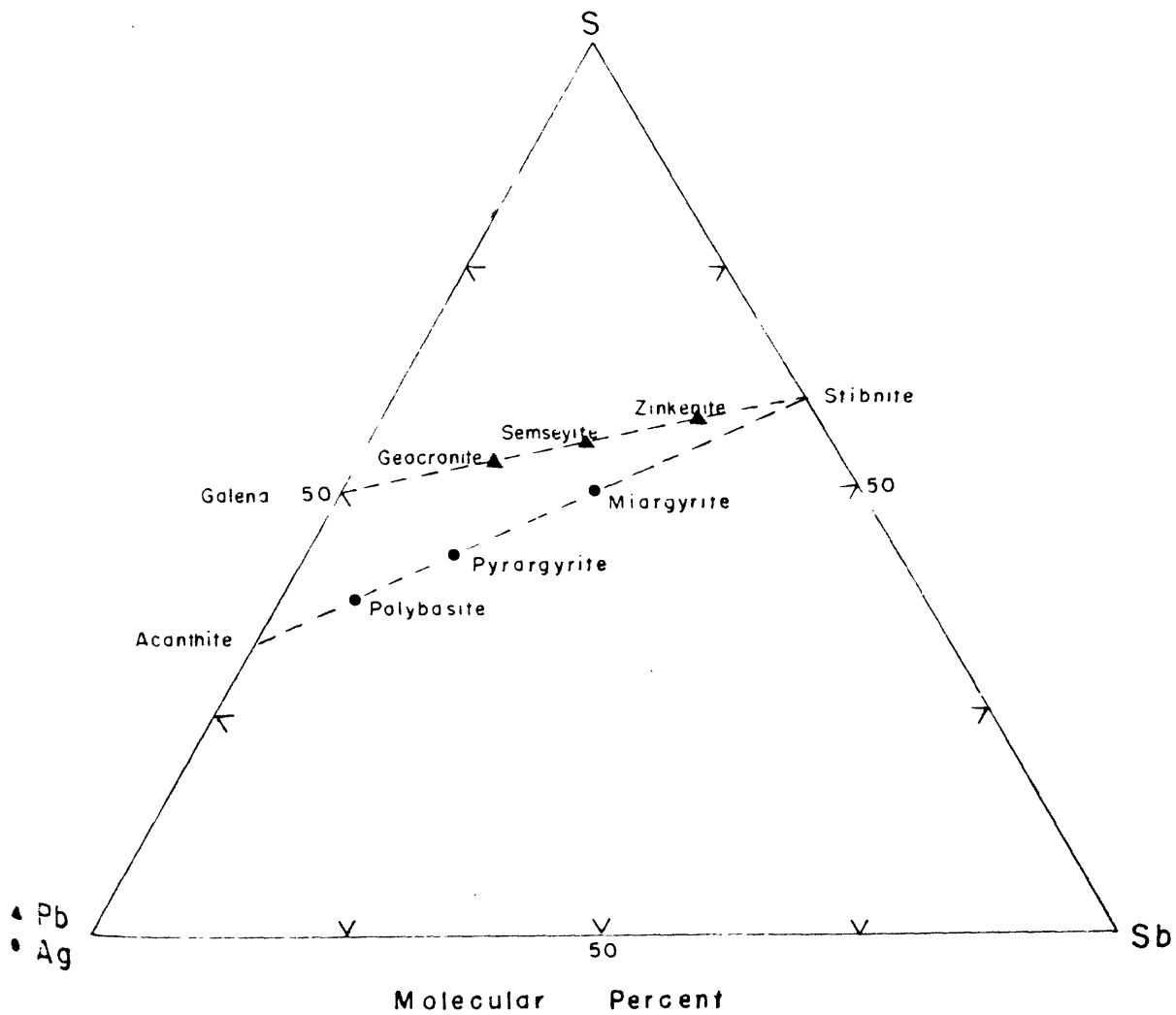


Figure 55 : Assemblage Diagram of Silver and Lead  
Sulfantimonides

pairs of the acanthite-stibnite transition series are never found closely associated in space. This suggests that most of the silver was precipitated directly as sulfantimonides from mineralizing fluids, in which the effective concentration of antimony increased with time as the mineralizing fluids underwent slight modifications. This also represents deposition in response to locally established equilibrium in a system undergoing constant change. These examples of deposition under conditions of highly localized equilibrium were recognized only because of progressive chemical zoning among related minerals, and are interpreted as typical of normal depositional processes.

Therefore, it is concluded that equilibrium conditions during the deposition of an assemblage cannot be assumed unless textures indicate simultaneous deposition (exsolution or pseudoeutectic textures) or show repeated mutual boundaries between three or more members. Since neither these textures nor these boundaries are common in the Castro-virreyne district, it is assumed that equilibrium was not always attained during deposition.

Second, it is difficult to assume similar conditions of deposition for two minerals in a system where slight changes in the physico-chemical environment were the causes of deposition.

Third, the formation of sulfantimonides from galena and acanthite, the hydrothermal leaching, and the hypogene enrichment of the silver ores indicate that post-depositional changes were important in determining the final composition and distribution of many minerals.

Fourth, although the role of colloids is not well understood, abundant colloform textures in quartz, pyrite, rhodochrosite, and allophane (see Figures 7 and 15); desiccation cracks in quartz; spongy

balls of pyrite (see Figure 19) suggest that colloidal deposition was important in the formation of these gangue minerals and possibly the simple sulfides of silver and lead during low temperature regimes.

Finally, the evaluation of the type and distribution of ionic species present and their relative activities was not feasible, because complex ions of antimony, silver, bismuth, arsenic, and possibly other metals played a predominant role both in metal transport and mineral formation. The role of complex ions is deduced from the fact that

- 1) the sequence of deposition does not follow the order of solubilities,
- 2) the formation of sulfantimonides is most satisfactorily explained by the reaction of simple sulfides with an antimony-sulfur complex, and
- 3) silver, antimony, and bismuth are precipitated in quantity only in late, low-temperature mineralization although they appear as minor or trace constituents earlier.

In order to apply the data of Holland (1959) and Barton (1957) to the problem of the composition of the mineralizing fluids, mineral assemblages were sought which appeared to have been deposited in equilibrium, which had not undergone post-depositional changes, and which did not involve colloidal deposition of sulfosalts. This excluded all assemblages containing lead, copper, or silver sulfantimonides or showing colloform banding. The only assemblages used were those whose components showed mutual boundaries and consistent relations with other minerals. These assemblages are referred to as equilibrium assemblages. Unfortunately, many of the possible assemblages that fit the textural conditions contained sulfosalts, for which there is no thermochemical data; and many of those that satisfied the chemical conditions did not show the proper textures. Exsolution, pseudocutectic, and granular

textures best fitted the stipulated conditions.

Six assemblages were found which met these conditions: 1) sphalerite-chalcopryrite (see Figure 28), 2) quartz-galena-sphalerite-chalcopryrite (see Figure 32), 3) quartz-hematite-siderite (see Figure 47), 4) quartz-rhodochrosite-stibnite, 5) galena-sphalerite-barite (see Figure 53), and 6) gypsum-sphalerite-stibnite (see Figure 6). The first and second assemblages are characteristic of the depositional phase of mineralization, the third and fourth assemblages are typical of the early part of the reworking phase, the fifth assemblage represents final hypogene mineralization late in the reworking phase, and the sixth assemblage is typical of supergene mineralization.

In applying these assemblages to the diagrams of Holland (1959) it was found that the stability fields for most of the component minerals were so large and overlapped so greatly that only relatively gross changes in the chemistry of the mineralizing fluids with time and in space could be calculated. Comparison of the equilibrium assemblages found at Castrovirreyña with Holland's diagrams for Sb-O-S, Pb-O-S, and Ag-O-S shows that sulfur decreased with falling temperatures and with the appearance of antimony and silver. A similar comparison with the diagrams for Ba-O-S and Ca-O-S shows that oxygen decreased with falling temperatures and with the appearance of  $\text{CaCO}_3$ . Consideration of the stability fields of lead, zinc, and iron sulfides shows that the mineralizing fluids were richer in sulfur and oxygen during the depositional phase than during the reworking phase; the limiting fugacities during the depositional phase for  $\text{S}_2$  were from  $10^{-10}$  to  $10^{-20}$ , and for  $\text{O}_2$  a fugacity of  $10^{-37}$  or less. Estimates of the fugacities of  $\text{CO}_2$  were not possible. They were

probably very low during the depositional phase because no carbonate minerals were recognized, but increased notably in the reworking phase with the appearance of carbonate minerals.

Mineralization during the reworking phase took place approximately between 300° and 400°K, and seems to fall within the limits determined by the quartz-siderite-hematite assemblage. According to Holland's Fe-O-S-C diagram at 300°K, a siderite-hematite assemblage indicates a CO<sub>2</sub> fugacity of greater than 10<sup>-1.5</sup>, a S<sub>2</sub> fugacity of 10<sup>-25</sup> to 10<sup>-35</sup>, and an O<sub>2</sub> fugacity of between 10<sup>-50</sup> and 10<sup>-70</sup>. The average values of the fugacities are plotted on Plate 4, where they can be compared with other chemical values.

Application of these equilibrium assemblages to the anionic activity ratio diagrams of Barton (1957) generally defines a chemical environment only within the wide range of Barton's Hydrothermal Region. Two ratios, however, show important changes in the chemistry of the mineralizing fluids. The appearance of siderite in preference to pyrite indicates a decline in the S<sup>2-</sup>/CO<sub>3</sub><sup>2-</sup> ratio to a point where neither iron nor lead nor zinc could be deposited as sulfides, although silver could be. Secondly, the occurrences at La Griega and Madona of calcite instead of gypsum as a late hypogene mineral indicate an increase in the CO<sub>3</sub><sup>2-</sup>/SO<sub>4</sub><sup>2-</sup> ratio at the end of hypogene mineralization, at these locales at least. These changes are in general agreement with the data obtained from Holland's diagrams, namely a decrease of S<sub>2</sub> and an increase of CO<sub>2</sub> with time.

Estimates of the hydrogen ion concentration (pH) during mineralization are based mostly on gangue minerals. The abundance of kaolinite in the argillized wallrock adjacent to the vein implies a slightly acid



environment (Folk, 1947, and Stringham, 1952) during the early stages of mineralization. The presence of wurtzite suggests continuing acidity (Allen and others, 1914) near maximum temperatures, in the depositional phase. On the other hand, the abundant carbonates and sericite deposited during the reworking phase indicate a neutral or slightly basic environment (Stringham, 1952). Furthermore, the formation of hematite in an environment of decreasing oxygen concentration would be facilitated by a more basic environment (pH above 7). The presence of allophane encrusting very late quartz, galena, and sphalerite crystals in vugs, indicates a shift to an acid environment (Stringham, 1952) in the final stages of hypogene mineralization. Despite these changes in the hydrogen ion concentration, it is doubtful that the pH varied more than a unit or two from neutral (Barton, 1959).

Although it is difficult to obtain precise information on the chemistry of the mineralizing fluids through the use of thermochemical diagrams, an estimate of the relative concentration of metal cations in time and space can be derived from the paragenetic sequence and zoning. The relative concentration is considered synonymous with ionic activity or the availability of an element for deposition. It should be emphasized that most of the principal elements found in the Castrovirreyna deposits were present in the mineralizing fluids throughout the depositional and reworking phases of mineralization, but they were deposited in greatly differing amounts, according to the time and place. Spectrographic analyses show that even when an element does not appear as a major constituent it is usually present in minor or trace amounts (see Appendix IV).

The relative concentration of the important metallic elements found in the Castrovirreyas deposits, as determined by their appearance in the paragenetic sequence, is plotted as a function of time in Plate 4. Comparing this graph with the accompanying paragenetic chart and the graphs of temperature, pH, and fugacities, the following conclusions can be reached: 1) base-metal mineralization is cyclic in response to a rise and fall in temperature; 2) base-metal deposition is favored by an acid environment and relatively high fugacities of  $O_2$  and  $S_2$ ; 3) at higher temperatures, with a low pH, and with relatively high fugacities of  $O_2$  and  $S_2$ , and a low fugacity of  $CO_2$ , silver, bismuth, manganese, and to a lesser extent antimony were soluble or formed complexes so that they were deposited in only minor and trace amounts; 4) the deposition of antimony, silver, bismuth, and manganese and the formation of sulfosalts was favored by low temperatures, a basic environment (pH above 7), relatively low fugacities of  $O_2$  and  $S_2$ , and a high fugacity of  $CO_2$ ; 5) remobilization of silver for hypogene enrichment was probably caused by an increase in the fugacity of  $CO_2$  and an increase in pH; 6) the final deposition of base-metal sulfides was caused by a shift to an acid environment and perhaps an increase in the fugacity of  $S_2$ . Therefore, it is concluded that the zoning and the complex paragenesis shown by the Castrovirreyas deposits reflect an intricate interplay between temperature, pH, ionic activity, and effective concentration in mineralizing fluids which were constantly reworking the products of their own deposition.

## L. Localization of ore shoots and zoning

The localization and character of vein material is controlled by two factors: the physical setting of deposition and the chemistry of mineralization. The physical setting determines the amount of vein material that can be deposited at any one site, whereas the chemistry of mineralization affects the character and distribution of ore minerals, i.e., zoning. Both of these environmental factors are interdependent, however, because mineralizing fluids that exercise control on the distribution of vein material need adequate channels and depositional sites to be effective and vice versa.

### 1. Structural controls

In the well-mineralized sections of the veins of the Castro-virreyna district the best ore shoots formed where the veins are widest. Thus, within a given environment, ore localization is principally a function of structural features, such as: the degree of offset along the fissure, vein configuration, and the competence of the wallrock.

During the early stages of mineralization, offset of the vein walls was minimal and ore shoots formed where brecciation and permeability were greatest, namely at flexure points and fracture junctions. These ore shoots are small, seldom exceeding 2 meters in width, 15 meters in length, and 25 meters in depth. They are best illustrated in veins at La Virreyna and Cerro Reliquias (see Figure 14 and Plates 14 and 15).

Continued movements along certain veins, principally along those at Caudalosa and San Genaro, during mineralization, increased brecciation at flexure points and augmented offset of vein walls. In the northwestward-trending Caudalosa and San Pedro veins, where the north walls moved down and slightly to the right (right-lateral reverse

displacement), oreshoots tended to form where the dip flattened or the strike veered northwards (see Figure 14). These oreshoots are up to 75 meters long, 40 meters deep, and 3 meters wide. At the San Genaro mine continued movements increased offset of the vein walls a meter or two, forming numerous oreshoots 10 to 50 meters long, 50 to 100 meters deep, and 1.5 to 2 meters wide at flexure points.

The formation of gash or tension fractures in veins trending northeasterly and northwesterly also helped localize ore accumulation. Ore pockets at gash fractures are generally about 5 meters long, 20 meters deep, and 1 to 3 meters wide (see Figure 14). The fractures themselves are seldom mineralized for more than 2 or 3 meters from the main vein.

The role of wallrock in controlling vein width was not fully evaluated because intense alteration next to vein walls usually obscured the nature of the wallrock. Generally the best ground for the formation of oreshoots is massive andesite lava. This rock, because of its high competence, showed maximum offset of vein fissure walls, brecciated without much comminution, and permitted persistence of open fractures. Pyroclastic rocks, on the other hand, permitted only a minimum displacement of walls as they probably yielded plastically. They also were easily triturated, thereby clogging vein channels. Thus, veins entering massive pyroclastic rock tend to be narrow, poorly mineralized, and commonly feather out into small fractures. This is well shown at the east end of the San Pedro vein on the 4510 level (see Plate 10).

## 2. Zoning

Vertical and horizontal zoning, which is used herein as recog-

nizable and consistent spatial grouping of minerals with respect to one another, is evident on all scales from microscopic to district-wide at Castrovirreyna.

On a microscopic to local scale, zoning is shown by a consistent order of deposition of different minerals in space, in response to changes in the chemistry of mineralizing fluids in time, namely banding. This banding may be concentric, as shown by Figure 16, or symmetrical. Small-scale zoning also formed in response to localized equilibrium conditions is illustrated by the zonal arrangement of lead sulfantimonides and, to a lesser degree, silver sulfantimonides around galena and acanthite in bands which increase in antimony content the farther away they are from the pure sulfides (see Figures 38 and 49).

Vertical zoning is evident throughout the district by changes in grade or character of ore with depth. Lead and zinc tend to concentrate near the surface and copper tends to increase slightly in tenor with depth. Furthermore, at the San Genaro mine silver minerals are concentrated near the surface in considerable quantities by hypogene processes; but with increasing depth silver mineralization diminishes below economic grade without commensurate increases in the base-metal content nor decrease in the total amount of vein material. Throughout the district, the grade of ore diminishes in depth without a proportional decrease in average vein width.

On a district-wide scale zoning is evident in the distribution of the types of mineral deposits of the district. Base-metal veins are found throughout the district but are best developed in the western half around La Virreyna and Cerro Reliquias (see Plate 3). Lead sulfantimonide mineralization is confined to veins in the center of the district at

Caudalosa, Candelaria, and Madona; and enargite and famatinite are found exclusively at Caudalosa. Hypogene silver sulfantimonide mineralization is found only at San Genaro and Astohuaraca in the eastern third of the district.

The decrease in the mineralization temperatures of the deposits to the east, and the zonal concentration of base-metals, lead-antimony minerals, and silver-bismuth-antimony minerals from west to east implies preferential separation of base-metal elements, antimony, and silver and bismuth along thermal and chemical gradients extending from a source west and below the district. The deposition of antimonian or argentian minerals following base-metal mineralization in the central and eastern portions of the district indicates the concentration of antimony and silver in time. Thus, zoning is the product of chemical differentiation along persistent physico-chemical gradients in time and space.

## CONCLUSIONS

### Economic

1. Supergene ores of the Castrovirreyña type deposits were shallow and usually have been mined out by colonial mining operations, except in blind or covered veins that should be looked for.

2. The shallowness of supergene silver mineralization does not preclude the presence of economic concentration of base-metal minerals. Thus the shallow, low temperature veins in the Andean andesite rocks should be re-evaluated as base-metal producers, even though colonial Spanish mining operations cleaned out surficial silver ores.

3. The concentration of silver near the surface at San Genaro was mainly a process of hypogene reworking which caused the migration of silver along physico-chemical gradients towards the surface (to environments with lower temperature and pressure). Thus, it is not likely that economic concentrations of silver minerals in this type of deposit will be found below the present limits of silver ore.

4. In the Castrovirreyña district future prospecting for silver ore should be confined to the San Genaro area and eastward. Veins more than 500 meters long, trending easterly or northeasterly should be primary targets. Prospecting should be done to at least 5 meters depth, to get below the oxidized and leached portions of the veins. Around the San Genaro mine extensive prospecting also should be done, on the surface and underground, for secondary fractures (splits) associated with the main veins which carry rich ore pockets but have no surface expression.

5. Since ore minerals at Castrovirreyña were zonally distributed along physico-chemical gradients in space from a source of mineraliza-

tion west of the district, it is unlikely that base-metal mineralization at the eastern-most deposits, such as San Genaro, will increase in tenor at depth.

6. Good base-metal mineralization can be expected at depth in the central and western parts of the Castrovirreyna district, especially in veins trending northwesterly. The Caudalosa structure, from Madona to Bonanza, is particularly promising and should be drilled between the Madona, Caudalosa, Candelaria, and Bonanza mines.

### General

1. The Castrovirreyna deposits are typical of the shallow veins formed during Andean orogenic activities in late Tertiary time, and which are most abundant in the volcanic rocks near the crest of the Andean Cordillera. Vein fissures were formed by orogenic forces equivalent to east-west compression and the fissures were reopened during mineralization by the release of these forces. Mineralizing fluids were derived from the underlying Andean batholith.

2. The Castrovirreyna deposits are relatively shallow deposits, in which physico-chemical gradients in time and space controlled the distribution of metals out from a single source west of and below the district. Gradients in time are reflected in the order of deposition of vein-forming minerals, and gradients in space controlled the horizontal and vertical zoning. Recognition of these gradients depends on not only the presence of detectable mineralogical and compositional changes, but also the survival of this record of change through subsequent chemical activity.

3. The Castrovirreyna deposits represent an open chemical system in which the mineralizing fluids were constantly modifying the deposi-



tional environment while they themselves were undergoing modification. Thus, these deposits formed in a general state of nonequilibrium and true equilibrium was attained only in a local and restricted sense.

4. Mineral deposition at any one location took place with both rising and falling temperatures, as the site heated up and then cooled, causing both normal and reversed paragenetic sequences. Most minerals deposited with rising temperatures were redissolved with subsequent increase in temperature, leaving only vestiges; the bulk of existing vein material was deposited with falling temperatures.

5. Post-depositional reworking (dissolution, reprecipitation, rearrangement, and alteration of vein-forming minerals by their own mineralizing fluids) was an important phenomenon at Castrovirreyne. Although this phenomenon was only confirmed by the formation of non-equilibrium sulfantimonide assemblages from simple sulfides, reworking could explain many of the complex and controversial textures found at Castrovirreyne in the base-metal sulfides, and thus, may be more common than heretofore realized.

6. Complex ions probably played a dominant role in keeping antimony, silver, and bismuth in solution until lower temperature regimens, permitting these elements to be concentrated in low temperature and pressure environments, and to record the phenomenon of in situ reworking, by their interaction with existing minerals.

7. The mineralization at Castrovirreyne is the resultant product of a long period of deposition, dissolution, migration, and reworking, and is at best a fragmentary record of the paragenesis.

8. Thermochemical data and physico-chemical diagrams were of limited use in interpreting the chemistry of mineralization of the

Castrovirreyña deposits, because 1) most mineral suites did not form under the ideal conditions required, or 2) the stability fields of component minerals was unknown or too great to be indicative.

9. In summary, the Castrovirreyña deposits were formed under predominantly nonequilibrium conditions, from fluids containing colloids and complex ions, and the resulting minerals were reworked by subsequent mineralizing fluids. These conditions are not ideal in a chemical sense and are probably common at low temperatures. Thus, a chemical approach to the problem of low-temperature mineralization should take these nonideal conditions into account. Furthermore, vein mineralogy should be studied not only to establish an order of deposition, but also to find and interpret mineral assemblages that provide clues to the processes involved in metal transportation and deposition, and which are indicative of particular chemical and physical environments or trends in both time and space (paragenesis in the European sense).

**APPENDIX I**

**Mine Descriptions**

#### A. Astohuaraca Mine

The Astohuaraca mine is in the northeast corner of the district about 6 kilometers north of Santa Inés and 2 kilometers west of the village of Choclococha (see Plate 2). It lies at about 4700 meters altitude and is accessible over 2 kilometers of trail from the Pisco-Huancavelica road along the north shore of Laguna Choclococha.

Andesitic tuffs and tuff breccias underlie the area. The mine explored seven veins, six of which lie in an area 600 meters wide by 200 meters long. These six veins strike from North to N. 10° E., and dip from 70° SE. to vertical. They are 200 to 500 meters long and contain 20 to 50 centimeters of brecciated wallrock, gouge, and quartz, small amounts of barite, and pods and disseminations of galena, sphalerite, pyrite, and pyrargyrite. Veins are enclosed by 2 to 4 meters of bleached, argillized wallrock. The seventh vein, two hundred meters south of the main group, strikes N. 45° E., and dips 80° E. It consists of 1.5 meters of altered rock, with 20 centimeters of gouge and quartz containing disseminations of galena, sphalerite, pyrite, and pyrargyrite.

The Astohuaraca mine was worked sporadically from early colonial time (Monroy, 1769) to the 19th century. The ruins of a large camp (300 to 400 inhabitants) and a small smelter still stand at the mine. According to local legend the Incas worked the mine before the coming of the Spanish. Few surface workings are visible and the extent of the underground workings is unknown, as they were inaccessible at the time of this study. Water has always been a serious problem in the mine and, together with controversies over ownership, has discouraged recent attempts to reopen the mine.

The name Astohuaraca is derived from the Spanish word asta, meaning lance or spear, and the Quechua word huraraca, meaning silver, in allusion to the native wire silver found in the early days.

#### B. La Griega Area

The La Griega area is on the northern edge of the district, 4 kilometers north of the San Genaro mine, 6 kilometers west of the Astohuaraca mine, and just south of the lakes, Laguna Ccesococha and Laguna Yanacocha (see Plate 2). It lies at 4750 meters altitude and is reached over 6 kilometers of unsurfaced road which branches off the San Genaro mine road at Laguna Orcococha.

The area is underlain by andesite flows and flow breccias that are intruded by a small body of adamellite surrounded by quartz latite, and a larger body of quartz latite porphyry.

The five principal veins of the La Griega area trend N.  $75^{\circ}$  E., and dip  $50^{\circ}$ - $75^{\circ}$  N. or  $70^{\circ}$ - $75^{\circ}$  S. They crop out for 500 to 1250 meters, and are branching and sinuous, averaging 1 meter in width. Mineralization is irregular and consists of banded, vuggy quartz and silicified wallrock with disseminations, knots, and irregular bands of galena, small amounts of chalcopyrite, sphalerite, rhodochrosite, and pyrite, and rarely tetrahedrite. Finely crystalline encrustations, grainy masses, and fibrous veinlets of calcite are characteristic of these deposits.

The four northernmost veins lie within the quartz latite-adamellite body. They are developed by the La Griega mine, which consists of two adits, each 100 meters long, and numerous small workings. The Mateo vein, which lies 700 meters south of the La Griega mine, follows the southern edge of the southernmost quartz latite intrusive and consists of 1 to 3 meters of quartz with scattered disseminations of sulfides.

In 1957 this vein was being explored by a 45 meter shaft.

### C. Rápida Area

The Rápida area is 5.5 kilometers southwest of Astohuaraca and 2 kilometers northeast of the San Genaro mine camp (see Plate 2). It is accessible by road from the San Genaro mine road. The area is 1.5 kilometers across and covers the eastern extension of the veins of the San Genaro mine. The mineralization in this area is the low-grade, galena-sphalerite mineralization characteristic of veins found away from the important mineralized centers, rather than the silver sulfantimonides of San Genaro. Veins in the Rápida area range from 50 to 300 centimeters wide, and generally consist of banded massive quartz, siliceous breccia, small amounts of manganiferous carbonate, and thin bands or disseminations of sphalerite, galena, occasionally pyrite, and a little chalcopyrite. Sulfide mineralization is erratic and tends to be richest nearest the surface.

The area was actively worked during the latter half of the 19th century and includes more than ten mines and prospects. The only mine active at the time of this study was the Rápida mine in the southwest corner of the area. The Castrovirreyna Metal Mines Company operated the Rápida mine on lease from the Corporación Minera Castrovirreyna from 1952 to 1956, and produced over 50,000 tons of lead ore, driving about 600 meters of workings on four levels over a vertical range of 100 meters.

The Rápida mine lies on the east end of the Rápida vein, whose outcrop extends 1500 meters to the west, into the San Julián section of the adjacent San Genaro mine. This vein strikes sinuously from N. 60° W. to due west, having an average trend of N. 70° W. The mine also

developed another vein striking N. 70° W., that lies 75 meters north of the Rápida vein, as well as a mineralized crossover between the Rápida vein and the N. 70° W. vein mentioned above. The crossover strikes N. 50° W. These three veins explored at the Rápida mine are nearly vertical or dip slightly to the north and average 125 centimeters wide.

Sulfide mineralization is concentrated near the surface in and around the crossover vein between the two east-west veins; ore tenor does not extend to more than 100 meters in depth and about 50 meters on either side of the crossover junctions. Vein widths do not decrease notably with the decline in tenor.

The Eleonora prospect, about 300 meters north of the Rápida mine, has several adits, inclined workings, open cuts, and pits which explore three veins trending N. 30° W. They dip steeply to the south, are 75 to 150 centimeters wide, and crop out for 150 to 250 meters..

At the Siglo Nuevo prospect, one kilometer north of the Rápida mine, four or five small inaccessible adits explore three small veins that strike N. 50°-70° E., dip 70° NW., and are 50 to 150 centimeters wide. Enoch (private report, 1905) stated that the quartzose gossan of these veins contained argentite and as much as an ounce of gold per ton, but that otherwise mineralization was poor. Masias (1929) reported that the ore generally ran 100 ounces of silver per ton and the ore pockets contained 2000 to 3000 ounces of silver per ton. Accessible vein exposures, both surficial and underground are not well mineralized.

The Aranzazu mine, about one kilometer west of the Rápida mine, explores the Aranzazu vein on two levels only 10 meters apart vertically and less than 100 meters long. This vein strikes from N. 55° to 80° W., trending N. 70° W., and dips steeply to the north. It crops out for

about 2000 meters and is the eastern extension of the Bella vein, of the San Julián section of the neighboring San Genaro mine. At the Aranzazu mine, the Aranzazu vein is low grade, consisting of massive quartz and minor galena and sphalerite, with erratic silver values. It averages about 150 centimeters wide.

The Pampamachay adit, 0.5 kilometers south of the Rápida mine, is 185 meters long. It was driven to cut the eastern end of the Trabajo (Grau) vein, which is one of the principal veins of the San Genaro mine. Although the Trabajo vein was not cut, a low-grade stringer was intersected at the face and developed for 20 meters before operations were stopped in 1955. This stringer strikes N. 60° W. and ranges in width from 10 to 100 centimeters.

#### D. San Genaro Mine

The San Genaro mine is the largest and one of the oldest in the district. It was worked in early colonial times and has been in operation more or less continuously since 1860. This mine lies 2.5 kilometers north of Laguna Orcococha, just northwest of Laguna Yanacocha (see Plate 2), and is reached by 7 kilometers of unsurfaced road that branches from the Pisco-Huancavelica road at the east end of Laguna Orcococha. Ore is concentrated in a 130 tons/day flotation mill, located a few hundred yards from the main portal. Power is supplied to the mine and mill by a 1500 kva hydroelectric plant at Santa Inés, 7 kilometers southeast of the mine, on the west shore of Laguna Choclococha.

The San Genaro mine has about 20 kilometers of workings on 13 levels, most of which are accessible. Present operations include the opening of old, near-surface workings. Vertical spacing between levels is 10 to 40 meters, and averages about 30 meters. The portal of the



principal or San Genaro level lies at an altitude of 4773 meters above sea level. The lowest level, the 105 level, lies at 4668 meters and the highest level is at 4956 meters altitude. The deepest workings, however, seldom extend more than 200 meters below outcrops. The mine has two shafts, one on the Trabajo vein which connects the San Genaro level with the 35, 70 and 105 levels, and another on the San Julián vein, from the 70 and 105 levels.

The best silver mineralization at San Genaro lies within an oval area, about 1200 meters by 800 meters, centered around Cerro Quespisisa (see Figure 56). This area is underlain by massive andesite and minor andesite igneous breccia, and is surrounded by bedded andesite lavas and pyroclastics that tend to dip away from Cerro Quespisisa, suggesting that it is the core of a volcanic vent. West of this area silver veins pinch out upon entering the bedded volcanic rocks. To the east the larger veins extend 500 meters or more into the bedded volcanic rocks, but beyond the limits of the massive andesite only contain mediocre to fair lead-zinc mineralization similar to that found throughout the district.

The larger veins at San Genaro are 50 to 200 centimeters wide, averaging 120 centimeters, and the smaller ones range from 10 to 50 centimeters wide and average about 30 centimeters. Vein material generally is not fractured but in places it has been brecciated and re-cemented during mineralization (see Figure 10).

The veins are typical of shallow epithermal bonanza-type silver deposits, and contain complex silver ores that are enriched towards the surface. Sulfide minerals are galena, sphalerite, chalcopyrite, tetrahedrite, pyrargyrite, polybasite, miargyrite, acanthite, pearceite,

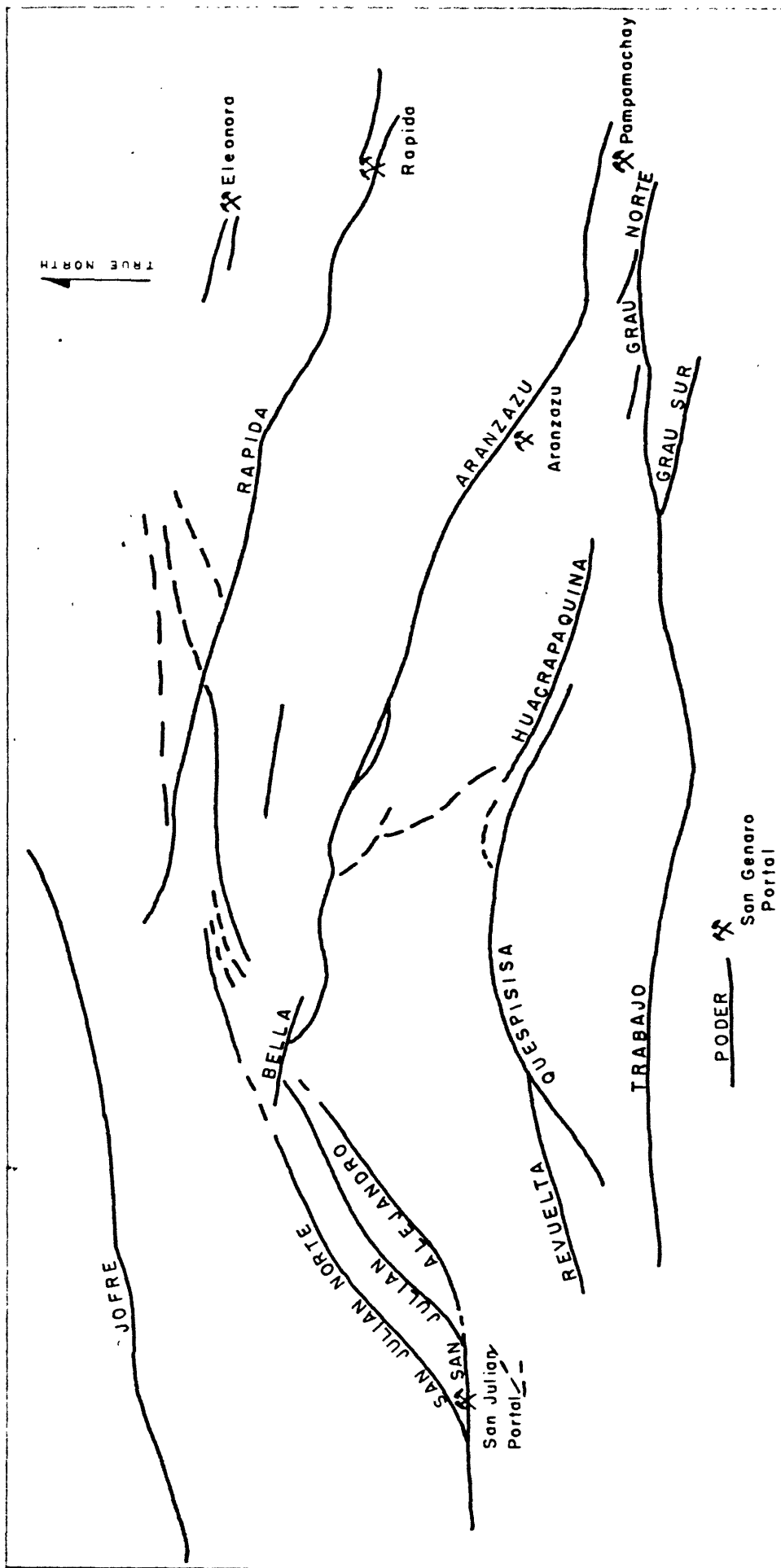


FIGURE 56 — SKETCH MAP SHOWING PRINCIPAL VEINS OF THE SAN GENARO AREA

After W. A. Lyons, 1961

aramayoite, and stibnite. Gangue minerals are quartz, pyrite, barite, siderite, rhodochrosite, hematite, marcasite, amethyst, quartz, clay minerals, and sericite. Vein material is porous and comb structures, vugs, and druses are abundant. Cavities are lined with small quartz crystals, or, less commonly, crystals of barite, galena, sphalerite, pyrargyrite, polybasite, miargyrite, and tetrahedrite. Crystals generally are not larger than 3 millimeters. Many cavities are completely filled with crustified aggregates of the above minerals.

Crustified banding is well developed, and cockade ore was noted where breccia fragments are present. Banding tends to be symmetrical and well-defined. Most bands are massive milky quartz containing disseminated sericite or hematite. Others are quartz with disseminated sulfides. Still other bands are green or amethystine quartz, sericite, siderite, or, rarely, pure galena or sphalerite. Banding is oscillatory in places and bands are sinuous, irregular, and even colloform, ranging in width from 0.5 to 30 centimeters. The generalized sequence from the center of a typical vein outward is: crystalline quartz with silver sulfide and sulfantimonides, milky quartz, quartz with hematite needles, quartz with massive chalcopyrite and disseminated pyrite, and, finally, quartz with disseminations of sphalerite and galena.

Silver mineralization can be grouped into five general types based on mode of occurrence and mineralogical associations.

1) Near-surface silver mineralization is characterized by sooty or plumose acanthite coating primary vein minerals, native wire silver enclosed in quartz and barite, and thin films of acanthite and pyrargyrite coating and replacing primary sulfides. Silver ores of this type are restricted to the upper 25 to 40 meters of the vein, and are most

abundant from 5 to 20 meters below the surface. Old reports stated that surficial ores, probably of this type, had as much as 5 percent silver. This mineralization is considered supergene.

2) The most important type of silver mineralization, from the standpoint of modern mining economy, is the enriched sulfide ore in the upper 100 meters of the veins. Silver content of this ore is lower than in the surficial ores but is notably higher than in the other types. In recent operations, ores of this type contain up to 5 kilograms of silver per ton, and average between 300 and 600 grams of silver per ton. This silver mineralization consists of massive to semiporous crystalline aggregates of pyrargyrite, miargyrite, and polybasite, associated with quartz and barite, and contains small amounts of sphalerite, galena, tetrahedrite, and aramayoite. Sulfide minerals cement brecciated vein quartz, line vugs in quartz, or form large pods; and are interpreted as products of hypogene enrichment.

3) A third type of silver mineralization, also common in the upper 100 meters of the veins, is associated with colloform banded gangue. Silver minerals are principally pyrargyrite and miargyrite, with lesser amounts of polybasite; they are invariably associated with siderite, quartz, sericite, pyrite, and tetrahedrite. Silver minerals are generally restricted to those bands containing quartz (see Figure 51) and were deposited prior to reworking and hypogene enrichment of silver.

4) A fourth type of silver mineralization consists of anhedral grains of pyrargyrite, miargyrite, polybasite, pearceite, and scanthite in narrow seams of quartz. Silver antimonides commonly form good crystals where quartz is vuggy. The quartz is clear and medium grained,

and contains only the aforementioned silver minerals and minor amounts of gold (see Figure 49). These quartz seams cut the base-metal portions of the veins and are common throughout the known extent of the silver veins. This type of silver mineralization represents unenriched hypogene ore.

5) The fifth and most widespread type of silver minerals consists of thin films of fine- to medium-grained crystalline aggregates of pyrargyrite and miargyrite filling or coating cracks in primary vein material. Silver minerals are associated with tetrahedrite, sericite, galena, and sphalerite and they coat both sulfide and gangue minerals along small irregular seams and cracks cutting massive vein material. These films of silver minerals are seldom more than 1 millimeter thick. They represent final hypogene mineralization.

Base-metal mineralization at San Genaro can be separated into two general types, representing early and late stages of mineralization. The older base-metal sulfides, which include galena, tetrahedrite, sphalerite, chalcopryrite, and pyrite, are found as fine-grained disseminations, pods or thin stringers in massive banded quartz. Bands containing these sulfides are 1 to 10 centimeters wide and are generally found nearer the vein walls than the centers. The silver content of these base-metal bearing bands is low, probably less than 100 grams per ton, even though galena and tetrahedrite carry silver (see Tables XXVIII and XXXVI). Silver minerals are rare and when present replace base-metal sulfides. Abundant quartz and disseminations of hematite are the principal gangue minerals associated with this type of mineralization.

The late base-metal mineralization consists of small amounts of galena, sphalerite, tetrahedrite, and pyrite disseminated in quartz bands, and coats or fills cavities in vuggy quartz as small crystals or grains. This late base-metal mineralization is associated with the last three types of silver mineralization.

In general base-metal tenor is too low to be mined alone economically: lead averages about 1 percent, zinc about 1.5 percent, and copper about 0.1 percent or less. Base-metal values are relatively constant in depth, increasing only slightly towards the surface, thus, where silver values are less than about 200 grams per ton mining becomes uneconomical. No attempt is made to recover the zinc at San Genaro, but copper and lead are recovered with the silver.

The San Genaro mine has exploited about seven strong veins and more than 13 minor veins in the southern and western portion of the vein network around San Genaro (see Figure 56). The eastern portion of this network is the Mpida area, discussed previously, and the northern portion is explored by a few inaccessible adits. The veins explored in the San Genaro mine lie in three systems 200 to 400 meters apart, each of which has a major vein and numerous splits (see Figure 56). The major veins, from north to south, are San Julián, Quespisisa, and Trabajo. The San Julián and Quespisisa vein systems are roughly parallel, trending northeasterly to northwesterly. The Trabajo vein, however, trends easterly throughout its length. Minor veins split off at small angles from either the footwall or the hanging wall of the major veins, and are, in general, narrow and low grade for the first 10 to 15 meters, after which they may increase in width and mineralization and strike parallel the parent vein.

The veins of the Trabajo and Quespisisa systems have been worked out, and activity is currently concentrated in the central and eastern part of the San Julián system.

The southernmost vein in the San Genaro mine, the Trabajo, trends N.  $85^{\circ}$  E., generally dips steeply north, and crops out for more than 2 kilometers. This vein has been worked from the surface to the 105 level, a vertical distance ranging from 140 to 170 meters, and has been explored for more than 2000 meters along the San Genaro and Niño Jesús levels (see Plate 5). Locally the Trabajo vein is sinuous and erratic in strike, dip, and width; strike ranges from N.  $60^{\circ}$  E. to N.  $70^{\circ}$  W., dip lies between  $70^{\circ}$  S. and  $60^{\circ}$  N., and width ranges from 20 to 200 centimeters. Vein material usually consists of strongly banded, massive quartz and silicified wallrock, with bands, disseminations, and pods of sulfides. The Trabajo and related veins are more massive than others in the mine, and contain more hematite, siliceous breccia, and less gouge and clay.

The widest and best mineralized sections of the Trabajo veins strike approximately east. These sections average 125 centimeters wide and are 50 to 300 meters long. They are connected to one another by narrow, weakly mineralized crossovers, which generally strike either N.  $60^{\circ}$  W. or N.  $60^{\circ}$  E. and are 30 to 200 meters long. The central and western parts of the Trabajo vein have yielded the largest amounts of ore, and are stoped over a vertical distance of about 75 meters, from the surface to below the 35 level (4738 meters elevation) and along the strike for nearly 600 meters. Silver content decreases steadily with depth and mineral exploitation was not economic beyond about 15 meters below the 35 level. Explorations on the 70 level (4703 meters eleva-

tion) and 105 level (4663 meters elevation) revealed only low-grade lead-zinc mineralization.

The eastern end of the Trabajo vein, called the Grau vein, is particularly erratic in both attitude and mineralization and is accompanied by numerous splits and parallel structures. The width of the Grau vein averages 60 centimeters, and metal content is lower than in other parts of the Trabajo vein, and only a few isolated shoots and splits have yielded ore. The eastern end of the Trabajo vein feathers out in bedded volcanics, whereas the western end terminates abruptly in pyroclastic rocks.

Minor veins associated with the Trabajo vein have produced good ore in limited amounts. They strike from N. 60° to 85° E. and dip steeply north or south, paralleling or diverging slightly from the Trabajo vein. These minor veins generally have a single ore shoot, 10 to 40 meters long by 20 to 50 meters high by 50 to 125 centimeters wide, located 15 to 40 meters from the main vein. In the eastern section, most of the minor veins lie on the north side of the Trabajo vein and trend east to northeast. Elsewhere, they lie on the south side of the Trabajo vein and trend southwest. From east to west these minor veins are: Grau Norte, Contacto, Escondido, Baertl, Milagro, Genarito, Salvadora, and Poder (see Plate 5). The Baertl, Milagro, Genarito and Salvadora veins have produced the most ore.

The Quispisisa vein lies about 200 to 300 meters north of the Trabajo vein (see Plate 5). It is arcuate, trending east to northeast, dips steeply to the northwest, and crops out for about 1000 meters. It has been explored for about 700 meters horizontally and over 200 meters vertically, from the surface to the 70 level. The western half of the



Quespisisa vein, which is the best mineralized, strikes from N. 45°-65° E. and dies out to the west shortly after entering the bedded volcanic rocks. The eastern part of the vein trends easterly and splits into several barren fractures, the largest of which strikes N. 80° E. to N. 80° W. Dips of the Quespisisa vein range from 50° to 75° NW. Vein width ranges from 75 to 150 centimeters, but is relatively constant in any one section.

Vein material usually is well-banded massive quartz with bands, disseminations, and pods of fine-grained sulfides. Silver minerals are more obvious in the Quespisisa vein than in the Trabajo vein, but not so prominent as in the San Julián section. The Quespisisa vein and its splits contain more manganiferous siderite and anathyst than the others. Silver ore in this vein bottoms near the 70 level (4703 meters altitude). The richest hypogene ore was in the central part of the vein between the 35 level (4738 meters altitude) and the San Antonio level, 90 meters above. The most famous of several excellent ore shoots was the Boya de la Cruz, yielded 3,000,000 ounces of silver (Masias, 1929).

Only two minor veins associated with the Quespisisa vein have produced ore: the Revuelta-340 and the Huacrapaquina veins. The Revuelta-340 vein splits to the northwest off the hanging wall of the Quespisisa vein (see Plate 5), and consists of a narrow crossover section called the 340 vein, and the Revuelta vein. The Revuelta vein roughly parallels the Quespisisa vein, strikes N. 60°-70° E., dips 70°-80° N., and is 150 to 190 meters long. The 340 vein segment of the split strikes N. 85° W., dips 80°-85° N. and is 100 to 150 meters long. It is weakly mineralized for the first 10 to 15 meters from the Quespi-

sis vein. The width of the Revualta-340 vein ranges from 10 to 300 centimeters and is erratic in attitude and metal content.

The Huacrapaquina vein splits off to the east from the footwall of the Quespisisa vein at about the San Antonio level. It trends east, dips about  $60^{\circ}$  N. and nearly parallels the easternmost, barren section of the Quespisisa vein. It has been explored on three levels for about 300 meters horizontally and probably 40 meters vertically. The vein averages 60 centimeters wide. It is largely mined out and most of the workings are now inaccessible.

The San Julián section is about 400 meters northwest of the Quespisisa vein and contains several long veins and important splits occupying a belt about 200 meters wide and 850 meters long (see Plate 5 and Figure 56). Most of these veins trend northeast and terminate against the north-westward-trending Bella-Aranzazu vein, which extends east to the Rápida area. The best ore has been found in the Bella vein and the western half of the San Julián veins.

The attitude of the San Julián veins is erratic; strikes range from N.  $40^{\circ}$  E. to E.-W., dips from  $65^{\circ}$  N. to  $60^{\circ}$  S., and widths from 20 to 300 centimeters. Minor veins, which generally split off the footwall of the principal veins at flexure points are abundant (see Plate 6). These minor veins are usually narrow, low grade, and die out within 5 to 10 meters. Some of them contain small pockets of ore and a few have sizable ore shoots.

Vein material of the San Julián veins consists of thinly banded, porous, variegated quartz, and thin bands, knots, and disseminations of sulfide minerals. Individual bands are thin and vugs and open comb structures are common. Clay and gouge are more abundant in the San

Julían veins than other veins at San Genaro; and vein material is slightly brecciated, as in the Trabajo vein, suggesting postore movement. The silver and copper content of the San Julián veins is higher than in the other veins at San Genaro, whereas the lead and zinc contents are slightly lower.

The San Julián vein is the principal vein of the group. It crops out for at least 750 meters, trends N.  $50^{\circ}$  E. and dips  $70^{\circ}$  N. to  $70^{\circ}$  S. The San Julián vein has been worked for 700 meters horizontally and on eight levels and numerous surface workings, to a depth of over 200 meters below its outcrop. Silver ore bottoms at the 70 level, 100 to 125 meters below the surface.

The San Julián Norte vein splits northeast off the hanging wall of the west end of the San Julián vein and strikes parallel to it, but has a lower dip, about  $75^{\circ}$  S. It crops out for at least 750 meters and may continue another 1000 meters to the northeast of the Bella-Aranzazu vein. The San Julián Norte vein has been worked from the surface to the 35 level, a vertical distance of about 140 meters.

The southernmost vein of the San Julián group is the Alejandro vein, which lies southeast of the San Julián vein, which it may join at its northeastern and southwestern ends. The Alejandro vein strikes N.  $40^{\circ}$  E., dips  $80^{\circ}$  N., and crops out for about 600 meters horizontally, on five levels over a vertical range of 130 meters.

The San Julián Sur vein, another important vein in this group, splits off to the southwest from the footwall of the western end of the San Julián vein, below the San Genaro level. It trends N.  $60^{\circ}$  E., dips steeply to the south but has no outcrop. This vein explored for 250 meters horizontally and from the 35 level (4738 meters elevation) to

the 105 level (4663 meters elevation), but has only produced ore from the San Genaro level (4773 meters elevation) to the 70 level (4733 meters).

The Bella vein, against which the San Julián veins terminate (see Figure 56) strikes N. 80° W. and dips 45° S. It has been explored for over 350 meters horizontally and 100 meters vertically on four levels. This vein is the western end of the Aranzazu vein and was opened up after the writer's last visit to the mine.

### E. The Madona Area

The Madona area is on the west shore of a northern arm of Laguna Orcococha, about 3 kilometers west of San Genaro and 1.5 kilometers east of Caudalosa (see Plate 2). The three principal mines of the area, Madona, Caudalosa No. 2, and Pitonisa, are owned by the Corporación Minera Castrovirreyna, but only the first two were active from 1954-1957.

Andesitic pyroclastics, mostly lapilli or ash tuffs, capped by andesite flow rocks underlie the Madona area. Four veins or mineralized zones striking N. 70°-85° W., and dipping 65° N. to vertical, were recognized in an area about 750 meters wide. These veins probably are the eastward continuation of the veins of the Caudalosa mine, the Pitonisa vein corresponding to the San Pedro vein and the Madona mineralized zone corresponding to the Caudalosa vein. The presence of small amounts of stibnite, zinkenite, and rhodochrosite, minerals characteristic of the San Pedro and Caudalosa veins, supports this structural correlation.

The northernmost vein, Pitonisa, trends about N. 80° W., and consists of a series of N. 70° W. veins in echelon and connected by

crossovers striking N.  $60^{\circ}$ - $85^{\circ}$  E. Individual veins dip  $70^{\circ}$  S. to vertical and consist of 1 to 2 meters of bleached, argillized rock enclosing 10 to 70 centimeters of breccia and gouge with 1 to 40 centimeters of quartz and small amounts of sphalerite, galena, tetrahedrite, stibnite, and pyrite. Mineralization is generally weak. An adit 120 meters long near the lake shore and several pits and trenches explore this vein.

The Caudalosa No. 2 vein lies about 300 meters north of the Pitonisa vein. It has been explored by an adit 200 meters long and a 30 meters winze. This vein strikes N.  $85^{\circ}$  W., dips  $70^{\circ}$  N. to vertical, and lies in andesitic tuff just below its contact with the overlying lava. A rich ore shoot in this vein was found just below the tuff-andesite contact; it was 100 meters long, about 15 meters high, and averaged over a meter wide. It is 40 to 100 centimeters wide and consists of a brecciated argillized wallrock impregnated with silica and disseminated galena and sphalerite, and cemented by quartz, rhodochrosite, and massive galena, sphalerite, chalcopryite, tetrahedrite, and small amounts of pyrite and hematite. To the west, approximately at the contact of the tuff with the overlying andesite, the Caudalosa No. 2 vein dies out against a weakly mineralized vein striking N.  $65^{\circ}$  W. and dipping  $70^{\circ}$  to vertical.

The Madona veins lie about 200 meters north of Caudalosa No. 2. They have been developed from two adit levels, 40 meters apart vertically, the lower adit having more than 770 meters of workings and the upper adit 300 meters. The veins lie in a zone 20 to 40 meters wide which trends N.  $75^{\circ}$  W. (see Plate 7). Within this zone, two long veins and various smaller veins and splits lace back and forth with two pro-

dominant trends, N. 85° E. and N. 65°-75° W. The veins are 20 to 125 centimeters wide and contain gouge and brecciated altered wallrock cemented and partially replaced by vein minerals or enclosing a stringer of vein minerals 10 to 40 centimeters wide. Vein minerals include quartz, rhodochrosite, calcite, galena, sphalerite, tetrahedrite, chalcopryite, and pyrite. Vein material is banded and medium- to coarse-grained. Vein walls are sharp and marked by 5 to 20 centimeters of gouge. Mineralization is erratic, and best developed in sections striking N. 65°-75° W. Ore shoots are small, seldom exceeding 10 meters in length, 1.5 meters in width, and 20 meters in height.

F. Caudalosa Mine

The Caudalosa mine is in the center of the district, 2 kilometers north of the west end of Laguna Orcococha (see Plate 2). It is reached over 3 kilometers of narrow unsurfaced road that connects with the Pisco-Huancavelica road just southwest of Laguna Orcococha. The mine explores two strong veins, the Caudalosa and the San Pedro veins, which are exposed on the face of a cliff of andesitic lavas and pyroclastic rocks. These veins were worked superficially during colonial times, but extensive underground operations were not started until the end of the 19th century. The mine has nearly 15 kilometers of galleries, and workings extend from 4530 to 4830 meters elevation (see Plate 8). A two compartment shaft extends from the surface to the 4570 meter level and services the three principal levels of the mine, the 4640, 4610, and 4570 meter levels. The upper workings are adit levels, eight of which are on the Caudalosa vein and four on the San Pedro vein. The lowest level (4530 meter level) was driven after the work for this report was done, so no information is available.

Lead, copper, and zinc are the principal metals mined and concentrated at Caudalosa. About 50 to 250 grams of silver per ton, 10 to 20 grams of bismuth per ton and 0.1 to 0.5 grams of gold per ton are also recovered in the lead-copper concentrates. Ore is concentrated at the mine in a sink-and-float and flotation plant, which can handle 150 tons per day. Power for the mine and mill are supplied by diesel engines located at the mine.

The Caudalosa and San Pedro veins trend west-northwest, and dip steeply to the south (see Plates 9 and 10). They diverge slightly towards the east, and lie 120 to 250 meters apart. These veins are at least two kilometers long, and probably extend at least from the Candalaria mine, northwest of Caudalosa, to the Madona area in the southeast, a total distance of 3 kilometers. These two veins average 90 centimeters wide but are up to 5 meters wide in places. They are composed of alternating bands, 1 to 75 centimeters wide, of gouge, breccia, altered wallrock, quartz, rhodochrosite, and sulfides. Sulfide stringers are 1 to 50 centimeters wide, and two or more stringers may be present. Both veins, and in particular the Caudalosa, are accompanied and in a few places cut by late gouge-filled faults containing stibnite. Surface mapping indicates reverse dip slip movement along the vein zones with an apparent vertical displacement of 25 to 30 meters.

Wallrock in the upper part of the Caudalosa mine is andesite lava, but below the Temerario level (4685 meters altitude) andesite pyroclastics predominate. These pyroclastic rocks consist of fine- to medium-grained andesite crystal and ash tuffs, scattered lenses of andesite, lava, and, in the lower portions, subordinate tuff breccias. This pyroclastic unit, 130 meters thick just south of the San Pedro

vein, can be traced to the Madona and San Genaro areas (see Plate 2).

Vein minerals consist of stringers, knots, and disseminations of sulfides in brecciated, partly silicified wallrock, gouge, quartz, some rhodochrosite, and barite; rarely gypsum, realgar, and orpiment. Galena, pyrite, sphalerite, stibnite, and sulfosalts of lead and copper are the abundant sulfides. The sulfosalts are predominantly antimonian, and are, in order of abundance, tetrahedrite, semseyite, geocronite, zinkenite, bournonite, enargite, famatinite, and chalcostibite. The lead antimonides, i.e., semseyite, geocronite, and zinkenite, are best developed between the San Felipe level (4760 meters elevation) and the 4610 meter level in the Caudalosa vein, and between the San Pedro level (4700 meters elevation) and the 4610 meter level in the San Pedro vein. Although both veins contain bournonite and tetrahedrite throughout, these and other copper sulfosalts are best developed at and below the 4610 meter level.

Banding of sulfides is well developed, although individual bands may be irregular or lenticular. The bands are from 1 to 75 centimeters wide. Although sulfides show symmetrical banding the vein as a whole is usually asymmetrically banded (see Figure 11). Vugs and cavities are not common, and when present are generally only 1 to 5 centimeters in diameter and usually lined with quartz, pyrite, sphalerite, or lead or copper sulfosalts, or late minerals such as stibnite, barite, or gypsum. Some cavities are filled with botryoidal growths of sulfides, individual knobs of which are 5 to 10 centimeters in diameter at the base and 1 to 5 centimeters high and are made up of concentric layers of different sulfides (see Figure 16). Mineralization is not uniformly distributed along the veins, and especially on the lower levels, and



long stretches of low-grade or barren material, consisting mainly of gouge, partly silicified breccia, and quartz are present.

The principal factor controlling ore deposition was vein attitude; the most favorable sites for ore accumulation were sections with low dips ( $45^{\circ}$ - $65^{\circ}$ ) (see Figure 14). Larger ore shoots attain lengths of 50 to 75 meters, heights of 20 to 40 meters, and range in width from 1 to 3 meters. Smaller ore pockets, 5 to 15 meters long, 5 to 20 meters high, and 1 to 2 meters wide, are common at flexure in both dip and strike.

Splits are not very important and usually mineralized for only short distances. The best mineralized of these are: 1) a loop splitting off the hanging wall of the Caudalosa from the Temerario to the San Felipe levels; 2) a vein splitting off to the east of the 4640 level of the Caudalosa vein and developed for 50 meters on the Temerario level; and 3) an unnamed vein developed for 75 meters on the Victoria Nueva level, that is probably a split to the southeast off the hanging wall of the San Pedro vein. Within 200 meters of either side of the main veins four or five weakly mineralized structures have been explored without promising results. These structures are parallel to the main veins and have no visible connection with them.

Caudalosa, the northernmost of the two major veins, is the best mineralized (see Plate 9). It has been developed for 245 meters vertically and 40 to 1200 meters horizontally on ten levels. It strikes N.  $80^{\circ}$  W. at the eastern end and N.  $60^{\circ}$  W. at the western end. Dips range from  $70^{\circ}$  S. to  $70^{\circ}$  N., but tend to be steeply southward. Width ranges from 10 to 200 centimeters and averages about 85 centimeters. Banding in the Caudalosa vein is more complex and individual widths narrower than in the San Pedro vein. Rhodochrosite, stibnite, and the

sulfosalts are more abundant in the Caudalosa vein, and enargite, famatinite, and chalcostibite are restricted to it.

The San Pedro vein has been developed for 260 meters vertically and for 60 to 100 meters on seven levels (see Plate 10). It strikes N.  $80^{\circ}$  E. at the eastern end and N.  $50^{\circ}$  W. at the western. Dips range from  $40^{\circ}$  S. on the upper levels to  $60^{\circ}$  N. on the lower. Widths range from 20 to 200 centimeters and average about 95 centimeters. Vein material is more siliceous, less mineralized, and contains more breccia than the Caudalosa vein. Barite is more common in the San Pedro vein, especially in the upper levels, than in the Caudalosa vein.

#### G. Candelaria Area

The Candelaria area is 1.5 kilometers northwest of Caudalosa (see Plates 2 and 3), at an altitude of 4750 to 4850 meters, and is only accessible by trail from Caudalosa.

The andesite flow rocks of the area are cut by a belt of weakly mineralized veins, which is 150 to 250 meters wide and over 1000 meters long. The belt trends N.  $70^{\circ}$  W. on its eastern end, and N.  $80^{\circ}$  E. to the west. This belt is probably the continuation of the Caudalosa and San Pedro veins of the Caudalosa mine, but correlation is tentative as the intervening area is covered with glacial debris.

Mineralization within this belt follows two principal sets of fractures, one striking N.  $70^{\circ}$  W. and dipping  $60^{\circ}$ - $90^{\circ}$  N. to vertical, and the other striking N.  $50^{\circ}$  W. and dipping  $70^{\circ}$ - $75^{\circ}$  N. A minor set of mineralized fractures striking N.  $60^{\circ}$ - $90^{\circ}$  E. and dipping  $70^{\circ}$ - $90^{\circ}$  N. is common in the western end of the zone.

The veins in the Candelaria area are 20 to 100 centimeters wide and crop out for 50 to 1000 meters. They contain principally breccia, gouge

and silicified rock, with 5 to 50 centimeters of quartz, pyrite, sphalerite, galena, tetrahedrite, geocronite, semseyite, sinkenite, and disseminated hematite. Overall mineralization is generally shallow and contains few sulfides. Mineable quantities of sulfides were only seen in one vein, striking N. 70° W.

The principal underground workings of the area are the three adits of the Candelaria mine. The lowest of these, level 1, lies at 4740 meters altitude, and explores the probable extension of the Caudalosa vein for more than 175 meters. Level 2, a 225 meter crosscut, lies 25 meters higher, and level 3 is a small crosscut. Elsewhere within the area the veins have been explored by numerous pits and small adits which are all inaccessible.

#### H. Bonanza-Seguridad-Yahuarcocha Area

The Bonanza-Seguridad-Yahuarcocha area is in the northwest corner of the district, about 3 kilometers north of Laguna La Virreyna (see Plates 2 and 3). This area is about 750 meters wide and extends from the north slope of Cerro Santa Cruz to Laguna Yahuarcocha, about 3.5 kilometers to the west. It is reached only by trail from Laguna La Virreyna or the Caudalosa mine. Altitudes of the mine workings range from 4500 to 4750 meters.

The veins of this area were certainly known to Spanish colonial mines, but apparently no extensive work was done until the end of the 19th century. Early in the 20th century Augustin Arias and others operated mines in this area, but production was small and mining activity short-lived. The ruins of two large mine camps at Bonanza and Yahuarcocha and remnants of a well-constructed wagon road indicate former activity, which opened an estimated 2500 meters of workings in

some 15 to 20 adits.

Flat-lying andesite flows and flow breccias interbedded with small amounts of andesitic pyroclastics underlie the area. On the north slope of Cerro Santa Cruz are a series of dike-like intrusions of quartz latite porphyry, which fall along a single arcuate line striking N.  $75^{\circ}$ - $90^{\circ}$  E.

The Bonanza-Seguridad-Yahuarcocha area has at least 20 veins that can be divided into two principal systems, one striking N.  $45^{\circ}$ - $65^{\circ}$  E. and the other striking N.  $60^{\circ}$ - $75^{\circ}$  W. Most veins dip steeply north or south, the only notable exception is the Bonanza vein which dips  $45^{\circ}$  S. Most veins are from 25 to 300 meters long; the Bonanza vein, however, on the east end and two veins on the west end of the area crop out for more than 1000 meters. Veins of both systems are weakly mineralized and consist of 20 to 100 centimeters of argillized or silicified, brecciated wallrock and gouge with sporadic stringers and lenses of quartz. The stringers of quartz are 10-40 centimeters wide and contain disseminations or veinlets of pyrite, sphalerite, some galena, and occasional tetrahedrite and chalcopyrite.

A third very weakly mineralized set of fractures strikes N.  $25^{\circ}$ - $30^{\circ}$  E. and dips about  $65^{\circ}$  S. These veins seldom exceed 20 centimeters in width and either split off the N.  $45^{\circ}$ - $65^{\circ}$  E. veins or cut them with a slight offset.

The easternmost mines and prospects of this area lie near the head of the valley Callejón Grande. Mineralized structures on both flanks of Callejón Grande have been explored by some 10 adits, most of which are inaccessible. Only the Bonanza vein, on the south side of the valley produced ore.

The principal workings on the Bonanza vein are the Ruperto adit, at the eastern end of the vein, and the Bonanza mine, 650 meters to the southwest. Both of these workings are inaccessible.

The Seguridad area is 1.5 kilometers southwest of the Bonanza mine, on the east side of Callejón Grande. The area has six inaccessible adits on five or six short veins.

The Yahuarcocha area lies 750 meters east of Seguridad on the west side of Callejón Grande. This area, which is just east of Laguna Yahuarcocha, has six adits on at least 10 mineralized structures.

#### I. Cerro Reliquias Area

The Cerro Reliquias area centers around Cerro Reliquias on the western end of the district, and is 4 kilometers west of the Caudalosa mine and 3 kilometers east of the Banco Minero's Pacococha mill (see Plate 2). The area is about 3 kilometers long by 1 to 1.5 kilometers wide and lies just east of Laguna La Virreyna and Laguna San Francisco.

The Cerro Reliquias area was one of the most active and productive during the early history of the district. More than 100 adits, inclines, trenches, opencuts, and pits are evident, but most of them are inaccessible. In recent years activity has been sporadic but steadily increasing. Early mining operators sought the enriched surficial native silver and silver sulfide ores, more recently silver antimonides and argentiferous tetrahedrite were exploited. Currently the area is producing principally lead and zinc, with minor amounts of copper and silver. By 1958, the Santa Teresita and Matilde mines together were producing almost 10,000 tons of ore per year.

Over 50 veins are known in the Cerro Reliquias (see Plate 9), ranging from 25 to 1200 meters long, and from 25 to 175 centimeters wide. Veins

of this area can be divided into two groups on the basis of attitude. The largest and most productive veins strike N.  $45^{\circ}$ - $70^{\circ}$  W. and dip  $60^{\circ}$  S., and include, from north to south, Yunque, Perseguida, Saca Si Puedes, Matilde, El Dollar, and Restauradora 1 and 2. A second group of veins range in strike from N.  $70^{\circ}$  E. to E.-W. and dip from  $65^{\circ}$  S.- $55^{\circ}$  N., and include Mata Caballo, Pozo Rico, and Restauradora 3. Veins of these two groups do not cross, but terminate against one another, in places showing decided decrease in mineralization near the intersection. Post-mineral left-lateral faults, striking N.  $45^{\circ}$ - $55^{\circ}$  E. and dipping  $50^{\circ}$  SE. to  $30^{\circ}$  NW., cut the Saca Si Puedes vein in the Santa Teresita mine.

In general, the veins in the Cerro Reliquias area have poorly defined walls and contain large amounts of brecciated wallrock cemented by quartz or rhodochrosite. Hypogene sulfide minerals include, in order of their abundance, sphalerite, galena, tetrahedrite, and chalcopryite. Supergene chalcocite, covellite, and rarely galena were also observed.

The high silver production during colonial times was probably derived from native silver, acanthite, pyrargyrite, and miargyrite. The only silver minerals noted in the Cerro Reliquias area in this study were pyrargyrite and miargyrite which coat thin cracks in the upper 50 meters of the Mata Cabello, Saca Si Puedes, and Perseguida veins.

Gangue minerals include quartz, rhodochrosite, barite, pyrite, sericite, and rarely hematite and amethyst. The sulfides are medium grained and are disseminated through the quartz or rhodochrosite, either indiscriminately or in vague bands. Crustified banding of vein

material is not well developed; on the other hand, cockade textures are common. Vugs are rare and where present are small.

Andesitic lava flows, 5 to 30 meters thick, interbedded with 1 to 5 meter beds of andesite flow breccia, underlie the area in flat-lying beds.

The only mines in the Cerro Reliquias area active at the time of this study were Santa Teresita and Matilde (see Plates 2 and 3). The Santa Teresita mine explores the two largest veins of the area, Saca Si Puedes and Mata Caballo (see Plate 12). The Santa Teresita mine is 1.5 kilometers east of the Lira mine, at the east edge of the Laguna La Virreyina basin, and can be reached over two kilometers of dirt road from the Lira mine. It develops the Saca Si Puedes vein from two adit levels 40 meters apart vertically; the lower or 420 level explores the vein for more than 450 meters, whereas the upper or 460 level explores it for about 300 meters. The Mata Caballo vein, which terminates against the Saca Si Puedes vein just north of the mine has been found in both the 420 and 460 levels. It appears on the 420 level as a weak 10-centimeters stringer splitting to northeast off the footwall of the Saca Si Puedes vein. On the 460 level the Mata Caballo vein consists of 50 centimeters of rhodochrosite, quartz, pyrite, sphalerite, galena, and chalcopyrite, and was found about 100 meters to the north of the Saca Si Puedes vein. On both levels, only about 50 meters of the Mata Caballo vein has been explored.

The Santa Teresita mine produces about 9,000 tons of lead-zinc-copper ore per year. All ore is shipped to the flotation mill at the Caudalosa mine.

The Matilde mine is about 0.5 kilometers northeast of Laguna San Francisco and 1 kilometer southeast of the Santa Teresita mine. It lies in the cliffs east of Laguna San Francisco and is reached only by mule trail. The mine consists of an adit about 250 meters long, and a lower, blind level about 150 meters long. The first 120 meters of the adit are driven along the Entrada vein that dies out against the Matilde vein. Production is about 1000 metric tons of lead-zinc-copper ore per year.

Table II is a resumé of all of the veins of importance in the Cerro Reliquias area. Many are inactive at present but all have been worked.

#### J. La Virreyna Area

The La Virreyna area lies on the south shore of Laguna La Virreyna, about 1 kilometer northeast of the Banco Minero's flotation mill at Laguna Pacococha and about 10 kilometers north of the town of Castro-virreyna (see Plates 2 and 3). The area has two principal mines, Lira and Carmen, and is the westernmost mineralized area of the district and the lowest in altitude, lying at about 4525 meters above sea level. The area is reached over 2 kilometers of all-weather unsurfaced road that leaves the Pisco-Huancavelica road at Laguna Pacococha.

Lira, the larger of the two mines, produces 3000 to 6000 metric tons of lead-zinc-copper ore per year, which is concentrated at Pacococha. The mine has exploited all but the southernmost veins of the area (see Plate 13), and has nearly 3 kilometers of underground workings on six levels over a vertical range of 65 meters (see Plate 14). These levels are, from top to bottom, the Justicia, Rosita, and Luz adit levels, and the Pique, Caldera, and 60 levels. The principal level,



the Caldera level, transects the area from north to south with a 340 meter crosscut and develops, to a greater or lesser extent, seven of the principal veins of this area. This level serves as the main haulage-way and is reached from the surface by the Caldera incline. The 60 level was being driven 30 meters below the Caldera level at the time of this study and is not shown on the maps.

The Carmen mine lies 1 kilometer south of the Lira mine and explores the southernmost veins of the area, the Carmen-Constante and Beatita veins (see Plate 13). The mine is owned and operated by César Pozo & Sons of Lima. The annual production is about 5000 metric tons of lead-zinc-copper ore which is treated at the Banco Minero mill at Pacococha. The mine is developed on three levels, the zero, 35, and 70 levels which are connected to the surface by a shaft and an incline. The mine has more than 900 meters of underground workings and extensive irregular surficial workings (see Plate 13). The 70 level was being opened at the time of this study and is not shown on the maps.

The area is underlain by andesite flow breccias which show no flow structures or bedding, are presumed to be flat-lying like the andesite flow rocks in the Cerro Reliquias area to the east.

The mineralized area of La Virreyana is 500 meters wide in a N.-S. direction by 750 meters long, and is cut by nine principal veins, 100 to 575 meters long (see Plate 13). The principal veins are, from north to south: Caldera, Del Camino, Sanchez Cerro, De La Cruz, Lira, Ika, San Antonio, Carmen-Constante, and Beatita. They can be divided into two groups on the basis of attitude, one striking N.  $55^{\circ}$ - $80^{\circ}$  E. and dipping either  $75^{\circ}$  N. or  $75^{\circ}$  S. and the other striking N.  $55^{\circ}$ - $90^{\circ}$  W. and dipping  $65^{\circ}$  N. to  $65^{\circ}$  S.

Veins striking N.  $55^{\circ}$ - $80^{\circ}$  E. are the best mineralized, and all but the San Antonio, Carmen-Constante, and some small unnamed veins belong to this group. They generally maintain constant strikes and dips; flexures are small usually involving changes in strike to due east for 5 to 25 meters, or localized changes in dip of 10 to 20 degrees. Splits both to the southeast and northwest are frequent and are favorable sites for ore accumulation. Vein widths range from 20 to 300 centimeters and average about 80 centimeters. The most productive veins of this group are the Caldera, Sanchez Cerro, Lira, and Beatita veins.

Veins of the second group strike N.  $55^{\circ}$ - $90^{\circ}$  W. and most of them are in the southwestern corner of the area between the Lira and Beatita veins, where they feather out to the northwest from the Beatita vein. Many of the small stringers that split off the N.  $50^{\circ}$ - $80^{\circ}$  E. group of veins have orientations of this second group. Veins of this N.  $55^{\circ}$ - $90^{\circ}$  W. group are shorter, generally narrower, more sinuous in course, and more erratic in mineralization than those of the former group. The only veins of this group with economic importance are the De La Cruz, an erratic split of the Sanchez Cerro vein, the San Antonio, and the Carmen-Constante.

Mineralization of both the N.  $50^{\circ}$ - $80^{\circ}$  E. and N.  $55^{\circ}$ - $90^{\circ}$  W. was probably contemporaneous. The San Antonio-Beatita intersection, the only vein-crossing observed, shows no offset. Generally vein intersections are either simple splits or pinch outs of mineralization against one another with no indication of faulting.

The veins of the La Virreyna area consist of sphalerite, galena, tetrahedrite, and chalcopyrite, pyrite, gouge, and rarely rhodochrosite

64-103

Table III: Miscellaneous mines in the Castrovirreyna District

Mine	Location	Strike	Dip	Outcrop length (meters)	Width (cm)	Mineralization
Atoccha	3km SSW of Caudalosa; 2km E. of Cerro Reliquias	N.50°W.	55°N.	200	100-200	Alt rk; 20-40 cm sil br,qtz, jasper,disem, sp,ga,chn
Itanayoc	2km S. of Caudalosa, 200m N. of Laguna Orcococho	N.50°W. stringers E-W	90° 90° 70°N-90°	1300 10-30 10-30	3-10m 0-10 0-10	fault zone with stringers of qtz,py,sp,ga adit (40m) 7 misc.
Fortuna	2.5km W. of Caudalosa	N.55°W.	60°N.	900	60-100	Br;0-20 qtz, py,stib,sp,ga (inac)
Margarita	2km W. of Caudalosa	N.85°W.	60°-80°N.	200	20-100	Br,sg, 0-20 qtz,disem,py, sp,ga adit (160)
	Cerro San Pablo, 1km W. of Lira	N.80°W.	80°-85°N.	300-600	50-100?	3 veins;worked out in colonial times 16 workings (inac) See Monroy, (1769)
Soracocha	3km W. of La Griega, 4km NW of San Genaro	N.55°W. E-W N.75°E.	? ? ?	50-200 100-300 50-100	? ? ?	From map by Masias (1929) Area not visited in this study.

For abbreviations see Table II.

set in quartz, brecciated and silicified or argillized wallrock. The sulfide minerals form massive bands and small stringers, or cement brecciated altered wallrock. They are medium to coarse grained. Vein material is heterogeneous or shows vague banding which tends to separate pyrite and chalcopyrite, tetrahedrite, and galena and sphalerite into bands. The banding is usually asymmetrical but follows a general pattern, from the center outward, of galena and sphalerite, tetrahedrite with or without quartz; and finally chalcopyrite, pyrite, and quartz. Veins are usually massive but contain elongate vugs lined with galena, sphalerite, tetrahedrite, or quartz crystals 1 to 5 centimeters across. Vein material is compact and not triturated, although crystal gliding and recrystallization due to shear are shown by galena in the Carmen-Constante vein. Vein walls are sharp and usually marked by 5 to 15 centimeters of gouge.

#### K. Miscellaneous Mines

Table III gives in abbreviated form the available information on a few scattered mines which have not been described in this report. Most of these mines were inaccessible so information is poor.

## **APPENDIX II**

### **Mine Production**

Table IV: Mine production and grade of ore, Carmen mine, 1941-1958

Year	Ore (metric tons)	Silver (grams/ton)	Lead (percent)	Copper (percent)	Zinc (percent)
1941	378	304	15.05	2.04	19.59
1942	No data				
1943	No data				
1944	326	208	7.3	1.8	9.6
1945	361	243	7.6	1.9	9.8
1946	669	132	6.5	1.1	
1947	No data				
1948	531	158	6.8	.8	7.5
1949	178	108	3.9		3.6
1950	No data				
1951	523	140	4.5	.75	3.0
1952	3,007	379	3.5	1.7	3.6
1953	3,581	512	2.9	2.5	3.9
1954	4,899	536	3.5	3.0	4.2
1955	No data				
1956	6,767	176	3.8	1.3	4.1
1957	6,631	298	2.0	1.7	2.2
1958	5,220	437	2.4	2.5	2.3

Source: Banco Minero del Perú

Table V: Metal production, Caudalosa mine, 1927-1957

Year	Gold (grams)	Silver (kilograms)	Copper (tons)	Lead (tons)	Zinc (tons)
1927	3,010	4,915	141	35	
1928	2,850	3,415	110	37	
1929	1,970	1,428	47		
1930	1,790	2,016	69		
1931	1,970	2,416	82		
1932-33	No data				
1939	503	418	9		
1940-48	No data				
1949	7,988	8,877	196	330	
1950	3,913	7,833		492	
1951		6,949	186	617	610
1952		4,001	97	709	610
1953		6,566	141	1,097	632
1954*	12,540	9,925	213	1,599	694
1955*	13,892	11,645	298	1,632	798
1956*	14,128	13,100	321	1,480	738
1957*	16,944	13,677	312	1,593	911

\* Includes production for Madona, Matilde, and Santa Terasita mines.

Source: Corporación Minera Castrovirreyna.

Table VI: Mine production and grade of ore, Lira mine, 1941-1958

Year	Ore (metric tons)	Silver (grams/ton)	Lead (percent)	Copper (percent)	Zinc (percent)
1941	431	261	8.45	1.2	5.8
1942	1,967	218	8.3	1.2	6.3
1943	No data				
1944	8,115	302	6.6	1.7	6.1
1945	1,067	271	5.4	.75	4.0
1946	3,275	324	6.3	1.5	6.5
1947	4,230	340	4.1	2.0	6.4
1948	6,791	231	3.1	1.0	3.9
1949	6,676	183	3.7	.8	3.65
1950	6,690	267	5.0	1.7	5.1
1951	7,192	213	4.1	1.2	3.7
1952	6,328	224	3.1	.7	3.4
1953	2,945	268	5.6	.35	4.0
1954	6,344	278	5.3	.4	3.7
1955	No data				
1956	3,051	228	4.15	.8	3.7
1957	2,785	155	4.3	.4	3.6
1958	4,567	183	3.6	.8	2.5

Source: Banco Minero del Perú



Table VII: Metal production, San Genaro mine, 1928-1955

Year	Gold (grams)	Silver (kilograms)	Copper (tons)	Lead (tons)	Zinc (tons)
1928	370	140			
1929	1,810	303		13	
1930	4,290	701		25	
1931-35	No production				
1936	4,556	735	9	28	
1937-43	No production				
1944	448	7,205			
1945	76,670	12,221	63	407	
1946	73,724	8,796	54	402	
1947	122,871	13,547			
1948	83,674	8,235		95	
1949	117	11,343	118	1,068	1,105
1950	100,085	19,872		1,167	992
1951	48,769	8,826		1,087	976
1952	48,267	10,993		993	954
1953*	79,687	18,342	93	1,850	1,083
1954*	64,889	14,711	36	540	201
1955*	117,569	21,723	35	503	106

\* Includes production for Rápida mine

Source: **Castrovirreyas Metal Mines Co.**

### **APPENDIX III**

#### **Mineralogical Investigations**

## A. Techniques

### 1. X-ray methods

X-ray powder diffraction methods were chosen as the principal means of mineral identification for the following reasons: 1) mineralogy of the Castrovirreyna deposits was complex and involved many unusual or rare sulfosalts, 2) the sulfosalts investigated were too closely related in chemical and physical properties to permit satisfactory identification by microscopic or microchemical means, and 3) much of the material was too fine-grained to permit identification by normal visual or chemical means.

Powder diffraction photographs were taken instead of using X-ray spectrometric powder techniques (X-ray diffractometry) because 1) the amount of pure material available was often too small even for spectrometric powder techniques and 2) maximum accuracy in determining  $d$ -spacing of the diffraction patterns of the sulfosalts was desired, as published information on these minerals is scarce.

The following technique was used: finely crushed material was formed into spheres about 0.3 millimeters in diameter with gum tragacanth or, preferably, with a small amount of vaseline, and mounted on the tip of a fine glass fiber. Powder diffraction photographs were taken with a Parrish modification of the 114.59 millimeter Buerger camera using  $\text{CuK}\alpha$  radiation, and with the film mounted according to the Straumanis method. Eastman No-screen X-ray film was used. The line intensities were estimated visually, using 10 for the darkest line and  $1/2$  for lines barely visible. The films were measured on an illuminated screen with a millimeter scale; all measurements were corrected for film shrinkage.

## 2. Spectrographic methods

All material used for spectrographic analyses was carefully selected for purity, using a binocular microscope; single crystals were used whenever possible. The material was cleaned manually, washed, crushed, cleaned of low density gangue with bromoform, washed, and finally manually picked over with a needle. This method reduced the amount of impurities well below the level detectable by X-ray diffraction methods, which lies around 2 to 4 percent of sample, but did not always eliminate all impurities. The relative amount of impurities left can best be estimated from the amount of Si, Al, and Ca found in the spectrographic analyses. In these analyses, however, standard purity graphite electrodes were used, and expected contamination of 0.03 to 0.06 percent Si, traces to 0.002 percent Al, and traces to 0.03 percent Ca were present in the electrodes.

Ten milligram samples were used and the sample burned to completion in a cup electrode. Spectrographs were taken on 35 millimeter film, with a dispersion of 2 angstroms per millimeter. The films were read on a film comparator microphotometer using Harvey's semiquantitative method (Harvey, 1947).

### B. Supporting Investigations

The following supporting investigations were undertaken or started in conjunction with this report: 1) the trace-element content of selected sulfides, 2) the variation of the iron content of sphalerite, and 3) the variation in the composition of tetrahedrite versus changes in the d-spacings.

The trace-element contents of selected sulfides were investigated in an attempt to distinguish or correlate stages of mineralization on

the basis of trace-element assemblages. The wide spread sulfides galena, sphalerite, and tetrahedrite were chosen for these analyses; about 15 samples of each were analyzed spectrographically. Although this approach was fruitful, lack of time and the difficulty in obtaining sufficient pure material precluded an adequate sampling, and only precursory results were obtained.

The iron contents of sphalerite were studied to determine the temperatures of formation of sphalerites from different veins and different parts of the same vein. Both spectrographic and X-ray diffraction data, however, showed that all sphalerites regardless of color or sample location contained less than 1.0 percent iron, a concentration below the limits of precise interpretation. Furthermore, almost all the sphalerite was associated with pyrite, not pyrrhotite, indicating that at best these values represent minimal temperatures.

A study of the relation between the d-spacings of the X-ray powder photographs of tetrahedrite and its composition was started. The extreme difficulty of purifying and even finding enough tetrahedrite for chemical analysis made it impractical to prepare the number of samples required by the variations in composition of tetrahedrite. The study was abandoned. It is hoped that this study of the tetrahedrite can be continued in the future using X-ray fluorescence methods, which requires only small amounts of material.

APPENDIX IV

X-ray Powder Diffraction Data

with

Commentary

# Acanthite

The X-ray powder diffraction data of the acanthite from San Genaro agrees with the data given by Ramsdell (1943) and Berry and Thompson (1962), both in d-spacings and intensities. It was possible, however, to resolve many of the doublets and triplets, especially of the intenser lines in the front reflection region, because a camera with a diameter of 114.59 millimeters was employed in this study.

Table VIII: X-ray powder diffraction pattern of acanthite

San Genaro mine Specimen C-228		Ramsdell (1943)				Berry and Thompson (1962)			
I	<u>d</u> (obs)	I	<u>d</u> (obs)	hkl	<u>d</u> (calc)	I	<u>d</u> (obs)	hkl	<u>d</u> (calc)
1/2	3.93	1	3.91	{200 202	3.92 3.87				
1	3.45			{002 210 212	3.43 3.41 3.37	1	3.45	{002 210 212	3.44 3.43 3.38
2	3.415	7	3.40			1/2	3.38		
1	3.365								
4H	3.08	8	3.07	012	3.075	3	3.09	012	3.08
5H	2.81					4	2.85	311	2.83
3H	2.667	6	2.66	311	2.665	2	2.67	121	2.66
10	2.596			{220 222	2.595 2.578	10	2.60	{220 222	2.61 2.58
4H	2.5675	10	2.58						
10B	{2.449 2.420	10	2.44	{113 022 313	2.453 2.435 2.415	8	2.45	{113 022	2.46 2.44
8	2.3705	9	2.37	402	2.36	5	2.38	402	2.38
4	2.204	7	2.205	131	2.21	3	2.22	131	2.21
4H	2.078	8	2.08	{123 202	2.09 2.07	4	2.09	{123 202	2.10 2.08
1/2	2.0625			{323 204	2.065 2.045	1/2	2.04	{323 204	2.07 2.05
1	2.036	4	2.05						

Table VIII (continued)

San Genaro mine Specimen C-228		Ramdell (1943)				Berry and Thompson (1962)			
I	d(obs)	I	d(obs)	hkl	d(calc)	I	d(obs)	hkl	d(calc)
1	1.989	4	1.99	$\begin{Bmatrix} 230 \\ 212 \\ 232 \end{Bmatrix}$	$\begin{Bmatrix} 1.988 \\ 1.984 \\ 1.981 \end{Bmatrix}$	1/2	2.00	$\begin{Bmatrix} 311 \\ 230 \\ 212 \end{Bmatrix}$	$\begin{Bmatrix} 2.01 \\ 1.995 \\ 1.995 \end{Bmatrix}$
2	1.957	5	1.96	$\begin{Bmatrix} 214 \\ 400 \end{Bmatrix}$	$\begin{Bmatrix} 1.962 \\ 1.96 \end{Bmatrix}$	1	1.961	$\begin{Bmatrix} \bar{2}14 \\ 422 \end{Bmatrix}$	$\begin{Bmatrix} 1.966 \\ 1.962 \end{Bmatrix}$
1	1.8975	4	1.905	$\begin{Bmatrix} 032 \\ 410 \end{Bmatrix}$	$\begin{Bmatrix} 1.914 \\ 1.885 \end{Bmatrix}$	1	1.910	$\begin{Bmatrix} 032 \\ 410 \end{Bmatrix}$	$\begin{Bmatrix} 1.919 \\ 1.901 \end{Bmatrix}$
1	1.859	4	1.865	$41\bar{4}$	1.86	1	1.870	$\begin{Bmatrix} \bar{4}14 \\ 113 \end{Bmatrix}$	$\begin{Bmatrix} 1.867 \\ 1.862 \end{Bmatrix}$
2	1.713	7	1.72	$\begin{Bmatrix} 13\bar{3} \\ 040 \\ 33\bar{3} \end{Bmatrix}$	$\begin{Bmatrix} 1.732 \\ 1.73 \\ 1.717 \end{Bmatrix}$	3	1.719	$\begin{Bmatrix} 333 \\ 004 \\ 420 \\ \bar{5}11 \end{Bmatrix}$	$\begin{Bmatrix} 1.722 \\ 1.720 \\ 1.716 \\ 1.716 \end{Bmatrix}$
						1/2	1.689	$\begin{Bmatrix} \bar{4}24 \\ \bar{1}41 \end{Bmatrix}$	$\begin{Bmatrix} 1.692 \\ 1.691 \end{Bmatrix}$
1H	1.579	5	1.58	$\begin{Bmatrix} 240 \\ 24\bar{2} \end{Bmatrix}$	1.595	2	1.580	$\begin{Bmatrix} \bar{2}42 \\ \bar{5}21 \end{Bmatrix}$	$\begin{Bmatrix} 1.582 \\ 1.577 \end{Bmatrix}$
1	1.551					2	1.556	$\begin{Bmatrix} 331 \\ 602 \end{Bmatrix}$	$\begin{Bmatrix} 1.554 \\ 1.553 \end{Bmatrix}$
2	1.536	4	1.54	$\begin{Bmatrix} 331 \\ 042 \\ 232 \\ 024 \end{Bmatrix}$	$\begin{Bmatrix} 1.546 \\ 1.545 \\ 1.541 \\ 1.537 \end{Bmatrix}$	1	1.542	$\begin{Bmatrix} 232 \\ 024 \\ \bar{6}04 \end{Bmatrix}$	$\begin{Bmatrix} 1.547 \\ 1.541 \\ 1.539 \end{Bmatrix}$
1H	1.509	4	1.51	$34\bar{1}$	1.507	1	1.512	$\begin{Bmatrix} \bar{6}12 \\ \bar{3}41 \\ \bar{5}15 \end{Bmatrix}$	$\begin{Bmatrix} 1.515 \\ 1.514 \\ 1.513 \end{Bmatrix}$
						1/2	1.484	$\begin{Bmatrix} \bar{4}34 \\ 133 \end{Bmatrix}$	$\begin{Bmatrix} 1.485 \\ 1.483 \end{Bmatrix}$
1H	1.479	3	1.475	133	1.477	1/2	1.475	$\bar{1}15$	1.471
		5	1.46	$11\bar{5}$	1.467				
2	1.4535	4	1.44	$\begin{Bmatrix} 14\bar{3} \\ 34\bar{3} \end{Bmatrix}$	$\begin{Bmatrix} 1.444 \\ 1.435 \end{Bmatrix}$	2	1.455	$\begin{Bmatrix} \bar{5}33 \\ 143 \end{Bmatrix}$	$\begin{Bmatrix} 1.459 \\ 1.447 \end{Bmatrix}$



Table VIII (continued)

San Genaro mine		Ramsdell (1943)				Berry and Thompson (1962)			
Specimen C-228									
I	d(obs)	I	d(obs)	hkl	d(calc)	I	d(obs)	hkl	d(calc)
1/2	1.41	1/2	1.41	622̄	1.407	1/2	1.412	622̄	1.417
								525̄	1.416
								402̄	1.408
								624̄	1.407
1/2	1.376	<1	1.38	034	1.376				
1/2	1.345	2B	1.335	335	1.343			341	1.337
1/2	1.330			341	1.331			242	1.333
1/2	1.330			242	1.328	1	1.336	713	1.331
1/2	1.318			204	1.32				
				600	1.31				
				250	1.305				
				214	1.30				
1/2	1.3055	1	1.30	422	1.296				
				440	1.296				
1/2	1.288			606̄	1.29				
				052	1.285				
1/2	1.267	1	1.265	323̄	1.27				
				351̄	1.26				
				224	1.236				
				226̄	1.228				
1H	1.224	3B		153̄	1.223				
				115	1.22				
				044	1.218				
1/2	1.189	<1	1.18	333	1.185				
				804	1.18				
				060	1.15				
		<1	1.15	252	1.15				
				234	1.15				
				254	1.145				
1/2	1.1265	<1	1.13	016	1.13				
		1/2	1.09	062	1.092				
				135	1.091				
1/2	1.034	1/2	1.04	337	1.03				

Table VIII (continued)

San Genaro mine	Ramadell (1943)	Berry and
Specimen C-228		Thompson (1962)

I	<u>d</u> (obs)	I	<u>d</u> (obs)	hkl	<u>d</u> (calc)	I	<u>d</u> (obs)	hkl	<u>d</u> (calc)
		1/2	1.01	{ 262	1.01				
				{ 361	1.01				
1/2	0.970	1/2	0.965	{ 800	0.98				
				{ 254	0.965				
1	0.958	1/2	0.94	{ 216	0.95				
				{ 226	0.95				

H - Hazy or diffuse line

B - Broad band; single measurement taken in middle, double measurement made on edges

# Aramayoite

The X-ray powder diffraction data of aramayoite from San Genaro coincides reasonably well with data given by Graham (1951) and Berry and Thompson (1962). The major difference is that Berry and Thompson obtained better resolution in the back reflection region and more lines than did the present author.

Table IX: X-ray powder diffraction pattern of aramayoite

San Genaro mine Specimen C-228					Graham (1951)					Berry and Thompson (1962)				
I	d <sub>(obs)</sub>	I	d <sub>(obs)</sub>	hkl	d <sub>(calc)</sub>	I	d <sub>(obs)</sub>	hkl	d <sub>(calc)</sub>	I	d <sub>(obs)</sub>	hkl	d <sub>(calc)</sub>	
5	3.425	2	3.43	012	3.428	2	3.44	012	3.43					
4	3.25	4	3.21	{ 022̄ 220	{ 3.244 3.213	4	3.22	{ 022̄ 220	{ 3.25 3.22					
3	3.16	1	3.15	210	3.146	1	3.15	210	3.15					
10	2.8395			{ 212̄ 202	{ 2.826 2.822			{ 212̄ 202	{ 2.83 2.83					
9	2.801	10	2.806	{ 030 030	{ 2.804 2.804	10	2.82	{ 212̄ 202 030	{ 2.83 2.83 2.81					
1	2.049	2	2.048	2̄32	2.047	2	2.05	232	2.05					
1	2.014	1/2	2.015	222	2.014	1/2	2.02	222	2.02					
1	1.971	1/2	1.967	2̄42̄	1.968	1/2	1.973	2̄42̄	1.972					
2	1.941	3	1.940	{ 232̄ 410	{ 1.936 1.930	3	1.945	{ 232̄ 410	{ 1.940 1.934					
1/2H	1.764	1/2	1.757	{ 214 204	{ 1.767 1.757	1/2	1.762	{ 214 204	{ 1.771 1.761					
1/2	1.739	1	1.738	042	1.742	1	1.743	042	1.745					
				{ 234̄ 024 224̄ 250 422	{ 1.716 1.714 1.704 1.693 1.691			{ 234̄ 024 224̄ 250 422	{ 1.719 1.717 1.707 1.701 1.694					
1	1.716	2	1.705			2B	1.710							

Table IX (continued)

San Genaro mine Specimen C-228		Graham (1951)		Berry and Thompson (1962)					
I	d(obs)	I	d(obs)	hkl	d(calc)	I	d(obs)	hkl	d(calc)
1	1.669	1	1.668	{ 402 432 052 240	{ 1.673 1.669 1.668 1.668	1	1.672	{ 402 432 052 240	{ 1.676 1.672 1.671 1.671
1	1.6155	1	1.614	{ 044 440	{ 1.622 1.607	1	1.618	{ 044 440	{ 1.625 1.610
1/2	1.583	1/2	1.578	420	1.573	1/2	1.583	420	1.576
1/2	1.4215	1/2	1.413	{ 424 404	{ 1.413 1.411	1/2	1.417	{ 424 404	{ 1.416 1.414
1/2	1.405	2	1.402	060	1.402	2	1.406	060	1.405
						1/2	1.349		
1/2	1.2855					1/2	1.297		
						1/2	1.287		
						1/2	1.274		
						1/2	1.242		
						1/2	1.158		
						1/2	1.138		
						1/2	1.089		
						1/2	1.074		

H - Hazy or diffuse line

B - Broad band, single measurement taken in middle

# Bourbonite

The d-spacings of the X-ray powder diffraction pattern of bourbonite from Caudalosa are consistently lower than the measured and calculated spacings of Leineweber (1956), and Berry and Thompson (1962) reported 14 lines in the back reflection region which neither Leineweber nor the author observed. Spectrographic analysis of the Caudalosa material shows appreciable amounts of arsenic and silver, and small amounts of iron and zinc which may account for the increase in cell dimension and ensuing decrease in d-spacings.

Table X: X-ray powder diffraction pattern of bourbonite

Caudalosa mine Specimen C-35		Leineweber (1956)				Berry and Thompson (1962)			
I	<u>d</u> (obs)	I	<u>d</u> (obs)	hkl	<u>d</u> (calc)	I	<u>d</u> (obs)	hkl	<u>d</u> (calc)
				100	8.14			100	
		3.5	5.97	110	5.97				
2	5.81	12.	5.81	011	5.82	3	5.79	011	5.81
1	5.63	7.5	5.64	101	5.65				
1	4.71	5.	4.73	111	4.74	1/2	4.75	111	4.73
2	4.32	15.5	4.35	020	4.36	4	4.37	020	4.35
2	4.01	20.	4.08	200	4.08	3	4.08	200	4.07
1	3.87	30.	3.90	002	3.90	8	3.90	002	3.90
5	3.83	37.5	3.84	120	3.84				
2	3.68	20.	3.69	210	3.70	2	3.68	210	3.69
				201	3.62				
				102	3.52				
				121	3.45				

Table X (continued)

Caudalosa mine Specimen C-35						Leineueber (1956)				Berry and Thompson (1962)			
I	d <sub>(obs)</sub>	I	d <sub>(obs)</sub>	hkl	d <sub>(calc)</sub>	I	d <sub>(obs)</sub>	hkl	d <sub>(calc)</sub>	I	d <sub>(obs)</sub>	hkl	d <sub>(calc)</sub>
1/2	3.33	3.5	3.34	211	3.34								
1	3.25	18.	3.27	122	3.27	2	3.27	112	3.26				
3	2.96	25.5	2.998	220	2.978	4	2.99	220	2.97				
2H	2.89	18.	2.910	022	2.908	1	2.90	022	2.90				
2	2.805	26.5	2.823	202	2.822	2	2.82	202	2.82				
1	2.768	12.	2.786	221	2.783								
10	2.727	100.	2.739	122	2.739								
				130	2.736	10	2.74	130	2.73				
		9.	2.725	{ 031 2.722 300 2.720									
6	2.667	45.5	2.687	212	2.685	4	2.69	212	2.68				
		26.	2.597	310	2.597	5	2.59	310	2.59				
5	2.585	9.	2.583	131	2.582								
1/2	2.557	7.	2.571	301	2.570								
				013	2.493								
				103	2.454								
				311	2.465								
		3.	2.388	113	2.385								
1	2.355	11.5	2.363	{ 222 2.368 230 2.366		1	2.37	{ 113 2.38 222 2.36					
1H	2.298	8.	2.303	320	2.308	1	2.30	320	2.30				
		3.	2.267	231	2.264	1	2.24	231	2.26				
1H	2.227	7.5	2.2413	132	2.2402								
		3.5	2.2339	302	2.2328								
				321	2.2123								
				203	2.1953								

Table X (continued)

Caudalosa mine Specimen C-35						Berry and Thompson (1962)			
I	d <sub>(obs)</sub>	I	d <sub>(obs)</sub>	hkl	d <sub>(calc)</sub>	I	d <sub>(obs)</sub>	hkl	d <sub>(calc)</sub>
1/2	2.161	3.5	2.1791	040	2.1781				
		4.	2.1621	312	2.1621				
				123	2.1552	1/2	2.16	123	2.15
				213	2.1290				
2	2.096	12.	2.1119	140	2.1035	2	2.09	140	2.10
				400	2.0316	1/2	2.02	400	2.04
1/2	2.026	5.	2.0316	141	2.0316				
				232	2.0234				
4	1.980	31.5	1.9853	{ 410 1.9868 322 1.9868 330 1.9853		3	1.985	{ 410 1.983 322 1.983	
				401	1.9746				
		15.5	1.9608	223	1.9616				
3	1.947	31.	1.9528	004	1.9528	3	1.945	004	1.950
		5.	1.9363	033	1.9371				
		5.	1.9209	{ 411 1.9255 331 1.9239 240 1.9216					
		4.5	1.9004	{ 042 1.9019 104 1.8989					
1/2	1.879	5.	1.8834	{ 133 1.8856 303 1.8805					
1/2	1.868			241	1.8660				
				114	1.8560				
3	1.846	32.	1.8503	{ 142 1.8524 420 1.8546		4	1.848	{ 142 1.850 420 1.845	

Table X (continued)

Caudalosa mine Specimen C-35				Leineweber (1956)				Berry and Thompson (1962)			
I	d(obs)	I	d(obs)	hkl	d(calc)	I	d(obs)	hkl	d(calc)		
1/2	1.819			313	1.8391						
				402	1.8084						
		9.	1.7984	421	1.7984						
1/2	1.791	9.	1.7865	024	1.7878						
5	1.765	52.	1.7672	{ 412 332	{ 1.7710 1.7697	6	1.765				
1	1.734	10.5	1.7585	204	1.7515						
						1/2	1.728				
						2	1.664				
						2	1.631				
						1/2	1.585				
						2	1.556				
						1	1.480				
						2	1.427				
						1	1.389				
						1	1.365				
						1	1.337				
						1/2	1.252				
						1	1.228				
						1	1.152				
						1/2	1.118				
						1	1.106				

H - Hazy or diffuse line



# Chalcostibite

The X-ray powder diffraction pattern of chalcostibite from Caudalosa agrees with data of Berry and Thompson (1962), but the Caudalosa material gave consistently lower values for d-spacings. The principal impurity of the Caudalosa chalcostibite is iron (see Table XXIV).

Table XI: X-ray powder diffraction pattern of chalcostibite

Caudalosa mine Specimen C-67		Berry and Thompson (1962)			
I	<u>d</u> (calc)	I	<u>d</u> (obs)	hkl	<u>d</u> (calc)
2	7.31	2	7.38	020	7.24
2	7.20				
1H	4.62	1	4.67	120	4.63
1H	3.62	1	3.65	{011 040}	3.66 3.62
10 8	{3.13 3.09}	10	3.13	{111 140}	3.13 3.10
10 8	{3.00 2.97}	9	3.00	{200 031}	3.01 2.98
1H	2.94				
1	2.768	1/2	2.79	220	2.78
1	2.542	1	2.56	230	2.55
1	2.398				
6	2.295	4	2.31	{240 051}	2.32 2.30
3	2.237	2	2.24	{160 221}	2.24 2.24
4	2.113	3	2.12	031	2.12
3	1.894	3	1.895	002	1.895

Table XI (continued)

Caudalosa mine Specimen C-67		Berry and Thompson (1962)			
I	$\underline{d}_{(calc)}$	I	$\underline{d}_{(obs)}$	hkl	$\underline{d}_{(calc)}$
4	1.826	4	1.831	{ 022 251	1.833 1.829
2H	1.807	1/2	1.817	{ 071 080	1.817 1.811
?	1.780				
5	1.7545	5	1.762	{ 311 340	1.761 1.756
1/2	1.736	1/2	1.743	171	1.739
?	1.709				
1H	1.683	1	1.687	261	1.686
2	1.6155	2	1.621	142	1.619
1/2	1.6025	1	1.603	202	1.603
?	1.5905				
2	1.548	1	1.554	{ 190 271 280	1.555 1.555 1.552
		3	1.441	{ 370 191 430 281	1.441 1.439 1.437 1.436
		1/2	1.372	{ 421 312	1.374 1.372
1H	1.345	1	1.344		
1/2	1.308	1	1.308		
3	1.2865	2	1.287		
1/2	1.258	1	1.258		
?	1.2225				
1	1.198	2	1.199		

Table XI (continued)

Caudalosa mine Specimen C-67		Berry and Thompson (1962)			
I	d(calc)	I	d(obs)	hkl	d(calc)
1/2	1.190	1/2	1.192		
?	1.155	1	1.160		
1/2	1.1425	2	1.143		
1/2	1.132	1	1.133		
?	1.093				
?	1.082	1	1.079		
1H	1.0675	1	1.068		
1/2	1.005	2	1.006		
1/2	0.979	2	0.980		
		1/2	0.960		
1/2	0.949	1	0.948		

H - Hazy or diffuse line

? - Possible faint line

# Enargite

Measurement of the  $d$ -spacings of enargite from Caudalosa agrees well with those given by Gaines (1942) and almost precisely with the data of Berry and Thompson (1962), except for the absence of a few lines in the photographs of the Caudalosa material, particularly in the back reflection region. Although Stevanović's (1903) analysis of enargite from Caudalosa indicates pure enargite, the spectrographic analysis shows appreciable amounts of antimony and several trace elements (see Table XXV), some of which may be due to inclusions of famatinite or tetrahedrite.

Table XII: X-ray powder diffraction pattern of enargite

Caudalosa mine Specimen C-122		Gaines (1942)		Berry and Thompson (1962)			
I	$d_{(obs)}$	I	$d_{(obs)}$	I	$d_{(obs)}$	hkl	$d_{(calc)}$
				1/2	6.46	100	6.41
				1/2	4.87	110	4.85
10	3.21	100	3.21	1/2	3.22	{ 120 200	{ 3.21 3.20
				10	3.22	{ 120 200	{ 3.21 3.20
9	3.08	80	3.08	4	3.08	002	3.07
				1/2	2.97	210	2.94
10	2.852	100	2.85	8	2.87	{ 121 201	{ 2.85 2.84
4	2.224	40	2.22	3	2.22	{ 122 202	{ 2.22 2.22
				1/2	2.06	310	2.05
				1/2	1.910	222	1.904

Table XII (continued)

Caudalosa mine Specimen C-122		Gaines (1942)		Berry and Thompson (1962)			
I	d(obs)	I	d(obs)	I	d(obs)	hkl	d(calc)
9	1.859	90	1.86	9	1.859	{040 320	1.855 1.852
8	1.731	60	1.73	6	1.731	{123 203	1.728 1.727
1/2	1.603			4	1.608	{240 400	1.606 1.603
5	1.59	50	1.59	5	1.59	{042 322	1.589 1.587
2	1.556	10	1.56	4	1.556	{241 401	1.554 1.551
1	1.423	5	1.43	1	1.425	{242 402 024	1.424 1.422 1.421
				1/2	1.349	{250 430	1.347 1.345
4	1.266	30	1.27	4	1.266	{243 510 403	1.264 1.263 1.263
2	1.215	10	1.22	4	1.221		
2	1.194	10	1.20	4	1.197		
3	1.151	10	1.15	1	1.155		
1	1.131	5	1.13	1	1.134		
2H	1.074	5	1.07	5	1.075		
4H	1.047	40	1.05	5	1.049		
				1/2	1.030		
2	1.015	20	1.01	3	1.015		
2	0.978	5	0.978	1	0.980		
1	0.929	5	0.928	4	0.932		

Table XII (continued)

Caudalosa mine Specimen C-122		Gaines (1942)		Berry and Thompson (1962)			
I	$\underline{d}_{(obs)}$	I	$\underline{d}_{(obs)}$	I	$\underline{d}_{(obs)}$	hkl	$\underline{d}_{(calc)}$
1	0.899	5	0.899	1/2	0.900		
1	0.891			2	0.893		
				1/2	0.886		
4H	0.865	5	0.861	2	0.868		
				1/2	0.858		
2	0.819	5	0.818	5	0.819		
				1/2	0.804		
				1/2	0.797		

H - Hazy or diffuse line

# Famatinite

The d-spacings of the X-ray powder diffraction photograph of famatinite from Caudalosa are slightly lower than the spacings given by Gaines (1957) and Berry and Thompson (1962). Moreover, Gaines obtained better resolution and many more lines. Both Stevanović's and the author's analysis of the Caudalosa material show appreciable amounts of arsenic (see Table XXVI), which could account for the shift in d-spacings from ideal values.

Table XIII: X-ray powder diffraction pattern of famatinite

Caudalosa mine Specimen C-122		Gaines (1957)				Berry and Thompson (1962)			
I	<u>d</u> <sub>(obs)</sub>	I	<u>d</u> <sub>(obs)</sub>	hkl	<u>d</u> <sub>(calc)</sub>	I	<u>d</u> <sub>(obs)</sub>	hkl	<u>d</u> <sub>(calc)</sub>
1/2	5.24	2	5.261	002	5.380				
1	4.72	3	4.731	101	4.811	2	4.77	012	4.77
						1/2	4.35	112	4.36
1/2	3.745	1	3.752	110	3.805				
10	3.05	10	3.071	112	3.106	10	3.08	222	3.08
1/2	2.935	2	2.952	103	2.984	1/2	2.96	023	2.96
3H	2.652	3	2.664	{004 200	2.690	3	2.67	004	2.67
1/2	2.3825	2	2.390	202	2.405				
1/2	2.318	3	2.336	211	2.348	1/2	2.33	124	2.33
		2	2.181	114	2.197	1/2	2.18	224	2.18
1/2	1.963	4	1.985	213	1.997	1/2	1.973	{025 234	1.982
8	1.870	8	1.895	220	1.903	7	1.838	044	1.837
		2	1.787	006	1.793				

Table XIII (continued)

Caudalosa mine Specimen C-122		Gaines (1957)				Berry and Thompson (1962)			
I	d(obs)	I	d(obs)	hkl	d(calc)	I	d(obs)	hkl	d(calc)
		2	1.763	301	1.768				
		1	1.693	310	1.701				
5	1.599	7	1.614	312	1.622	5	1.610	226	1.609
1H	1.5875	2	1.597	303	1.603				
1	1.530	3	1.547	224	1.553	1	1.542	444	1.540
		1	1.485	206	1.492	1/2	1.473	046	1.480
		2	1.469	321	1.477				
		2	1.434	314	1.437				
		2	1.373	323	1.377				
2	1.3285	5	1.342	008 400	1.345	3	1.336	008	1.334
1H	1.319	1	1.304	402	1.304				
		2	1.294	411	1.295				
		1	1.266	330	1.268				
4H	1.216	{ 6	1.232	332	1.234	4	1.226	266	1.224
		{ 1	1.225	413	1.226				
		{ 4	1.200	420	1.203				
1/2	1.188	1	1.174	422	1.174	1	1.197	048	1.193
		1	1.164	307	1.166	1/2	1.167	248	1.164
		1	1.145	334	1.147				
		1	1.114	415	1.115				
4H	1.084	6	1.099	424	1.098	4	1.090	443	1.089
		1	1.072	431	1.070				



Table XIII (continued)

Caudalosa mine Specimen C-122		Gaines (1957)				Berry and Thompson (1962)			
I	d <sub>(obs)</sub>	I	d <sub>(obs)</sub>	hkl	d <sub>(calc)</sub>	I	d <sub>(obs)</sub>	hkl	d <sub>(calc)</sub>
2H	1.022	{ 1 5	{ 1.055 1.037	510 512	1.055 1.035	3	1.028	2.2.10 6 6 6	1.027
		1	0.9960	521	0.9948				
		2	0.9628	523	0.9638				
		4	0.9491	440	0.9516	1	0.943	088	0.943
2H	0.939								
		5	0.9105	516	0.9097	3	0.902	2.6.10	0.902
2H	0.899	1	0.8974	{ 600 0.0.12	0.8967				
1/2H	0.894*	2	0.8815	611	0.8813				
		2	0.8736	534	0.8730				
		1	0.8588	613	0.8584				
		5	0.8510	620	0.8506				
2	0.842	1	0.8405	{ 446 622	0.8402	2	0.845	0.4.12	0.844
1/2	0.836*	1	0.8304	518	0.8300				
		4	0.8208	536	0.8208				
1/2	0.812	1	0.8120	624	0.8112	1	0.813	6.6.10	0.814
		2	0.8018	606	0.8020				
		1	0.7929	3 1.12	0.7933				
		2	0.7836	633	0.7825				
		4	0.7768	448	0.7767				

\* - Possibly due to impurities

H - Hazy or diffuse line

# Ferrous sulfates

Comparison of the d-spacings of the powder photograph of melanterite from the Caudalosa mine with the ASTM card shows good general agreement. It is obvious, however, that the photograph of the Caudalosa material gave superior resolution, as five doublets appear where heretofore single lines were reported.

An X-ray powder diffraction photograph taken of a dessication product of melanterite was similar to the ASTM card for pozenite,  $\text{FeSO}_4 \cdot 4\text{H}_2\text{O}$ , except that the ASTM material showed better resolution and more lines.

Table XIV: X-ray powder diffraction pattern of ferrous sulfates

Melanterite			Pozenite			
Caudalosa mine Specimen C-90		ASTM Card No. 3.0796	Caudalosa mine Specimen C-90		ASTM Card No. 13-103	
I	d <sub>(obs)</sub>	d <sub>(obs)</sub>	I	d <sub>(obs)</sub>	I	d <sub>(obs)</sub>
1/2	6.75	6.8	4	6.84	50	6.89
		6.0	8	5.45	90	5.48
2D	5.485	5.5	1/2	5.17	10	5.18
10	4.89	4.9	1	4.75	30	4.76
1	4.54	4.55	10	4.47	100	4.50
1D	4.02	4.02	7	3.99	80	3.979
7	3.78	3.78			10	3.840
1/2	3.38		1	3.62	20	3.682
3	3.25	3.23	4	3.403	80	3.410
1	3.196		4HB	{ 3.289 3.224	20	3.295
1	3.103	3.09			70	3.239

Table XIV (continued)

Melanterite			Pozenite			
Caudalosa mine Specimen C-90		ASTM Card No. 3.0796	Caudalosa mine Specimen C-90		ASTM Card No. 13-103	
I	$\frac{d}{(obs)}$	$\frac{d}{(obs)}$	I	$\frac{d}{(obs)}$	I	$\frac{d}{(obs)}$
1	3.007		5	2.969	70	2.993
1	2.930	2.92			80	2.973
3HB	2.7965 2.727	2.75			10	2.899
			1	2.7675	20	2.776
3HB	2.6595 2.6218	2.63	1	2.7310	40	2.738
2	2.485	2.50	3	2.5749	70	2.579
1	2.4296	2.42	1/2	2.4780	10	2.478
1	2.3888		2	2.4265	70	2.436
2	2.3150	2.31	2H	2.3704	70	2.381
1/2	2.1835	2.17			70	2.327
		2.11			10	2.293
1	2.0837	2.07	2	2.2669	50	2.272
1/2	2.0557				10	2.247
2	2.0159	2.01			10	2.223
2	1.9704	1.96	1/2	2.1886	10	2.183
					20	2.148
1	1.8863	1.87	1/2	2.1154	10	2.116
2	1.8647		1/2	2.0445	10	2.058
			2	1.9713	50	1.973
					20	1.952
			2	1.9010	30	1.900
			1	1.8736	20	1.876

Table XIV (continued)

Melanterite			Pozenite			
Caudalosa mine Specimen C-90		ASTM Card No. 3.0796	Caudalosa mine Specimen C-90		ASTM Card No. 13-103	
I	<u>d</u> (obs)	<u>d</u> (obs)	I	<u>d</u> (obs)	I	<u>d</u> (obs)
					20	1.863
					10	1.825
			2	1.7990	50	1.798
			1	1.7590	30	1.759
			1	1.7267	30	1.728
			1	1.6776	20	1.679
			1/2	1.6356	20	1.659
			+ 9 additional lines to 1.29		+ 16 addi- tional lines to 1.015	

# Geocronite

The d-spacings in the X-ray powder diffraction photograph of geocronite from Caudalosa agrees with the data of Douglas and others (1954). The Caudalosa material, however, gave rather hazy photographs so that the weaker lines noted by Douglas were not discernable, especially in the front reflection region.

Spectrographic analysis of geocronite from Caudalosa shows noticeable amounts of only arsenic and silver (see Table XXIX).

Table XV: X-ray powder diffraction pattern of geocronite

Caudalosa mine Specimen C-170		Douglas and others (1954)			
I	<u>d</u> (obs)	I	<u>d</u> (obs)	hkl	<u>d</u> (calc)
		10H	6.91	120	7.08
		10	6.74	{ 021 121	{ 6.77 6.75
		20-	6.36	130	6.34
		20-	6.12	{ 031 131	{ 6.12 6.10
		20+	5.49	{ 041 141	{ 5.45 5.44
		10-H	4.95	150	4.96
		10H	4.84	151	4.84
1/2	4.50	40	4.46	{ 101 201 111	{ 4.48 4.46 4.44
		10-	4.33	{ 061 161	{ 4.33 4.32
1/2	4.21	10+	4.21	112	4.20
		10+	4.13	{ 131 231	{ 4.13 4.12

Table XV (continued)

Caudalosa mine  
Specimen C-170

Douglas and others  
(1954)

I	d(obs)	I	d(obs)	hkl	d(calc)
		20-	3.93	{ 200 170 210 071	{ 3.95 3.94 3.92 3.89
1/2	3.32	40-	3.83	220	3.84
1	3.715	60	3.71	{ 012 230 212	{ 3.72 3.71 3.70
2	3.68				
1/2	3.62	20	3.64	{ 022 222	{ 3.64
1	3.53	100	3.54	{ 240 032 232	{ 3.54 3.53 3.52
5	3.375	80	3.39	{ 042 242	{ 3.38 3.38
10	3.165	30B	3.18	{ 052 252 0.10.0 260	{ 3.23 3.22 3.18 3.17
7	3.05	90	3.06	{ 062 262	{ 3.059 3.052
5	2.98	70	2.98	270	2.985
7	2.885	90	2.89	{ 072 272	{ 2.891 2.884
3	2.7965	50H	2.80	{ 280 132 332 191	{ 2.806 2.796 2.784 2.779
3	2.719	50	2.72	{ 082 142 282 342	{ 2.727 2.723 2.722 2.712

Table XV (continued)

Caudalosa mine Specimen C-170		Douglas and others (1954)			
I	d(obs)	I	d(obs)	hkl	d(calc)
1/2	2.6365	20	2.63	152 300 352 310	2.638 2.637 2.628 2.628
		10	2.59		
		10	2.55		
		20B	2.49		
		10	2.44		
1	2.392	30-	2.39		
		10+	2.33		
		10	2.29		
10H	2.232	90	2.235		
4	2.1155	60	2.122		
1H	2.083	30	2.086		
1H	2.049	40+	2.052		
1H	2.029	40-	2.030		
1	1.9715	30+	1.973		
4	1.941	20	1.984		
2	1.8845	40	1.889		
1/2	1.843	30	1.850		
7H	1.8275	80	1.831		
		10	1.791		
5H	1.7635	70	1.765		
2	1.723	40	1.744		
1/2	1.692	30	1.694		

Table XV (continued)

Caudalosa mine Specimen C-170		Douglas and others (1954)			
I	$\underline{d}_{(obs)}$	I	$\underline{d}_{(obs)}$	hkl	$\underline{d}_{(calc)}$
1/2	1.676	20	1.677		
		20	1.651		
		10	1.618		
1H	1.593	30	1.597		
		10H	1.565		
1/2H	1.486	30	1.489		
1/2H	1.464	40H	1.469		
1/2H	1.445	40	1.448		
1/2	1.4275	20	1.428		
1/2H	1.405	40	1.409		
plus + 9 lines		plus + 20 lines			

H - Hazy or diffuse line



# Miargyrite

The d-spacings in the X-ray powder photograph of miargyrite from San Genaro are slightly lower than those given by Graham (1951) and Berry and Thompson (1962). Both authors give 10 lines in the back reflection region which were not observed in the films of the San Genaro material. Moreover, the eight powder diffraction photographs taken of different miargyrites from San Genaro have five lines not reported by Graham nor by Berry and Thompson. Their presence has not been explained as they do not correspond to the strong lines of suspected impurities, nor did spectrographic analyses reveal trace-elements in quantities sufficient to cause these lines (see Table XXX).

Table XVI: X-ray powder diffraction pattern of miargyrite

San Genaro mine Specimen C-144		Graham (1951)				Berry and Thompson (1962)			
I	<u>d</u> (obs)	I	<u>d</u> (obs)	hkl	<u>d</u> (calc)	I	<u>d</u> (obs)	hkl	<u>d</u> (calc)
8	3.43	9	3.443	211	3.423	9	3.45	211	3.43
3	3.165	2	3.178	044	3.171	2	3.19	004	3.18
3	3.085	2	3.091	40 $\bar{2}$	3.091	2	3.10	$\bar{4}$ 02	3.10
10	2.880	10	2.877	21 $\bar{3}$	2.881	10	2.88	$\bar{2}$ 13	2.89
9	2.7355	8	2.739	402	2.734	8	2.75	402	2.74
1	2.2015	1/2	2.205	020	2.195	1/2	2.21	020	2.20
1H	2.1835								
1/2	2.099								
5	2.0055	4	2.005	215	2.004	4	2.01	215	2.01
5	1.965	4	1.963	61 $\bar{1}$	1.963	4	1.965	$\bar{6}$ 11	1.967
3	1.9085	3	1.909	40 $\bar{6}$	1.909	3	1.914	$\bar{6}$ 04	1.913

Table XVI (continued)

San Genaro mine Specimen C-144				Graham (1951)				Berry and Thompson (1962)			
I	d(obs)	I	d(obs)	hkl	d(calc)	I	d(obs)	hkl	d(calc)		
?	1.872										
3H	1.8055	1	1.799	024	1.805	1	1.804	024	1.809		
3H	1.7895	2	1.792	422	1.790	2	1.797	422	1.794		
1	1.7145	1/2	1.712	422	1.712	1/2	1.719	422	1.716		
3H	1.6835	3	1.682	{613 217	{1.684 1.679	3	1.686	{613 217	{1.687 1.682		
1H	1.6555	1	1.657	{406 615	{1.663 1.655	1	1.661	{406 615	{1.666 1.658		
1/2	1.633	1/2	1.624	800	1.628	1/2	1.629	800	1.631		
1/2	1.613										
2H	1.588	2	1.586	008	1.585	2	1.590	008	1.588		
2	1.548	2	1.544	804	1.545	2	1.549	804	1.548		
1/2H	1.488	1/2	1.488	-	-	1/2	1.492	-	-		
1/2	1.440	1/2	1.445	426	1.440	1/2	1.449	426	1.443		
1/2	1.419	1/2	1.415	231	1.414	1/2	1.419	231	1.417		
1	1.371	1	1.368	804	1.368	1	1.372	804	1.371		
1/2	1.3235	1/2	1.327			1/2	1.331				
1	1.3095	1/2	1.311			1/2	1.315				
1H	1.286		1.280			1/2	1.285				
1/2	1.279										
1	1.265	1/2	1.263			1/2	1.266				
2	1.248	2	1.246			2	1.249				
1/2B	1.2295	1/2	1.229			1/2	1.233				
	1.223	1/2	1.224			1/2	1.228				
1/2	1.163	1/2	1.162			1/2	1.166				

Table XVI (continued)

San Genaro mine Specimen C-144				Graham (1951)		Berry and Thompson (1962)			
I	d(obs)	I	d(obs)	hkl	d(calc)	I	d(obs)	hkl	d(calc)
1	1.144	1/2	1.144			1/2	1.147		
1	1.1305	1/2	1.126			1/2	1.129		
1/2	1.106	1/2	1.106			1/2	1.109		
1/2	1.0985	1/2	1.100			1/2	1.103		
1/2	1.0865	1/2	1.085			1/2	1.088		
1/2	1.0775	1/2	1.076			1/2	1.079		
1/2	1.0655	1/2	1.062			1/2	1.065		
		1/2	0.987			1/2	0.990		
		1/2	0.975			1/2	0.978		
		1	0.955			1/2	0.958		
		1/2	0.924			1/2	0.927		
		1/2	0.902			1/2	0.905		
		1/2	0.896			1/2	0.898		
		1/2	0.878			1/2	0.881		
		1/2	0.867			1/2	0.870		
1/2	0.843	1/2	0.843			1/2	0.845		
		1/2	0.823			1/2	0.825		
		1/2	0.795			1/2	0.798		

H - Hazy or diffuse line

B - Broad band, single measure taken in middle

? - Possible faint line

# Pearceite

Measurements of the X-ray powder diffraction pattern agree fairly well with the data of Peacock and Berry (1947) and Berry and Thompson (1962), although they are somewhat lower. The San Genaro material gave three weak lines and one diffuse band which are not reported by others. The  $d$ -spacings of these lines approximate lines found in polybasite, the antimonian analog of pearceite. Perhaps the shift of spacings and the extraneous lines are caused by the presence of antimony.

Table XVII: X-ray powder diffraction pattern of pearceite

San Genaro mine Specimen C-144		Berry and Thompson (1962)			
I	$d_{(obs)}$	I	$d_{(obs)}$	hkil	$d_{(calc)}$
4	11.86				
1	6.395	6.51		10 $\bar{1}$ 0	6.40
1/2	5.99	6.07		0002	5.97
2	3.715	3.72		11 $\bar{2}$ 0	3.69
1/2	3.57	3.56		11 $\bar{2}$ 1	3.53
1	3.435				
1/2	3.325				
7	3.11	5	3.11	{ 11 $\bar{2}$ 2 20 $\bar{2}$ 1	{ 3.14 3.09
10	2.99	10	3.00	0004	2.99
9	2.822	9	2.84	20 $\bar{2}$ 2	2.82
1/2	2.707				
4	2.4975	4	2.50	20 $\bar{2}$ 3	2.49
2	2.373	3	2.37	21 $\bar{3}$ 1	2.37
3	2.327	5	2.33	11 $\bar{2}$ 2	2.32

Table XVII (continued)

San Genaro mine Specimen C-144		Berry and Thompson (1962)			
I	$\underline{d}(\text{obs})$	I	$\underline{d}(\text{obs})$	hk1l	$\underline{d}(\text{calc})$
1/2	2.2295	1/2	2.24	$\begin{cases} 21\bar{1}32 \\ 10\bar{1}15 \end{cases}$	$\begin{matrix} 2.24 \\ 2.24 \end{matrix}$
3	2.1835	3	2.19	20 $\bar{2}$ 4	2.18
1/2	2.137	1/2	2.15	30 $\bar{3}$ 0	2.13
2	2.099	2	2.10	30 $\bar{3}$ 1	2.10
10	2.067	2	2.07	21 $\bar{3}$ 3	2.07
3	2.010	4	2.01	$\begin{cases} 30\bar{3}2 \\ 11\bar{2}5 \end{cases}$	$\begin{matrix} 2.008 \\ 2.006 \end{matrix}$
3	1.914	1	1.914	$\begin{cases} 20\bar{2}5 \\ 1016 \end{cases}$	$\begin{matrix} 1.914 \\ 1.901 \end{matrix}$
1/2	1.888	1/2	1.884	$\begin{cases} 30\bar{3}3 \\ 21\bar{3}4 \end{cases}$	$\begin{matrix} 1.880 \\ 1.879 \end{matrix}$
3	1.8485	5	1.852	22 $\bar{4}$ 0	1.846
1/2H	1.824	1/2	1.824	22 $\bar{4}$ 1	1.825
1HB	$\begin{matrix} 1.7875 \\ 1.7605 \end{matrix}$				
1H	1.692	3	1.698	$\begin{cases} 31\bar{4}2 \\ 21\bar{3}5 \\ 20\bar{2}6 \end{cases}$	$\begin{matrix} 1.700 \\ 1.699 \\ 1.690 \end{matrix}$
1/2	1.666	1/2	1.678	22 $\bar{4}$ 3	1.675
1/2	1.6315				
1/2	1.569	1/2	1.570	22 $\bar{4}$ 4	1.570
		1/2	1.547	$\begin{cases} 11\bar{2}7 \\ 40\bar{4}2 \end{cases}$	$\begin{matrix} 1.548 \\ 1.545 \end{matrix}$
1H	1.506	1	1.510	20 $\bar{2}$ 7	1.505
1H	1.487	1	1.492	0008	1.493

Table XVII (continued)

San Genaro mine Specimen C-144		Berry and Thompson (1962)			
I	$\underline{d}(\text{obs})$	I	$\underline{d}(\text{obs})$	hk11	$\underline{d}(\text{calc})$
1/2	1.461	1	1.463		
1/2	1.409	1	1.410		
1/2	1.355	1	1.358		
1/2	1.2495	1	1.252		

H - Hazy or diffuse line

B - Broad band, single measurement taken in middle

# Polybasite

The d-spacings in the X-ray powder diffraction photographs of polybasite from San Genaro are slightly lower than those for the pure material given by Peacock and Berry (1947) and Berry and Thompson (1962). Seven extraneous lines appeared in the six different diffraction patterns photographed, which are not reported by previous authors. Five of these lines can be matched reasonably well with lines in the pearceite pattern. The first three lines have d-spacings above 5.9 and may not have been detected by smaller diameter cameras.

Spectrographic analysis of the San Genaro polybasite shows appreciable percentages of copper and arsenic.

Table XVIII: X-ray powder diffraction pattern of polybasite

San Genaro mine Specimen C-144		Peacock and Berry (1947)				Berry and Thompson (1962)			
I	<u>d</u> (obs)	I	<u>d</u> (obs)	hkil	<u>d</u> (calc)	I	<u>d</u> (obs)	hkil	<u>d</u> (calc)
1H	11.86								
?	6.42								
1/2	5.97								
1/2	3.61	1	3.61	{ 31 $\bar{4}$ 0 22 $\bar{4}$ 2	{ 3.622 3.594	1	3.62	{ 31 $\bar{4}$ 0 22 $\bar{4}$ 2	{ 3.63 3.60
1/2	3.42	1/2	3.47	31 $\bar{4}$ 2	3.466	1/2	3.48	31 $\bar{4}$ 2	3.47
1/2	3.23	1/2	3.27	40 $\bar{4}$ 0	3.265	1/2	3.28	40 $\bar{4}$ 0	3.27
7	3.14	9	3.18	22 $\bar{4}$ 4	2.186	9	3.19	22 $\bar{4}$ 4	3.19
10	2.93	10	2.99	{ 32 $\bar{5}$ 0 0003	{ 2.996 2.980	10	3.00	{ 32 $\bar{5}$ 0 0003	{ 3.00 2.99
1/2	2.91								

Table XVIII (continued)

San Genaro mine Specimen C-144		Peacock and Berry (1947)				Berry and Thompson (1962)			
I	$\bar{d}_{(obs)}$	I	$\bar{d}_{(obs)}$	hkil	$\bar{d}_{(calc)}$	I	$\bar{d}_{(obs)}$	hkil	$\bar{d}_{(calc)}$
5	2.8615	8	2.87	$\begin{Bmatrix} 40\bar{4}4 \\ 41\bar{5}0 \end{Bmatrix}$	$\begin{Bmatrix} 2.864 \\ 2.850 \end{Bmatrix}$	8	2.88	$\begin{Bmatrix} 40\bar{4}4 \\ 41\bar{5}0 \end{Bmatrix}$	$\begin{Bmatrix} 2.87 \\ 2.86 \end{Bmatrix}$
2	2.776	1/2	2.76	11 $\bar{2}$ 8	2.771	1/2	2.77	11 $\bar{2}$ 8	2.78
2	2.675	5	2.69	$\begin{Bmatrix} 31\bar{4}6 \\ 32\bar{5}4 \end{Bmatrix}$	$\begin{Bmatrix} 2.677 \\ 2.677 \end{Bmatrix}$	5	2.70	$\begin{Bmatrix} 31\bar{4}6 \\ 32\bar{5}4 \end{Bmatrix}$	$\begin{Bmatrix} 2.68 \\ 2.68 \end{Bmatrix}$
4	2.521	6	2.52	$\begin{Bmatrix} 40\bar{4}6 \\ 33\bar{6}0 \end{Bmatrix}$	$\begin{Bmatrix} 2.523 \\ 2.513 \end{Bmatrix}$	6	2.53	$\begin{Bmatrix} 40\bar{4}6 \\ 33\bar{6}0 \end{Bmatrix}$	$\begin{Bmatrix} 2.53 \\ 2.52 \end{Bmatrix}$
6	2.414	4	2.42	42 $\bar{6}$ 2	2.417	4	2.42	42 $\bar{6}$ 2	2.42
1	2.392								
1	2.341	2	2.33	22 $\bar{4}$ 8	2.337				
1	2.312								
?	2.253								
4	2.1965	2	2.20	40 $\bar{4}$ 8	2.201	2	2.21	40 $\bar{4}$ 8	2.205
1H	2.142	1/2	2.14	$\begin{Bmatrix} 2.1.3.10 \\ 4370 \\ 60\bar{6}2 \end{Bmatrix}$	$\begin{Bmatrix} 2.147 \\ 2.147 \\ 2.141 \end{Bmatrix}$	1/2	2.15	$\begin{Bmatrix} 2.1.3.10 \\ 4370 \\ 60\bar{6}2 \end{Bmatrix}$	$\begin{Bmatrix} 2.151 \\ 2.151 \\ 2.145 \end{Bmatrix}$
1HB	2.1175								
	2.094	2	2.10	$\begin{Bmatrix} 43\bar{7}2 \\ 32\bar{5}8 \\ 42\bar{6}6 \end{Bmatrix}$	$\begin{Bmatrix} 2.113 \\ 2.113 \\ 2.097 \end{Bmatrix}$	2	2.11	$\begin{Bmatrix} 43\bar{7}2 \\ 32\bar{5}8 \\ 42\bar{6}6 \end{Bmatrix}$	$\begin{Bmatrix} 2.117 \\ 2.117 \\ 2.101 \end{Bmatrix}$
1H	2.049	1	2.06	$\begin{Bmatrix} 52\bar{7}2 \\ 41\bar{5}8 \end{Bmatrix}$	$\begin{Bmatrix} 2.060 \\ 2.059 \end{Bmatrix}$	1	2.07	$\begin{Bmatrix} 52\bar{7}2 \\ 41\bar{5}8 \end{Bmatrix}$	$\begin{Bmatrix} 2.064 \\ 2.063 \end{Bmatrix}$
1	2.025	3	2.02	$\begin{Bmatrix} 51\bar{6}6 \\ 43\bar{7}4 \\ 2.2.4.10 \end{Bmatrix}$	$\begin{Bmatrix} 2.020 \\ 2.020 \\ 2.015 \end{Bmatrix}$	3	2.02	$\begin{Bmatrix} 51\bar{6}6 \\ 43\bar{7}4 \\ 2.2.4.10 \end{Bmatrix}$	$\begin{Bmatrix} 2.024 \\ 2.024 \\ 2.019 \end{Bmatrix}$
1/2	1.987	1/2	1.971	$\begin{Bmatrix} 52\bar{7}4 \\ 61\bar{7}2 \end{Bmatrix}$	$\begin{Bmatrix} 1.973 \\ 1.964 \end{Bmatrix}$	1/2	1.977	$\begin{Bmatrix} 52\bar{7}4 \\ 61\bar{7}2 \end{Bmatrix}$	$\begin{Bmatrix} 1.977 \\ 1.968 \end{Bmatrix}$
1/2	1.9105	1	1.928	$\begin{Bmatrix} 4.0.4.10 \\ 33\bar{6}8 \\ 1.1.2.12 \end{Bmatrix}$	$\begin{Bmatrix} 1.925 \\ 1.921 \\ 1.921 \end{Bmatrix}$	1	1.933	$\begin{Bmatrix} 4.0.4.10 \\ 33\bar{6}3 \\ 1.1.2.12 \end{Bmatrix}$	$\begin{Bmatrix} 1.929 \\ 1.925 \\ 1.925 \end{Bmatrix}$



Table XVIII (continued)

San Genaro mine Specimen C-144		Peacock and Berry (1947)				Berry and Thompson (1962)			
I	d <sub>(obs)</sub>	I	d <sub>(obs)</sub>	hkil	d <sub>(calc)</sub>	I	d <sub>(obs)</sub>	hkil	d <sub>(calc)</sub>
				4376	1.839			4376	1.893
3	1.888	6	1.886	6174	1.889	6	1.892	6174	1.893
				4480	1.865			4480	1.889
1/2	1.861	1/2	1.854	5276	1.851	1/2	1.859	5276	1.855
1/2	1.845								
				6282	1.791			6282	1.795
1/2	1.7895	1	1.785	5384	1.780	1	1.791	5384	1.784
				6176	1.780			6176	1.784
				4378	1.742			4378	1.745
1/2H	1.742	1	1.738	3.1.4.12	1.742	1	1.743	3.1.4.12	1.745
				6284	1.733			6284	1.736
				4486	1.703			4486	1.706
1	1.701	3	1.702	0.0.0.14	1.703	3	1.707	0.0.0.14	1.706
				4.0.4.12	1.697			4.0.4.12	1.700
				3.2.5.12	1.656			3.2.5.12	1.659
1/2	1.658	2	1.654	6178	1.656	2	1.658	6178	1.659
				5492	1.656			5492	1.659
1/2	1.623	1	1.616	8082	1.617	1	1.621	8082	1.620
				4.3.7.10	1.595			4.3.7.10	1.598
1/2	1.595	2	1.590	4488	1.593	2	1.595	4488	1.596
				6394	1.586			6394	1.589
				7186	1.586			7186	1.589
				2.2.4.14	1.552			2.2.4.14	1.555
1/2	1.549	1	1.549	6288	1.548	1	1.554	6288	1.551
				4.2.6.12	1.548			4.2.6.12	1.551
				5.1.6.12	1.516			5.1.6.12	1.519
1H	1.5125	4	1.512	8192	1.516	4	1.517	8192	1.519
				8086	1.510			8086	1.513
				4.0.4.14	1.510			4.0.4.14	1.513
1/2	1.4805	1	1.484	0.0.0.16	1.490	1	1.488	0.0.0.16	1.493
		1/2	1.459			1/2	1.463		
		2	1.431			2	1.435		

Table XVIII (continued)

San Genaro mine Specimen C-144		Peacock and Berry (1947)				Berry and Thompson (1962)			
I	$\frac{d}{d}(\text{obs})$	I	$\frac{d}{d}(\text{obs})$	hkil	$\frac{d}{d}(\text{calc})$	I	$\frac{d}{d}(\text{obs})$	hkil	$\frac{d}{d}(\text{calc})$
		1	1.359			1	1.363		
		1	1.538			1	1.342		
		1/2	1.224			1/2	1.228		
		1	1.208			1	1.212		
		1/2	1.179			1/2	1.182		
		1/2	1.169			1/2	1.173		
		1/2	1.153			1/2	1.157		
		1	1.127			1	1.130		
		1	1.091			1	1.094		
		1	1.069			1	1.072		

H - Hazy or diffuse band

? - Possible faint line

# Pyrargyrite

X-ray diffraction data of pyrargyrite from San Genaro show the d-spacings to be slightly, yet consistently, lower than the values given by Berry and Thompson (1962), probably because of the presence of arsenic. The X-ray diffraction patterns of the Castrovirreyna material are more complete than those of Berry and Thompson, not only resolving many doublets, but also revealing many more lines, especially in the back reflection region. Spectrographic analysis indicates that the Castrovirreyna pyrargyrite is quite pure except for 1 to 2 percent arsenic (see Table XXXII).

Table XIX: X-ray powder diffraction pattern of pyrargyrite

San Genaro mine Specimen C-143		Berry and Thompson (1962)			
I	<u>d</u> (obs)	I	<u>d</u> (obs)	hkl	<u>d</u> (calc)
1	4.14	1	4.00	01 $\bar{1}$ 2	3.97
1	3.945				
6	3.33	5	3.35	21 $\bar{1}$ 1	3.34
6	3.21	8	3.21	30 $\bar{3}$ 0	3.19
6	3.17				
10	2.776	10	2.79	12 $\bar{3}$ 2	2.79
1/2H	2.751				
7	2.564	5	2.58	11 $\bar{2}$ 3	2.58
7	2.5355	5	2.54	13 $\bar{4}$ 1	2.54
2	2.2615	1	2.26	31 $\bar{4}$ 2	2.27
2	2.1225	1	2.13	{ 10 $\bar{1}$ 4 32 $\bar{5}$ 1	{ 2.13 2.13
1H	2.0875	1/2	2.09	{ 41 $\bar{5}$ 0 14 $\bar{5}$ 0	{ 2.09 2.09
1/2	1.997				

Table XIX (continued)

San Genaro mine Specimen C-143		Berry and Thompson (1962)			
I	$\underline{d}(\text{obs})$	I	$\underline{d}(\text{obs})$	hk11	$\underline{d}(\text{calc})$
1/2	1.955	2	1.965	2352	1.963
3	1.861	2	1.870	2134	1.871
1	1.8345	1/2	1.845	3360	1.844
1/2	1.768	1	1.755	5052	1.755
3	1.748				
2H	1.6805	1	1.689	5161	1.688
				1344	1.687
1/2	1.6635	1/2	1.675	4262	1.672
1/2	1.608	1/2	1.600	4044	1.614
				1562	1.601
				6060	1.597
				0660	1.597
2H	1.594				
1/2	1.568				
?	1.549				
2H	1.530	1/2	1.537	5270	1.534
				2570	1.534
?	1.5125				
?	1.480				
2H	1.452				
1	1.4005				
1H	1.390				
1	1.3805				
1/2H	1.3505				
1/2	1.267				
1	1.2105				
1/2	1.192				

Table XIX (continued)

San Genaro mine Specimen C-143		Barry and Thompson (1962)		
I	$\underline{d}(\text{obs})$	I	$\underline{d}(\text{obs})$	$\underline{d}(\text{calc})$
1	1.179			
1/2	1.157			
H	1.128			
1/2	1.066			
?	1.050			
1/2	1.0425			
?	0.897			
?	0.820			
?	0.815			

H - Hazy or diffuse line

? - Possible faint line

# Semseyite

X-ray diffraction data for semseyite from Caudalosa agree closely with the measured values given by Berry and Thompson (1962) and even better with data of Nuffield and Peacock (1945). The author's data coincide better with calculated values given by others, when careful measurement is made of the limits of the hazy bands that comprise most of the diffraction pattern. Spectrographic analysis indicates that the notable impurities are arsenic and silver, which apparently have not affected the cell dimensions (see Table XXXIII).

Table XX: X-ray powder diffraction pattern of semseyite

Caudalosa mine Specimen C-70		Nuffield and Peacock (1945)				Berry and Thompson (1962)			
I	d <sub>(obs)</sub>	I	d <sub>(obs)</sub>	hkl	d <sub>(calc)</sub>	I	d <sub>(obs)</sub>	hkl	d <sub>(calc)</sub>
1/2	6.565	1/2	6.59	220	6.55	1/2	6.61	200	6.56
1/2	5.43	1/2	5.46	113	5.40		5.47	113	5.41
1/2	4.50	1/2	4.56	{ $\frac{114}{115}$	{ $\frac{4.54}{4.52}$	1/2	4.58	{ $\frac{114}{115}$	{ $\frac{4.54}{4.53}$
2	4.21	1/2	4.20	{ $\frac{221}{223}$ 024	{ $\frac{4.21}{4.20}$ 4.20	1/2	4.21	{ $\frac{221}{223}$ 024	{ $\frac{4.22}{4.21}$ 4.21
7HB	$\frac{3.87}{3.81}$	5	3.84	{ $\frac{314}{130}$	{ $\frac{3.86}{3.82}$	5	3.85	{ $\frac{314}{130}$	{ $\frac{3.87}{3.83}$
2H	3.72	1/2	3.75	{ $\frac{131}{132}$	{ $\frac{3.73}{3.72}$	1/2	3.75	{ $\frac{131}{132}$	{ $\frac{3.73}{3.73}$
3H	3.56	2	3.59	{ $\frac{315}{225}$	{ $\frac{3.58}{3.57}$	2	3.59	{ $\frac{315}{225}$	{ $\frac{3.59}{3.58}$
4	3.355	8	3.37	{ $\frac{116}{117}$	{ $\frac{3.36}{3.36}$	8	3.38	{ $\frac{116}{117}$	{ $\frac{3.38}{3.37}$

Table XX (continued)

Caudalosa mine Specimen C-70		Nuffield and Peacock (1945)				Berry and Thompson (1962)			
I	$\underline{d}_{(obs)}$	I	$\underline{d}_{(obs)}$	hkl	$\underline{d}_{(calc)}$	I	$\underline{d}_{(obs)}$	hkl	$\underline{d}_{(calc)}$
10B	$\left\{ \begin{array}{l} 3.29 \\ 3.24 \end{array} \right.$	10	3.26	$\left\{ \begin{array}{l} 026 \\ \bar{3}16 \\ 400 \\ \bar{2}26 \\ 404 \end{array} \right.$	$\left\{ \begin{array}{l} 3.29 \\ 3.29 \\ 3.27 \\ 3.25 \\ 3.23 \end{array} \right.$	10	3.27	$\left\{ \begin{array}{l} 400 \\ \bar{2}26 \\ \bar{4}04 \end{array} \right.$	$\left\{ \begin{array}{l} 3.28 \\ 3.26 \\ 3.24 \end{array} \right.$
1H	3.02			$\left\{ \begin{array}{l} 040 \\ \bar{3}31 \\ 118 \end{array} \right.$	$\left\{ \begin{array}{l} 3.00 \\ 2.99 \\ 2.97 \end{array} \right.$			$\left\{ \begin{array}{l} 041 \\ \bar{1}17 \\ \bar{1}18 \end{array} \right.$	$\left\{ \begin{array}{l} 2.98 \\ 2.98 \\ 2.97 \end{array} \right.$
5B	$\left\{ \begin{array}{l} 2.965 \\ 2.935 \end{array} \right.$	9	2.97	$\left\{ \begin{array}{l} 041 \\ \bar{2}25 \\ 117 \\ \bar{2}27 \\ 008 \end{array} \right.$	$\left\{ \begin{array}{l} 2.97 \\ 2.97 \\ 2.97 \\ 2.96 \\ 2.95 \end{array} \right.$	9	2.98	$\left\{ \begin{array}{l} \bar{2}25 \\ \bar{2}27 \\ 008 \end{array} \right.$	$\left\{ \begin{array}{l} 2.97 \\ 2.96 \\ 2.95 \end{array} \right.$
4B	$\left\{ \begin{array}{l} 2.8755 \\ 2.848 \end{array} \right.$	4	2.86	$\left\{ \begin{array}{l} 420 \\ \bar{4}24 \\ 331 \\ 135 \end{array} \right.$	$\left\{ \begin{array}{l} 2.87 \\ 2.86 \\ 2.86 \\ 2.86 \end{array} \right.$	4	2.87	$\left\{ \begin{array}{l} 420 \\ \bar{4}24 \\ 331 \\ 135 \end{array} \right.$	$\left\{ \begin{array}{l} 2.88 \\ 2.87 \\ 2.87 \\ 2.86 \end{array} \right.$
3B	$\left\{ \begin{array}{l} 2.7715 \\ 2.6905 \end{array} \right.$	1	2.77	$\left\{ \begin{array}{l} \bar{4}25 \\ 421 \\ 318 \end{array} \right.$	$\left\{ \begin{array}{l} 2.77 \\ 2.77 \\ 2.75 \end{array} \right.$	1	2.78	$\left\{ \begin{array}{l} 421 \\ \bar{4}25 \end{array} \right.$	$\left\{ \begin{array}{l} 2.78 \\ 2.77 \end{array} \right.$
		4	2.70	$\left\{ \begin{array}{l} \bar{2}26 \\ \bar{2}28 \end{array} \right.$	$\left\{ \begin{array}{l} 2.70 \\ 2.69 \end{array} \right.$	4	2.71	$\left\{ \begin{array}{l} \bar{2}66 \\ \bar{2}28 \end{array} \right.$	$\left\{ \begin{array}{l} 2.71 \\ 2.70 \end{array} \right.$
2H	2.446	1	2.48	$\left\{ \begin{array}{l} 243 \\ \bar{5}16 \\ \bar{2}27 \\ \bar{2}29 \end{array} \right.$	$\left\{ \begin{array}{l} 2.49 \\ 2.47 \\ 2.47 \\ 2.46 \end{array} \right.$	1	2.49	$\left\{ \begin{array}{l} 243 \\ \bar{2}27 \\ \bar{5}16 \end{array} \right.$	$\left\{ \begin{array}{l} 2.49 \\ 2.47 \\ 2.47 \end{array} \right.$
		1/2	2.37	$\left\{ \begin{array}{l} 424 \\ \bar{2}44 \\ \bar{2}46 \\ 423 \\ 0.0.10 \end{array} \right.$	$\left\{ \begin{array}{l} 2.37 \\ 2.37 \\ 2.37 \\ 2.36 \\ 2.36 \end{array} \right.$	1/2	2.38		
3	2.246	3	2.25	$\left\{ \begin{array}{l} 2.2.10 \\ \bar{6}02 \\ \bar{6}04 \\ \bar{5}13 \\ \bar{2}45 \\ \bar{1}39 \\ \bar{5}18 \\ \bar{4}42 \\ 247 \end{array} \right.$	$\left\{ \begin{array}{l} 2.26 \\ 2.26 \\ 2.26 \\ 2.26 \\ 2.25 \\ 2.25 \\ 2.25 \\ 2.25 \\ 2.25 \end{array} \right.$	3	2.25		

Table XX (continued)

Caudalosa mine Specimen C-70		Nuffield and Peacock (1945)				Berry and Thompson (1962)			
I	d(obs)	I	d(obs)	hkl	d(calc)	I	d(obs)	hkl	d(calc)
3	2.2215								
4H	2.1515	3	2.15	$\begin{cases} 441 \\ \bar{4}45 \\ \bar{1}55 \\ 514 \\ 318 \end{cases}$	$\begin{cases} 2.16 \\ 2.16 \\ 2.15 \\ 2.15 \\ 2.15 \end{cases}$	3	2.16		
		1/2	2.11	$\begin{cases} \bar{3}51 \\ \bar{6}23 \\ 622 \\ 043 \end{cases}$	$\begin{cases} 2.12 \\ 2.12 \\ 2.11 \\ 2.10 \end{cases}$	1/2	2.11		
1H	2.0515	1	2.05	$\begin{cases} 532 \\ 636 \\ 2.0.10 \\ 2.0.12 \end{cases}$	$\begin{cases} 2.07 \\ 2.05 \\ 2.95 \\ 2.04 \end{cases}$	1	2.06		
1/2H	2.0015	1/2	2.00	$\begin{cases} 060 \\ 1.1.11 \\ 1.1.12 \end{cases}$	$\begin{cases} 2.00 \\ 2.00 \\ 2.00 \end{cases}$	1/2	2.01		
1/2	1.963	1/2	1.975	$\begin{cases} 156 \\ \bar{1}57 \\ 049 \\ 062 \end{cases}$	$\begin{cases} 1.980 \\ 1.979 \\ 1.973 \\ 1.970 \end{cases}$	1/2	1.981		
3H	1.918	2	1.916	$\begin{cases} \bar{7}14 \\ \bar{2}61 \\ 338 \\ \bar{5}.1.11 \end{cases}$	$\begin{cases} 1.917 \\ 1.917 \\ 1.916 \\ 1.914 \end{cases}$	2	1.922		
1/2	1.888	1/2	1.897	$\begin{cases} 357 \\ 248 \end{cases}$	$\begin{cases} 1.899 \\ 1.897 \end{cases}$	1/2	1.903		
1H	1.8555	1	1.858	$\begin{cases} 262 \\ \bar{2}64 \\ 0.4.10 \end{cases}$	$\begin{cases} 1.863 \\ 1.862 \\ 1.854 \end{cases}$	1	1.863		
1H	1.8005	1	1.802	$\begin{cases} 711 \\ 2.2.11 \\ \bar{3}21 \\ \bar{3}22 \\ 339 \\ \bar{1}58 \\ 2.2.13 \\ 159 \end{cases}$	$\begin{cases} 1.805 \\ 1.804 \\ 1.804 \\ 1.803 \\ 1.801 \\ 1.799 \\ 1.799 \\ 1.793 \end{cases}$	1	1.807		



Table XX (continued)

Caudalosa mine Specimen C-70		Nuffield and Peacock (1945)				Berry and Thompson (1962)			
I	d(obs)	I	d(obs)	hkl	d(calc)	I	d(obs)	hkl	d(calc)
1	1.7715	1/2	1.763	$\begin{Bmatrix} \bar{5}55 \\ 646 \end{Bmatrix}$	$\begin{Bmatrix} 1.776 \\ 1.761 \end{Bmatrix}$	1/2	1.768		
1/2H	1.725	1	1.720	$\begin{Bmatrix} \bar{2}67 \\ 3.1.14 \end{Bmatrix}$	$\begin{Bmatrix} 1.722 \\ 1.721 \end{Bmatrix}$	1	1.725		
1/2H	1.6865	1	1.687	$\begin{Bmatrix} 737 \\ 2.4.10 \\ 642 \\ \bar{3}.3.13 \\ 172 \\ 171 \\ \bar{2}.4.12 \\ 648 \\ 2.2.12 \\ 0.0.14 \end{Bmatrix}$	$\begin{Bmatrix} 1.691 \\ 1.691 \\ 1.691 \\ 1.691 \\ 1.690 \\ 1.690 \\ 1.688 \\ 1.687 \\ 1.685 \\ 1.685 \end{Bmatrix}$	1	1.692		
1/2	1.4775	1	1.478			1	1.482		
1/2	1.344	1/2	1.337			1/2	1.341		
1/2	1.279	1/2	1.280			1/2	1.284		
1/2	1.263	1/2	1.260			1/2	1.264		
		1/2	1.234			1/2	1.237		
1/2	1.21	1/2	1.211			1/2	1.215		
1/2	1.655	1/2	1.179			1/2	1.182		

H - Hazy or diffuse line

B - Broad band, single measurement taken in middle  
double measurement taken on edges.

# Zinkenite

Measurements of X-ray powder diffraction photographs of zinkenite from Caudalosa agree in general with the observations of Nuffield (1946) and Berry and Thompson (1962), coinciding better with their calculated values than with the observed ones. Diffraction patterns of the Caudalosa material showed 13 lines not previously reported.

Copper and silver are the principal impurities found by spectrographic analysis (see Table XXXVII).

Table XXI: X-ray powder diffraction pattern of zinkenite

Caudalosa mine Specimen C-33		Nuffield (1946)				Berry and Thompson (1962)			
I	$\underline{d}(\text{obs})$	I	$\underline{d}(\text{obs})$	hkil	$\underline{d}(\text{calc})$	I	$\underline{d}(\text{obs})$	hkil	$\underline{d}(\text{calc})$
1/2H	10.99								
?	10.4								
1H	7.195								
2	5.505	1/2	5.49	44 $\bar{8}$ 0	5.51	1/2	5.50	44 $\bar{8}$ 0	5.52
1/2	5.275								
1/2	4.77	1/2	4.79	08 $\bar{8}$ 0	4.77	1/2	4.80	08 $\bar{8}$ 0	4.78
1	4.36		4.41	4.6. $\bar{1}$ 0.0	4.37	1/2	4.42	4.6. $\bar{1}$ 0.0	4.39
2	4.12								
4	3.91	1	3.94	04 $\bar{4}$ 2	3.92	1	3.95	04 $\bar{4}$ 2	3.93
2	3.705								
3	3.555	1	3.55	06 $\bar{6}$ 2	3.56		3.56	06 $\bar{6}$ 2	3.57
7	3.45	10	3.44	2.10. $\bar{1}$ 2.0	3.43		3.45	2.10. $\bar{1}$ 2.0	3.43
10	3.41	1	3.36	44 $\bar{3}$ 2	3.39		3.36	44 $\bar{3}$ 2	3.40
6	3.33								
1H	3.19								

Table XXI (continued)

Caudalosa mine Specimen C-33			Huffield (1946)			Berry and Thompson (1962)				
I	d <sub>(obs)</sub>		I	d <sub>(obs)</sub>	hkil	d <sub>(calc)</sub>	I	d <sub>(obs)</sub>	hkil	d <sub>(calc)</sub>
2	3.13									
4		1	3.07	{ 4. 6. $\overline{10.2}$ 4.10.14.0		3.07 3.06	1	3.08	{ 4. 6. $\overline{10.2}$ 4.10.14.0	3.07 3.06
4	2.98	2	3.01	2. 8. $\overline{10.2}$		2.99	2	3.02	2. 8. $\overline{10.2}$	3.00
1/2	2.905	1/2	2.90	2.12. $\overline{14.0}$		2.91	1/2	2.91	2.12. $\overline{14.0}$	2.91
7	2.792	4	2.80	6. 6. $\overline{12.2}$		2.79	4	2.81	6. 6. $\overline{12.2}$	2.80
5	2.7595									
1	2.6925	1/2	2.69	2.10. $\overline{12.2}$		2.68	1/2	2.70	2.10. $\overline{12.2}$	2.68
1/2H	2.5425	1/2	2.54	{ 0.12. $\overline{12.2}$ 6. 8. $\overline{14.2}$ 2.14. $\overline{16.0}$		2.56 2.53 2.53	1/2	2.54	{ 0.12. $\overline{12.2}$ 6. 8. $\overline{14.2}$ 2.14. $\overline{16.0}$	2.56 2.54 2.53
2	2.4075	1	2.41	{ 2.12. $\overline{14.2}$ 6.12. $\overline{18.0}$		2.41 2.40	1	2.42	{ 2.12. $\overline{14.2}$ 6.12. $\overline{18.0}$	2.41 2.41
2	2.301	1/2	2.30	{ 0.14. $\overline{14.2}$ 6.10. $\overline{16.2}$		2.30 2.30	1/2	2.30	{ 0.14. $\overline{14.2}$ 6.10. $\overline{16.2}$	2.31 2.31
3	2.253	1	2.25	{ 4.12. $\overline{16.2}$ 2.16. $\overline{18.0}$		2.25 2.23	1	2.25	{ 4.12. $\overline{16.2}$ 2.16. $\overline{18.0}$	2.26 2.24
5	2.149	1	2.15	{ 0004 6.14. $\overline{20.0}$		2.15 2.15	1	2.16	{ 0004 6.14. $\overline{20.0}$	2.15 2.15
5	2.125	2	2.13	{ 8.10. $\overline{18.2}$ 0.13. $\overline{18.0}$		2.12 2.12	2	2.13	{ 8.10. $\overline{18.2}$ 0.13. $\overline{18.0}$	2.13 2.12
1	2.083	2	2.06	{ 4.16. $\overline{20.0}$ 4.14. $\overline{18.2}$		2.08 2.05	2	2.06	{ 4.16. $\overline{20.0}$ 4.14. $\overline{18.2}$	2.09 2.05
5	1.9795	3	1.980	{ 2.16. $\overline{18.2}$ 8.14. $\overline{22.0}$		1.982 1.978	3	1.985	{ 2.16. $\overline{18.2}$ 8.14. $\overline{22.0}$	1.986 1.982
4	1.8735	1	1.875	{ 4.16. $\overline{20.2}$ 0.10. $\overline{10.4}$		1.874 1.873	1	1.881	{ 4.16. $\overline{20.2}$ 0.10. $\overline{10.4}$	1.878 1.877
6	1.8205	3	1.823	2.10. $\overline{12.4}$		1.823	3	1.828	2.10. $\overline{12.4}$	1.827

Table XXI (continued)

Caudalosa mine Specimen C-33				Nuffield (1946)		Berry and Thompson (1962)			
I	$\underline{d}(\text{obs})$	I	$\underline{d}(\text{obs})$	hkil	$\underline{d}(\text{calc})$	I	$\underline{d}(\text{obs})$	hkil	$\underline{d}(\text{calc})$
10H	1.770		1.763	$\left\{ \begin{array}{l} 6.16.\overline{22}.2 \\ 6.18.\overline{24}.0 \end{array} \right.$	$\left\{ \begin{array}{l} 1.766 \\ 1.764 \end{array} \right.$	1/2	1.768	$\left\{ \begin{array}{l} 6.16.\overline{22}.2 \\ 6.18.\overline{24}.0 \end{array} \right.$	$\left\{ \begin{array}{l} 1.770 \\ 1.768 \end{array} \right.$
2	1.716	1	1.711	4.20. $\overline{24}.0$	1.713	1	1.716	4.20. $\overline{24}.0$	1.716
		1/2	1.687	$\left\{ \begin{array}{l} 12.12.\overline{24}.2 \\ 0.14.\overline{14}.4 \\ 6.10.\overline{16}.4 \end{array} \right.$	$\left\{ \begin{array}{l} 1.688 \\ 1.688 \\ 1.688 \end{array} \right.$	1/2	1.692	$\left\{ \begin{array}{l} 12.12.\overline{24}.2 \\ 0.14.\overline{14}.4 \\ 6.10.\overline{16}.4 \end{array} \right.$	$\left\{ \begin{array}{l} 1.691 \\ 1.691 \\ 1.691 \end{array} \right.$
2H	1.6555	1	1.654	$\left\{ \begin{array}{l} 2.22.\overline{24}.0 \\ 8.18.\overline{26}.0 \end{array} \right.$	$\left\{ \begin{array}{l} 1.654 \\ 1.654 \end{array} \right.$	1	1.658	$\left\{ \begin{array}{l} 2.22.\overline{24}.0 \\ 8.18.\overline{26}.0 \end{array} \right.$	$\left\{ \begin{array}{l} 1.657 \\ 1.657 \end{array} \right.$
1/2	1.573	1/2	1.579	$\left\{ \begin{array}{l} 4.14.\overline{18}.4 \\ 4.22.\overline{26}.0 \\ 12.14.\overline{26}.2 \end{array} \right.$	$\left\{ \begin{array}{l} 1.580 \\ 1.575 \\ 1.575 \end{array} \right.$	1/2	1.583	$\left\{ \begin{array}{l} 4.14.\overline{18}.4 \\ 4.22.\overline{26}.0 \\ 12.14.\overline{26}.2 \end{array} \right.$	$\left\{ \begin{array}{l} 1.583 \\ 1.578 \\ 1.578 \end{array} \right.$
1/2H	1.521	1/2	1.519			1/2	1.523		
1	1.499								
1/2	1.4765					1	1.463		
3	1.457	1	1.459						
1H	1.440	1/2	1.445			1	1.449		
1H	1.4115	1/2	1.408			1/2	1.412		
1H	1.390	1	1.389			1	1.393		
1/2	1.369	1/2	1.366			1/2	1.370		
3H	1.340	1	1.340			1	1.344		
1	1.313	1/2	1.313			1/2	1.316		
1H	1.2935	1/2	1.292			1/2	1.296		
1/2	1.1825								
1/2	1.292								
1/2	1.142	1/2	1.143			1/2	1.147		

Table XXI (continued)

Caudalosa mine  
Specimen C-33

Nuffield (1946)

Berry and  
Thompson (1962)

I	$\underline{d}_{(obs)}$	I	$\underline{d}_{(obs)}$	hkil	$\underline{d}_{(calc)}$	I	$\underline{d}_{(obs)}$	hkil	$\underline{d}_{(calc)}$
2H	1.123	1/2	1.123			1/2	1.126		
1/2	1.0675	1/2	1.066			1/2	1.069		
1	1.0225	1/2	1.028			1/2	1.031		

H - Hazy or diffuse line

? - Possible faint line

## APPENDIX V

### Spectrographic Analyses

Table XXII: Spectrographic analysis of aramayoite

Major constituents	( > 10%)	Ag, Sb
Minor constituents	(0.1-10%)	Si
Traces	( < 0.1%)	Fe, Cu
Locality: A level, San Julián vein, San Genaro mine		
Specimen: C-228		

Table XXIII: Spectrographic analyses of bournonite

	<u>1.</u>	<u>2.</u>
Over 10%	Pb	Pb
3 to 30%	Cu, Sb	Cu, Sb
1 to 10%		Ag, As
0.3 to 3%	Ag, As	Si*
0.1 to 1%	Zn	Fe
0.03 to 0.3%		Zn
0.01 to 0.1%	Si*, Fe, Bi	Mn, Cd, Bi
Traces	Mg*, Mn	Al*, Mg*, In (?)

\* - Possibly due to impurities

1. Caudalosa vein, Pompeyo level, Caudalosa mine  
(specimen C-283)
2. Caudalosa vein, 570 level, Caudalosa mine  
(specimen C-173)

Table XXIV: Spectrographic analysis of chalcostibite

Major constituents	( > 10%)	Cu, Sb
Minor constituents	(0.1-10%)	Fe
Traces	( < 0.1%)	Ag, Si, Mg
Locality: 610 level, Caudalosa vein, Caudalosa mine		
Specimen: C-30		

Table XXV: Analyses of enargite

<u>1.</u>		<u>2.</u>
S	32.42	Over 10% Cu
Cu	48.53	3 to 30% As
As	<u>19.08</u>	1 to 10% Sb
	100.03	0.3 to 3% Ag
		0.1 to 1% Hg
		0.03 to 0.3% Sn, Si*
		0.01 to 0.1% Mn, Fe
		Traces Bi, In, Al*, Mg*, Ca*

\* - Possibly due to impurities

1. Chemical analysis of enargite from Caudalosa mine, Stevanović (1903).
2. Spectrographic analysis of enargite from 610 level, Caudalosa vein, Caudalosa mine (specimen C-122).



Table XXVI: Analyses of famatinite.

	<u>1.</u>		<u>2.</u>
S	31.01	Over 10%	Cu
Sb	12.74	3 to 30%	Sb
As	9.09	1 to 10%	As
Cu	45.43	0.3 to 3%	Ag, Hg
Fe	0.67	0.1 to 1%	Sn
Resid.	<u>0.65</u>	0.03 to 0.3%	Tl, Si*
	99.59	0.01 to 0.1%	Fe
		Traces	Bi, In, Mo, Mn
			Al*, Ca*, Mg*

\* - Possibly due to impurities

1. Average of two chemical analyses of famatinite from Caudalosa mine, Stevanović (1903).
2. Spectrographic analysis of famatinite from 610 level of Caudalosa vein, Caudalosa mine (specimen C-122).

Table XXVII: Spectrographic analysis of ferrous sulfate (pozenite)

Major constituents: Fe

Minor constituents: Cu, Ag

Traces : Mg, Si

Locality : 640 level, San Pedro vein, Caudalosa mine.

Specimen : C-90A

Occurrence: Dessication product of melanterite.

Table XXVIII: Spectrographic analysis of galena

	1	2	5	14	17a	17b	18	21	22	23	27	28
Boron	-	-	tr	-	-	tr	-	-	-	-	tr	-
Silicon	.01	.06	.06	.06	.01	.16	.06	.03	.12	.12	.12	.12
Aluminum	tr	tr	.004	tr	tr	tr	.002	.002	tr	.006	.006	.002
Magnesium	tr	tr	-	tr	tr	tr	-	tr	tr	-	tr	-
Calcium	.04	.04	.04	.04	.02	.02	.04	.04	.04	.04	.04	.04
Iron	.015	.015	.015	.010	.007	.015	.010	.015	.015	.030	.040	.010
Manganese	tr	tr	.01	tr	tr	tr	tr	tr	tr	tr	tr	tr
Zinc	tr	tr	tr	tr	tr	tr	tr	tr	.20	.40	.07	tr
Cadmium	-	-	-	-	-	-	-	-	-	tr	-	-
Lead	30	30	30	30	30	30	30	30	30	30	30	30
Copper	tr	tr	.01	tr	.01	.05	.08	.01	tr	.10	.01	tr
Silver	.01	.10	.01	.10	.10	.01	.01	.01	.10	.01	.01	.01
Bismuth	tr	tr	tr	tr	tr	tr	tr	tr	tr	tr	tr	tr?
Antimony	.02	.24	.02	.02	.24	.10	.40	.08	.40	.24	.24	.01
Arsenic	-	-	-	-	-	-	-	tr	-	tr	tr	-
Indium	-	-	tr?	tr?	-	-	-	-	tr?	-	-	tr?

Elements looked for but not found: alkalis, Ba, Sr, Be, Ti, V, Cr, Co, Ni, Au, Hg, Sn, Ta, Zr, Hf, Nb, Ta, Mo, W, Re, Pt, Sc, Y, Th, U, P, Ga, Ge, Tl.

Localities

1. Caldera vein, Caldera level, Lira mine, specimen C-145
2. Lira vein, Caldera level, Lira mine, specimen C-220
5. Mata Cabello vein, 480 level, Sta. Teresita mine, specimen C-187
14. Caudalosa vein, 570 level, Caudalosa mine, specimen C-217
- 17a. San Pedro vein, 610 level, Caudalosa mine, specimen C-90 coarse grained
- 17b. San Pedro vein, 610 level, Caudalosa mine, specimen C-90 fine-grained
18. San Pedro vein, 610 level, Caudalosa mine, specimen C-241
21. No. 1 vein, 580 level, Madona mine, specimen C-180
22. San Julián North vein, A level, San Genaro mine, specimen C-283
23. San Julián vein, A level, San Genaro mine, specimen C-25
27. Quacpisisa vein, 35 level, San Genaro mine, specimen C-24
28. Bella-Aranzazu vein, Dump, Rápida mine, specimen C-226

Table XXIX: Spectrographic analyses of geocronite

	<u>Massive</u>	<u>Sooty</u>
Over 10%	Pb	Pb
3 to 30%	Sb	Sb
1 to 10%	As	As
0.3 to 3%	Si*, Ag	Si*, Ag
0.1 to 1%		
0.03 to 0.3%		Cu, Fe
0.01 to 0.1%	Zn, Fe	Mn, Tl
Traces	Al*, Mg*, Bi,	Al*, Mg*, Cd,
	Cu, Sn, Tl	Sn, Bi

\* - Possibly due to impurities

Locality: 570 level, Caudalosa vein, Caudalosa mine

Specimen: C-101

Table XXX: Spectrographic analysis of miargyrite

Over 10%	Ag, Sb
3 to 30%	
1 to 10%	
0.3 to 3%	
0.1 to 1%	Hg, Pb, As
0.03 to 0.3%	Zn
0.01 to 0.1%	Si*, Cu
Traces	Al*, Mg*, Fe

\* - Possibly due to impurities

Locality: San Genaro level, San Julián vein, San Genaro mine

Specimen: C-144

Table XXXI: Analyses of polybasite

	<u>1.</u>		<u>2.</u>
Ag	67.95	Over 10%	Ag
Cu	6.07	3 to 30%	Sb
Sb	5.15	1 to 10%	
As	3.38	0.3 to 3%	Cu, Fe, As
S	16.37	0.1 to 1%	Pb
Resid.	<u>0.76</u>	0.03 to 0.3%	Zn, Si*
	100.18	0.01 to 0.1%	
		Traces	Bi, Mg*

\* - Possibly due to impurities

1. Analysis of polybasite from "Quispesisa vein" (San Genaro),  
Castrovirreyna, Boddlander (1895).
2. Spectrographic analysis of polybasite from San Julián vein,  
San Genaro mine (specimen C-144).

Table XXXII: Spectrographic analyses of pyrargyrite from the San

Genaro mine

	<u>1.</u>	<u>2.</u>	<u>3.</u>
Over 10%			
3 to 30%	Ag, Sb	Ag, Sb	Ag, Sb
1 to 10%	As		
0.3 to 3%			
0.1 to 1%			
0.03 to 0.3%	Cu	Cu	Cu, Si, Mg*
0.01 to 0.1%	Si*, Al*	Si*, Fe, Pb	
Traces	Mg*, Mn, Fe, Bi	Al*, Mg*, Bi	

\* - Possibly due to impurities

1. Milagro vein, Niño Jesús level, San Genaro mine (specimen C-143)
2. San Julián vein, A level, San Genaro mine (specimen C-144)
3. San Julián north vein, B level, San Genaro mine (specimen C-225)

Table XXXIII: Spectrographic analysis of semseyite

Over 10%	Pb
3 to 30%	Sb
1 to 10%	
0.3 to 3%	Ag, As
0.1 to 1%	
0.03 to 0.3%	
0.01 to 0.1%	Si*, Fe
Traces	Al*, Na*, Mg*, Cu, Sn (?), Bi

\* - Possibly due to impurities

Locality: 610 level, Caudalosa vein, Caudalosa mine

Specimen: C-70

Table XXXIV: Spectrographic analyses of sphalerite

	1	4	5	6	8	9	10	11	14	17	18a	18b	19	21	22	23	26	27	28
Boron	-	-	-	-	-	tr	-	tr	-	-	-	-	-	-	-	-	-	-	tr
Silicon	.06	.03	.06	.12	.03	.008	.2	.4	.01	.02	.03	.03	.06	.01	.7	.03	.12	.03	.70
Aluminum	.03	-	.002	tr	tr	-	tr	.004	tr	-	tr	-	tr	-	-	tr	-	-	.004
Magnesium	tr	tr	.03	tr	tr	.01	-	tr	tr	tr	tr	tr	tr	-	tr	tr	tr	tr	.03
Calcium	.02	tr	.04	tr	tr	-	tr	.02	tr	tr	.03	.05	.02	tr	tr	tr	tr	tr	.04
Barium	-	-	-	-	-	-	-	-	-	-	-	-	-	-	.05	-	-	-	-
Iron	.03	.88	.10	.015	.08	.01	.69	.006	.57	.86	.015	.15	.03	.76	.03	.23	.70	.40	.15
Manganese	.002	.014	.05	.011	tr	.002	.008	.02	.004	.004	.007	tr	.007	.002	tr	.008	.018	.006	.05
Zinc	>30	>30	>30	>30	>30	>30	>30	>30	>30	>30	>30	>30	>30	>30	>30	>30	>30	>30	>30
Cadmium	.02	.02	.09	.02	.23	.8	.35	.20	.21	.024	.01	.02	.02	.14	.02	.17	.13	.04	.30
Lead	-	-	tr	-	-	.01	.03	.90	-	-	.03	tr	-	-	.06	-	-	-	.30
Copper	.002	.002	.01	.005	.003	.01	.35	.20	.001	.05	.05	.005	.005	.002	.25	tr	.002	.001	.01
Gold	-	-	-	-	-	-	.002	-	-	-	-	-	-	-	-	-	-	-	-
Silver	tr	-	tr	>.01	tr	>.01	>.01	>.01	tr	tr	>.01	tr	>.01	tr	>.01	tr	tr	tr	tr
Bismuth	.08	-	-	-	-	tr	-	tr	-	-	-	-	-	-	-	-	-	-	-
Mercury	-	.08	-	tr	.24	-	.16	.07	tr	.24	.08	.16	.08	tr	.16	tr	.05	tr	-
Tin	-	-	-	-	-	-	-	.004	-	.004	-	-	-	-	-	-	-	-	-
Antimony	-	-	-	-	-	tr	.015	.04	-	.015	.15	tr	-	-	-	-	-	-	tr
Arsenic	-	-	-	-	-	-	-	.30	-	-	-	-	-	-	-	-	-	-	-
Gallium	-	-	tr	.03	-	.025	.03	.01	-	.01	.02	.005	.02	.005	.005	-	-	-	-
Germanium	-	-	-	.002	.02	.004	.002	.002	-	tr	.002	-	.003	-	-	-	-	-	-
Indium	.006	.02	-	.01	-	.01	.006	.025	-	.37	.010	.025	.006	-	-	-	tr	-	tr

Elements looked for but not found: alkalies, Be, Sr, Ba, Ti, V, Cr, Co, Ni, Ta, Zr, Hf, Nb, Ta, Mo, W, Re, Pt, Sc, Y, Th, U, B, P, Tl.

Localities

1.	Caldera vein,	Caldera level,	Lira mine,	specimen	C-145
4.	Lira vein,	" "	" "	"	C-235
5.	Mata Caballo vein,	480 level,	Sta. Teresita mine,	"	C-187
6.	Caudalosa vein,	San Felix level,	Caudalosa mine,	"	C-107
8.	" "	610 level,	" "	"	C-30
9.	" "	" "	" "	"	C-219
10.	" "	" "	" "	"	C-173
11.	" "	570 level,	" "	"	C-225
14.	" "	" "	" "	"	C-217
17.	San Pedro vein,	610 level,	" "	"	C-90
18a.	" " "	" "	" "	"	C-241, fine grained
18b.	" " "	" "	" "	"	C-241, coarse-grained
19.	" " "	" "	" "	"	C-240
21.	Entrada vein,	580 level,	Madona mine,	"	C-180
22.	San Julián Norte vein,	A level,	San Genaro mine,	"	C-283
23.	San Julián vein,	San Genaro level,	" " "	"	C-25
26.	" " "	" " "	" " "	"	C-28
27.	Quespisisa vein,	35 level,	" " "	"	C-24
28.	Bella-Aranzazu vein,	Dump,	Rápida mine,	"	C-226

Table XXV: Spectrographic analysis of stibnite

Over 10%	Sb
3 to 30%	
1 to 10%	
0.3 to 3%	Zn, As
0.1 to 1%	Pb
0.03 to 0.3%	
0.01 to 0.1%	Si*, Al*, Mg*, Fe, Cu, Bi
Traces	Mn

\* - Possibly due to impurities

Locality: 570 level, Caudalosa vein, Caudalosa mine

Specimen: C-150

Table XXXVI: Spectrographic analyses of tetrahedrite

	1	3	5	7	12	13	15	16	17	18	20	21	22	23	24	25
Boron	-	-	-	-	tr	-	-	-	-	-	-	-	-	-	-	-
Silicon	.12	.032	.06	.2	.024	.20	.06	.03	.016	.04	.12	.06	.12	.40	.30	.30
Aluminum	-	tr	tr	tr	-	tr	.02	tr	-	tr	tr	tr	.01	.04	tr	-
Magnesium	tr	-	tr	-	-	tr	-	tr	.005	tr	tr	tr	tr	tr	tr	tr
Calcium	tr	.03	tr	tr	.005	tr	-	-	-	-	tr	-	-	-	-	tr
Iron	.2	.7	.26	.4	4.0	.45	.007	.54	1.5	.4	.225	.006	.4	.4	.54	.11
Manganese	.025	.40	.40	.005	.04	.2	.007	.006	.002	.007	.4	.025	.001	.002	.4	.002
Zinc	-	.9	2.5	2.5	.9	1.2	.1	1.0	1.2	2.5	1.0	2.5	2.5	2.5	1.2	-
Cadmium	.05	-	.03	.05	.3	.03	.01	.02	.1	.05	.01	.1	.1	.05	.02	.1
Lead	.20	.01	.08	1.95	-	.12	3.0	-	.05	.02	.04	.45	.2	1.2	.04	.75
Copper	10	10	10	10	10	10	10	10	10	10	10	10	10	10	10	10
Silver	.1	1.0	1.0	1.0	1.0	1.0	.01	1.0	.1	1.0	.1	1.0	1.0	1.0	1.0	1.0
Bismuth	-	tr	-	.15	1.0	.3	tr	.8	3.0	.5	.02	tr	tr	tr	.5	.03
Mercury	tr	-	-	.90	-	.5	-	-	.15	1.0	.7	.5	.7	.6	.6	.9
Antimony	10	10	10	10		6.5	10	10	10	10	5	10	10	10	10	10
Arsenic	6.0	.05	10	3.0	8.0	3.0	4.0	6.0	6.0	4.0	8.0	6.0	3.0	2.0	6.0	3.0
Tin	-	-	-	-	-	.002	-	-	-	-	.10	-	-	-	-	-
Molybdenum	tr	-	tr	-	-	tr	.004	.002	-	-	-	-	-	-	-	tr
Indium	tr	-	.005	.02	.025	.02	-	-	.025	.02	.005	tr	-	-	-	tr
Thallium	-	-	-	-	-	-	-	.16	-	-	-	-	-	-	-	-

Elements looked for but not found: alkalis: Be, Sr, Ba, Ti, V, Cr, Co, Ni, Au, Te, Zr, Hf, Nb, Ta, W, Re, Pt, Sc, Y, Th, U, B, P, Ga, Ge.

Localities				
1.	Caldera vein,	Caldera level,	Lira mine,	specimen C-145
3.	Lira vein,	" "	" "	" C-149
5.	Mata Caballo vein,	480 level,	Sta. Teresita mine,	" C-187
7.	Caudalosa vein,	Pompeyo level,	Caudalosa mine,	" C-37
12.	" "	570 level,	" "	" C-219
13.	" "	530 level,	" "	" C-230
15.	" "	570 level,	" "	" C-160
16.	San Pedro vein,	640 level	" "	" C-108
17.	" " "	610 level	" "	" C-90
18.	" " "	" "	" "	" C-241
20.	Bonanza vein,	Dump	Bonanza mine,	" C-117B
21.	Entrada vein,	580 level,	Madona mine,	" C-180
22.	San Julian Norte vein,	A level,	San Genaro mine,	" C-283
23.	San Julian vein,	San Genaro level,	" " "	" C-25
24.	" " "	" " "	" " "	" C-191
25.	" " "	" " "	" " "	" C-190



Table XXXVII: Spectrographic analysis of zinkenite

Major constituents	( > 10%)	Pb, Sb
Minor constituents	(0.1-10%)	Si, Cu, Ag
Traces	( < 0.1%)	--
Locality:	570 level, Caudalosa vein, Caudalosa mine	
Specimen:	C-33	

BIBLIOGRAPHY

1. Allen, E. T., Crenshaw, J. L., and Merwin, H. E., 1914, Effect of temperature and acidity in the formation of marcasite ( $\text{FeS}_2$ ) and wurtzite ( $\text{ZnS}$ ): A contribution to the genesis of unstable forms: Amer. Jour. Sci., v. 38, p. 393-431.
2. Barnes, H. L., 1956, Mineral zoning and ore transport (abs.): XX Internat. Geol. Cong, Mexico; Resúmenes de los trabajos presentados, p. 208.
3. \_\_\_\_\_, and Kullerud, Gunnar, 1957, Relations between composition of ore minerals and ore solutions: Econ. Geology, v. 52, p. 825-830.
4. Barton, P. B., Jr., 1957, Some limitations on the possible composition of the ore-forming fluid: Econ. Geology, v. 52, p. 333-354.
5. \_\_\_\_\_, 1959, The chemical environment of ore deposition and the problem of low-temperature ore transport: in Abelson, P. H., Researches in geochemistry: New York, John Wiley & Sons, p. 279-300.
6. \_\_\_\_\_, and Kullerud, Gunnar, 1957, Preliminary report on FeS-ZnS system and implications regarding use of sphalerite geothermometer (abs.): Geol. Soc. America Bull., v. 68, p. 1699.
7. Bastin, E. S., 1950, Interpretation of ore textures: Geol. Soc. America Mem. 45, p. 101.
8. \_\_\_\_\_, and others, 1931, Criteria of age relation of minerals, with special reference to polished sections of ore: Econ. Geology, v. 26, p. 561-610.

9. Bateman, A. M., 1951, The formation of mineral deposits: New York, John Wiley & Sons, 371 p.
10. Bellido, Eleodore; Narvaz, Sigfredo; and Simons, F. S., 1956, Mapa geologico del Peru: Soc. Geol. del Peru, scale 1:2,000,000, 2 sheets.
11. Berry, L. G. and Thompson, R. M., 1962, X-ray powder data for ore minerals: The Peacock Atlas: Geol. Soc. America Mem. 85, 309 p.
12. Billings, M. F., 1942, Structural geology: New York, Prantica-Hall, 473 p.
13. Bodenlos, A. J., 1957, Base-metal deposits of the Cordillera Negra, Departamento de Ancash, Peru: U. S. Geol. Survey Bull. 1040.
14. B  dlander, G., 1895, Zusammensetzung des Polybasits: Neues Jahrb. Min., B. 1, p. 98-99.
15. Brode, W. R., 1946, Chemical spectroscopy: 2nd edition, New York, John Wiley & Sons, 677 p.
16. Brown, J. S., 1936, Supergene sphalerite, galena, and willemite at Balmat, New York: Econ. Geology, v. 31, p. 331-334.
17. Buerger, H. W., 1934, The unmixing of chalcopyrite from sphalerite: Am. Mineralogist, v. 19, p. 525-530.
18. Cooke, H. C., 1913, The secondary enrichment of silver ores: Jour. Geology, v. 21, p. 1-28.
19. Creasey, S. C., 1959, Some phase relations in the hydrothermally altered rocks of porphyry copper deposits: Econ. Geology, v. 54, p. 351-394.

20. Crosnier, Leon, 1852, *Geologie du Perou: Notice geologique sur les departments de Huancavelica et d'Ayacucho: Annales des mines (Paris) Ser. 5, v. II, p. 1-107.*
21. Curtis, G. H., 1954, *Mode of origin of pyroclastic debris in the Mehrten formation of the Sierra Nevada: Univ. California, Pub., Geol. Sec., v. 29, no. 9, p. 453-502.*
22. Douglas, R. M., Murphy, M. J., and Pabst, A., 1954, *Geocronite: Am. Mineralogist, v. 39, p. 908-928.*
23. Edwards, A. B., 1954, *Textures of the ore minerals and their significance: 2nd edition, Melbourne, Australian Institute of Mining and Metallurgy, 242 p.*
24. Emmons, W. H., 1917, *The enrichment of ore deposits: U. S. Geol. Survey Bull. 625, 530 p.*
25. Folk, R. L., 1947, *The alteration of feldspar and its products as studied in the laboratory: Am. Jour. Sci., v. 245, p. 388-394.*
26. Gaines, R. V., 1957, *Luzonite, famatinite, and some related minerals: Am. Mineralogist, v. 42, p. 766-779.*
27. Garrels, R. M., 1960, *Mineral equilibria at low temperature and pressure: New York, Harper and Brothers, 254 p.*
28. George, W. O., 1924, *The relation of physical properties of natural glass to their chemical composition: Jour. Geology, v. 32, p. 353-372.*
29. Graham, A. R., 1951, *Matildite, aramayoite, miargyrite: Am. Mineralogist, v. 36, p. 436-449.*
30. Gratton, L. C., 1933, *The depth zones of ore deposition: Econ. Geology, v. 28, p. 514-541.*

31. Guild, F. N., 1917, A microscopic study of silver ores and their associated minerals: *Econ. Geology*, v. 12, p. 298-353.
32. \_\_\_\_\_, 1928, The enrichment of silver ores: in Fairbanks, E. E., The laboratory investigations of ores: New York, McGraw-Hill, p. 201-242.
33. Harcourt, G. A., 1942, Tables for the identification of ore minerals by X-ray powder patterns: *Am. Mineralogist*, v. 27, p. 63-113.
34. Harrison, G. R., 1939, Massachusetts Institute of Technology Wave Length Tables: New York, John Wiley & Sons, 429 p.
35. Harvey, C. E., 1947, A method of semiquantitative spectrographic analysis: Glendale (California), Applied Research Laboratory, 285 p.
36. Holland, H. D., 1956, The chemical composition of vein minerals and the nature of ore forming fluids: *Econ. Geology*, v. 51, p. 781-797.
37. \_\_\_\_\_, 1959, Some applications of thermochemical data to problems of ore deposits. I. Stability relations among oxides, sulfides, sulfates and carbonates of ore and gangue minerals: *Econ. Geology*, v. 54, p. 184-233.
38. Ingerson, Earl, 1955, Methods and problems of geologic thermometry: *Econ. Geology*, 50th Anniv. Vol., pt. 1, p. 341-410.
39. Klug, H. P., and Alexander, L. E., 1954, X-ray diffraction procedures for polycrystalline and amorphous material: New York, John Wiley & Sons, 716 p.

40. Kullerud, Gunmar, 1953, The Fe-ZnS system as a geological thermometer: Norsk geol. Tidssk., v. 32, p. 61-147.
41. \_\_\_\_\_, 1959, Sulfide systems as geological thermometers: in Abelson, P. H., Researches in geochemistry, New York, John Wiley & Sons, p. 301-335.
42. Kracek, F. C., 1942, Melting and transformation temperatures of mineral and allied substances, Handbook of Physical Constants: Geol. Soc. America Spec. Paper 36, p. 139-174.
43. Lacy, W. C. and Hosmer, H. L., 1956, Hydrothermal leaching in central Peru: Econ. Geology, v. 51, p. 69-71.
44. Lasky, S. G., 1930, A colloidal origin of some of the Kennecott ore minerals: Econ. Geology, v. 25, p. 737-763.
45. Laineweber, Günter, 1956, Struktur-Analyse des Bournonite und seligmannite mit Hilfe der Superpositions-Methoden: Zeitschr. Kristallographic, Bd. 108, p. 161-184.
46. Lewis, R. W., Jr., 1956, Geology and mineralogy of the Castrovirreyne mining district, Huancavelica: Soc. Geol. Peru, t. 30, p. 217-224.
47. Lindgren, Waldemar, 1907, The relation of ore deposition to physical conditions: Econ. Geology, v. 2, p. 105-127.
48. \_\_\_\_\_, 1933, Mineral deposits: 4th edition, New York, McGraw-Hill, 930 p.
49. \_\_\_\_\_, 1937, Succession of minerals and temperatures of formation in ore deposits of magmatic affiliation: Am. Inst. Mining Metall. Engineers Trans., v. 126, p. 356-376.

50. Lyons, R. J. P., 1959, Time aspects of geothermometry: *Am. Inst. Mining Metall. Engineers Trans.*, v. 214, p. 1145-1151.
51. Manetti, José M., 1945, Noticias referentes a la representación de don Alvaro Monroy: in Masias, 1929, *Soc. Geol. Perú Bol.*, v. 3, p. 92.
52. Masias, Aurelio, 1929, Geología de la región minera de Castrovirreyna: *Soc. Geol. Perú Bol.*, v. 3, p. 59-108.
53. McKinstry, H. E., 1945, Structure of hydrothermal veins: *Econ. Geology*, 50th Anniv. Vol., pt. 1, p. 170-225.
54. \_\_\_\_\_, and Kennedy, G. C., 1957, Some suggestions concerning the sequence of certain ore minerals: *Econ. Geology*, v. 52, p. 379-390.
55. Monroy, Alvaro, 1769, Representación dirigida al Virreynato del Perú en junio de 1769 para el restablecimiento del mineral de Castrovirreyna en el departamento de Huancavelica: in Masias, 1929, *Soc. Geol. Perú Bol.*, v. 3, p. 83-93.
56. Montesinos, Fernando, 1591, *Memorias Antiguas: Historiales del Perú*: Translated and edited by Means, P. A., 1920, London.
57. Huffield, E. W., 1946, Studies of mineral sulfosalts: XII - Fulbypite and zinkenite: *Univ. Toronto, Geol. Ser.*, no. 50, p. 49-62.
58. \_\_\_\_\_, and Peacock, M. A., 1945, Studies of mineral sulfosalts: VII - Plagionite and semseyite: *Univ. Toronto, Geol. Ser.*, no. 49, p. 17-39.
59. Oppenheim, Victor, 1948, Theory of Andean orogenesis: *Am. Jour. Sci.*, v. 246, p. 578-590.

60. Palache, C., Berman, H. and Frondel, C., 1944, The system of mineralogy of James Dwight Dana and Edward Salisbury Dana, 7th edition, v. 1, Elements, sulfides, sulfosalts, oxides: New York, John Wiley & Sons, 834 p.
61. \_\_\_\_\_, 1951, The system of mineralogy of James Dwight Dana and Edward Salisbury Dana, 7th edition, v. 2, Halides, nitrates, borates, carbonates, sulfates, phosphates, arsenates, tungstates, molybdenates, etc.: New York, John Wiley & Sons, 1124 p.
62. Park, C. F., Jr., 1955, The zonal theory of ore deposits: Econ. Geology, 50th Anniv. Vol., pt. 1, p. 226-248.
63. Peacock, M. A. and Berry, L. G., 1947, Studies of mineral sulfosalts: XII Polybasite and pearceite: Mineralogy Mag., v. 28, no. 196, p. 1-13.
64. Pettijohn, F. S., 1957, Sedimentary rocks: New York, Harper & Brothers, 2nd edition, 718 p.
65. Ramdohr, Paul, 1955, Die Erzminerale und ihre Verwachsungen: Berlin, Akademie Verlag, 875 p.
66. Ransome, F. L., 1910, Criteria of downward sulfide enrichment: Econ. Geology, v. 5, p. 205-220.
67. Ravicz, L. G., 1915, Experiments in the enrichment of silver ores: Econ. Geology, v. 10, p. 378-384.
68. Robinson, S. C., 1948, Synthesis of lead sulphantimonides: Econ. Geology, v. 43, p. 293-312.
69. Ross, Virginia, 1954, The formation of intermediate sulfide phases in the solid state: Econ. Geology, v. 49, p. 734-752.



70. Sales, R. H., and Meyer, Charles, 1948, Wallrock alteration at Butte, Montana: Am. Inst. Mining Metall. Engineers, Tech. Pub. 2400.
71. \_\_\_\_\_, 1949, Results from preliminary studies of vein formation at Butte, Montana: Econ. Geology, v. 44, p. 465-484.
72. Schwartz, G. M., 1932, Microscopic criteria of hypogene and supergene origin of ore minerals: Econ. Geology, v. 27, p. 533-553.
73. \_\_\_\_\_, 1959, Hydrothermal alteration: Econ. Geology, v. 54, p. 161-183.
74. Short, M. N., 1940, Microscopic determination of the ore minerals: U. S. Geol. Survey Bull. 914, 2nd edition, 311 p.
75. Skinner, B. J., 1960, Assemblage enargite - famatinite, a possible geologic thermometer (abs): Geol. Soc. America Bull., v. 71, p. 1975.
76. \_\_\_\_\_, Barton, P. B., Jr., and Kullerud, Gunnar, 1959, Effect on the unit cell edge of sphalerite. A revision: Econ. Geology, v. 54, p. 1040-1046.
77. Smith, F. Gordon, 1954, Composition of vein-forming fluids from inclusion data: Econ. Geology, v. 49, p. 205-210.
78. Stevanovic, S., 1903, Ueber einige Kupfererze und Beiträge zur Kenntniss der Zirkongruppe; ueber Stylotyp, Famatinit und Enargit: Zeits. Krist., Bd. 37, p. 235-244.
79. Stone, J. G., II, 1958, Ore genesis in the Naica District, Chihuahua, Mexico: Ph.D. thesis, Stanford University.

30. Stringham, Bronson, 1952, Fields of formation of some common hydrothermal alteration minerals: Econ. Geology, v. 47, p. 661-664.
31. Thompson, J. B., Jr., 1959, Local equilibrium in metasomatic processes: in Abelson, P. H., Researches in geochemistry: New York, John Wiley & Sons, p. 427-457.
32. Van Hise, C. R., 1902, Some principles controlling the deposition of ores: in Fosvpepny, Franz, The genesis of ore deposits, 2nd edition, New York, Am. Inst. Mining Metall. Engineers, p. 282-432.
33. Vitaliano, C. S., and Mason, Brian, 1952, Stibiconite and cervantite: Am. Mineralogist, v. 37, p. 982-999.
34. Wahlstrom, E. E., 1955, Petrographic mineralogy: New York, John Wiley & Sons, 408 p.
35. White, D. E., 1955, Thermal springs and epithermal deposits: Econ. Geology, 50th Anniv. Vol., pt. 1, p. 99-154.
36. Williams, Howell, Turner, F. J., and Gilbert, C. M., 1958, Petrography: San Francisco, W. H. Freeman & Co., 406 p.
37. Winchell, A. N., and Winchell, Horace, 1951, Elements of opitical mineralogy: Part II, Description of minerals: 4th edition, New York, John Wiley & Sons, 423 p.